

Design and Development of Atraumatic Vacuum Assisted Delivery Devices

Baboo Dushyantsingh Goordyal

Submitted in accordance with the requirements for the degree of
Doctor of Philosophy

The University of Leeds
School of Mechanical Engineering

February 2020

Declarations

The candidate confirms that the work submitted is his/her own and that appropriate credit has been given where reference has been made to the work of others.

This copy has been supplied on the understanding that it is copyright material and that no quotation from the thesis may be published without proper acknowledgement.

The right of Baboo Dushyantsingh Goordyal to be identified as Author of this work has been asserted by Baboo Dushyantsingh Goordyal in accordance with the Copyright, Designs and Patents Act 1988.

© 2020 The University of Leeds and Baboo Dushyantsingh Goordyal

Acknowledgements

I would like to acknowledge my family for their love and support during the highs and lows of this PhD especially my parents. The research outcomes of this PhD would never have been presented if it wasn't for the innovative, amicable & professional guidance provided by Pete Culmer, Matthew Tulley & Ali Alazmani. The supervision provided allowed me to develop my independent academic thinking whilst keeping originality at heart. I would also like to thank Dr John Anderson for providing clinical output during the definition phase of the project.

The development of the VAD simulator and the presented research outcomes would not have been possible without the technical know-how of Tony Wiese, Dave Readman, Reese Moore & Graham Brown. Special thanks to Eakin group Ltd for collaborating with the research team on this project. I would like to present my sincere gratitude to friends who have kindly agreed to review the contents of this thesis namely: SA Mohammed, Arturo Andersen Chinbuah, Abimbola Oladokun, Mustafa Kadhim & Mark Slade.

Special mentions to Kow Jun Wai for being ever so present through my time as a postgraduate researcher (PGR). The countless runs for coffee refills, Chinese/Malaysian food runs & tantrums thrown at each other will always remain enjoyable moments to be forever remembered. To all PGRs encountered during my time of study at the University of Leeds, I was embraced by your presence and hope to see you again in the near future.

Abstract

Vacuum-Assisted Delivery (VAD) is an obstetric practice used to assist child delivery during the second stage of labour. During the procedure, the obstetric professional attaches the VAD device to the scalp of the foetus through suction and tractive force is then applied alongside maternal contractions to assist the baby's passage through the delivery channel. VAD is more prevalent than obstetric forceps due to its ease of use, lower maternal morbidity and improved cosmetic outcome for the mother and her baby. However, safety concerns such as unintentional cup detachment or high vacuum, can lead to induced trauma to the foetus. Since its original inception, there have been limited efforts to evaluate the safety of VAD devices or optimise their design and operation. Here, an engineering approach to assess the devices' failure modes is proposed to inform training, best obstetric practice and improved VAD design.

An instrumented experimental recreation of VAD has been developed to achieve a comprehensive understanding of the mechanics of VAD devices and the associated trauma. It features an instrumented adaptation of a commercially available VAD device (the Kiwi® Omnicup™) connected to a tensile testing machine to simulate obstetric traction onto a head scalp model (fabricated using textile reinforced silicone). A pneumatic control system provides an actively controlled vacuum to the instrumented device. Optical markers, placed onto the scalp model, combined with a high-speed camera system provide tracking of scalp deformation during the mechanical simulation of an obstetric traction. Experimental factors such as traction speed, magnitude of vacuum imposed & changes to the design geometry of the VAD cup and pneumatic architecture including the consideration of frictional attributes of the maternal environment, were investigated. The results from the experimental studies show that a simulated obstetric VAD traction produces a characteristic response from which a number of key clinically relevant metrics can be determined and highlight the association of clinical factors and mechanical factors to device performance. The research informed on the conception of an atraumatic concept to prevent cup detachment. Upon evaluation of the technical and commercial feasibility of the concept, commercial and research opportunities were identified, which could help improve the performance of VAD devices, in the future.

Table of Contents

Chapter 1 Introduction to Research	1
1.1 Research aim & Objectives	2
1.2 Thesis Overview	2
Chapter 2 Literature Review	5
2.1 Vaginal Birth	6
2.2 Instrumental Vaginal Delivery.....	9
2.2.1 Obstetric Forceps.....	12
2.2.2 VAD Systems	13
2.3 Interaction of VAD with Foetal head	17
2.4 Associated Trauma with VAD & Cup Detachment.....	19
2.5 Design Evolution of VAD	22
2.6 VAD Mechanics behind Cup Detachment	27
2.7 Literature Summary	30
2.8 Conclusion.....	31
Chapter 3 Development of a VAD simulator	32
3.1 Research Motivation.....	33
3.2 Clinical Simulation Requirements.....	34
3.3 Design Requirements of a VAD simulator	37
3.4 Load Measurement & Simulation of Traction.....	41
3.4.1 Instrumentation of VAD Device	42
3.4.2 Foetal Head Scalp Model.....	43
3.5 Chapter Summary	43
Chapter 4 Design and Development of an Experimental Measurement System to detect Cup Detachment	44
4.1 Introduction.....	45
4.2 Development of a Foetal Head Scalp Model	46
4.2.1 Initial Development.....	47
4.2.2 Development of a silicone-textile composite scalp	52
4.2.3 Fabrication of Silicone-textile Scalp Composite	59
4.3 VAD Pneumatic Instrumentation	61
4.3.1 Pneumatic Controller unit.....	62
4.3.2 VAD sensing Unit.....	63
4.3.3 Calibration of VAD Pneumatic controller and Sensing Units	63
4.4 Experimental methodology to detect cup detachment.....	66
4.4.1 Test Assembly.....	67

4.4.2	Test Methodology	69
4.4.3	Visual Detection of Cup Detachment with Pin Markers	70
4.5	Dynamics of Cup Detachment.....	73
4.5.1	Data Processing.....	73
4.5.2	System dynamics.....	77
4.5.3	Repeatability and Reproducibility.....	80
4.6	Chapter Summary	84
Chapter 5	Experimental Evaluation of VAD Systems	85
5.1	Investigation of Clinical and Mechanical Factors affecting VAD Performance.....	86
5.2	Parametric experimental Study	87
5.2.1	Test Protocol.....	87
5.2.2	Study 1: Vacuum magnitude inside instrumented VAD.....	90
5.2.3	Study 2: Traction Speed.....	90
5.2.4	Study 3: Changes in Cup Geometry	90
5.2.5	Study 4: Frictional Attributes of the Maternal Environment ...	93
5.2.6	Study 5: Changes in Pneumatic VAD Configuration	94
5.3	Experimental Results	96
5.4	Experimental Evaluation.....	103
5.5	Discussion.....	111
5.6	Chapter Summary	112
Chapter 6	Translating research outcomes to the design of a commercial system.....	113
6.1	Assessment of Clinical and Commercial Opportunities	114
6.2	Assessing technical opportunities to improve VAD performance .	118
6.2.1	Evaluation of Design Opportunities.....	118
6.2.2	Concept for an atraumatic VAD device	121
6.2.3	Intellectual Property (IP) Analysis	122
6.2.4	Regulatory requirements.....	125
6.3	Discussion.....	127
6.4	Chapter Summary	127
Chapter 7	General Discussion, Future Works and Conclusion	128
7.1	Assessment of Research Objectives.....	129
7.2	General Discussion and Future works.....	132
7.2.1	Discussion.....	132
7.2.2	Future Works	134
7.3	Concluding Remarks	139

References.....	140
Appendices.....	147

List of Tables

Table 2-1 - Factors assessed at vaginal examination which could impact labour. Extracted and modified from (13, 21).....	8
Table 2-2: Instrumental delivery rates in EU Countries(23)	9
Table 2-3: shows the desired outcomes of the stakeholders identified during the identification of the clinical care pathway (26)	11
Table 2-4: Mechanical properties of tested scalps. Left: Tested regions of the scalp. Right: Table with reported values of mechanical properties of human scalp tested against ISO 527-2 (55)	19
Table 3-1: Summary of the model features, the simulation requirements and the system specifications of the VAD simulator	39
Table 3-2: Calculations for the average speed of traction during VAD extracted from Saling’s Traction Experiments (91)	42
Table 4-1 :Summary of the material evaluation for implementation in the head scalp model.....	57
Table 4-2 shows a summary of Simulation Control & Sensing Hardware	61
Table 4-3: Summary of the testing variables measured by the hardware and operated by its designated software utilised in the test measurement system.....	66
Table 5-1: Test protocol matrix during this parametric study of clinical and mechanical factors.....	88
Table 5-2: Cup profile tested with their cross section, surface area, contact volume and schematic upon combination with the respective insert.	91
Table 5-3: List of lubricants used during the study of assessing the impact of lubricant on the traction force	93
Table 5-4: The pneumatic configuration and the effective volume after valve based on the schematic shown in Figure 5-1 & Table 5-1....	95
Table 6-1 : Market opportunity analysis based Total Available Market (TAM), Serviceable available market (SAM), and serviceable obtainable market (SOM) of the identified countries with a receptive VAD market in Table 2-2.....	116
Table 6-2: Estimated calculations for the cost saving potential of the proposed device in UK.....	117
Table 6-3: IP Analysis to identify IPs which can be a barrier to innovation. The relevance in risk is colour coded. Green-Free to operate, Yellow- Presented IP might be a concern but there might be workability around it.....	123
Table 6-4: Regulatory pathway of predicate/substantially equivalent VAD devices following the 510(k) route in USA	126
Table 7-1: Risk register for Future works of technical and commercial development of VAD device	135

List of Figures

- Figure 2-1: Timeline of normal delivery events. A: Foetus aligns to the bony maternal pelvis in a cephalic presentation(vertex/head first), B: Baby progressing through the stations of delivery, C:Baby's head scalp is visible at the introitus, D: Delivery of the baby is completed where the body delivers, either spontaneously or with the healthcare professional (accoucheur) holding the foetal head, sometimes to help delivery of the shoulders. This also marks completion of the second stage of labour(14). E: Front view of stations of delivery gauged with respect to the ischial spine (-3 to +3). Zero station is achieved when the head is aligned to the ischial spine. Each 1 cm increment from this reference constitutes of an increase of +1 delivery station(15).7**
- Figure 2-2: Examples of obstetric forceps. Top: Key design features of Kielland Forceps(34), Bottom: Illustration of Simpson Forceps(35)12**
- Figure 2-3: Modern adaptations of conventional VAD system and their design features. A: Medela Basic Electric pump for VAD use, B: Medela Manual Pump VAD system, C: Utah Med Ltd VAD system, D: Cooper Surgical MityVac VAD system.....13**
- Figure 2-4: Two- handed traction technique with the Kiwi OmniCup(46, 47)15**
- Figure 2-5: Process steps during VAD. A: Cup placement-A vacuum source is applied to create a chignon by manual/electric pumping after placement on the flexion point. On caption-Illustration of Malmstrom's cup placement on a foetal head (36), B: Traction-Applied traction with a counter traction used to overcome resistant introitus, C: Cup Release: VAD is released after the crowning of the head and clinician proceeds to crown delivery.16**
- Figure 2-6: Diameter of circle represents the suboccipitobregmatic diameter (SOB). Picture courtesy of Sorbe et al. (38).....17**
- Figure 2-7 : Distinctive layers of the scalp present on the cranium: Skin & Dense connective tissue, Epicranial Aponeurosis, Loose areolar connective tissue & Pericranium onto the skull ((56)).....18**
- Figure 2-8 :Trauma associated with VAD. A:Elevation of scalp after VAD(36), B: Dissipation of caput succedaneum after a few hours leading to a cup mark (36) C: Baby head with SGH (56) D: All trauma levels associated with VAD.....21**
- Figure 2-9:Single Use VAD Systems. A & B:Examples of Single Use Instrumented devices with a reusable pump. C: Cooper Surgical Mystic 2 VAD system, D: Clinical Innovation Kiwi Omni Cup.....24**
- Figure 2-10: Evolutionary trail of modern VAD devices. A: Medela conventional cup system (80), B: Description of the features of the VAD cups in panel A.....24**

Figure 2-11: Evolutionary track of VAD device design A:James Young Simpson’s ‘Air Tractor’(81), B:Saleh’s rubber cup with finger grips(71), C: McCahey’s designs, D:Stillman’s design(71), E: Couzigou’s ventouse eutocique(81), F:Finderle’s horn VAD device(81), G: Malmstrom’s VAD device proposed in 1968(81), H: Bird’s modified VAD device proposed in 1969(81)	25
Figure 2-12: Replotted Traction Experiments by Malmstrom (27) VE60:60mm diameter cup, VE50:50mm diameter cup, VE40: 40mm diameter cup. Predicted curves displays Force values (calculated by the multiplication of the Vacuum Induced by the contact cross-sectional area of cup onto scalp).....	27
Figure 2-13: Attachment of cup onto flexion point and creation of chignon and overview of the contact angles of scalp present at the entry of VAD cup system.	28
Figure 3-1: Key VAD procedural steps demonstrated by Dr John Anderson on a VAD Training Model. A&B: Identification phase, C,D&E: Application and Insertion phase of VAD, F&G: Traction Phase, H:End of VAD Procedure-Crowning and release of vacuum on foetal head.	35
Figure 3-2 : A coronary view of the stations of delivery used to assess descent of the baby with the SOB shown as the major presenting diameter to be accounted for (Adapted from:(15) (9))	36
Figure 3-3: Kiwi Omni Cup™ MTE (with traction indicator)	37
Figure 3-4: Design concept of VAD Simulator with model features highlighted to simulate the clinical use of VAD. An overview of phase development of the process of development of this concept model can be seen from Appendix A2.....	38
Figure 4-1: Control schematics of interaction of different developed instrumented units of the in-vitro simulation of VAD set up to capture the dynamics of cup detachment on a developed VAD simulator	46
Figure 4-2: Silicone-textile composite scalp placed onto the hemispherical head model based on requirements provided in Table 3-1.	47
Figure 4-3: First iteration of the head model	48
Figure 4-4: Fabrication steps to create a Scalp. Step 1: Silicone Preparation and Pouring, Step 2: Casting, Step 3: Curing Step 4: Demoulding Removal of top mould from bottom mould.....	49
Figure 4-5 : Experimental overview of silicone casting. A-Top Mould, B-Bottom Mould, C- Silicon Curing, D- Demoulded Silicone Scalp ..	50
Figure 4-6: Optimised head model with grooved walls for improved contact with the moulded scalp surrogate.....	51
Figure 4-7: Evolution of head scalp models in the VAD simulator A: Over elongation of the material with the original conception. B: Vacuum controlled scalp with the optimised head model. C: Silicone-textile Scalp	52

Figure 4-8: Tensile specimen dimensions based on ASTM D412-06a standards. A- Length of test specimen, B-Breadth of the barbell ends for clamping, C: Thickness of sample, D-Gauge length of elongation.....	54
Figure 4-9: Tensile Stress-Strain Curve for Scalp testing alongside the representation of the tensile specimen at different stages of the test.	54
Figure 4-10: Preparation steps of the silicone-textile composites. A- First layer (2mm) silicone preparation, B-First layer cured and laser cut textile sheet to fit tensile template C- Placement of textile sheet, D-secure clamping of tensile set for second layer silicone preparation (2mm), E- Curing and setting of samples	56
Figure 4-11: Tensile testing of material evaluated in the conception of a silicone-textile scalp. A-Tensile testing of silicone-textile barbell specimen, B- Tensile testing of SynDaver 4N Skin Simulant	56
Figure 4-12 : Data for the Mean Elastic Modulus for $0 < e < 15.48\%$ (Left y axis- Blue) & Mean Stress at $e=38.87\%$ (Right y axis-Red)	58
Figure 4-13: Overview of scalps manufactured over the time of study. A- Silicone scalp, B-Loose PTE fibre scalps, C-Sulky scalps, D- Lyocell scalp and list of associated defects with the current manufacturing technique.....	60
Figure 4-14: Pneumatic components used to pneumatically instrument the VAD cup	61
Figure 4-15: Instrumentation of the VAD controlled by the VAD Pneumatic controller and the vacuum recorded by the VAD Sensing Unit. Both systems are monitored by the DAQ.	62
Figure 4-16: Schematic of the electro-pneumatic Vacuum Regulator showing the feedback control schematic of a set pressure based on an input signal(113)	63
Figure 4-17: Calibration Curve for voltage input to the vacuum sensor as result of vacuum changes created by the pump and validated by the Digital Manometer (n=48).	64
Figure 4-18: Calibration curve for the voltage output from the electro-pneumatic regulator to control the vacuum sensed by the calibrated vacuum sensor. The supply of vacuum to the regulator was -80 kPa and generated by the pump (n=39).	65
Figure 4-19: Calibration curve for the voltage input to electro-pneumatic regulator against vacuum levels changes generated by the pump (n=39).	65
Figure 4-20: Assembly components of the VAD simulator. The foetal head scalp model and the pneumatically controlled VAD cup onto an Instron E10000 and a high speed camera records the test performed.	68
Figure 4-21: Details of how a synchronisation signal is sent from the NI DAQ to start the data acquisition of the load & vacuum and recording of the high speed camera	68

Figure 4-22 : Test flowchart with the 2 interfacing software used during the data acquisition of the test method to simulate an overtraction. A: The test flowchart associated with the LabView Interface. B: The test flowchart associated with the Instron Interface.	69
Figure 4-23: Pin markers onto Scalp. A: Schematic of pin markers placement position on foetal head scalp model at indicated by distances a,b,c & d, B: Experimental placement of pin markers on foetal head scalp model and identification of the side pins	70
Figure 4-24: pixel displacement calibration using calibrated meter rule & setting of ROI using image detection algorithm (Harris-Stephens) on Matlab	71
Figure 4-25: Automatic tracking of the pin position at frames elapsed from Trigger. Red marked shows the start of the test. Blue markers show End of the Test.....	72
Figure 4-26: Image analysis flowchart to obtain the y displacement of the side pins	72
Figure 4-27: Data Processing flowchart for the acquired pin markers and DAQ data sets	74
Figure 4-28: Time-series data acquisition of the traction load and vacuum level for the experimental capture at 100Hz	75
Figure 4-29: Post-Processed Time-series data acquisition of the displacement of the pin markers displacement (mm) data for the experimental capture at 100Hz. T_{pin} shows initial movement of the pin markers, T_{max} is the maximum identified Traction load. T_{pop} is the detected time at which Pop Off arises through threshold setting on the differentiated time series profile of the acquisition of the displacement of the pin markers.....	75
Figure 4-30: Chain of events at different time points registered on the test and the relevant capture image of the test associated with each time stamp described in Figure 4-29.....	76
Figure 4-31: Time-series data acquisition of the traction load and vacuum level for the experimental capture at 1600Hz	77
Figure 4-32 : Pin Marker Threshold setting of 0.04mms-1 to detect the Pop-Off event on the differentiated displacement pin markers dataset (velocity) against time elapsed from trigger for the experimental capture at 1600Hz.	78
Figure 4-33: Time-series data acquisition centred around T_{max} of the traction load and vacuum level for the experimental capture at 1600Hz. T_{max} is the maximum traction load identified. T_{pop} is the location of the pop-off event. Events of $T_{pop} \pm 10$ frames or $\pm 0.000625s$ are also indicated.	78

- Figure 4-34: Chain of events leading to a cup detachment starting from T_{max} to $T_{pop+10\text{ Frames}}$. The time points registered on the test and the relevant capture image of the test associated with each time stamp described in Figure 4-33. On left a schematic on the net flowrate (Q_{net}) inside the cup is shown at various time events during the test. Q_{out} represents suction flow rate towards the vacuum supply or the sensor. Q_{leak} represents the leak introduced in the closed system.79**
- Figure 4-35: Interval plots of L_{max} , V_{max} , and T_{max} for evaluating Two manufactured scalps. Y axis represents the L_{max}, V_{max} & T_{max} and X axis represents tested scalps.....81**
- Figure 4-36: Interval plots of L_{pop} , V_{pop} , and T_{pop} for evaluating Two manufactured scalps. Y axis represents the L_{pop}, V_{pop} & T_{pop} and X axis represents tested scalps.....81**
- Figure 4-37: Times-series plot f 5 experimental repeats of the load (N) & Vacuum (-kPa) acquired at 5000Hz with load and vacuum markers at T_{max} and T_{pop} reported for the evaluation of 2 scalps.....82**
- Figure 4-38 :Time series plot in Figure 1 37, centred around T_{max} with load and vacuum markers at T_{max} and T_{pop} reported for the evaluation of 2 scalps.....83**
- Figure 5-1: Pneumatic Test configurations for the study of the regulated buffered vacuum source. The configuration 1, state 1 is the control simulations for all the cases in all presented studies. (a)- relates to changes in cup geometry , (b)-relates to changes in traction speed, (c)-relates to addition of lubricants on the surface of the foetal head scalp, (d) relates to pneumatic changes in the control & delivery of the vacuum by the pneumatic unit.....89**
- Figure 5-2: Cup Geometry changes in instrumented VAD. In diagram annotations shows the cup geometry changes upon insertion of fabricated inserts to reduce the contact area of the scalp and volume capacity of the VAD cup. In the displayed constitutive equation, the impact of F_m will be investigated through different addition of inserts. F_{lumped} will contain the terms (F_v :Force due to the applied vacuum and F_f :Force due to frictional effects). T represents the Tension in the scalp.....92**
- Figure 5-3: Investigation of the Frictional Attributes of the maternal environment using different formulation of lubricants (low viscosity to high viscosity) to provide an insight the tribology of the cup interaction. (μ_k -Sliding Coefficient of Friction). In the displayed constitutive equation, the impact of F_f will be investigated through application of different lubricant formulations on the foetal head scalp model. F_{lumped} will contain the terms (F_v :Force due to the applied vacuum and F_m :Force due to mechanical interlock). T represents the Tension in the scalp.....94**
- Figure 5-4: Pneumatic Architecture volumetric flow rate changes as a function of volume.....96**

Figure 5-5: A representative time centred series centred plot at maximum traction time ($T=T_{max}$) of the sensory output of the load and the vacuum detected by the VAD simulator with graph markers indicated at T^*_{Pop} ($T=T_{max}-T_{pop}$) for each Test configuration in Study ID 1	97
Figure 5-6: A representative time centred series centred plot at maximum traction time ($T=T_{max}$) of the sensory output of the load and the vacuum detected by the VAD simulator with graph markers indicated at T^*_{Pop} ($T=T_{max}-T_{pop}$) for each Test configuration in Study ID 2	98
Figure 5-7: A representative time centred series centred plot at maximum traction time ($T=T_{max}$) of the sensory output of the load and the vacuum detected by the VAD simulator with graph markers indicated at T^*_{Pop} ($T=T_{max}-T_{pop}$) for each Test configuration in Study ID 3	99
Figure 5-8: A representative time centred series centred plot at maximum traction time ($T=T_{max}$) of the sensory output of the load and the vacuum detected by the VAD simulator with graph markers indicated at T^*_{Pop} ($T=T_{max}-T_{pop}$) for each Test configuration in Study ID 4	100
Figure 5-9: A representative time centred series centred plot at maximum traction time ($T=T_{max}$) of the sensory output of the load and the vacuum detected by the VAD simulator with graph markers indicated at T^*_{Pop} ($T=T_{max}-T_{pop}$) for each Test State in Pneumatic VAD configuration 1 in Study ID 5	101
Figure 5-10: A representative time centred series centred plot at maximum traction time ($T=T_{max}$) of the sensory output of the load and the vacuum detected by the VAD simulator with graph markers indicated at T^*_{Pop} ($T=T_{max}-T_{pop}$) for each Test State in Pneumatic VAD configuration 2 in Study ID 5.	102
Figure 5-11: Regression line showing relationship between $L_{max}(N)$ and V_{max} for each tested Traction speed (mm/min) for Study 1	104
Figure 5-12: Interval plot of T_{max} (N) against tested Traction speed (mm/min) conditions for Study 2	105
Figure 5-13: Regression line showing relationship between $T_{max}(s)$ and tested Traction speed (mm/min) conditions for Study 2	105
Figure 5-14: Interval Plot of L_{max} (N) against changes in cup geometry for Study 3	106
Figure 5-15: Tukey simultaneous analysis of means of L_{max} against tested experimental condition for study ID 3. Only Insert B showed difference in means compared to unchanged configuration.....	107
Figure 5-16: Interval plot of L_{max} (N) against test lubricant formulation in Study 4	108
Figure 5-17: Tukey simultaneous analysis of means of L_{max} against tested across all tested experimental condition and the scalps control for study ID 4.....	108

Figure 5-18: Comparison of means of Lmax (N) against tested Pneumatic configuration ID for study 5.....	109
Figure 5-19: Comparison of means of Vmax (kPa) against tested Pneumatic configuration ID for study 5.....	110
Figure 5-20: Interval plots of test metrics- Lmax(N), Vmax(kPa), Tmax(s) against tested Pneumatic configuration ID for study 5.....	110
Figure 6-1: Clinical care pathway behind operative delivery and clinical outcomes in the event of VAD failure (21, 119).....	115
Figure 6-2: Reimbursement chart showing NHS operational cost associated with clinical costs linked to clinical care pathway as shown in Figure 6-1 (119).....	117
Figure 6-3: Design aspects considered during the conception of an atraumatic VAD cup system. A: Changing the cup geometry to improve scalp retention. B: Integration of a reservoir to provide a continuous volumetric flow rate to the pneumatic architecture C: Sensing unit integration in the dynamically sensing the vacuum inside the VAD cup system.....	119
Figure 6-4 : Concept of the device operation to reduce cup detachment by an adaptive tensioning mechanism triggered by vacuum sensing input. Left: Device and Operations. Right: Dynamic monitoring control and monitoring of cup detachment.....	121

Abbreviations/Glossary of Terms

Term	Explanation/Definition
ACOG	American College of Obstetricians and Gynecologists
Caput Succedaneum	During labour, the serosanguinous fluid accumulating in the subcutaneous tissue of the foetal scalp & the periosteal tissue of the foetal skull, is similar to oedema but termed caput succedaneum.
Cervical Effacement & dilation	As labour progresses the cervix shortens and thins out, a process termed effacement. The cervix also stretches open, termed dilatation, allow the passage of the baby through the birth canal.
Chignon	Build-up of bloody fluid caused by induced pressure by the application of a VAD device to create cohesion between the cup effector and the scalp.
Episiotomy	Surgical incision of the perineum and posterior vaginal wall
Flexion Point	Located 3 cm forward of the posterior fontanelle along the sagittal suture and is the ideal application point for VAD to be placed to maintain flexion of the foetal head during traction
Fontanelles	Gaps between the foetal skull bones which allows the passage of the baby through the maternal pelvis
Gravida/Parity	Primigravida: A woman pregnant for the first time Multigravida: A woman pregnant multiple times
Introitus	Entrance to the vaginal canal
Ischial spine	Anatomical bony landmark in pelvis
Mento-vertical diameter	Engagement diameter of baby head during cephalic delivery
Moulding	Suture apposed(+1): Fetal head bones touching and not overlapping Sutures overlapped but reducible (+2): Fetal head bones gently overlapping and can be restored back to position with a gentle touch Suture overlapped and not reducible(+3): The extreme case leading to overlapping of bones not easily restored to position.

Term	Explanation/Definition
OA, OT, OP position: Orientation of foetal head	<p>OA: Occipito anterior- Occipital bone positioned towards mother's belly</p> <p>OP: Occipito posterior- Occipital bone positioned away from mother's belly</p> <p>OT: Occipito transverse- Occipital bone positioned sideways to the mother's belly</p>
Oedema	<p>Oedema is any serous fluid collection in extra vascular tissue and can be the result of multiple causes e.g. infection, inflammation or trauma. During labour, the serosanguinous fluid accumulating in the subcutaneous tissue of the fetal scalp & the periosteal tissue of the foetal skull, is similar to oedema but termed caput succedaneum.</p>
Presentation of fetal body	<p>Cephalic: Baby's head presenting downwards to pelvis</p> <p>Breech: Baby's buttock presenting downwards to pelvis</p>
RCOG	Royal College of Obstetricians and Gynaecologists
Serosanguinous	Referring to blood and the serum liquid part of blood.
Stations of Delivery (-1 to +5)	<p>The station of delivery is used to describe the position of the presenting part of the baby in relation to a bony anatomical landmark in the maternal pelvis, the ischial spines. This is conventionally measured in centimetres, above (minus) or below (plus) the ischial spines. The clinical description "-3 above spines" would therefore represent a high head, the leading edge of which sitting at a plane where it is only just entering the maternal true pelvis. +1 represents a head which has advanced 1cm beyond the the plane of the ischial spines.</p>
Subgaleal haematomas	Bleeding in between the skull periosteum and the scalp galea aponeurosis
Terms of delivery	<p><u>UK</u> Pre Term: Delivery at a gestational age of 24-36 weeks and 6 days pregnancy (~11%). Full Term: Delivery at a gestational age of 37-40 completed weeks pregnancy (~80%). Post Term: Delivery at a gestational age of >40 weeks pregnancy (~10 %).</p> <p><u>USA</u> Early term- (37 0/7 weeks of gestation through 38 6/7 weeks of gestation) Full term- (39 0/7 weeks of gestation through 40 6/7 weeks of gestation) Late term- (41 0/7 weeks of gestation through 41 6/7 weeks of gestation), Post term- (42 0/7 weeks of gestation and beyond) to more accurately describe deliveries occurring at or beyond 37 0/7 weeks of gestation.</p>
Type of labour	<p>Unaided/spontaneous vaginal delivery (ie., no instruments required), In the UK an unaided or spontaneous normal delivery is usually managed by a trained midwife, without the involvement of a physician. In other parts of the developed world, physicians may routinely attend normal deliveries. In developing nations, if a woman is cared for in labour by a trained birth attendant, their skills will be more akin to that of a midwife.</p> <p>Iatrogenic: Medically caused. An induced labour is iatrogenic.</p>

Chapter 1

Introduction to Research

Complications during childbirth result in the need for obstetricians to use 'assisted delivery' in over 12% of cases. Whilst this is preferable to the risk of maternal and foetal trauma imposed by emergency C-Section, assisted delivery systems remain poorly understood and under-developed (1).

Vacuum-Assisted Delivery (VAD) is a mainstay of assisted delivery techniques utilised during the second stage of labour. During the procedure, the obstetric professional attaches the VAD device to the scalp of the foetus using negative pressure and tractive force is then applied alongside maternal contractions to assist the baby's passage through the delivery channel. VAD is more established than obstetric forceps due to its ease of use, lower maternal morbidity and improved cosmetic outcome for her baby. However, safety concerns, such as unintentional cup detachment or high vacuum, can lead to induced trauma to the foetus (2, 3). Single-use integrated hand-pump VAD systems such as the Kiwi Omni Cup™ developed by Clinical Innovations Inc. (CI) have been dominating the VAD market for the past two decades but they have not shown significant improvement on delivery rate success in comparison to their predicates (4). Despite their growing prevalence, there has been a limited effort to evaluate the safety of VAD devices or attempts to optimise their design and operation.

Formed in 1994, Pelican Feminine Healthcare Group (PFH), part of the Eakin Healthcare Group, is a small-medium enterprise (SME) specialising in the manufacture of disposable medical products for the UK and Irish market, such as stoma care and general feminine healthcare. PFH acted as the exclusive distributor of the Kiwi Omni Cup™ in the UK until CI established its own distribution channels. Commercially, PFH identified that there was a marketing prospect to regain market coverage. Driven by this identified commercial need, PFH collaborated with the University of Leeds under a Medical Research Council industrial grant, to lead on informing novel, original and innovative research in the field in an effort to aid their aspiration of developing of a VAD device capable of improving clinical outcomes.

1.1 Research aim & Objectives

The research aim is to achieve an engineering understanding of the key design parameters of commercially available VAD devices and their impact on performance and trauma in order to inform the design of a less traumatic device. The research objectives are organized as follows:

- Objective 1 Perform a review of published literature to identify the clinical gaps of understanding in VAD device design

- Objective 2 Understand and characterise the mechanics of VAD device performance based on the most prevalent form of trauma during VAD: Cup Detachment

- Objective 3 Investigate VAD device design improvements to improve VAD performance

- Objective 4 Recommend engineering design inputs for an atraumatic VAD device and evaluate the feasibility of commercial translation and clinical implementation

1.2 Thesis Overview

The thesis spans 7 chapters which address the research objectives and then provide a general discussion and reflection of their potential to inform future opportunities in this field. A brief synopsis is presented below:

Chapter 2: Literature Review

This chapter provides an overview of the existing literature published on modern obstetrical practices related to Vacuum Assisted Delivery (VAD) since its original inception in 1968. The clinical use behind the operation of their medical use was understood and the design evolution of the VAD systems leading the current state

of art is discussed. The findings from this literature review revealed a paucity of engineering understanding behind the operational use of VAD devices and subjective evidence on how the device performance impacts the most prevalent form of trauma identified: cup detachment. This presented a real opportunity for driving forward research to achieve a better understanding of VAD operation from an engineering perspective.

Chapter 3: Development of a VAD simulator

The clinical outcomes identified in the literature overview showed that the most prevalent indication of trauma associated with VAD usage was cup detachment. A VAD simulator concept was conceived based on guidance from an experienced clinician to establish its core design requirements. This informed the basis for the design and development of a test measurement system to understand the dynamics of cup detachment.

Chapter 4: Design and Development of an Experimental Measurement System to detect Cup Detachment

This chapter looked at the development of an experimental VAD model to develop a comprehensive understanding of the mechanics behind VAD devices and any associated trauma. The tensile mechanical properties of different silicone-textile assembly formulations were benchmarked against scalp mechanical properties reported in the literature. The best formulation was then used in the fabrication of the head scalp model. The Kiwi Omnicup™ was used as a template for instrumentation of the VAD cup system. The control, sensing & data acquisition aspects were devised to control and provide sensory feedback on the vacuum inside the VAD cup. Optical markers, placed onto the scalp model, combined with a high-speed camera system provide tracking of scalp deformation during mechanical simulation of obstetric traction. The evaluation of the measurement system has shown that a simulated obstetric VAD traction produces a characteristic response from which a number of key clinically relevant metrics can be determined. Image analysis shows that loss of vacuum is strongly affected by the geometry and physical properties of the VAD device during its interaction with the scalp. Experiments will be devised from the proposed methodology to investigate clinical and mechanical factors related to device performance.

Chapter 5: Experimental Evaluation of VAD Systems

This chapter details the experimental approach taken to identify key influencing clinical and mechanical factors capable of affecting the propensity of cup detachment. The learnt outcomes from the experimental efforts lead to suggestion of engineering improvements to drive innovation in the form of an atraumatic VAD cup system concept in an effort to reduce VAD trauma by avoiding cup detachments. The technical and commercial feasibility of the concept based on the engineering suggestions will be evaluated with a view towards commercialisation in the form of a new product introduction (NPI) to the market in the following chapter.

Chapter 6: Translating research outcomes to the design of a commercial system

The concept of a portable atraumatic VAD device used in emergency child birth to assist delivery of babies that allows medical professionals to perform safer VAD delivery during difficult labour, was evaluated in this chapter. Unlike the passive vacuum assisted device from current competitors, the proposed innovation will reduce unintentional cup detachments. The costs to healthcare provision behind the occurrence of a VAD cup detachment was then calculated based on the clinical care path decisions associated with this undesired healthcare outcome. An IP analysis was performed to understand the patent landscape and a regulatory pathway then analysed to discuss future consideration for the device development process. This work was performed in collaboration with the industrial partner of this project.

Chapter 7: General discussion, Conclusion & Future works

The concluding chapter of this thesis gives a general discussion of the outputs and findings from the presented research. The research objectives were reviewed in context of the produced work and suggestions about future work for continuation of the proposed research to propose value creation in the form of more innovative atraumatic VAD devices.

Chapter 2

Literature Review

This chapter provides a resumé of literature published on modern obstetrical practices related to Vacuum Assisted Delivery (VAD). The clinical use behind the operation of their medical use is understood and the design evolution of the VAD systems leading the current state of art is discussed. The acquired knowledge is then used to provide suggestions of improvement in the field and the motivation behind the research aim of this thesis in an effort to create an atraumatic VAD device.

2.1 Vaginal Birth

Parturition (human Labour) can be regarded as the most exciting epilogue of life. After months of foetal development and maternal delivery anticipation, it represents the most unpredictable and complex stage where both mother and her child are at maximum risk. Maternal biological pathways are triggered to maintain the rhythmic coordination between the contraction of the corpus and the yielding (cervix effacement) of the uterine cervix to prepare the birth canal for foetal progression(5)

The process of normal delivery can be summarized in 7 discrete steps, also called the cardinal movements of birth: Engagement, Descent, Flexion, Internal Rotation, Extension, Restitution & external rotation and Expulsion. During the first stage of normal/classic labour (5-8 hours on average depending on parity), the foetus' head moves to its best presenting diameters to the maternal pelvis by rotating anteriorly and changing its shape from a nearly circular shape to an elliptical one due to changes in uterine pressure (6, 7). The foetus aligns itself to the bony pelvis and engages in a cephalic (vertex) presentation; accounting for nearly 95% of all births (Figure 2-1) (8, 9).

At this instant, the mother achieves full cervical dilation (opening up to 10-12cm) and full effacement (thinning of cervix to 100 %). She enters the second stage of labour (2-3 hours) in an effort to push down her new-born through the birth canal via series of expulsive contractions.

Hereafter, third stage of labour is reached once the baby is delivered with her placenta removed straight after. If normal vaginal delivery is not possible due to associated factors as shown in Table 2-1, the obstetric team have two main options; providing additional assistance to the mother through Instrumental Vaginal Delivery, or performing an emergency caesarean ('C-Section') (10, 11). However, the emergency C-Section is typically only used as a last resort (when instrumental delivery is not achievable or fails) because it risks significantly greater maternal morbidity (more blood loss and postnatal aftercare) (12) (13).

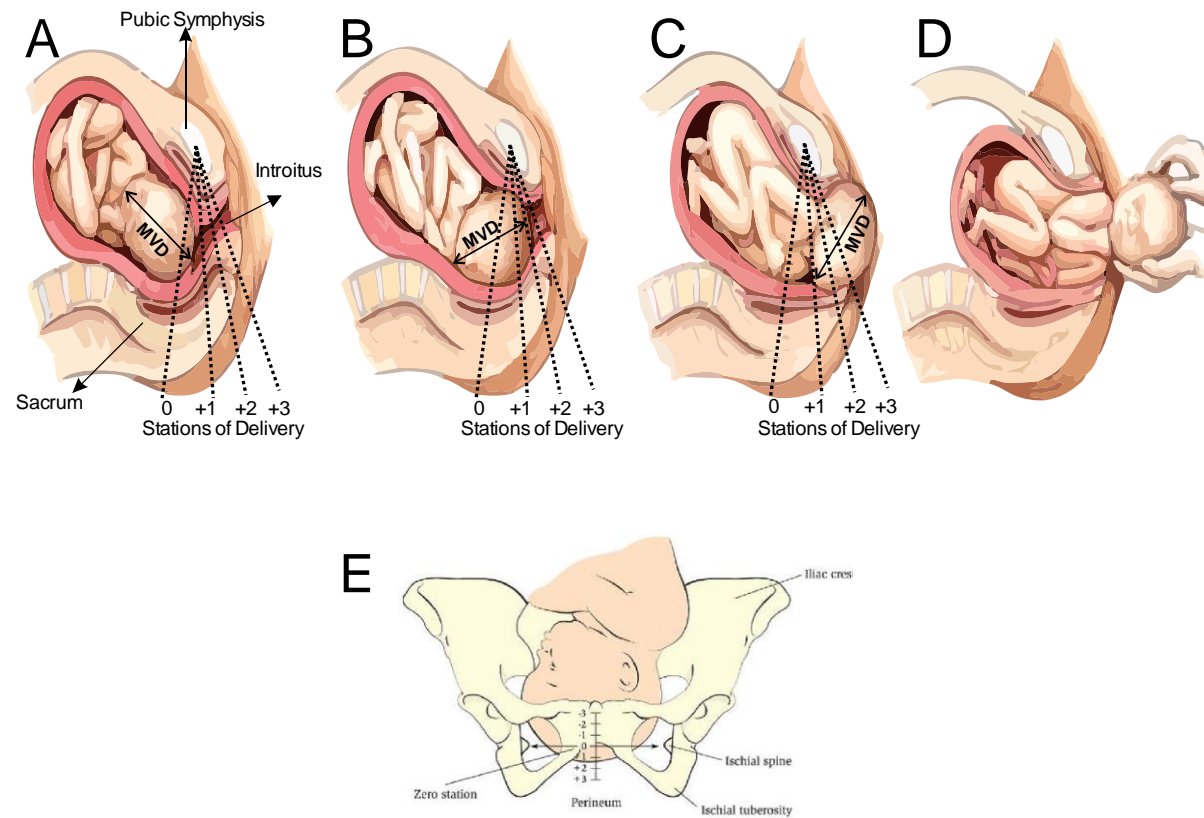


Figure 2-1: Timeline of normal delivery events. A: Fetus aligns to the bony maternal pelvis in a cephalic presentation(vertex/head first), B: Baby progressing through the stations of delivery, C:Baby's head scalp is visible at the introitus, D: Delivery of the baby is completed where the body delivers, either spontaneously or with the healthcare professional (accoucheur) holding the foetal head, sometimes to help delivery of the shoulders. This also marks completion of the second stage of labour(14). E: Front view of stations of delivery gauged with respect to the ischial spine (-3 to +3). Zero station is achieved when the head is aligned to the ischial spine. Each 1 cm increment from this reference constitutes of an increase of +1 delivery station(15).

Table 2-1 - Factors assessed at vaginal examination which could impact labour. Extracted and modified from (13, 21)

Term	Factors	Examples
Power	Reduction of expulsive force	<ul style="list-style-type: none"> • Insufficient cervical effacement and dilation • Abnormal volume of maternal amniotic fluid • Not ruptured maternal membrane
Passenger	Foetal Complication	<ul style="list-style-type: none"> • Unsuitable position: Breech or shoulder • Persistent malposition • Twin Pregnancy • Abnormality of foetal head (too big) • Entanglement with Umbilical Cord Presence of excess Caput, hydrocephalus asynclitism due to unfavourable positions & stations or excessive moulding
Passage	Maternal/Birth Canal complication	<ul style="list-style-type: none"> • Contraction or deformation of bony pelvis • Abnormality in pelvis (too small) • Tumours or infection • Scars from previous injuries • Presence of Oedema

2.2 Instrumental Vaginal Delivery

Instrumental Vaginal Delivery is a clinical means of providing additional mechanical assistance to the mother's contractions, providing both additional force and guidance to baby during the second stage of labour (when the mother's cervix is fully dilated and the baby's head has made contact with the bony pelvis). Instrumented delivery comprises two families of instruments: Obstetric Forceps and Vacuum Assisted Delivery (VAD) devices. Combined these have a reported usage in 12-15% of registered deliveries in the UK (11, 16) and approximately 5% in USA (17). Obstetric professionals are trained per professional body guidelines such as the USA & UK College of obstetricians (ACOG or RCOG) to identify the prerequisites for instrumental vaginal delivery (18). In addition, simulation based techniques such as mannequins or computational visualisation are used to complement or improve their proficiency (19, 20). Instrument selection is driven by the clinical training received to identify complicated birth scenarios (21). Other contributing factors are linked to the stations of delivery and orientation of the foetal head (anterior or posterior); VAD can be preferred over the forceps for low cavity (+3) as well as posterior mid-cavity (0 to +2) delivery but no clear preference for normal mid-cavity delivery (22). In countries with significant instrumental delivery rates (IDR>10%) as indicated in Table 2-2, lower caesarean delivery rates were observed (23). It is interesting to note that there exists a wide range of differing practices with regards to instrumental delivery and the selection of instruments is motivated by the training and decision making abilities of the healthcare professional (21, 24).

Table 2-2: Instrumental delivery rates in EU Countries(23)

Instrumental Delivery Rate (IDR)	Countries
IDR < 5%	Bulgaria, Czech, Estonia, Greece, Croatia, Italy, Cyprus, Latvia, Lithuania, Hungary, Malta, Poland, Portugal, Romania, Slovenia, Slovakia
5 % < IDR < 10% (Average: 7.64 %)	Belgium, Denmark, Germany, Netherlands, Austria, Finland, Sweden, Iceland

Instrumental Delivery Rate (IDR)	Countries
IDR>10% (Average: 12.5 %)	Ireland,Spain,France,Luxembourg,UK, Norway,Switzerland

In the UK, the decision to perform instrumental is associated and influenced by the desired outcomes of key stakeholders involved in the clinical care pathway. The latter includes the clinical operative staff responsible for performing VAD delivery (Obstetricians & Trained midwives), the community responsible for managing the pre-birth (midwives) & after-birth care (nurses), the mother & baby and the purchasing unit of the hospital trust (Table 2-3). In the event that a birth requires an assisted delivery, the clinician must review a number of prerequisites (often termed 'indications for use') before they proceed. The main prerequisites comprise of ensuring that the mother has an empty bladder and rectum (This is to ensure that there is more space for the baby's passage and ensuring less damage to those organs), that there is full cervical dilation and that the position of the baby's head is in the appropriate station of 0 to +5, as shown in Figure 2-1 (such that the baby's head is sufficiently exposed for VAD attachment or forceps contact) (25).

Table 2-3: shows the desired outcomes of the stakeholders identified during the identification of the clinical care pathway (26)

Desired Outcomes of Product	Stakeholders for Clinical Care Pathway in UK			
	Obstetricians/Senior Midwives	Nurses & Midwives (Community & Clinical)	Mother & Baby	NHS Supply Chain Purchasing/CCGs/Hospitals/Trusts
	Better Patient outcomes	Reduction of time in aftercare	<ul style="list-style-type: none"> • Aesthetically pleasing, reassuring design, • Non-invasive 	<ul style="list-style-type: none"> • Improve revenue stream • Increase productivity • Less number or less qualified staff required Reduce waiting lists • Reduce theatre time, re-admissions, complications, length of patient stay
	Easy to use and safe familiar device supplied with good training material	More focused on Patient's welfare.	Safe for baby and not uncomfortable during procedure	<ul style="list-style-type: none"> • A Cost-Effective Solution and popular solution with good supply chain. • Minimal product variability (One standard size), Minimal recycling
Help to shorten time to care	No additional processing i.e. sterilization or machine set up	No adverse consequences to future development of baby		

2.2.1 Obstetric Forceps

Modern obstetrical forceps, usually made of stainless steel, were first introduced in the 16th century to help assist troublesome child birth. Key design elements feature a curved blade, shaped to match the contours of the baby head and provide easy manoeuvrability through the birth canal. Forceps are available in a wide variety of designs to accommodate differing delivery needs, as shown in Figure 2-2. For example Simpson's forceps are widely used for outlet deliveries because they conform well to the baby's head, Keilland's forceps are used to assist rotational delivery due to their narrow profile. Closed blade systems like Simpson-Luikart forceps were designed to conform to the curve of the maternal pelvis (cephalic pelvic curve) (27-30). The use of the forceps requires extensive training but remains clinically challenging (31), with links to increased maternal morbidity (e.g. anal sphincter injury) and cosmetic damage to the baby's head (32). As a consequence, use of VAD devices has increased in the past decade, pursued as a less traumatic alternative to forceps (33).

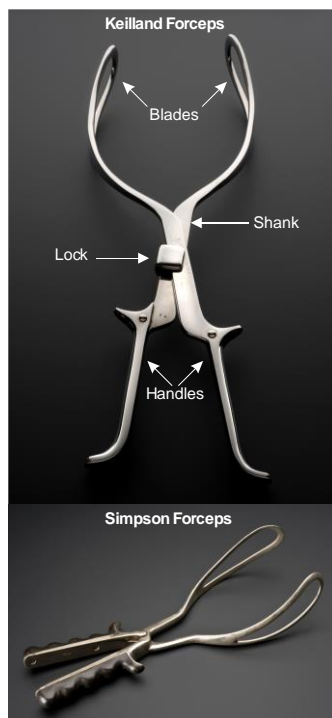


Figure 2-2: Examples of obstetric forceps. Top: Key design features of Keilland Forceps(34), Bottom: Illustration of Simpson Forceps(35)

2.2.2 VAD Systems

Vacuum Assisted delivery (VAD) was brought into widespread clinical use through the introduction of a system proposed by Malmström (36), aiming to impart assistive forces through a suction interface on the baby's head. In general the VAD consists of a suction cup which is placed on the flexion point of the scalp, a negative pressure is then applied (either via manual or electric pump) (Figure 2-3) such that the healthcare professional can assist by pulling the VAD handle in tandem with the mother's contractions (37).

Since the original VAD device from Malmström, there has been little evidence of innovation in device design or function. While this is not uncommon in surgical instrumentation it should be considered in the context of growing clinical evidence (emergence of developing countries and improved quality of care) that VAD systems could, and should, be improved for improved safety and efficiency.

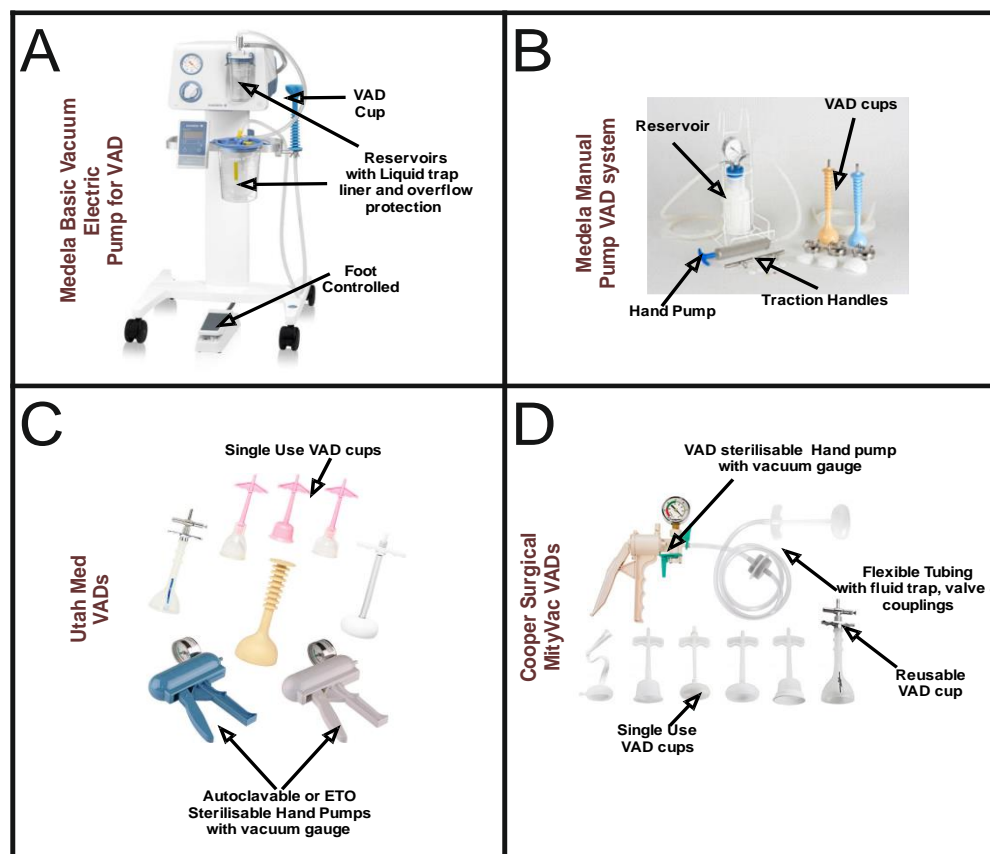


Figure 2-3: Modern adaptations of conventional VAD system and their design features. A: Medela Basic Electric pump for VAD use, B: Medela Manual Pump VAD system, C: Utah Med Ltd VAD system, D: Cooper Surgical MityVac VAD system

The first step is critical in which the clinician must identify the correct location for VAD attachment on the baby's scalp; the flexion point situated 30mm from the anterior fontanelle and 60mm from the posterior fontanelle in the direction of the sagittal suture, as shown in (Figure 2-5) (38). The VAD device is then manoeuvred through the delivery channel onto this point and a vacuum is applied to create a secure attachment with the scalp. This differential pressure with the atmosphere causes the first intermittent layers of the scalp to expand outwards from the aponeuric galea to fill inside the cup. The result is an elevated region of scalp filled with fluid, known as the caput succedaneum (or colloquially as a 'chignon' or 'localized oedema') which forms a mechanical scalp-device interface (39-41).

After a caput is formed and held, the VAD device can be employed by the clinician to assist the mother using the VAD handle during each maternal contraction. This process has two main aims; firstly to ensure correct orientation of the baby's head, secondly to assist descent (movement) through the birth canal. The clinician angles each pull to promote flexion of the baby's head, bringing the chin towards the chest and orientating the occipital end of the scalp toward the pelvis (42) (Figure 2-1). Full flexion is achieved when the 'Mento-Vertical Diameter (MVD, the vector between the chin and VAD flexion point) points towards the entrance to the birth canal (42, 43). The procedure typically lasts around 10 minutes over 2-3 pulls, each exerting a force up to 115N (44). This process achieves a success rate of over 80% when used with a commonly available VAD device (Kiwi OmniCup™) (44).

The position of the baby is constantly monitored by the clinician's other hand. In some cases a 'counter-traction' is applied, a force opposing the main direction of movement in order to maintain device position and orientation during traction. This technique is also reported to help the clinician gauge and regulate the tractive force, particularly during outlet deliveries when the foetal head must pass through a narrow (and thus restrictive) introitus (44, 45) (Figure 2-5).

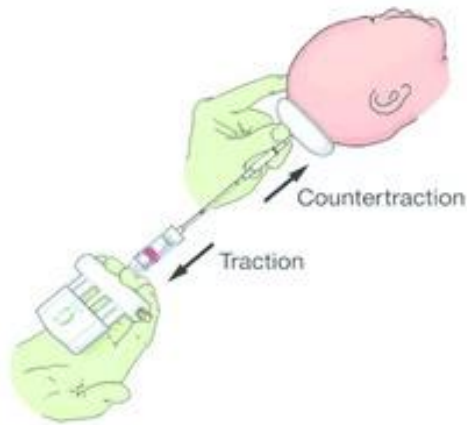


Figure 2-4: Two- handed traction technique with the Kiwi OmniCup(46, 47)

The VAD device is used until the emergence of the baby's head past the introitus, termed 'crowning'. At this point further assistance is typically not required since the baby's head represents the most significant resistance to movement during the birth process. Ending use of VAD consists of releasing the vacuum to prepare for crown delivery, where the clinician or midwife guides the final emergence of the baby. In some cases, a VAD is required to assist in rotational delivery which involves addressing a malposition of the baby's head. This follows the same basic procedure described above but with a redirection of traction along the axis of the maternal pelvis (37).

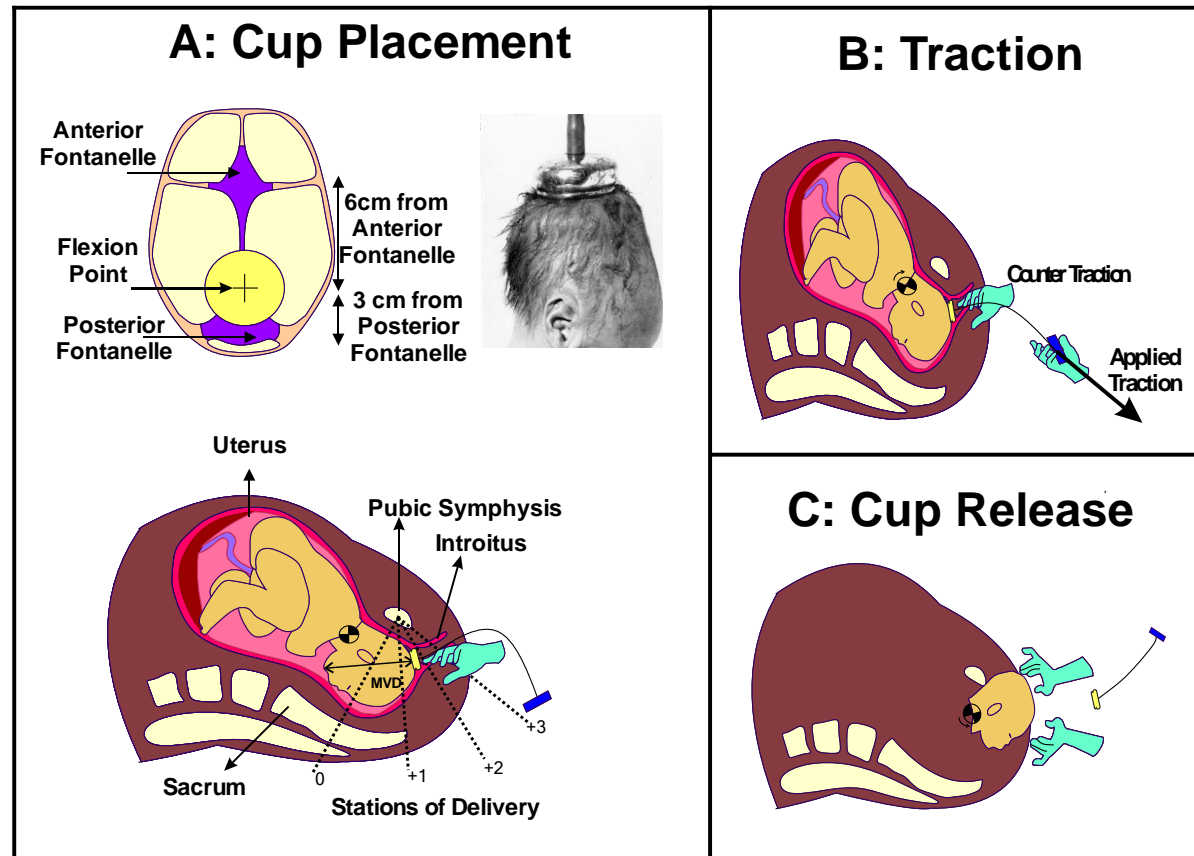


Figure 2-5: Process steps during VAD. A: Cup placement-A vacuum source is applied to create a chignon by manual/electric pumping after placement on the flexion point. On caption-Illustration of Malmstrom's cup placement on a foetal head (36), B: Traction- Applied traction with a counter traction used to overcome resistant introitus, C: Cup Release: VAD is released after the crowning of the head and clinician proceeds to crown delivery.

2.3 Interaction of VAD with Foetal head

In order to perform VAD, there needs to be first a continuous attachment of the cup effector onto the foetal head. The cup is first positioned by the healthcare professional over the flexion point (Figure 2-5) of the presenting part of the foetal head called suboccipitobregmatic diameter (SOB) located on the parietal region reported to be $11.54 \pm 0.62\text{cm}$ (N=319) (9) (Figure 2-6). The scalp is displaced by the suction to fill the resultant void inside the cup. The deformation experienced by the scalp is linked to its intrinsic mechanical properties. The thickness of the scalp of the parietal region of 1 month old baby was 3.5mm in median with a range of 1.9 to 9.1mm on the parietal region (48).

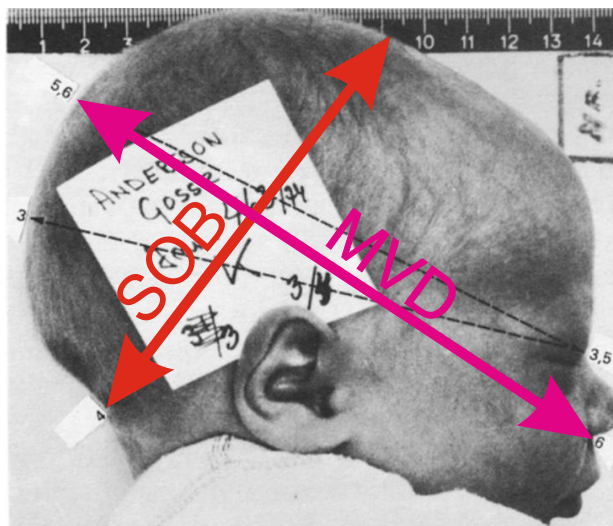


Figure 2-6: Diameter of circle represents the suboccipitobregmatic diameter (SOB). Picture courtesy of Sorbe et al. (38)

The compliance of scalp is dependent on the mobility of its constituent parts the skin, subcutaneous tissue, the galea aponeurotica, the subaponeurotic connective tissue over the fixed pericranium onto the cranium (49-52). Gel-like chemicals, glycosaminoglycans binding the skin to surrounding tissues and the fibrous structure of the collagen & elastin present in the skin dermis contributes to the non-linear viscoelastic properties of the scalp (53, 54). The toughness of scalp is characterised by the keratinised epidermis, collagen-rich and fibrous dermis and amorphous gel-like deep reticular layers of the dermis present on the skin (55). In the parietal region where the VAD cup is applied, the region is tighter when compared to other regions of the head due to the presence of a dense galeal layer (Figure 2-7).

Research behind the characterisation of mechanical properties of human foetal head scalp is understated due to the amount of studies produced in the area and the complex structure of the scalp. However, a recent study by Falland-Cheung et al. (55) conveyed information about the elastic modulus, tensile strength, strain at maximum load and strain to failure of different scalp regions of adult human heads (left temporal, frontal parietal, right temporal, occipital) (Table 2-4). The tests were performed against ISO 527-2 using pre conditioned tissue (8mmx4mm) at 20mm/min. Out of this data, it is important to note that the Young's modulus at the occipital end was 19.10 MPa (SD: 6.74 MPa) at a strain at the maximum force of 20.27% (SD: 4.79%) and the tensile strength was 2.75 MPa (SD: 0.96MPa) at a strain to failure of 29.35% (SD: 9.52%).

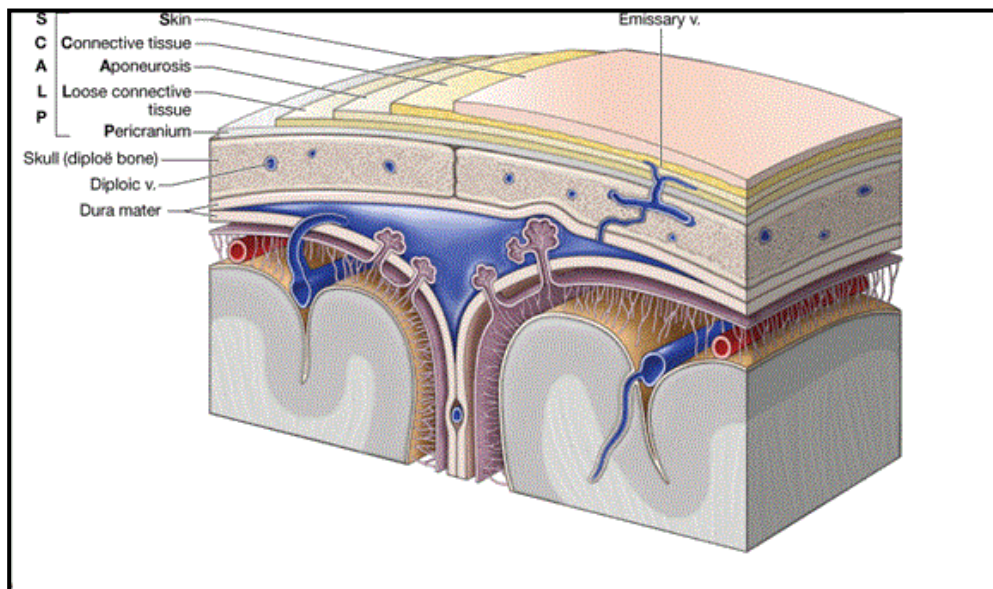
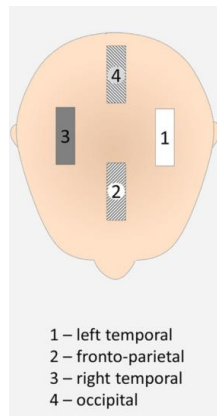


Figure 2-7 : Distinctive layers of the scalp present on the cranium: Skin & Dense connective tissue, Epicranial Aponeurosis, Loose areolar connective tissue & Pericranium onto the skull ((56)).

Table 2-4: Mechanical properties of tested scalps. Left: Tested regions of the scalp. Right: Table with reported values of mechanical properties of human scalp tested against ISO 527-2 (55)



Region	Elastic Moduli (MPa)	Tensile Strength (MPa)	Strain at Fmax (%)	Strain to failure (%)
Left temporal	24.3±	3.42±	19.09±	28.74±
	10.67	1.49	4.56	9.06
Fronto-Parietal	22.31±	3.11±	20.21±	30.45±
	9.31	1.28	5.26	10.4
Right Temporal	25.2±	3.61±	18.89±	27.11±
	9.1	1.52	4.04	7.35
Occipital	19.10±	2.75±	20.27±	29.35±
	6.74	0.96	4.79	9.52

2.4 Associated Trauma with VAD & Cup Detachment

Despite being an established instrument in labour wards across the world, there remain safety concerns behind the use of VAD devices. The chignon created by the vacuum action of the VAD device, shown in Figure 2-8, creates a striking visual impression of trauma, but in actuality it typically only persists for a few hours before dissipating, with associated cup-marks healing within one to four hours post partum (57).

The adverse events which cause more profound trauma to the baby are less common, but also less visually apparent, making detection challenging. The mechanical interaction between VAD device and scalp can result in damage to the underlying scalp anatomy to varying degrees (58). Subgaleal haematomas (SGH) occur in approximately 6 in 10, 000 VAD deliveries, when excess blood from the emissary veins accumulates beneath the epicranial aponeurosis (galea). This requires immediate attention as the blood can spread across the entire calvarial vault. If not diagnosed promptly, the resultant blood loss could lead to a life threatening hypovolemic shock (a 1 cm depth increase in subgaleal space could accommodate up to 260mL of blood (59-61), approaching the circulation volume of a 3kg baby (62-64). The occurrence of SGH is strongly linked to inappropriate cup placement in VAD(65). In the majority of SGH cases, the

leading edges of the cup were located too close to the anterior fontanelle (less than the recommended 30mm) (66) and even small errors in placement can lead to severe injury (67). High traction forces increases the propensity of unintentional cup detachments (often termed 'pop-offs')(68). Whilst the determination of safe traction levels remains highly subjective by obstetricians, there is a real need to investigate the impact of cup detachment (3). This is problematic firstly because an uncontrolled cup detachment can cause, or exacerbate, head trauma to the baby (as noted in Cephalohaematomas and SGH) but also because it can impose a profound change in the delivery plan. In the UK, after two or three pop-offs have occurred the delivery team must revert to an emergency caesarean section with significantly higher risks of morbidity and poorer outcomes for mother and baby alike (10, 11).

This creates a more prolonged second stage labour where the baby experiences more stress but can also lead to more maternal frustration, in an already delicate situation. Therefore, it is critical to evaluate the suitability of the VAD device and proceed to the right care decision whilst preventing unnecessary delay to the delivery of the baby.

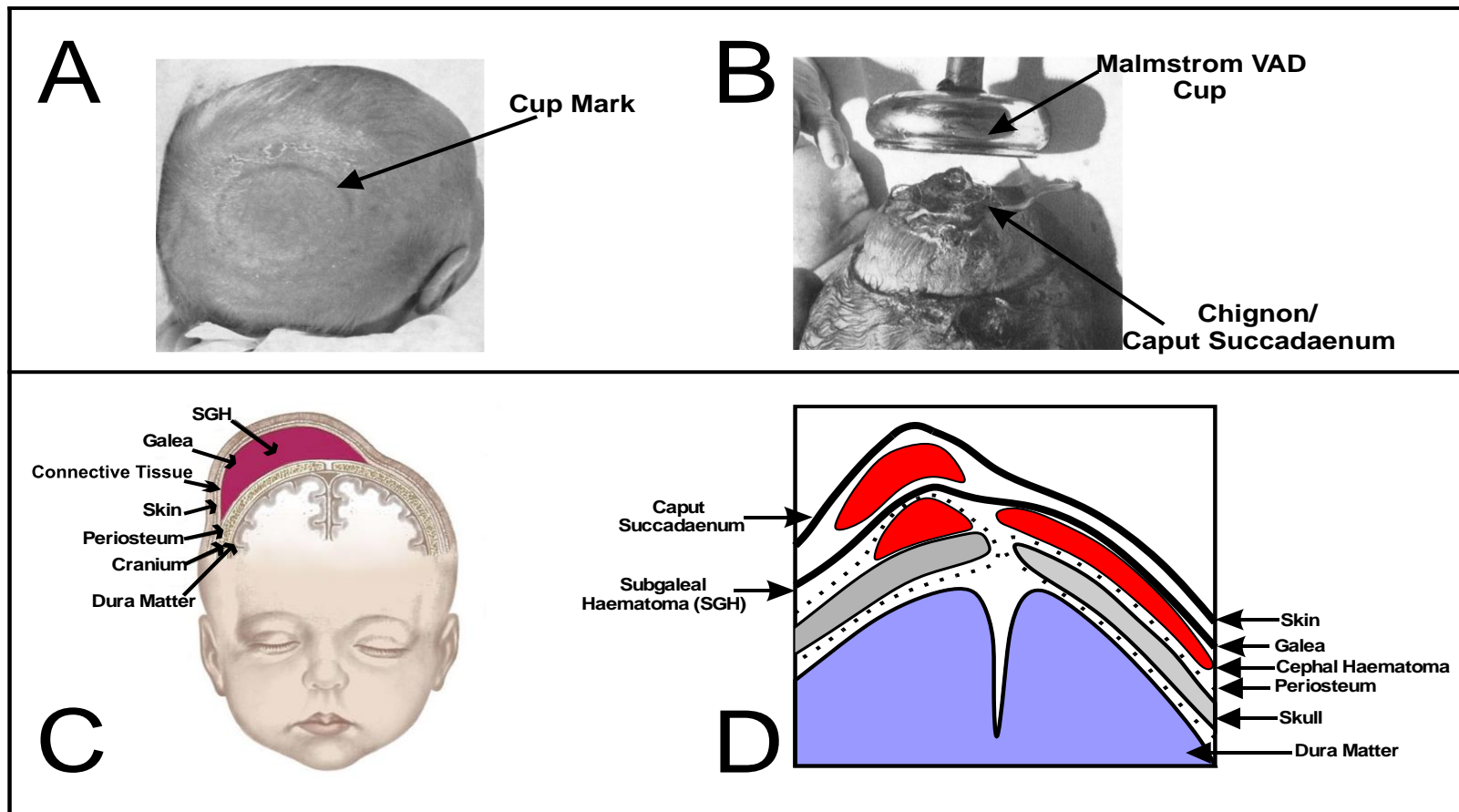


Figure 2-8 :Trauma associated with VAD. A:Elevation of scalp after VAD(36), B: Dissipation of caput succedaneum after a few hours leading to a cup mark (36) C: Baby head with SGH (56) D: All trauma levels associated with VAD

2.5 Design Evolution of VAD

Given the wide use of ventouse delivery for operative delivery it is instructive to consider how VAD device design, function and performance has evolved since their inception.

Although wide-scale use of VAD techniques has only occurred since the 1950's, the concept and early prototype systems have been in existence far longer. In 1848 Sir James Young Simpson, inventor of the Simpson's forceps also proposed their alternative; the 'Air Tractor' can be credited as the first VAD device, motivated in an effort to reduce maternal trauma (69). The device comprised of a brass syringe attached to a 3 inch diameter cup made of vulcanized rubber covering a metal insert. Entry to the cup was covered by a brass wire gauze where a piece of sponge or flannel was housed to inherently prevent obstruction of the vacuum inlet (70). The device wasn't widely adopted due to reported concerns behind its limited suction force leading to Simpson to concentrate on the commercialisation of his forceps invention. Despite not being popular in the UK, Simpson's work inspired others. In 1886 French inventor Soubhy Saleh produced a rubber cup connected to a separate vacuum pump while in the USA Stillman patented a VAD-like device in 1875 comprising of an oval cup with collapsible rings to facilitate entry, coupled to a traction handle (71). The 'Atmospheric Tractor' from McCahey followed in 1890 featuring a near-hemispherical rubber cup which was depressed, much like a plunger, onto the baby's head without an external vacuum pump (36). In 1912 Kuntzsch developed the "vakuumhelm" which employed a manometer to gauge the vacuum level inside an attachment cup. This was used in two successful trials on still-born infants but, like the devices preceding it, was not developed or used clinically (39).

It was only after several more decades and the introduction of the 'ventouse eutocique' device in 1947 that VAD devices achieved clinical recognition (72). This device consisted of a straight sided aluminium cup (diameter 40-65mm) and a braided pull cord for improved angular manipulation (73). Vacuum was generated in the cup using an electric pump which included a waste trap for amniotic fluid and blood (74). A similar approach was patented by Finderle in 1952, albeit with a horn-shaped cup, but despite a reported 221 successful cases the device was discontinued (75). However, it was the introduction of Malmström's VAD system in 1953 which brought more widespread clinical use and closely represents those systems used today(76). Malmström produced improved designs between 1957-1968 (36). The latter consisted of a vacuum cup

with a curved cross-section (diameter 33-60mm), designed to create a mechanical interlock with scalp tissue when a vacuum was applied through an external pump. Traction is controlled by metal chain and handle to the cup. While it represented a step-change in VAD device design, there were some limitations in performance: the metal cup caused scalp bruising and when posterior delivery was attempted, the device would fail due to leverage movement caused by the metal chain onto the suction tube (77). Stöstedt and Bird (74) addressed these problems through the design of a shallower profile cup for easier vaginal insertion and a neoprene or polypropylene mesh inlay for less traumatic scalp interaction. Bird also emphasised the need to place the cup over the flexion point in the median position to promote flexion toward the narrowest diameter of the foetal head. To facilitate this, he separated the suction and traction ports, moving the suction port to the side of the cup, enabling placement over the flexion point even in problematic positions(43). Bird's modification of the Malmstrom cup, coupled with the emphasis on correct placement over the flexion point, and his advice on the finger-thumb traction technique remain the basis of best practice in vacuum-assisted delivery. Further variations on this design were introduced by O'Neil et al. in 1987, replaced the chain attachment with a curved metal rod linked to the cup by a ball joint, intending to improve manipulation (78). However, across three studies (627 women) results showed there was no difference in maternal and neonatal outcome between these three variations on a metal cup design (1).

Driven by concerns that rigid metal cups could lead to scalp trauma on the infant, the 1970s saw the introduction of pliable cups made from elastomeric materials (57, 59). Kobayashi introduced a VAD system consisting of a hemi-ellipsoid Silastic™ cup with a 65mm opening and a central stem (see Figure 2-9). The compliance of the elastomeric material allowed it to be folded to ease insertion with minimal maternal trauma (77). Other VAD devices, such as the Menox Silc™ cup and the Mityvac™ cup, employed similar approaches and used elastomers to provide a 'soft' inner cup which helped to enhance contact area between scalp and cup. Obstetricians using these devices reported well-controlled delivery with minimal trauma (79). However they also showed significant limitations because they could only be used to assist outlet delivery stations (+3 or +5, see Figure 2-1) and were not advised for deliveries requiring rotation of the baby's head due to their compliant nature inhibiting the application of torque.

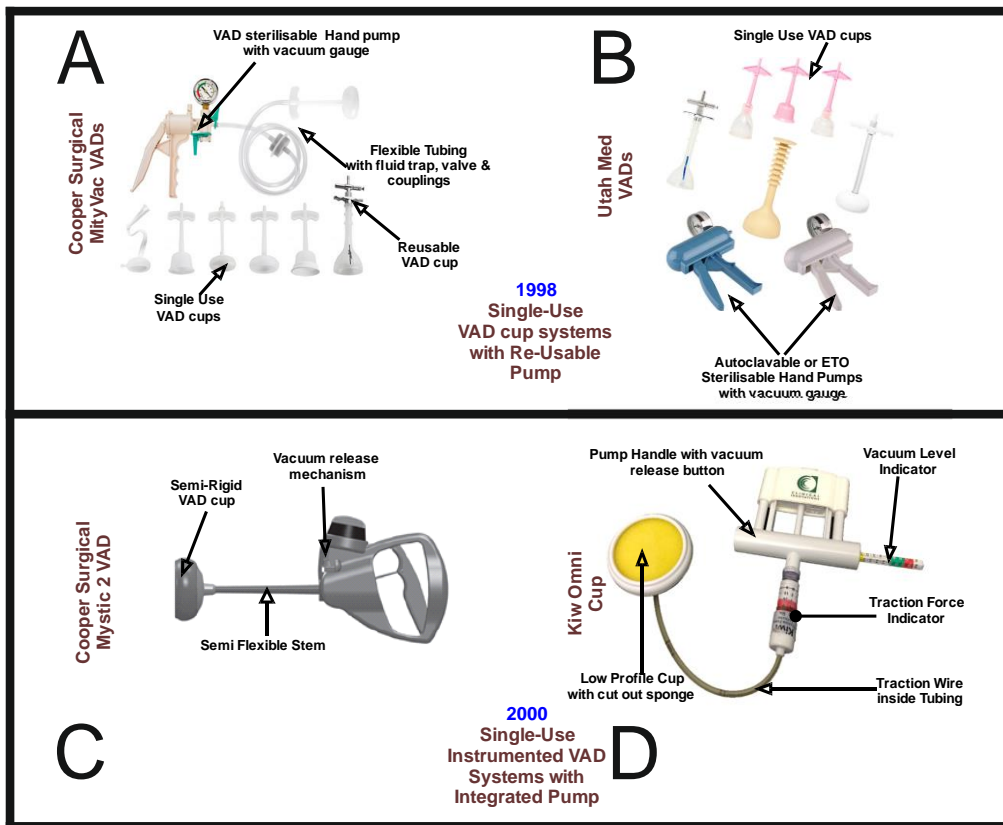


Figure 2-9: Single Use VAD Systems. A & B: Examples of Single Use Instrumented devices with a reusable pump. C: Cooper Surgical Mystic 2 VAD system, D: Clinical Innovation Kiwi Omni Cup

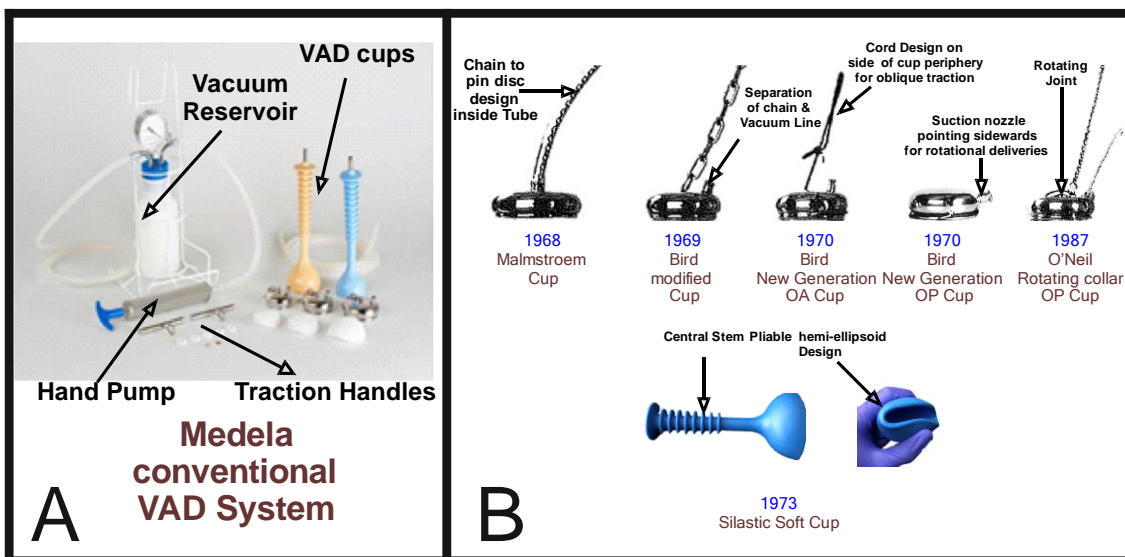


Figure 2-10: Evolutionary trail of modern VAD devices. A: Medela conventional cup system (80), B: Description of the features of the VAD cups in panel A.

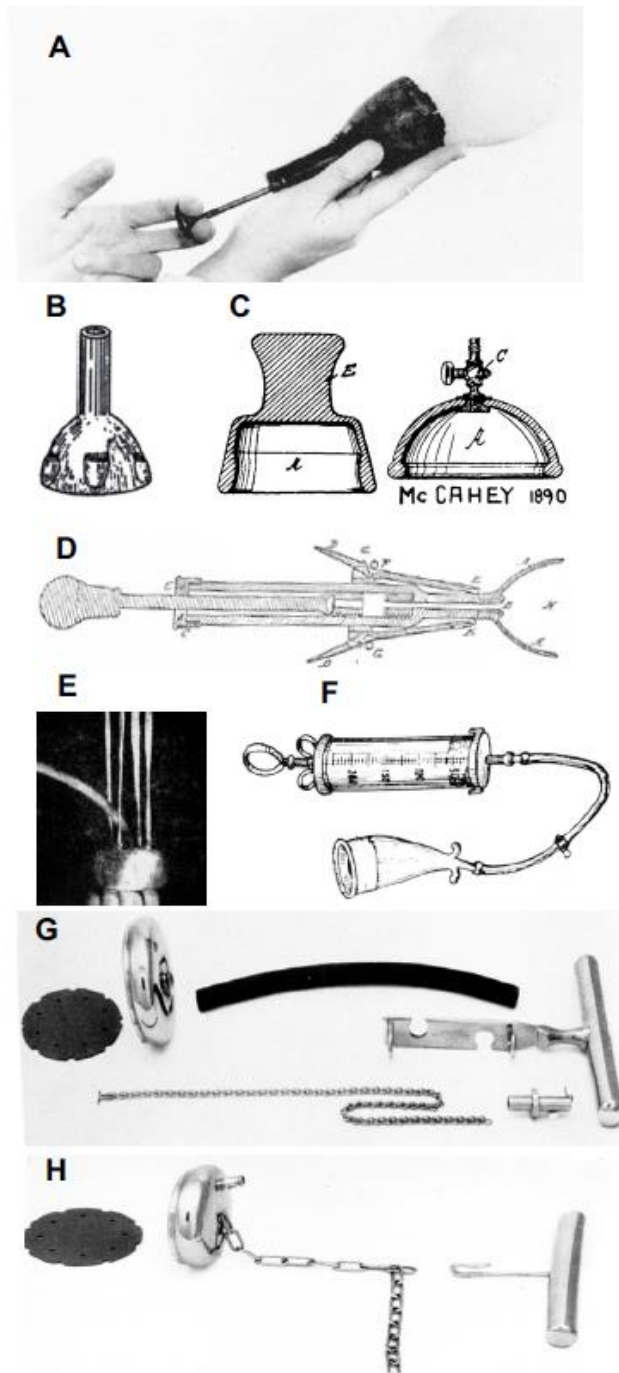


Figure 2-11: Evolutionary track of VAD device design A:James Young Simpson's 'Air Tractor'(81), B:Saleh's rubber cup with finger grips(71), C: McCahey's designs, D:Stillman's design(71), E: Couzigou's ventouse eutocique(81), F:Finderle's horn VAD device(81), G: Malmstrom's VAD device proposed in 1968(81), H: Bird's modified VAD device proposed in 1969(81) .

The last major innovation to VAD systems came during the 1990s, catalysed by moves to reduce transmissible infection through single-use instrumentation. In response, two single use VADs, complete with integrated hand-pumps entered the market; the MityOne™ (also known as the Mystic II) by Cooper Surgical Ltd and the Kiwi Omni Cup by Clinical Innovations Inc. The MityOne™ has two models with different cup designs, the M-Style (mushroom-shaped cross-section) cup is a clear polyethylene cup with a flexible coupling to account for bending during delivery and the MitySoft™ which features a more rigid shaft but a larger softer cup suited for low-station delivery (82). The Kiwi Omni cup was developed at a similar time and comprises a low-profile rigid plastic cup accommodating an integrated suction tube connected to a manual hand-pump via a flexible wire. Like the 'air tractor', a sponge is placed inside the cup to avoid obstruction to the vacuum inlet. The handle also features indicators to display vacuum-level and traction level during use (83, 84). However despite the addition of instrumentation, the device has not shown significant improvement on delivery rate success in comparison to older cups (e.g. Malmström or Bird's cups) and actually presents higher rates of cup detachment (up to 30%)(84-86).

The evolution of VAD devices described here provides an insight into the motivations driving change and the relatively modest innovations which have occurred as a result. Key advances addressed easing cup insertion and handling inside the birth canal, reduction of device failure rate and the use of instrumentation to help regulate the procedure. However, much of this evidence is circumstantial and there is no direct literature on the assessment of VAD device design attributes of commercially available VAD devices. With the growing popularity of VAD, there is an urgent need to evaluate the performance of design attributes of VAD devices especially when little is known on how these factors contribute to maternal/foetal trauma during operational device failure.

2.6 VAD Mechanics behind Cup Detachment

Understanding the mechanics of VAD use is central to inform improvements in both device design and clinical utility. However, much like the limited evidence available to explain VAD device evolution, there is a paucity of literature on how these systems behave during their interaction with the scalp of a baby and how device performance could be quantified.

The most expansive research in this area was conducted by Malmström to inform development of his VAD system in the 1960s. Studies focused on optimising the maximum traction forces the VAD can exert until cup detachment (pop-off). A rubber ball was used to simulate the scalp of the baby to which a VAD was attached and loaded using fixed weights. The study investigated the effect of applying different levels of vacuum (30-80kPa) across a range of cup diameters (40-60mm), as shown in Figure 2-12 (36). The results are intuitive, showing increased levels of maximum tractions as a function of increasing vacuum and cup diameter.

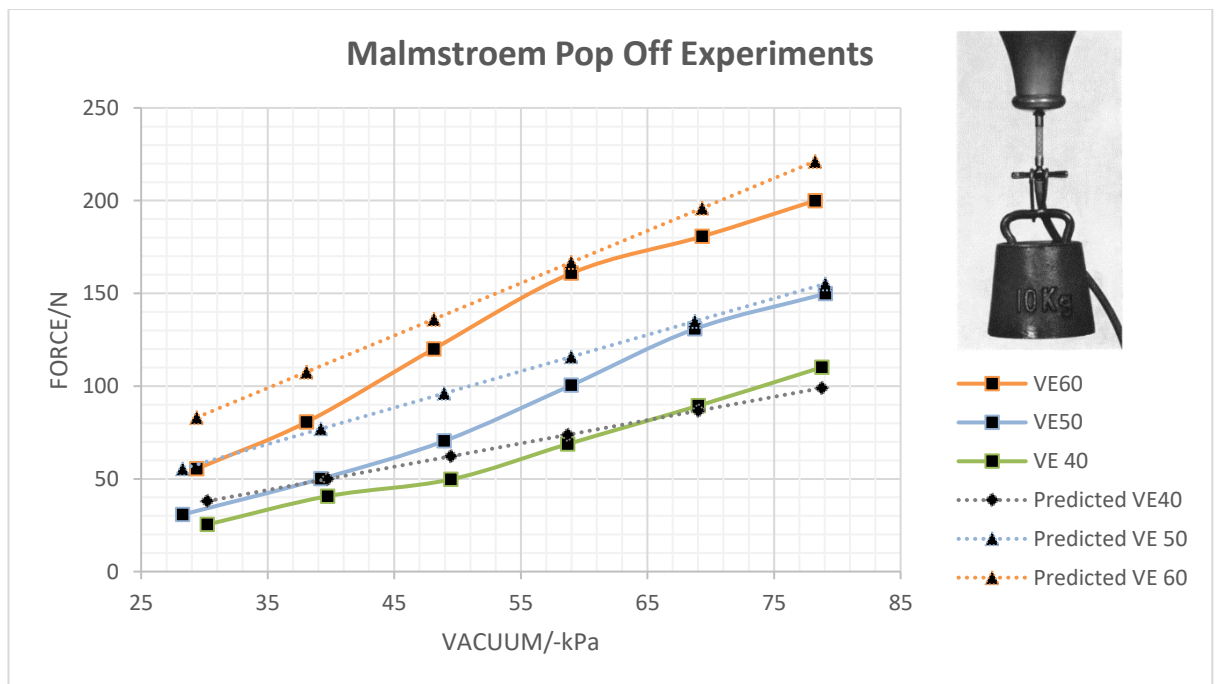


Figure 2-12: Replotted Traction Experiments by Malmstrom (27) VE60:60mm diameter cup, VE50:50mm diameter cup, VE40: 40mm diameter cup. Predicted curves displays Force values (calculated by the multiplication of the Vacuum Induced by the contact cross-sectional area of cup onto scalp).

Based on these experiments and his personal experience, Malmström recommended that his VAD system would be safe and clinically effective if the vacuum is achieved at a rate of -20kPa/min up to a maximum of -80kPa (87). The rationale was that this would allow the soft tissue layers of the scalp to conform inside the hemispherical suction cup, thereby creating a chignon (Figure 2-13). However, Svenningsen challenged this approach, proposing that the vacuum be rapidly applied to -80kPa as a time saving measure. This was supported by a study (n=60) which showed no difference in VAD traction forces compared to a slower vacuum rate, although consideration of how this may result in tissue trauma was not detailed (88).

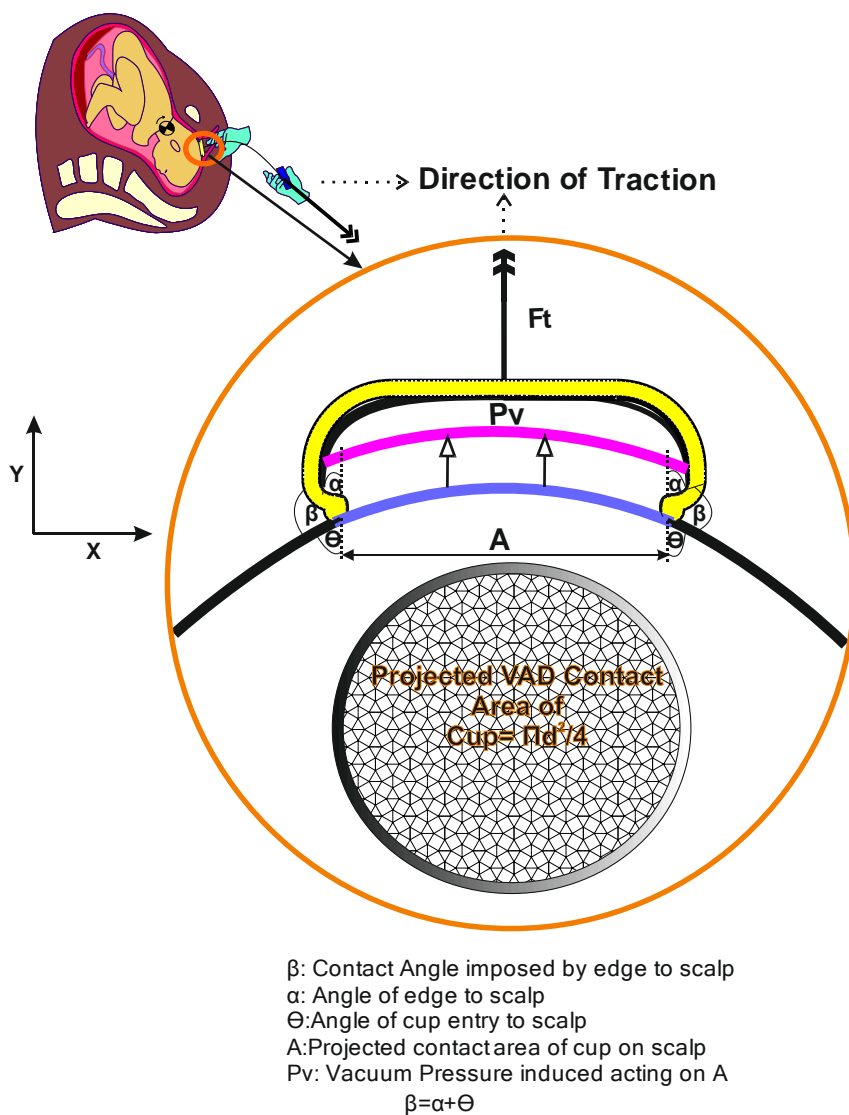


Figure 2-13: Attachment of cup onto flexion point and creation of chignon and overview of the contact angles of scalp present at the entry of VAD cup system.

Litigation related to malpractice in VAD has catalysed research into improved safety and clinical outcome, which have typically been associated with the characteristics of applied traction (89). Vacca reported that a traction force of 115N would be sufficient for successful delivery in 80% of cases but that the traction should not exceed 135N as this would significantly increase the risk of maternal sphincter damage and scalp injury to the baby (39). This is supported by an investigation by Saling into the traction forces recorded during clinical use of the Malmström device (60mm Malmström Cup) which reported a maximum force of 125N for successful delivery. This revealed that neonatal birthweight and progression of delivery (i.e. the station) has a causative link with the tractive force required. Revealingly it also highlighted a need to investigate the effect of applied traction on foetal morbidity (e.g. traumatic lesions and foetal head compressions) (90, 91). Building on this work, Muise et al. investigated the effect of applying angular traction using a range of modern VAD devices. These experiments used a scalp model (*ex vivo* canine hind quarters) and found that the application of angled traction resulted in a linear reduction in the safe maximal tractive force which could be applied (92-94).

With the growing popularity of VAD over the forceps to assist vaginal delivery in the past decade, VAD is associated with less morbidity to the mother(95). However, the latter may be associated with more serious complications in the newborn (65, 96). Incorrect cup placement can intensify unintentional cup detachments(95). Bestgen et al. recreated experimentally cup detachments on porcine belly (97). This work introduced the concept of defining a maximum traction force to avoid both scalp trauma and cup detachment, now seen in instrumented VAD systems like the Kiwi OmniCup™(44). However, definition of what constitutes a safe level of traction force remains subjective and strongly dependent on device type (68). Accordingly, these must be informed by a more rigorous evidence-base, in particular on the biomechanics of VAD systems and how these relate to device performance and clinical outcomes.

2.7 Literature Summary

Since its introduction, VAD has established itself as a vital tool in the limited array of choices available to clinicians when complications occur in vaginal delivery. The underlying approach, to create a negative pressure against the baby's exposed scalp which can support the application of assistive force, is well-suited to the clinical workflow and has remained fundamentally unchanged through the history of VAD systems. Nevertheless, VAD technology has evolved over time with key drivers being increased safety (e.g. use of softer materials for the cup), ease of use (e.g. lower profile cups to facilitate placement) and prevention of adverse events (e.g. repositioning cables for rotational delivery). Latterly there has also been the introduction of single-use systems and a focus on feedback mechanisms to inform best practice (e.g. alarms to alert the clinician to loss of suction (98-100) and force sensors to detect the level of traction (3, 101).

It is questionable if these features and development are clinically valuable, or rather serve to provide product differentiation in a highly competitive and risk-averse commercial market. This perhaps best explains the incremental nature of innovation in VAD systems to date where it is difficult to obtain the engineering knowledge necessary to inform and justify more radical design changes and the potentially expensive regulatory approval they would incur. Nevertheless, the clinical evidence-base provides a strong argument that more significant innovation is required to make VAD systems safer and easier to use.

2.8 Conclusion

The ease of use and lower maternal morbidity associated VAD devices can make them an appealing delivery option. However, to further improve these devices to improve factors ranging from clinical usability through to maternal and foetal morbidity, requires a better understanding of the mechanical interaction between the VAD and the foetal scalp.

Since mainstream adoption in 1968 design changes have been reported, motivated by usability enhancement for easier clinical use inside the birth canal, the desire to reduce device failure rates during rotational delivery and gauging of vacuum/force feedback during traction. However, there exists a paucity of engineering understanding behind operational use of VAD devices. There is minimal evidence to inform VAD device design or clinical use and with the growing popularity of VAD, there is an urgent need to evaluate the performance of these medical devices.

This presents a real opportunity for driving research in achieving a better understanding of VAD operation from an engineering perspective. Supported evidence to quantify physical parameters such as safe tractive forces as well prevention of unintentional cup detachments could influence VAD best practice and perhaps provide insight on how future devices can be engineered to make VAD less traumatic.

Chapter 3

Development of a VAD simulator

This chapter formulates the research motivation in improving clinical outcomes associated with VAD use from an engineering perspective. A VAD simulator concept inspired by observation of the clinical requirements of VAD use will be introduced. The design requirements of model features of the VAD simulator will be established to account for simulation aspects of clinical and mechanical factors capable of influencing the dynamics of an identified trauma associated with the performance of VAD delivery: Cup detachment. The detailed design and development of the VAD simulator to investigate the failure dynamics associated with this trauma mode, will then be further discussed in the following chapter.

3.1 Research Motivation

Poor clinical judgement leading to the wrong VAD device selection and incorrect VAD usage have been shown to intensify cup detachment (102). This can lead to profound changes in the delivery plan leading to complicated clinical outcomes for the mother and her baby in the event of an unsuccessful VAD.

Training workshops with VAD simulators have been formulated to improve & reaffirm the technical competence of obstetric trainees in performing instrumental delivery (103). However, they do not provide a quantitative understanding of important clinical factors leading to cup detachment such as insufficient vacuum application, high axial/side forces or wrong vector of pull due to oblique traction or incorrect cup placement. Providing an evidence based understanding on the impact of such factors during VAD can help supplement the training of the clinical professionals; thereby inform best practice in the field and introduce best control measures to ensure safer VAD.

Whilst the cup-scalp interface is poorly understood but fundamental to device performance (ability to apply traction) and clinical outcome (i.e. scalp trauma), the mechanics of the cup-scalp interlock requires much improved definition, in particular how it correlates to clinical & mechanical factors associated with the design of VAD cup systems and their respective pneumatic architecture. Understanding the dynamics of chignon formation would allow investigation into how the vacuum should be applied (rate and magnitude) and how it should be maintained over time. Interlinked with these factors are the mechanical properties of the cup which will dictate the relative level of scalp and cup deformation (and thus stress at the interface) during use. These properties have been explored (through metal, plastic and elastomeric cup designs) but without rigorous quantification of the resultant performance. Furthermore, the mechanics at the skin-cup interface should not be neglected; the surface tribology will determine how the scalp moves relative to the cup during chignon formation and pop-off, while localised mechanical properties will dictate how the cup surface accommodates the presence of hair or caput (leading to potential pressure loss).

Another area of impact is the application of tractive effort and how the characteristics of this relate to device performance. Although this is partially governed by the needs of the mother and baby, it remains uncertain how the magnitude, rate and direction of traction relate to device performance and outcome. Clinicians currently acknowledge that the force during VAD is transferred to the scalp; producing a compressive force on the skull and forming a compound structure resembling a "sliding bag" (104). Clinical experience

provides intuition behind the end use of the device. However the current field of research necessitates much detailed engineering explanation of how the device operating procedures impact the trauma level linked with VAD end use. Upon achievement of a thorough understanding of the influence of mechanical & clinical factors, innovations to improve safety, such as instrumented VAD systems which can guide the user to maximise device performance, minimise potential device failures and improve maternal outcomes.

In this chapter, the design requirements of a physical experimental test set up will be addressed to inform on the biomechanics of VAD device design interaction during the dynamic simulation of an over traction the most concerning adverse event of VAD delivery: Cup detachment.

3.2 Clinical Simulation Requirements

Since the current research field surrounding the discussion of VAD devices still remains clinically driven, it was critical to outline an approach to define design and simulation requirements for the VAD simulator with an experienced clinical user of VAD cup system.

Dr John Anderson, Consultant Obstetrician & Gynaecologist, Bradford Teaching Hospitals NHS Trust, assisted the research team with his clinical expertise around VAD. Dr Anderson, performed a VAD demonstration with a CI Kiwi OmniCup™ on an instrumental delivery birth simulator (MODEL-med® Lucy and Lucy's Mum) (Figure 3-1). The training session provided an appreciation of the technical procedural steps in achieving VAD and helped in the definition of the essential simulation requirements of the VAD simulator concept discussed in the next section.

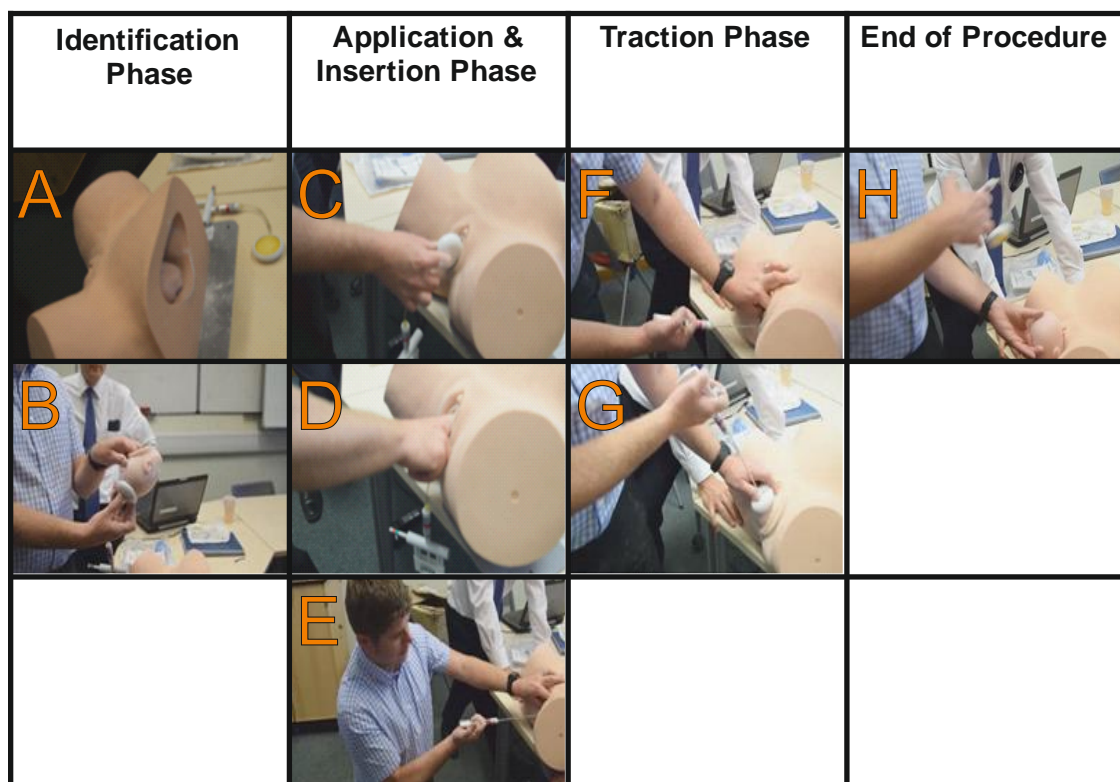


Figure 3-1: Key VAD procedural steps demonstrated by Dr John Anderson on a VAD Training Model. A&B: Identification phase, C,D&E: Application and Insertion phase of VAD, F&G: Traction Phase, H:End of VAD Procedure-Crowning and release of vacuum on foetal head.

The first step in VAD comprises of the identification of the flexion point on the foetal head. The health care professional uses his middle finger to estimate the insertion distance. After applying obstetric cream on the outside of the cup, the cup is then inserted immediately after a contraction onto the flexion point located on the presenting SOB diameter ($11.54 \pm 0.62\text{cm}$) during cephalic presentation of the baby's head (Figure 3-2). The cup positioning is performed by one hand operation with the thumb applying on the dome and two fingers resting on the rim. The second hand is then used to sweep any present maternal issue from the periphery of the cup to prevent entrapment. Upon satisfactory correct placement, the healthcare professional immediately creates a vacuum attachment by generating a negative pressure either by manual or electric pumping. The recommended safe level of vacuum magnitude on a Kiwi Omni Cup™ ranges in between 60-80kPa (46).

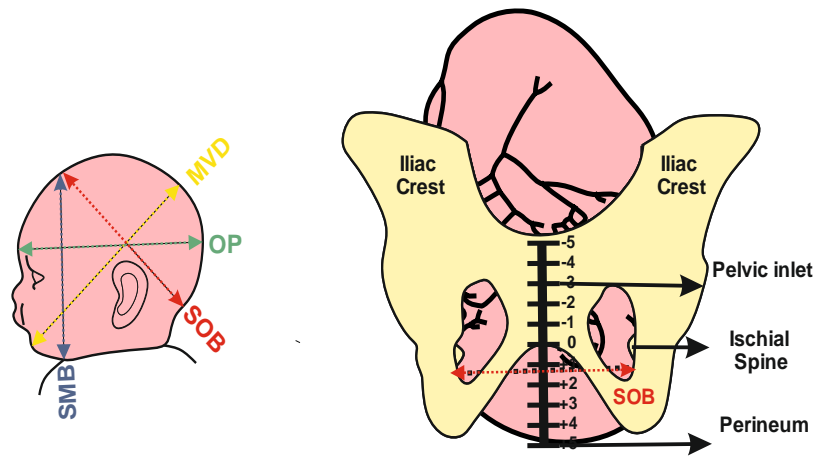


Figure 3-2 : A coronary view of the stations of delivery used to assess descent of the baby with the SOB shown as the major presenting diameter to be accounted for (Adapted from:(15) (9))

Once cup placement is achieved, the clinician adopts a kneeling position or sits on a low stool to perform the traction procedure. During the traction phase, traction is performed as a two-handed procedure with the pulling hand applying the tractive force and the other used to monitor the descent but also to apply a counter traction/counter pressure. This gesture complements the mother's pushing efforts or the involuntary uterine contractions to encourage flexion exposing the foetus to favourable presenting diameters necessary to achieve spontaneous delivery. For high to mid outlet foetal head positions (descent phase), a downward tractive force is applied along the axis of the pelvis in tandem with the maternal contraction. The procedure is continued until the foetal scalp becomes visible or reaches the pelvis outlet (perineal phase). The vector of tractive forces is then gradually changed upwards with the clinician adopting a standing position. The direction of pull has been shown to be most effective when it is applied perpendicular to the cup (93). At the end of the VAD procedure, baby's head is seen at the entry of the introitus and the operator presses on a valve and releases the imposed vacuum to complete birth.

Based on the comprehension of the clinical requirements presented above, an experimental concept will be introduced in the following section to establish the core simulation requirements required to be considered during a VAD simulation leading to a cup detachment. With an appropriately designed VAD simulator, the biomechanics of VAD device performance can be characterised to help advance understanding in this field of research and provide a foundation with which to improve our limited understanding of VAD biomechanics during cup detachment.

3.3 Design Requirements of a VAD simulator

This section will relate to the definition of design requirements of the VAD simulator to emulate the clinical interaction of an adapted instrumented version of the Kiwi® Omni Cup™ system (Figure 3-3) onto a representative foetal head exposed under controlled traction. Inspired by the clinical simulation requirements established above, the model features of the proposed concept will comprise of three main interfacing units as shown in Figure 3-4. Further design requirements of a representative foetal head scalp model will be discussed. The baseline instrumentation aspects of the adapted VAD device will focus on supply and control of safe coverage of vacuum levels as indicated by the graduations of the Kiwi Omni Cup system and design considerations to emulate the pumping architecture atypical of VAD devices. During VAD, Vacuum levels or magnitude is measured by the amount of air evacuated out of the VAD device either by manual or electric pumping and is measured in kPa or mmHg or psi. Cup geometry changes to the current cup design will also be accounted for to demonstrate the design intent of the recessed edges and its importance for scalp retention in the event of cup detachment. The vacuum levels inside the VAD device will be dynamically detected by a vacuum transducer. The motion of the device will be actuated by the actuator frame of uni-axial tensile testing machine to re-enact obstetric traction. A detailed summary of the key model features and design specifications of the VAD simulator can be viewed in Table 3-1.

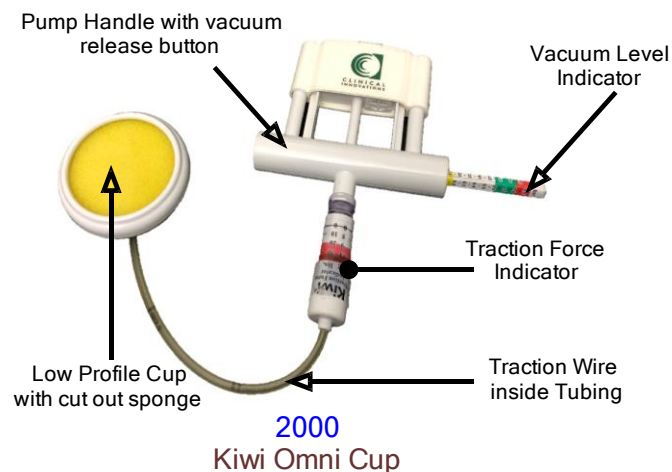


Figure 3-3: Kiwi Omni Cup™ MTE (with traction indicator)

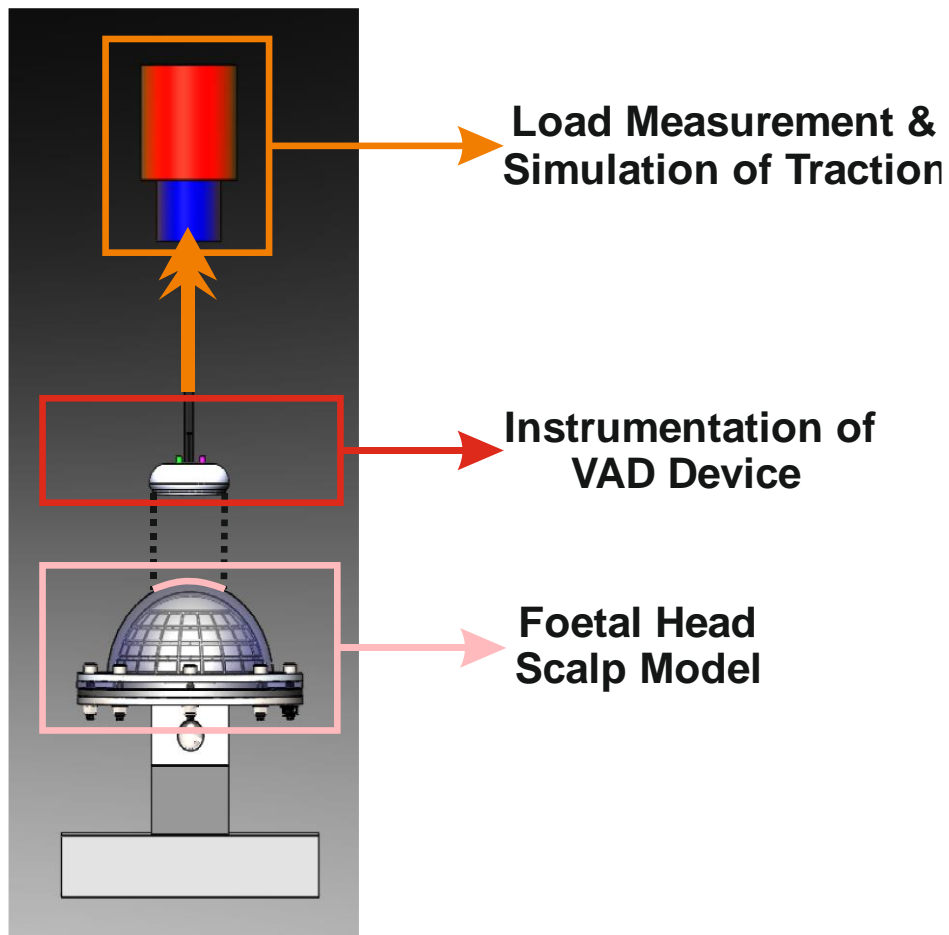


Figure 3-4: Design concept of VAD Simulator with model features highlighted to simulate the clinical use of VAD. An overview of phase development of the process of development of this concept model can be seen from Appendix A2

Table 3-1: Summary of the model features, the simulation requirements and the system specifications of the VAD simulator

Model Features	Simulation Requirement	System specifications
Foetal Head Scalp Model & Frictional attributes of the maternal environment	<ul style="list-style-type: none"> • Replicate the cup placement of the VAD device onto the presenting SOB diameter of the baby’s head: (11.54 ±0.62cm) (9) • Utilise a head scalp surrogate exhibiting the similar mechanical characteristics as foetal head scalp with the capability of enduring repetitive straining during testing. • Simulate exposure to the aqueous environment of maternal fluid surrounding the baby’s head 	<ul style="list-style-type: none"> • An equivalent model of the foetal head scalp will need to be developed with a conformable material capable of being moulded onto a presenting diameter of 12cm. • The Scalp element will need to reflect the mechanical properties addressed in the literature review. • Different lubricants with viscosity <1.17cP applied onto soft scalp (105)
Load Measurement & Simulation of Traction	<ul style="list-style-type: none"> • Simulation of over traction with tractive forces up to 200N at over a range of speed of traction(106) 	<ul style="list-style-type: none"> • A Uni-axial tensile system with a capable load cell (200N) should be selected to measure the range forces to be simulated to achieve VAD delivery at cover a range of tractive speed (50 to 200 mmmin⁻¹)(90)

Model Features	Simulation Requirement	System specifications
<p>Vacuum Measurement inside Instrumented VAD Cup System</p>	<ul style="list-style-type: none"> Capable of measurement changes in vacuum inside VAD device during the simulation of a traction leading to a cup detachment. 	<ul style="list-style-type: none"> Transducer should be sensitive enough to detect the vacuum changes inside the cup of the VAD device. The system should be able to accurately detect the event of cup detachment.
<p>Vacuum Control and supply inside Instrumented VAD Cup System</p>	<ul style="list-style-type: none"> Control of Vacuum Supply using commercial pneumatic architecture within recommended ranges described by the device manufacturer 	<ul style="list-style-type: none"> Selection of pneumatic components to reflect commercial pumping architecture System should be able to deliver a vacuum of a range covering 60kPa-80kPa (39)
<p>Cup Geometry Changes to instrumented VAD Cup System</p>	<ul style="list-style-type: none"> Limit the coverage of the mechanical interlock by design of changes in the cup geometry of a VAD cup system. 	<ul style="list-style-type: none"> Design adaptations to Kiwi Omni Cup to reduce the effect of mechanical interlock.

3.4 Load Measurement & Simulation of Traction

Traction or tractive force is defined as the application of an axial force in line with the maternal pelvis to aid the presentation foetal head to favourable diameters biomechanically advantageous for spontaneous delivery. It is measured in Newton (N). During VAD, the traction is expected to be applied constantly over a maternal contraction is observed. By a steady traction, the foetal head progresses through stations of delivery through a defined speed of traction (tractive speed) measured in mmmin^{-1} (Figure 3-2)(Table 3-2).

Exertion of high axial tractive forces (overtraction) is known to increase the propensity of unintentional cup detachment. Based on graduation on the traction indicator of the Kiwi Omni Cup, high tractive forces range in between 90N to 140N. This implies that a suitable force measurement system will need to be selected to axially apply forces to cover that range but as well monitor the load during the simulation of an overtraction.

From Malmström experiments, the maximum retention forces ranged between 30N and 200N for the respective applied vacuum magnitude range of 30 and 80kPa (36). Calculations from Saling's traction experiments indicate that the average traction speed ranges between 40-80 mm/min (90) (Table 3-2). This can also be defined In the event of an overtraction leading to a cup detachment, it is expected that speed of traction would be slightly more elevated. As such, a commendable range of speed of traction simulation of 50 to 200 mmmin^{-1} would be suitable for investigation. Currently there are no clear definition of traction levels, qualitative terms are used during the procedure. Gentle traction is first encouraged during the first minute to allow for the chignon to equilibrate. Strong traction is then applied depending on the magnitude of the vacuum originally applied. Higher forces are generally expected during the perineal phase due to the narrowing of the birth canal at the pelvic floor and the presentation of the widest diameter of the foetal head.

Table 3-2: Calculations for the average speed of traction during VAD extracted from Saling’s Traction Experiments (91)

Station of Delivery from Perineum	Distance from Perineum (mm)	Number of Traction (Rounded to nearest)	Duration of applied Traction (min) (Rounded to)	Speed of Traction (mm/min)
Pelvic inlet (-3)	80	3	3	80
Ischial Spine (0)	50	3	2	75
Pelvic outlet (+3)	20	2	1	40

3.4.1 Instrumentation of VAD Device

The event of a cup detachment has been perceived to be too fast to allow for corrective obstetric device manoeuvres (77). This suggests that it is likely that to be able to capture the dynamics of cup detachment, the VAD simulator will need to feature a pneumatically controllable instrumented VAD device equipped with sensors responsive to fast changes to the applied vacuum.

The Kiwi Omni Cup™ MTE (with traction indicator) will be used as a template for evaluation due to its robustness as well as ability to be instrumented. This device consists of an integrated suction tube connected to a manual hand-pump via a flexible wire and tube (Figure 3-3). The handle also features indicators to display vacuum-level and amount of traction the VAD device experienced during an obstetric pull. The flexible wire (16.5cm) is coupled with 4mm vacuum tubing connected to the hand pump. The traction cord loops around an anchor point which also comprises of 2 inlet holes to aid suction flow. A soft spherical cut out sponge is glued on the anchor point to prevent obstruction to the inlet holes but also to distribute the vacuum evenly. It will be critical that the alignment of the wire to the cup is central during simulation of traction experiments. Appropriate fixtures would need to be designed to secure the attachment of the VAD device onto a load cell and then onto the frame of the tensile testing machine. Understanding the impact of the recessed edges contributing to the mechanical interlock will be an area which will need to be explored.

3.4.2 Foetal Head Scalp Model

As highlighted in Chapter 2, despite previous attempts in the use of physical scalp models made from rubber and a variety of ex vivo tissues, there has been no reflection on how accurately they represent the anatomy of a baby's head as well as the geometry and mechanical properties of the scalp during the application of vacuum and traction. Whilst, in-Silico simulation requires well defined biomechanical parameters and obtaining data from real cases is difficult and inherently limited in scope; there exists a need to develop improved VAD models. As such there is a need to develop a higher fidelity physical head scalp model to test and evaluate VAD devices in order to improve our limited understanding of VAD biomechanics as highlighted in Section 3.1.

Since the primary point of action of VAD happens on the foetal head, it is critical that the simulation comprises of an appropriate foetal head scalp model on which the mechanics of the cup interaction can be characterised. It can be a considerable challenge to model the complex compound structure of the scalp, a simplified approach would be to develop a scalp surrogate reflecting the non-linear viscoelastic mechanical properties reported in Section 2.3. In the occipital region, the Young's Modulus of the tested scalp was reported to be 19.10 MPa (SD: 6.74 MPa) at a strain at the maximum force of 20.27% (SD: 4.79%) and the tensile strength was 2.75 MPa (SD: 0.96MPa) at a strain to failure of 29.35% (SD: 9.52%) (Table 2-4). The surface tribology can impact the relative motion of the scalp inside cup during chignon formation and cup detachment whereby localised mechanical properties can dictate how well the cup surface can accommodate the scalp. The simulation should also account for the aqueous maternal environment such as the amniotic environment with reported viscosity (water-like) of less than 1.17 Cp (105).

3.5 Chapter Summary

From the previous chapter, the clinical outcomes behind from the most prevalent indication of trauma associate with VAD usage: Cup Detachment, have been translated to form an engineering perspective on the scale of future innovation in VAD device design. This led to the conception of a VAD simulator and the definition of its system requirements to simulate clinically relevant operating procedures of VAD. This will form the basis of the design and development of a test measurement system presented in the next chapter to understand the dynamics of a cup detachment.

Chapter 4

Design and Development of an Experimental Measurement System to detect Cup Detachment

This chapter presents the development of an instrumented experimental re-enactment of VAD to achieve a comprehensive understanding of the mechanics of VAD devices and the associated trauma: Cup Detachment. It features the development of a representative head-scalp model on which a commercially available, instrumented VAD device (the Kiwi® Omnicup™) interfaces to simulate an obstetric traction. Upon creation of a measurement system alongside defined experimental methodology, an insight into the dynamics of a cup detachment will be provided.

4.1 Introduction

Following the design specifications of a VAD simulator presented in the previous chapter, the design and development of a configurable pneumatic experimental set up to control and sense the vacuum magnitude inside an instrumented Kiwi Omni during the simulation of an obstetric traction on a uni-axial testing machine (Instron E10000), will be presented in this chapter.

First, since there was no account of a reliable head scalp model presented in literature, a representative simple model of the foetal head scalp replicating the clinical situation upon which VAD needed to be developed. Considering that the clinical performance of a VAD device relies on the deformation of scalp inside the cup contributing to the chignon, a suitable scalp surrogate had to be developed to meet the design specifications. Based on initial developments, the learning from past creations will be used to consolidate the approach to develop a robust head scalp model. The mechanical performance of various fabricated silicone-textile composite formulations will be evaluated against those requirements for integration into the final assembly of the foetal-head scalp model. A quantifiable approach using engineering metrics of securing the capture of the dynamics of a cup detachment with the VAD simulator will then be proposed. This will consist of development robust experimental methodology behind the dynamic in-vitro simulation of an overtraction to understand the chain of events leading to a cup detachment. The obstetric traction will be emulated and sensed by the frame and load cell on a uni-axial tensile tester respectively. Local deformations on the scalp simulant arising due to VAD will be observed through the displacement of placed pin markers onto the developed foetal head scalp by high speed imagery whilst data acquisition of physical parameters such as vacuum level inside the instrumented VAD cup, load experienced during traction will be provided by a Data Acquisition and Control Unit (DAQ). The latter will also be utilised to synchronise the activation of the high-speed camera to record the motion of the pin markers ensuring a real-time observation of the dynamics of cup detachment. A schematic of the interacting components and their association to the relevant sections can be seen from Figure 4-1.

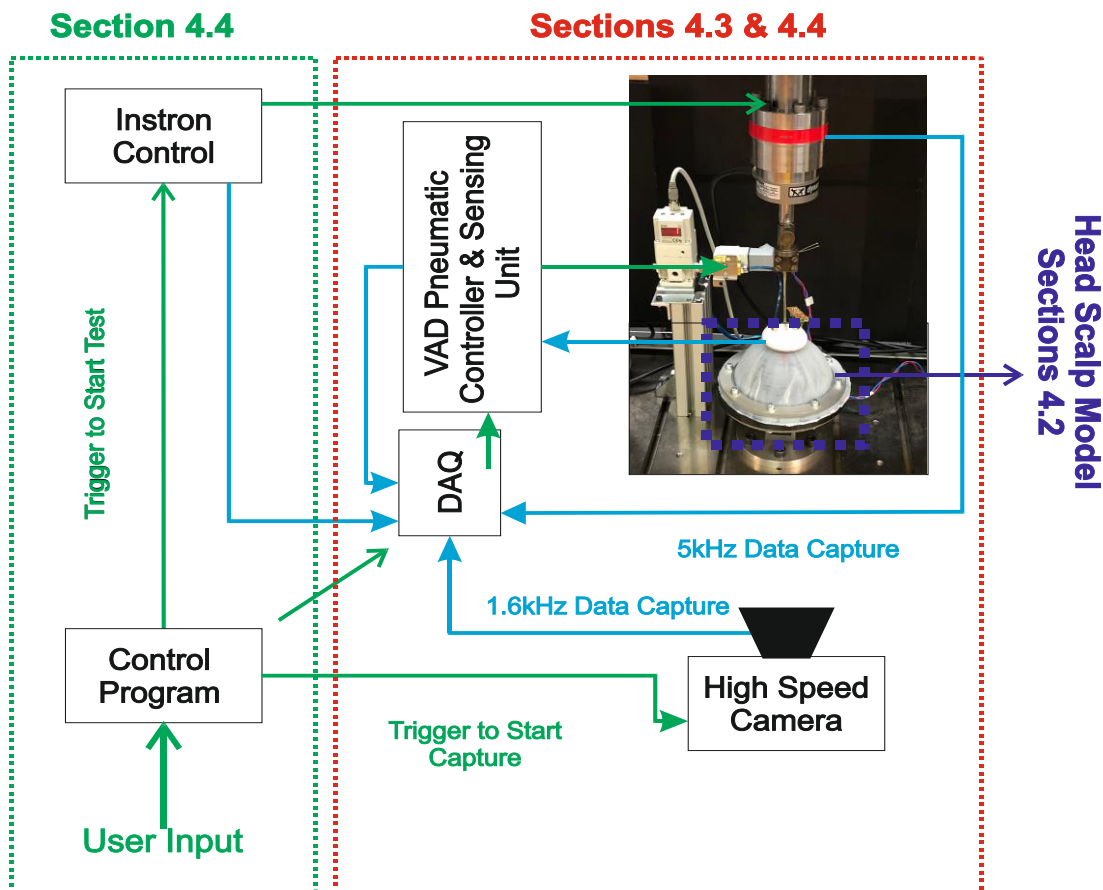


Figure 4-1: Control schematics of interaction of different developed instrumented units of the in-vitro simulation of VAD set up to capture the dynamics of cup detachment on a developed VAD simulator

4.2 Development of a Foetal Head Scalp Model

This section will present the work behind the development of a foetal head scalp model against the design specifications addressed in the previous chapter (Figure 4-2). Skin substitutes made out of soft elastomeric material have been extensively used during design verification processes of consumer products such as electric shavers to complex drug delivery medical systems (107). Such materials exhibit great resistance to stress/impact due to their reactive ability to absorb energy; making them ideal for repetitive testing (108). The feasibility of the manufacture of a soft elastomeric foetal head scalp and placement onto the developed head model, will be assessed through a preliminary evaluation. The learning from this evaluation will then be utilised to formulate an approach to reinforce the initially developed elastomeric material with a textile constraint layer and replicate the mechanical requirements of the foetal head scalp. Different formulations will be manufactured and tested per an iteration of the ASTM D412-06a standard (Section 4.2.2.1). The chosen formulation which meet the desired

specification will then be integrated into the final configuration for the evaluation of the measurement system in Section 4.5.3.

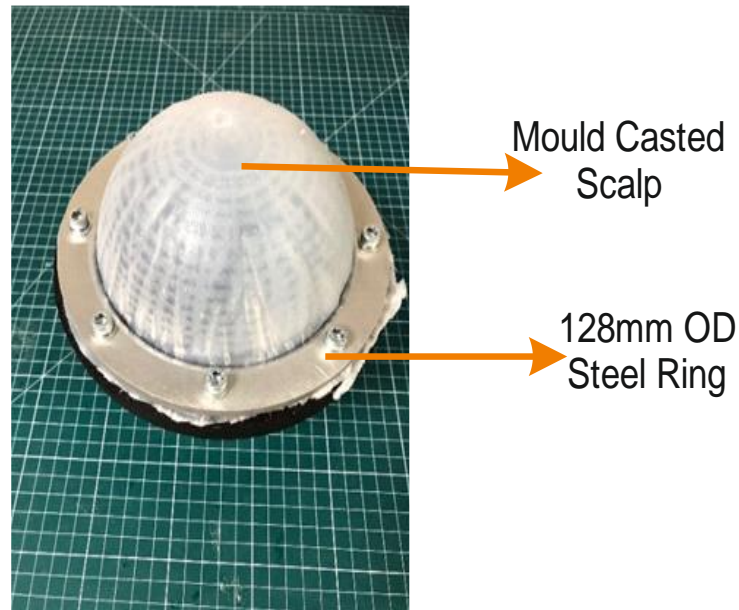


Figure 4-2: Silicone-textile composite scalp placed onto the hemispherical head model based on requirements provided in Table 3-1.

4.2.1 Initial Development

The first iteration of the foetal head model consisted of the design of a 120mm outer diameter (OD) hemisphere to model the presenting SOB diameter with an extended square profile (Figure 4-3). With the advent of rapid prototyping using 3D printed technologies, the head model was manufactured out of Nylon by Multi Jet Fusion (MJF) (HP Designjet 3D colour printer). MJF involves the infra-red thermal fusing of polymer based powder particles layer by layer with fusing & detailing agents ((109)).

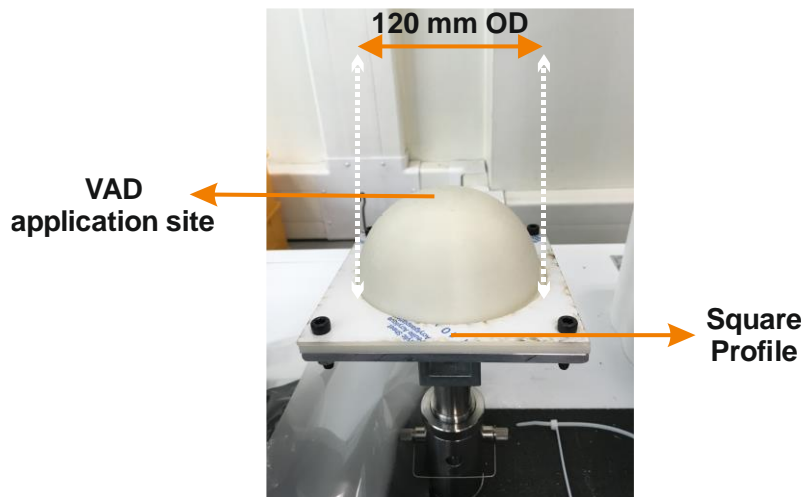


Figure 4-3: First iteration of the head model

Cured silicone elastomers have been shown to effectively mimic specific mechanical behaviour of tissues during the in-vitro simulation of tissue biomechanics (110). In this preliminary evaluation, a similar approach will be undertaken. Ecoflex 00-30, known for its excellent mechanical properties and ease of manufacture, was chosen to be integrated as the surrogate in the head scalp model. With an elastic modulus of 10 psi (68.95kPa) at 100% deformation and a durable pot life of 45 min, Ecoflex 00-30 is a platinum-catalysed rubber silicones curable at room temperature (4 hours at 23 °C) with relatively minimal shrinkage. Its low viscosity (3000 cps) allows it to be easily mixed and dispensed. Equally proportioned Part A and Part B of Smooth On™ Ecoflex 00-30 silicone was first thoroughly mixed and degassed in a planetary mixer (THINKY,ARA-250,Intertronics) for 90s at 2000rpm. Prior to silicone pouring, a mould release agent (Smooth On Universal™ Mould release) has been applied and left to settle for 5 minutes on both moulds. All presenting holes were covered with a non-adhesive filler to prevent silicone leakages. The prepared silicone (240g) was then transferred into a two-part designed cavity moulds and allowed to rest for 3 hours (Figure 4-4)(Figure 4-5). At the end of silicone curing, the moulds are pulled apart and the scalp is peeled off the bottom top mould for integration into the head scalp model.

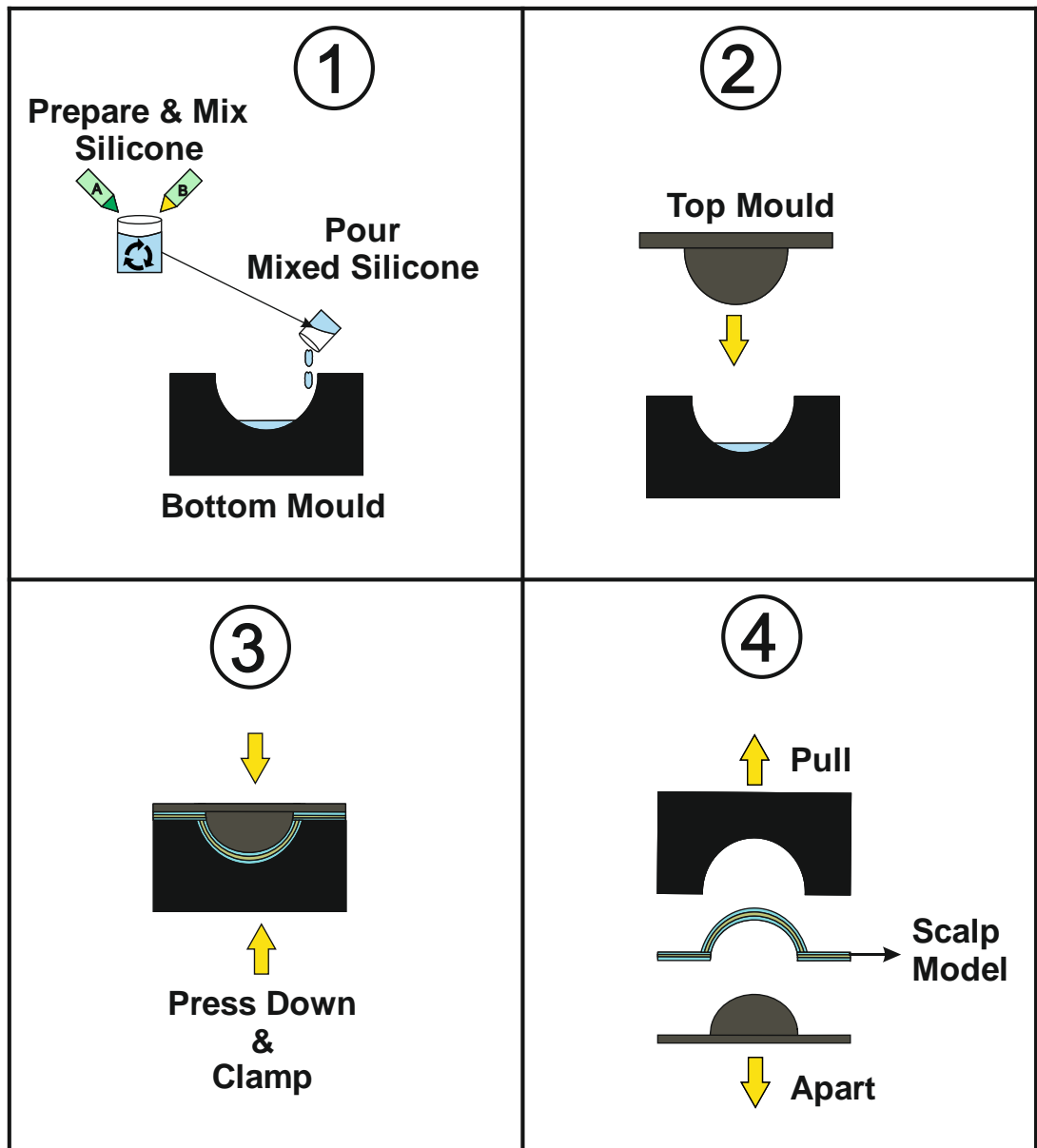


Figure 4-4: Fabrication steps to create a Scalp. Step 1: Silicone Preparation and Pouring, Step 2: Casting, Step 3: Curing Step 4: Demoulding Removal of top mould from bottom mould

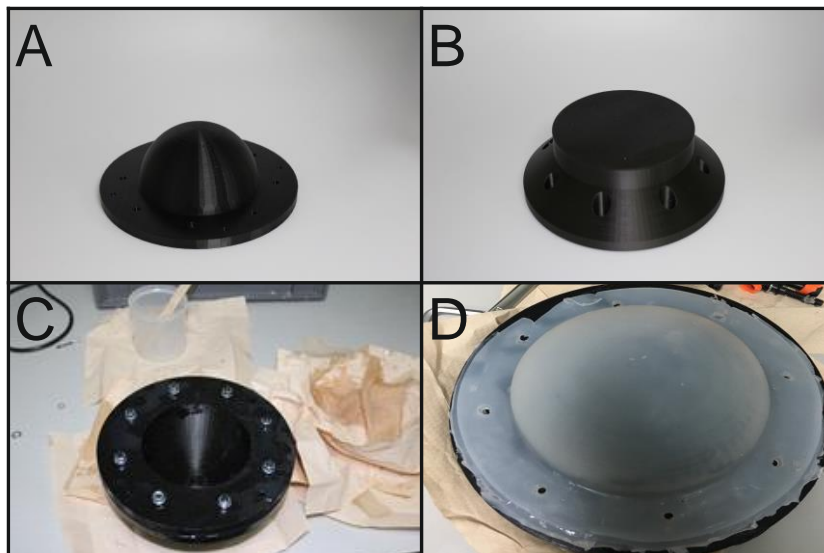


Figure 4-5 : Experimental overview of silicone casting. A-Top Mould, B-Bottom Mould, C- Silicon Curing, D- Demoulded Silicone Scalp

In earlier trials on identifying the right scalp surrogate, it was quickly realised that the silicone material experienced too much elongation over strain and the clamps were not rigid enough to contain the deformation of the material. This prompted to the second iteration of the design. Hereafter, the foetal head model featured an improved redesign of the original conception but manufactured by plastic extrusion based additive manufacturing technology with recyclable Polylactic Acid (PLA) filaments (Ultimaker 2 Extended +). The top of the construct followed the unaltered hemispherical curvature whereas sides of the design are grooved to achieve good surface contact area with the developed enveloped soft material. Surrounding the hemispherical construct, an extended circular profile (5mm from the epicentre) with 8x 5mm holes will provides space to attach a 128 mm OD steel ring to prevent the unwanted scalp movement on the side by providing a clamp down force (Figure 4-6). Perforations around the side of the construct were made to allow the flow of air during application of a vacuum to control the stiffness of the scalp to prevent over elongation of the scalp.

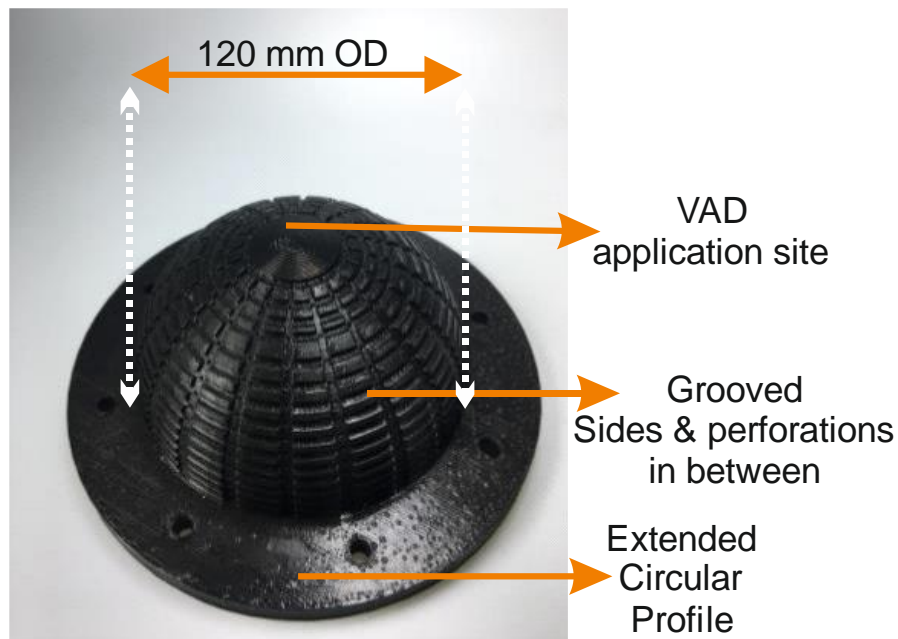


Figure 4-6: Optimised head model with grooved walls for improved contact with the moulded scalp surrogate

Despite the original efforts, it was hard to quantify the stiffness of the scalp exposed to a vacuum underneath. The applied vacuum was found to be interfering with local deformation of the scalp surrounding the VAD. As such, exploratory work on assessing less invasive improvements to the mechanical properties of silicone was required.

In a recent effort by Tausif et al. at the School of Design, University of Leeds, non-woven textile material such as Polyethylene (PET), regenerated cellulose (Lyocell) and Polyphenylene terephthalamide (PPTA) have been added to an elastomeric material (thermoplastic polyurethane(TPU)) to improve its tensile modulus and tensile strength (111). The presented study was a good basis to explore the integration of a constraint layer such as a textile material to reinforce the cured silicone matrix to improve its mechanical properties. With a better cure time and ease of manufacture than TPU, an initial effort was made by combining silicone with loose Polyethylene (PET) fibres (Figure 4-7). The outcome of this exploration motivated the evaluation of more silicone-textile configurations with a view to mimic a more realistic mechanical response similar to biological scalp in the next section.

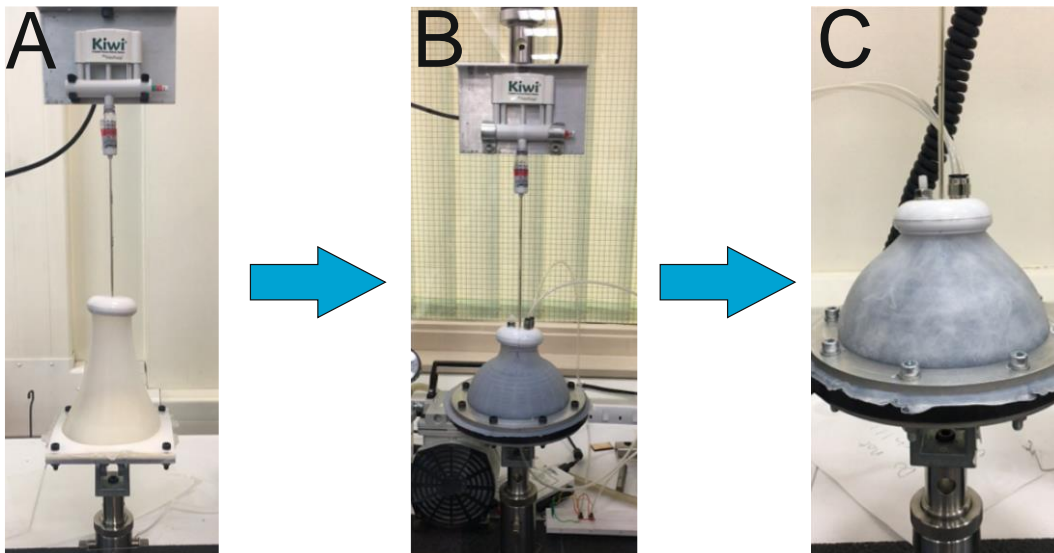


Figure 4-7: Evolution of head scalp models in the VAD simulator A: Over elongation of the material with the original conception. B: Vacuum controlled scalp with the optimised head model. C: Silicone-textile Scalp

4.2.2 Development of a silicone-textile composite scalp

In this section, different woven and non-woven textile material will be combined with the manufacture of Ecoflex 00-30 into tensile die sets dimensioned as per ASTM 412-06a standard. The resulting composite will then be evaluated against the mechanical properties defined in the system requirements in Chapter 3. The chosen formulation will then be integrated into the construction of the foetal head scalp to envelop the construction of a hemispherical foetal head model as shown in Figure 4-2.

4.2.2.1 Mechanical Testing

As highlighted in the Section 2.3, the developed scalp material should have an anticipated elastic modulus in the range of 1.91 ± 0.67 MPa within the lower specification of 20.27 ± 4.79 % elongation: 15.48 % elongation. A desirable tensile strength will allow for the material to withstand tensile forces without the occurrence of yielding or rupture under tensile loading. As such, the tested material should exhibit good tensile strength properties with the desired configuration able to withstand stresses more than 1MPa at an elongation of Upper Specification Limit (USL) of 29.35 ± 9.52 %:38.7% (Section 3.3). The reported values are consistent with the deformation profile of skin tensile tests in the forearm region whereby initial stretching of the collagen fibres observed at 40% elongation (112).

ASTM D412-06a, an internationally recognised test method for evaluating vulcanised rubber and thermoplastic elastomers under tension will be used for the mechanical evaluation of test samples manufactured to the correct dimensions as shown in the tensile test specimen in Figure 4-8.

After manufacture, the test samples will then need to be appropriately clamped in a uni-axial tensile testing apparatus. The test will be performed at a standard speed of 100mm/min until at least 100% elongation of the gauge length or breaking. The collected data (stress against % strain/elongation graph) will then be analysed to determine the modulus of elasticity or Young's modulus (E) from the gradient of the straight line portion as shown in Figure 4-9 (Equation 4-1). The Tensile Strength (TS) can be obtained by calculating the Load divided by the cross-sectional area at the % elongation at break as can be seen below (Equation 4-2 & Equation 4-3).

$$\text{Young's Modulus (E)} = \frac{\sigma}{\varepsilon} = \left(\frac{\text{gauge length}}{\text{cross - sectional area}} \right) \times \text{slope} \quad \text{Equation 4-1}$$

$$\text{Tensile Strength } \left(\frac{F}{A} \right) = \frac{\text{Load}}{\text{Cross - Sectional Area}} \quad \text{Equation 4-2}$$

$$\% \frac{\text{Strain}}{\text{Elongation}} = \left(\frac{L - L_0}{L_0} \right) \times 100\% \quad \text{Equation 4-3}$$

where L : Extended length

and L₀: Original Gauge Length

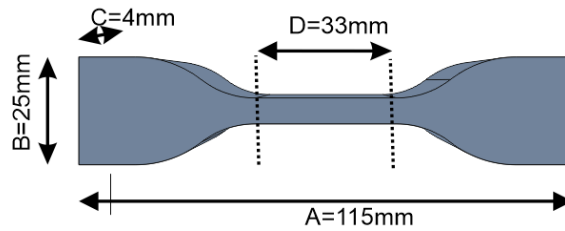


Figure 4-8: Tensile specimen dimensions based on ASTM D412-06a standards. A- Length of test specimen, B-Breadth of the barbell ends for clamping, C: Thickness of sample, D-Gauge length of elongation

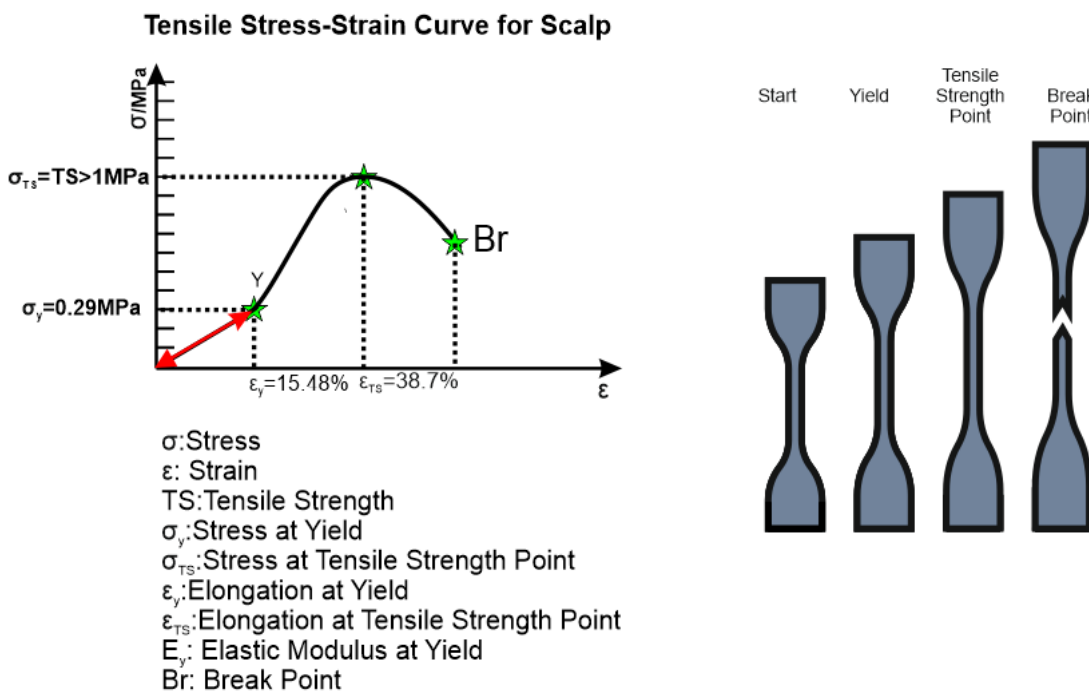


Figure 4-9: Tensile Stress-Strain Curve for Scalp testing alongside the representation of the tensile specimen at different stages of the test.

4.2.2.2 Materials and method

Commercially available Samuel Taylor Spandtex N64 and Sulky® Soft'n Sheer™ non-woven nylon cut-away permanent stabilizer as well as textile assemblies provided by the School of Design, University of Leeds, were combined with a silicone base (Ecoflex 00-30) to produce elastomeric composites. Woven samples of preformed carded Polyethylene terephthalate (PET) (1.6 decitex (dtex), 38mm) and non-woven Polyphenylene terephthalamide (PPTA/para-aramid) (1.7 dtex, 58mm), regenerated cellulose (Lyocell) (1.7 dtex, 38mm) will be included in this study. All non-woven preforms were carded (nominal mass area density of 70gm^{-2} , parallel-laid) and pre-neededled ($42\text{ punches cm}^{-2}$). One woven format of the same Lyocell formulation was also included in this test evaluation. The silicone was manufactured as detailed in section 4.3.2. The prepared silicone was then poured into 2mm or 4mm deep acrylic laser cut Stencils designed to fit 5 ASTM D412-06a (Die C- Tensile Set dimensions- 6mmx33mm) test specimens. A sheet of textile material (School of Design, University of Leeds) was sandwiched in between 2mm deep stencils whereas Ecoflex 00-30 sample was produced using a 4mm stencils. Once set, the silicone or the silicone composite is allowed to rest at room temperature for 3 hours and then demoulded to be trimmed to shape for tensile testing (Figure 4-10).

The prepared 5 test specimens were then securely positioned at the tag ends into pneumatically controlled Instron 250N Gripper set (2712-052) (Figure 4-11). A tensile test was then performed at 100mm/min with a 50mm end extension on an Instron 5500 equipped with a 500N load cell. Data were collected at intervals of 2 ms (500Hz) via the Bluehill™ Universal machine control interface.

In addition to the silicone composite testing, the mechanical properties of 2 synthetic skin simulants: SynDaver 4N & 10N (Adult Skin, SynDaver Labs, FL, USA, SKU:141503 & 141514) were also tested to establish recognised baselines in testing. The tissue simulants were first stored in saline solution and cut to size (15mmx70mm). The average thickness of the SynDaver 4N and SynDaver 10N were 1.9mm and 2.4mm respectively. The skin simulants were securely positioned into a pneumatically controlled Instron 250N Gripper set (2712-052) to expose a gauge length of 30mm. Destructive tensile test was then performed at 100mm/min on an Instron 3369 equipped with a 500N load cell. Data was collected at intervals of 2ms (500Hz) via the Bluehill™ Universal machine control interface.

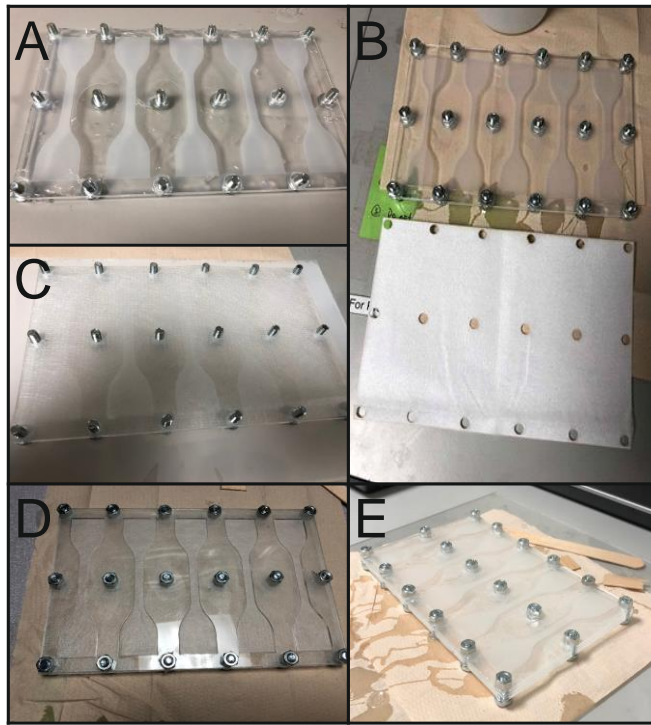


Figure 4-10: Preparation steps of the silicone-textile composites. A- First layer (2mm) silicone preparation, B-First layer cured and laser cut textile sheet to fit tensile template C- Placement of textile sheet, D-secure clamping of tensile set for second layer silicone preparation (2mm), E- Curing and setting of samples

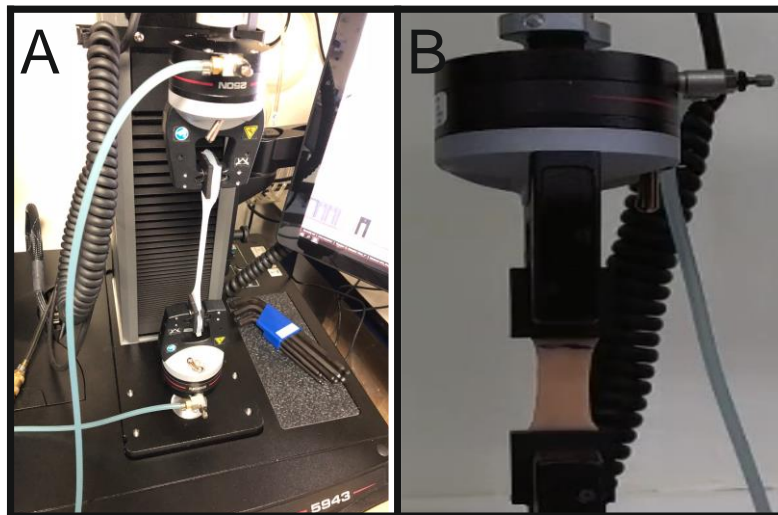


Figure 4-11: Tensile testing of material evaluated in the conception of a silicone-textile scalp. A-Tensile testing of silicone-textile barbell specimen, B- Tensile testing of SynDaver 4N Skin Simulant

4.2.2.3 Results and Evaluation

The graphical results of this characterisation work can be viewed in Appendix A1. A summary of results based on defined metrics, introduced in Figure 4-9, is displayed on Table 4-1 and a graphical representation of the observed results can be viewed in Figure 4-12.

Table 4-1 :Summary of the material evaluation for implementation in the head scalp model

Material Evaluated	Mean Elastic Modulus (MPa) at $0 < \epsilon < 15.48\%$ (n=5) \pm Standard Deviation (SD)	Mean Stress (MPa) at $\epsilon=38.87\%$ (n=5) \pm Standard Deviation (SD)
Ecoflex 00-30	0.04 \pm 0.01	0.01 \pm 4.34E-04
Ecoflex 00-30 + Carded PET 1.6 dtex, 38mm	0.06 \pm 0.04	0.03 \pm 4.79E-04
Ecoflex 00-30+Spandtex (A6 Polyester +Nylon)	0.05 \pm 0.014	0.02 \pm 3.08E-04
Ecoflex 00-30+Sulky	1.65 \pm 0.50	0.48 \pm 4.55E-04
Ecoflex 00-30 +PPTA 1.7dtex, 58mm	0.96 \pm 0.20	0.20 \pm 2.46E-04
Ecoflex 00-30+Lyocell 1.7 dtex ,38mm	1.04 \pm 0.21	0.34 \pm 3.16E-04
Ecoflex 00-30+Woven Lyocell 1.7 dtex 38mm	1.50 \pm 0.58	1.19 \pm 0.0012
SynDaver 4N	1.30 \pm 0.10	0.24 \pm 3.00E-05
SynDaver 10N	9.47 \pm 1.18	1.88 \pm 2.71E-04
Desired Mechanical Properties	1.91 \pm 0.67	>1MPa

The mean elastic modulus of PET 1.6 dtex 38mm and Spandtex composite didn't defer from Ecoflex 00-30. However, there were strong indication of good silicone-textile integration with the Polyphenylene terephthalamide (PPTA/para-aramid) (1.7 dtex, 58mm). However only the combination of the Sulky® Soft'n Sheer™ non-woven nylon cut-away permanent stabilizer and the woven regenerated cellulose (Lyocell) (1.7 dtex, 38mm) Ecoflex 00-30 met the desired mean elastic modulus properties at 38.97%. It is interesting to note that the SynDaver 4N was close to the desired range for the elastic modulus but didn't have the required tensile strength properties whilst SynDaver 10N displayed the opposite characteristics. Ecoflex 00-30 with woven regenerated cellulose (Lyocell) (1.7 dtex, 38mm) met the second requirement of the design

specifications by exhibiting good tensile strength properties (>1MPa). This lead to the consideration of this evaluated silicone-textile configuration to be integrated into the final design of the foetal head scalp model (Figure 4-12).

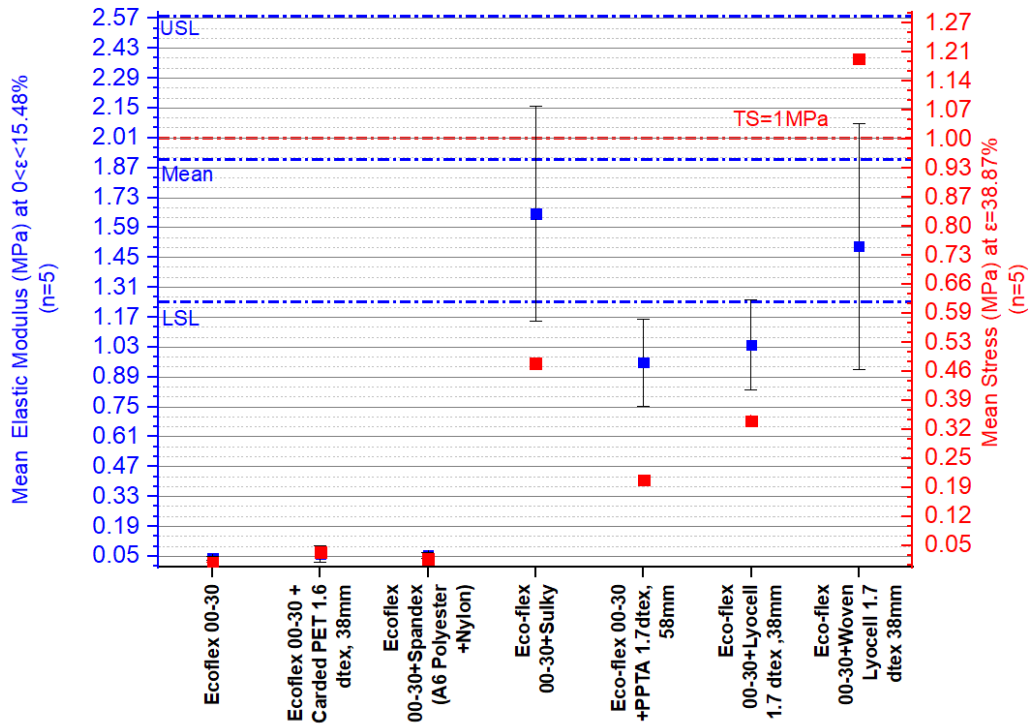


Figure 4-12 : Data for the Mean Elastic Modulus for $0 < \epsilon < 15.48\%$ (Left y axis-Blue) & Mean Stress at $\epsilon=38.87\%$ (Right y axis-Red)

4.2.3 Fabrication of Silicone-textile Scalp Composite

The fabrication of the silicone-textile scalp involved the same process steps as indicated in the manufacture of the silicone scalp in section 4.2.1. Half of the silicone prepared (120g) was first added into the bottom mould. The top mould was then gently pressed to ensure the silicone flows on the side of the circular profile. After this process step, a layer of the textile material was then positioned and then the remaining the silicone was dispensed. A centred bottom cast part was then pressed and secured into place by bolts and nuts. The unit is left to cure for 3 Hours. Once cured, the bolts are removed and an external pressure source (1bar) was applied to the relief hole on the top part to separate the newly moulded silicone from the top cast. The top cast is slowly levered off with a flat head screwdriver from the bottom cast to reveal the scalp model. Upon release of the scalp, the flashes of silicone are carefully removed by blowing pressurised air and then rinsed with distilled water. The moulds are then allowed to air dry for 2 days until next usage.

Throughout the time of study, the silicone-textile composite manufacturing technique has been conceived during the fabrication and trial of various formulation of scalps (Figure 4-13). Due to the physical manipulation of samples and the compressive nature of the moulding process, it is recognised that misalignment and pre-stressing of the imbedded textile material can happen This can cause defects and artefacts such as bubble entrapment, uncured silicone, residual silicone flashes and thinning layer (Figure 4-13). The conformance of a flat sheet of textile onto a hemisphere can lead to material overlapping i.e. creases. The quality of the composite scalps manufactured has been controlled through visual inspection in an effort to discard scalps prone to the defects and artefacts. In section 4.5, an evaluation of silicone scalp composed of the chosen formulation will be presented during the combined measurement system evaluation.

Timeline of Scalp Development

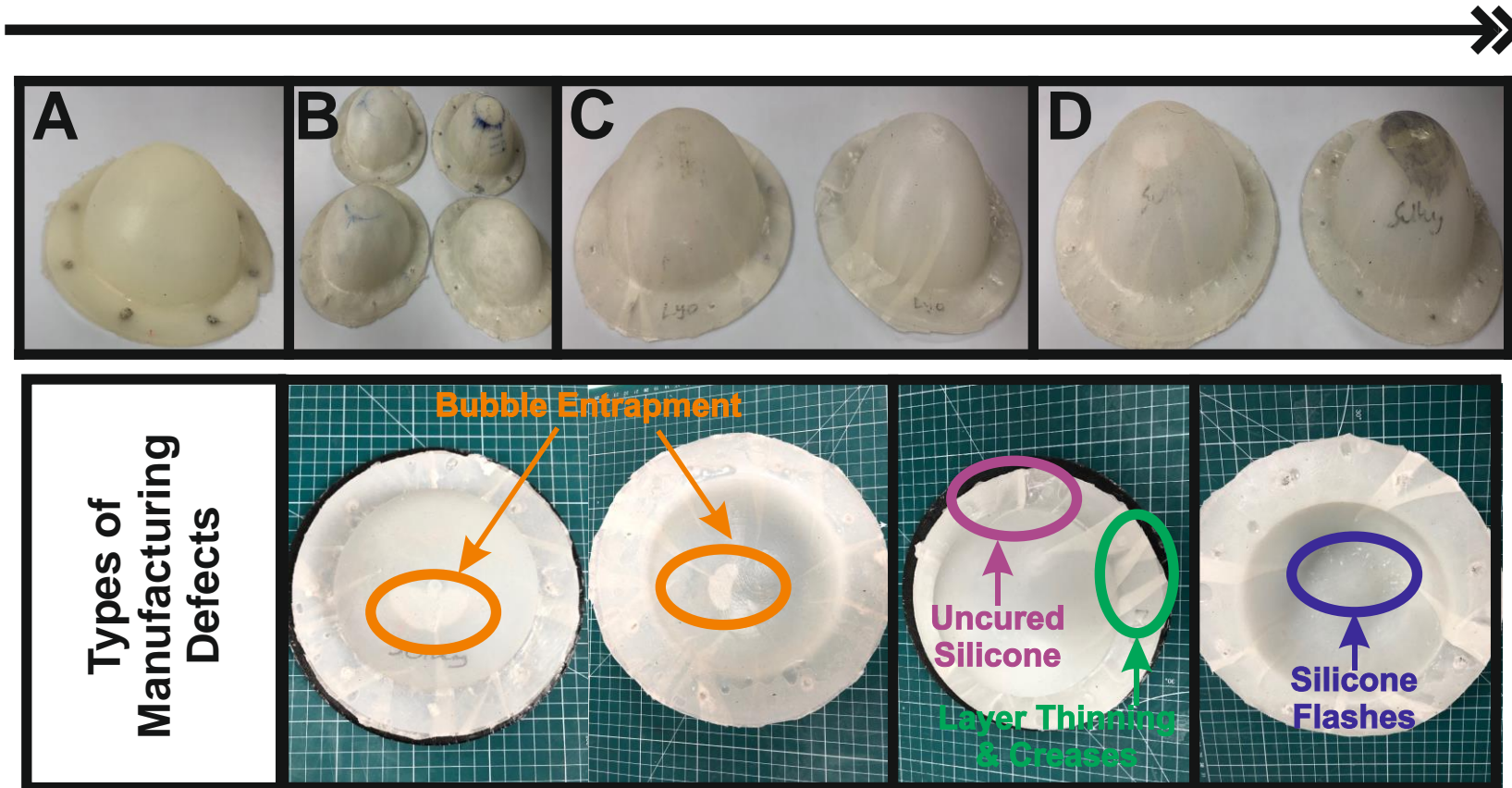


Figure 4-13: Overview of scalps manufactured over the time of study. A-Silicone scalp, B-Loose PTE fibre scalps, C-Sulky scalps, D- Lyocell scalp and list of associated defects with the current manufacturing technique

4.3 VAD Pneumatic Instrumentation

As highlighted in Chapter 3, the Kiwi Omni Cup will be used as a template for investigation. In this section, the technical aspects of the VAD pneumatic controller alongside the sensing unit to pneumatically instrument VAD cup will be covered (Figure 4-14). A summary of the hardware configuration utilised to construct the pneumatic sensing and control units can be seen from Table 4-2.

Table 4-2 shows a summary of Simulation Control & Sensing Hardware

Testing Variable	Unit	Hardware	Manufacturer & Model
Vacuum Pressure	Vacuum Sensing	Vacuum Sensor	Panasonic ADP5110
Vacuum output	Pneumatic Controller	Vacuum Regulator, valve & Pump with reservoir	SMCITV2090-21F2BSS, Normally closed Valve SMC VX214AA & Medap Venta Multi Care 26 Pump with Festo Air Reservoir 2L, G 1/2, CRVZS Series,

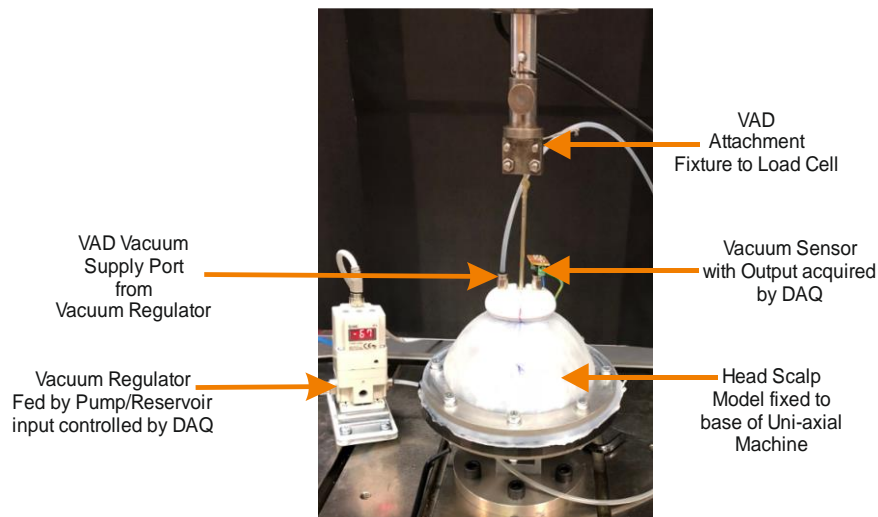


Figure 4-14: Pneumatic components used to pneumatically instrument the VAD cup

4.3.1 Pneumatic Controller unit

The pneumatic control kit comprises of a vacuum pump, reservoir, regulator & in-line control valve for a controlled supply of the vacuum level inside the interfacing VAD device (Figure 4-15).

Connected in line with the pump by 8mm OD tubing, a 2L vacuum reservoir (Festo Air CRVZS) is used to counteract any vacuum disturbances created by the vacuum pump (Medap Venta) but also used in buffered vacuum regulation experiments in the following chapter to emulate different VAD pneumatic architecture. The output of the vacuum is controlled electronically by using a vacuum regulator (SMC ITV2090) with high sensitivity (0.2% FS) and repeatability (0.5% FS). An electro-pneumatic solenoid based vacuum regulator can be set up to deliver vacuum to the VAD cup up to -80kPa with supply vacuum pressure ranges between -13.3kPa to -101kPa via a 4mm SMC push fit connector with a response time of 0.1s (10Hz) (Figure 4-16). The NI DAQ 6211 is central towards the control of the input of the regulator to deliver the supply of vacuum to the instrumented VAD whilst acquiring the changes in vacuum levels via the sensing unit.

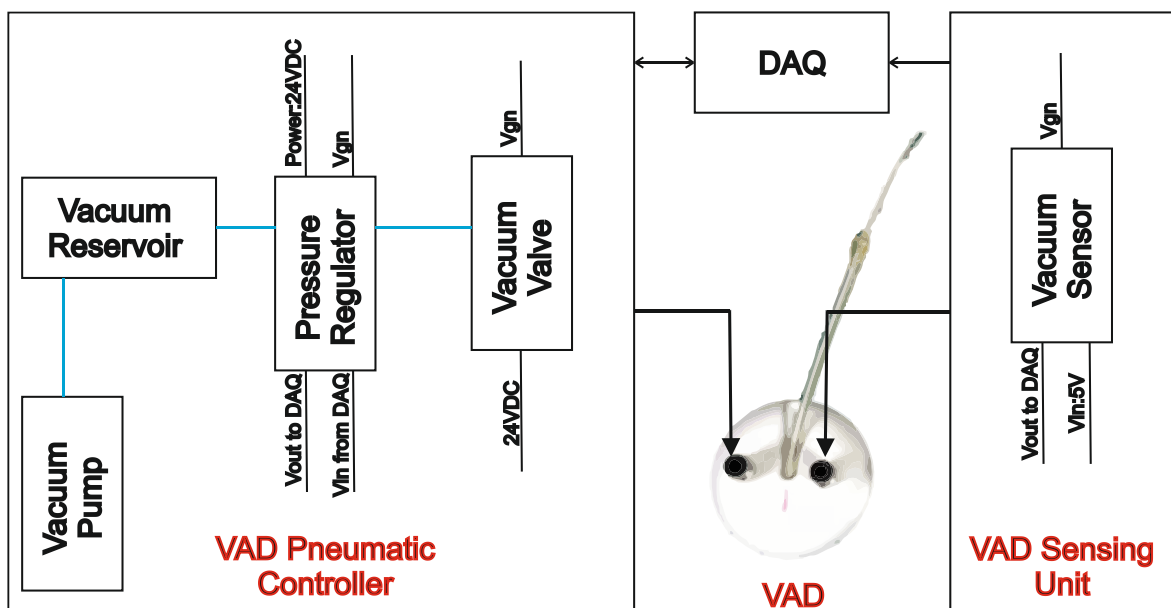


Figure 4-15: Instrumentation of the VAD controlled by the VAD Pneumatic controller and the vacuum recorded by the VAD Sensing Unit. Both systems are monitored by the DAQ.

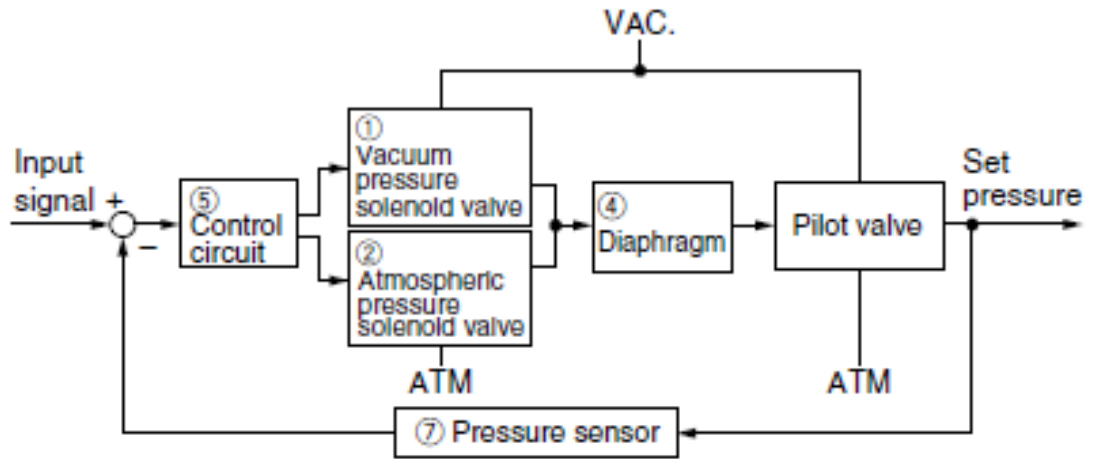


Figure 4-16: Schematic of the electro-pneumatic Vacuum Regulator showing the feedback control schematic of a set pressure based on an input signal(113)

4.3.2 VAD sensing Unit

Whilst, it is anticipated that the cup detachment is a very fast event, it is important that the vacuum sensor is fast and sensitive to any vacuum changes experienced in the cavity of the instrumented cup. Measurement of vacuum can be achieved by an either absolute or gauge pressure sensor relative to atmospheric pressure (101.3kPa). As a result, negative readings are obtained. The instrumentation of the VAD cup features the use of an analogue gauge vacuum sensor (Panasonic ADP 5110) connected to the analogue input of the DAQ and powered by 5V input. With a built in amplifier, temperature compensating circuit and compact in size, the negative pressure measurement sensor can record vacuum changes of up to -100 kPa with high accuracy ($\pm 1.25\%$ FS). To optimize sensing, the sensor was placed within close proximity of the interfacing port hole (4mm SMC push fit connector) (Figure 4-14).

4.3.3 Calibration of VAD Pneumatic controller and Sensing Units

Linearity & calibration tests were performed to evaluate the response of the Vacuum sensor & regulator present in the sensing and pneumatic controller units respectively, upon incremental vacuum changes. A linear regression fit was applied to obtain the characteristic correlation between the voltage output from the sensor to the connecting DAQ unit and the vacuum level acquired by a calibrated Digitron 2022P digital manometer ($R^2= 0.9998$, $n=48$) (Figure 4-17). Once calibrated, the relationship between the voltage input of the pneumatic

controller to delivery of the vacuum was cross-verified with the already calibrated vacuum sensor. A linear regression fit was applied to obtain the characteristic correlation between the voltage input and vacuum supplied by the pneumatic controller ($R^2= 0.9997$, $n=39$) (Figure 4-18). In addition, the in-built vacuum sensor providing the display of the vacuum levels on the electro-pneumatic regulator was calibrated accordingly ($R^2= 0.9999$, $n=39$). (Figure 4-19).

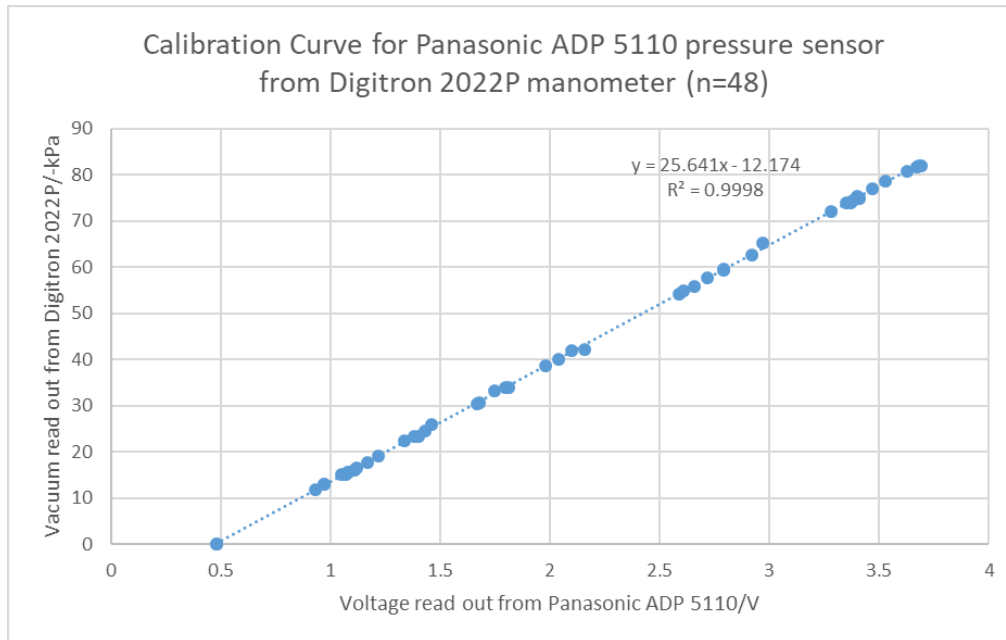


Figure 4-17: Calibration Curve for voltage input to the vacuum sensor as result of vacuum changes created by the pump and validated by the Digital Manometer (n=48).

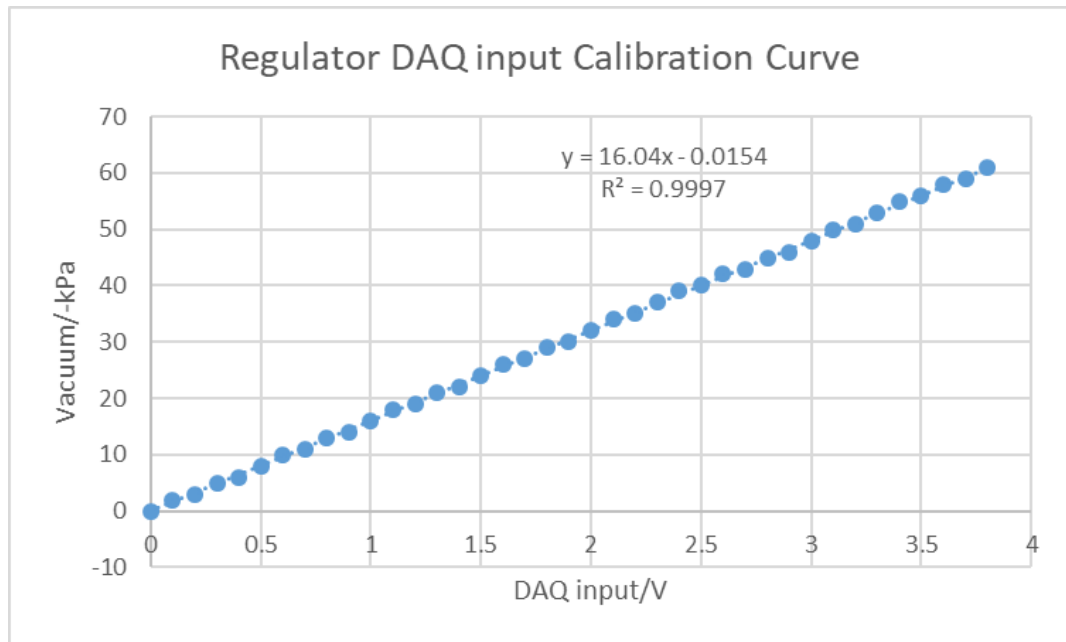


Figure 4-18: Calibration curve for the voltage output from the electro-pneumatic regulator to control the vacuum sensed by the calibrated vacuum sensor. The supply of vacuum to the regulator was -80 kPa and generated by the pump (n=39).

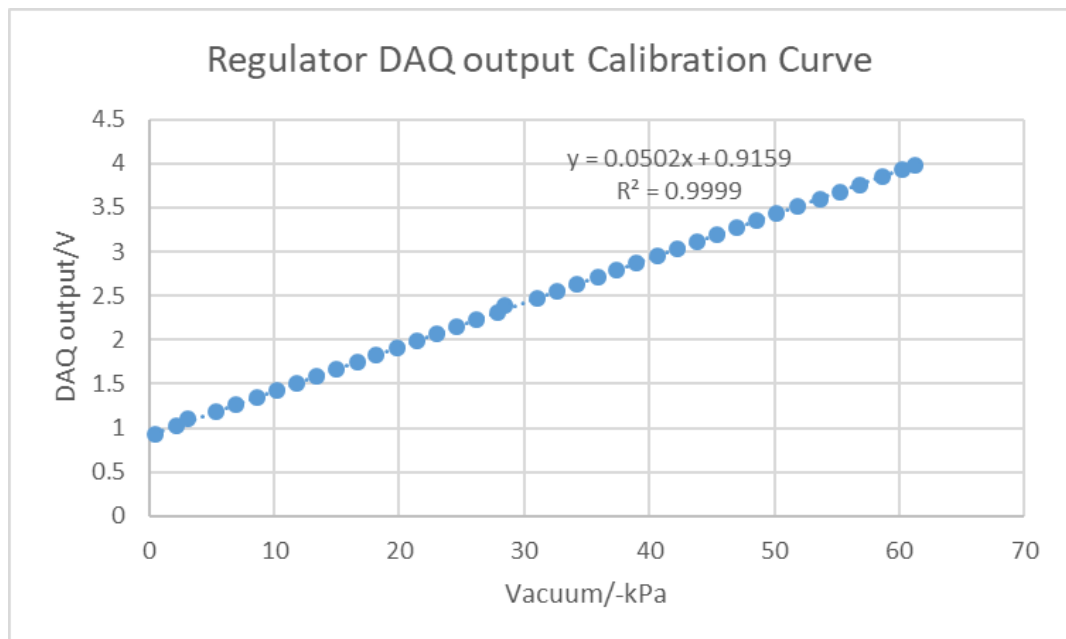


Figure 4-19: Calibration curve for the voltage input to electro-pneumatic regulator against vacuum levels changes generated by the pump (n=39).

4.4 Experimental methodology to detect cup detachment

Following the creation of the foetal head scalp model and the instrumentation of the VAD cup, the Instron E10000 was chosen as the uni-axial tensile test platform to develop the experimental methodology behind the in vitro simulation of an over traction. The testing methodology behind the interaction of essential hardware components utilised for detection or control of testing variables will be discussed in this section. A summary of the testing variables and detection hardware/unit alongside their operating software can be viewed in Table 4-3: Summary of the testing variables measured by the hardware and operated by its designated software utilised in the test measurement system.

Table 4-3: Summary of the testing variables measured by the hardware and operated by its designated software utilised in the test measurement system

Testing Variable	Hardware/Detection Unit	Operating Software
Vacuum Pressure	VAD Sensing Unit	National Instrument (NI) LabVIEW Virtual interface
Vacuum output	VAD Pneumatic Controller Unit	National Instrument (NI) LabVIEW Virtual interface
Traction Load (N)	Instron Load Cell (200N)	Instron Wavematrix Software
Traction Speed (mm/min)	Instron Frame with associated couplings & Software	Instron Wavematrix Software
5V Digital Synchronisation signal Output signal	Generated by DAQ and Supplied to Instron Controller by BNC cable	National Instrument (NI) LabVIEW Virtual interface
Visual detection of cup detachment & scalp deformation	High speed camera (Phantom V9.0) & 2mm studded pin markers	Phantom Camera Control (PCC)

4.4.1 Test Assembly

The Instron Electropuls E10000 equipped with a 200N load cell was chosen due to its extensive actuator stroke coverage (60mm) with configurable workspace (Tee slotted test base & Extended frame) and direct output of unfiltered acquired Force data (5000Hz) from its controller unit. With the head scalp model affixed to the Tee slotted base of the machine, traction simulation can be performed through the coupling of the pneumatically instrumented cup to the load-cell equipped actuator (Figure 4-20).

A commercially available VAD device (Kiwi Omni Cup) was modified to expose only the 16.5cm wire in bracket and the anchor point was sealed with epoxy glue to prevent unwanted vacuum interferences from the pump handle. Two precisely tap threaded 4mm holes were made to fit in 4mm push fit connectors to accommodate the vacuum control and sensing lines from the pneumatic controller and sensing unit developed in the abovementioned section (Figure 4-14). The wire was secured with a gripping fixture. The coupled assembly was then directly connected to the load cell affixed to the actuator of the frame via a designated piggy back fixture (See Appendix A2 for Fixtures Design).

A specialised National Instrument (NI) LabVIEW Virtual interface (VI) was created to allow the user to initialise the vacuum inside the cup via the regulator and record the output from the sensors input via buffered acquisition to the DAQ NI-6211 (Panel A in Figure 4-22). The back end of the LabVIEW software was programmed to acquire 5000 samples of data at a sampling frequency of 5000Hz in the acquisition control loop. Digitally controlling the initiation of the test is another benefit of using the E10000. The 5V synchronisation signal with 1 μ S delay (Low to high) was used to trigger the start of the test on the Instron Wavematrix directly from the NI LabVIEW VI (Figure 4-21). The same signal was used with a pre-set delay to activate the recording of the test with a high speed camera (High to Low); whereby the displacement of affixed pin markers was tracked to provide a visual perspective of the occurrence of cup detachment. This technical aspect will be discussed in the following section.

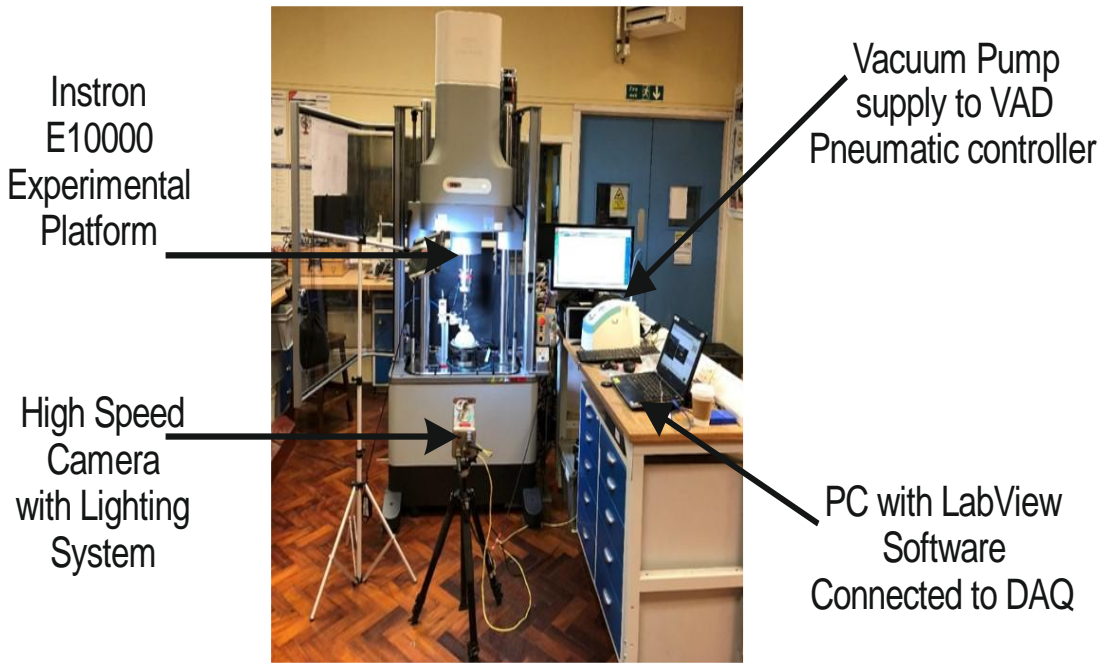


Figure 4-20: Assembly components of the VAD simulator. The foetal head scalp model and the pneumatically controlled VAD cup onto an Instron E10000 and a high speed camera records the test performed.

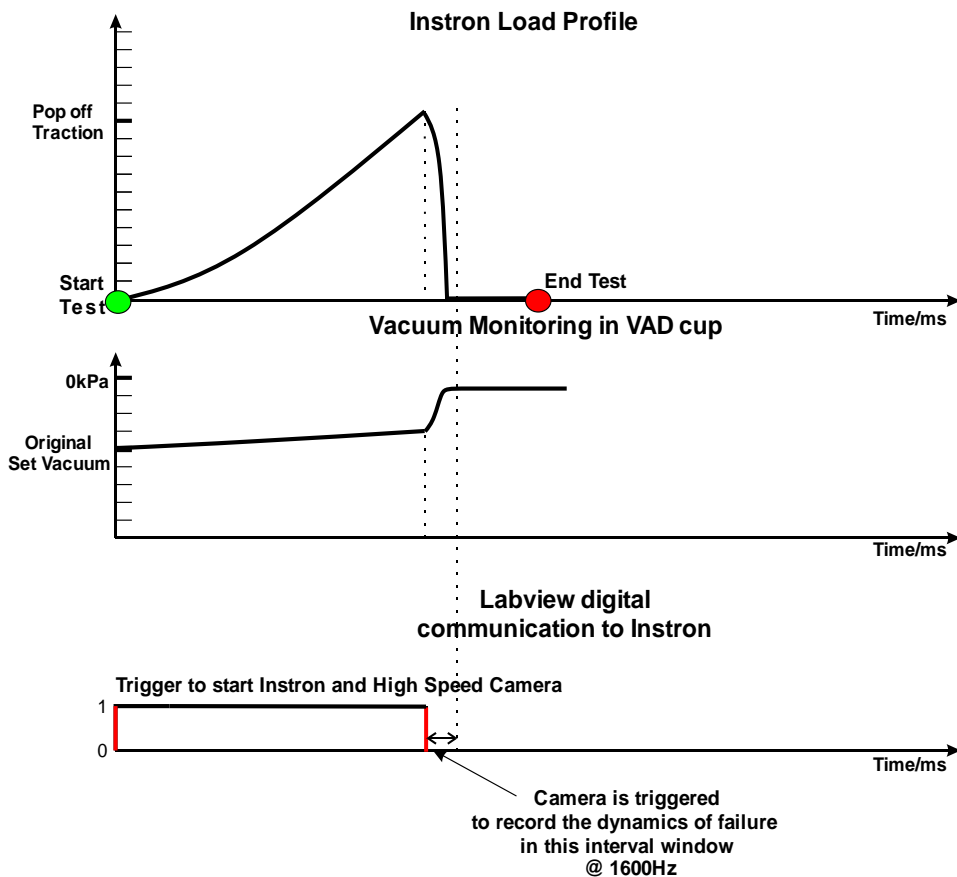


Figure 4-21: Details of how a synchronisation signal is sent from the NI DAQ to start the data acquisition of the load & vacuum and recording of the high speed camera

4.4.2 Test Methodology

First, the head scalp model is affixed at the bottom base of the Instron machine. A liquid leveller is used to ensure that the head scalp model is horizontal to the platform of the uni-tensile machine. The instrumented cup is then attached to the cross head and the 200N load cell with the coupling fixtures (Figure 4-20). The machine cross head is then adjusted so that the cup touches the periphery of the head scalp model and is coincident with a scribed marking. A reference-graded metre rule is placed adjacent to the foetal head scalp. The High-Speed camera is then focussed on the pin markers to capture the interaction region of VAD cup with the foetal head scalp model as addressed in the following section. Once in position, the flowchart of the test protocol is then followed to perform a simulation of an over traction by operating the created LabVIEW VI and the Wavematrix software (Figure 4-22).

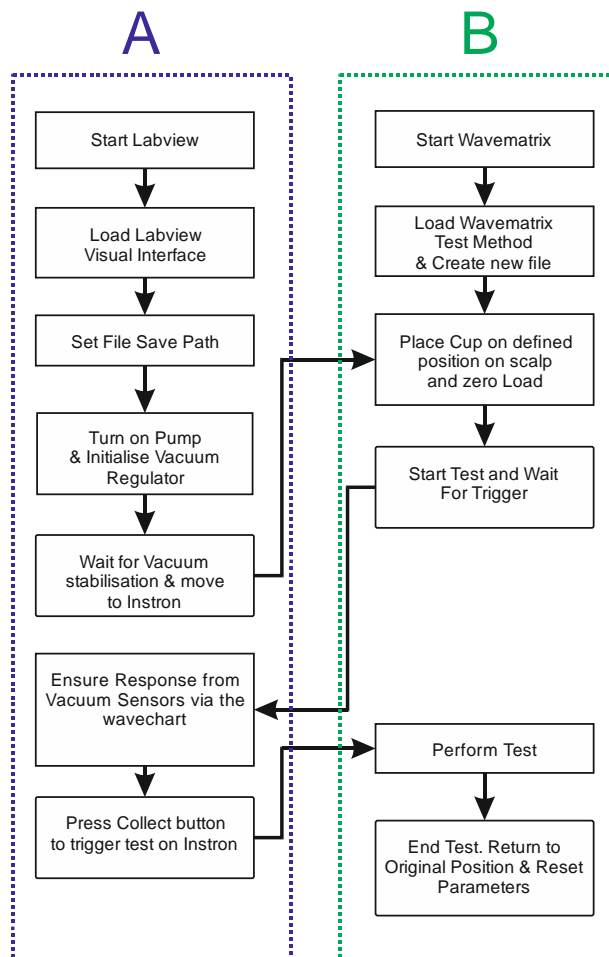


Figure 4-22 : Test flowchart with the 2 interfacing software used during the data acquisition of the test method to simulate an overtraction. A: The test flowchart associated with the LabView Interface. B: The test flowchart associated with the Instron Interface.

4.4.3 Visual Detection of Cup Detachment with Pin Markers

During simulation of an over traction, true strain information on the scalp around the periphery of the interfacing cup would be useful to indicate on the visual detection of a cup detachment. In this original effort, spanned over 10mm, three in-line visual markers (2mm studded steel pins) were inserted 2 mm apart from each other just directly underneath the instrumented cup in the head scalp model at 4 distinctive positions (left & right sides and ± 10 mm away from the centre) as shown in Figure 4-23. A laser-cut paper template was applied onto the head scalp model to help the placement of the pins. A high speed camera (Phantom V9.0), triggered by the synchronisation signal (T_{Trigger}) via capture serial connection, was programmed to capture the full coverage of the test at 100 Second (FPS) or by inducing a timed delay to focus at 1600 Second (FPS) the coverage on the failure dynamics of the cup detachment. During the physical simulation, a meter rule was placed in the frame of view to aid in the measurement of the displacement of the pin position. However, due to the convex structure of the scalp model, technical difficulties persisted in assessing the characterisation of the true strain information from all the slotted pin markers. The consideration of an additional vision system would need to be integrated in the overall rig assembly to obtain information about strain radially; however this wasn't feasible during the time of study and is further discussed in Section 7.2. Only axial vertical deformation information from the side pins could be interpreted (Panel B of Figure 4-23). However, the displacement of the side pin markers can still be used to provide a visual indication of the relative motion of the scalp to the cup during the occurrence of the cup detachment event.

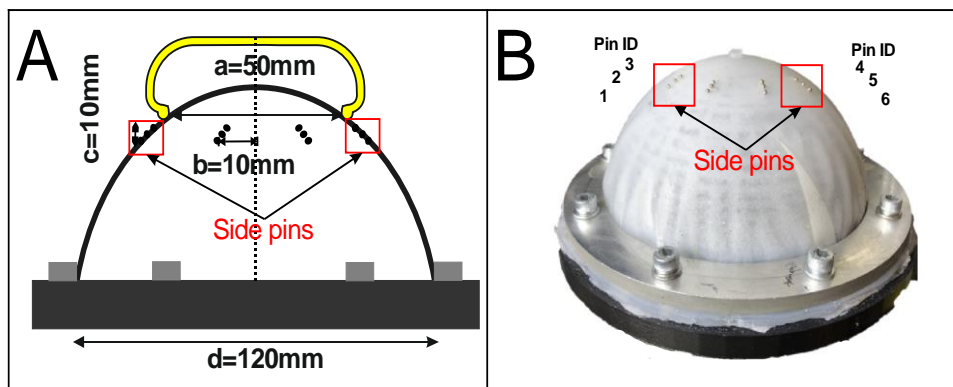


Figure 4-23: Pin markers onto Scalp. A: Schematic of pin markers placement position on foetal head scalp model at indicated by distances a,b,c & d, B: Experimental placement of pin markers on foetal head scalp model and identification of the side pins

After acquisition of the test footage, the video file was then analysed to extract information about the change in displacement of the placed pin markers. A standard image gamma adjustment curve with brightness 13.1%, Gain: 2.427AU,

Gamma: 1 AU, Toe: 1 AU is applied to the generated video file using the Phantom Camera Control (PCC) Software. Each frame is then converted into TIFF format. Upon conversion, the images are then imported into Matlab and an image tracking corner detection algorithm (Harris-Stephens) is used to detect the coordinates of the side pins on each recorded frame in a specified region of interest (ROI) (114)(Figure 4-24). Each image is composed of rows and columns of pixels. By calculating the number vertical pixels in a known distance (20mm) from the graduated scale present on the placed meter rule, the pixel axis to Cartesian axis is known. The initial coordinates of each pin marker at the start of the image detection (TTrigger) is then used as a reference to calculate the change in length for all the resulting frames at each point location based on the pixel calibrated axis (Figure 4-25). The resolution pin marker detection by this method is 0.01mm/pixel. The file is then saved containing the change in vertical displacement profile of the side pins. A flowchart of the image analysis process can be seen on Figure 4-26.

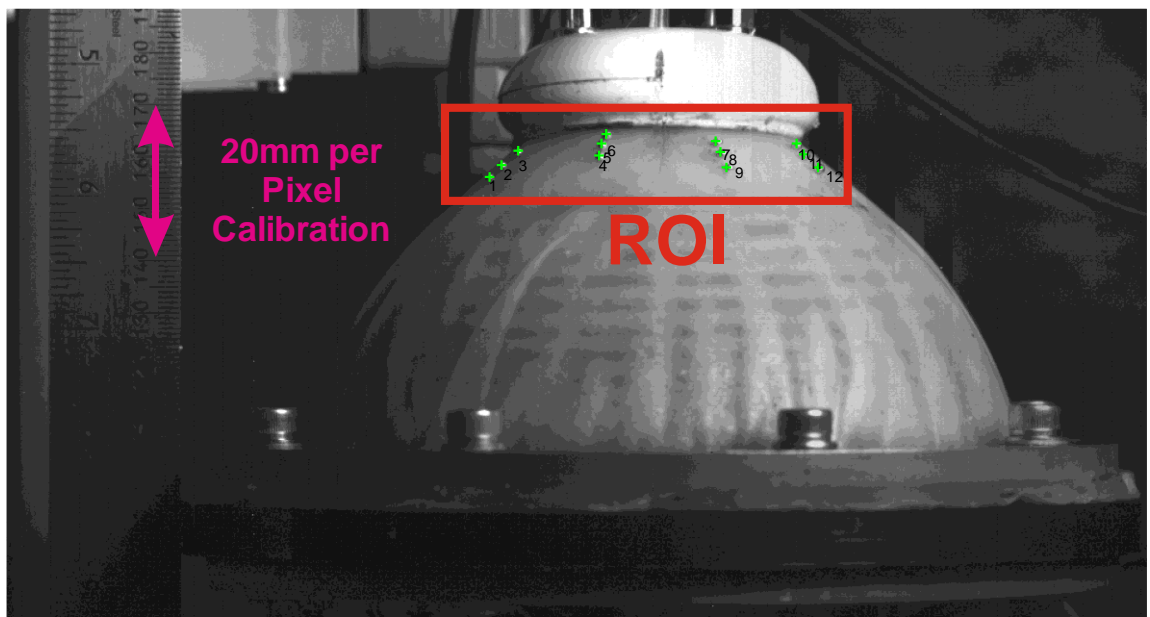


Figure 4-24: pixel displacement calibration using calibrated meter rule & setting of ROI using image detection algorithm (Harris-Stephens) on Matlab

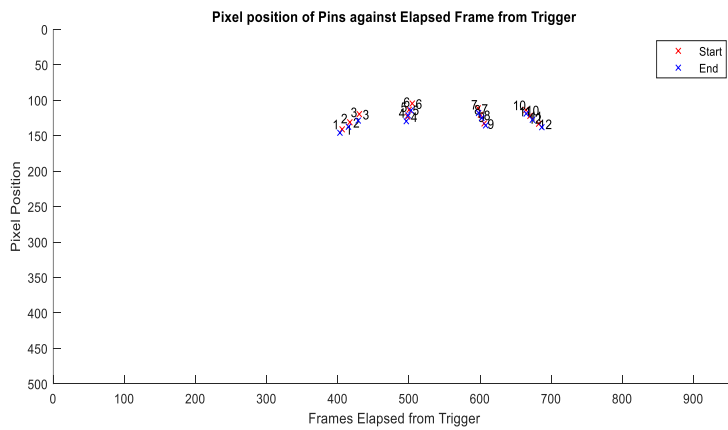


Figure 4-25: Automatic tracking of the pin position at frames elapsed from Trigger. Red marked shows the start of the test. Blue markers show End of the Test.

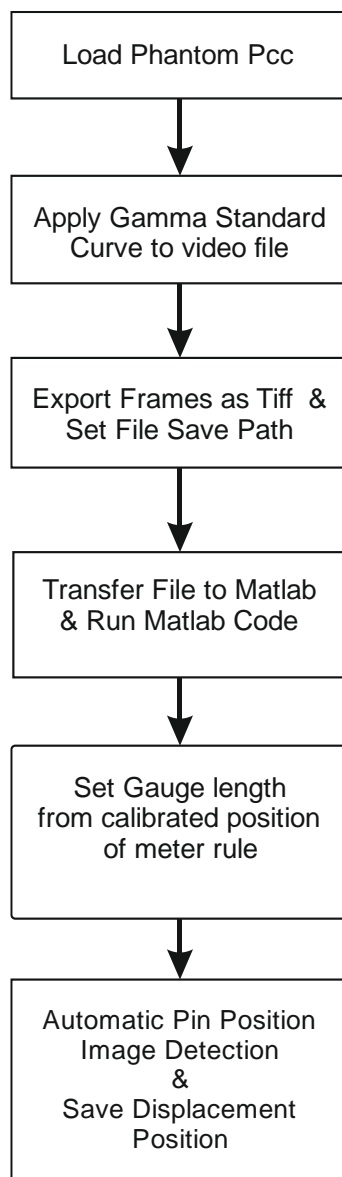


Figure 4-26: Image analysis flowchart to obtain the y displacement of the side pins

4.5 Dynamics of Cup Detachment

An experimental simulation of over traction at 100mm/min using the developed test assembly and test methodology was performed on a manufactured silicone-textile scalp with an applied vacuum level of -70kPa. The experiment was first recorded with the developed vision system at 100Hz to understand the chain of events leading to cup detachment. The same experiment was then repeated with the vision system capture rate increased to 1600 Hz to isolate the cup detachment event and inform on the dynamics of cup detachment.

4.5.1 Data Processing

Prior to the evaluation of the data acquired during the simulation, data processing of the acquired datasets was first required (Figure 4-27). The DAQ raw dataset for each experimental repeat contains time-series data on vacuum magnitude, the traction load & the synchronisation signal acquired captured at 5000Hz whilst the dataset for the pin markers contains pin displacement information either sampled at 100Hz or 1600Hz. Considering the difference in sampling rates, the two datasets had to be aligned around the common reference point Trigger time index (T_{Trigger}) (Figure 4-28 & Figure 4-29). T_{Trigger} was set to 0s and 6s for the experiments performed at 100 and 1600Hz respectively and can be identified when the synchronisation signal drops from a high to low value (5V to 0V) (Figure 4-21).

A resampling coefficient of $d(100/5000)$ or $(1600/5000)$ to align the DAQ acquired dataset to the nearest frame of the pin markers dataset. Once aligned, a threshold magnitude of 0.04 was applied to the differential of the pin position dataset (velocity) to identify the frame at which negative displacement is observed and the relevant time index is reported (T_{pop}). The maximum load was then detected and the time index is reported (T_{max}). The time series data of the load and vacuum data are concatenated around this new reference (T_{max}) to understand the dynamics of the system prior to cup detachment (Figure 4-33 & Figure 4-34).



Figure 4-27: Data Processing flowchart for the acquired pin markers and DAQ data sets

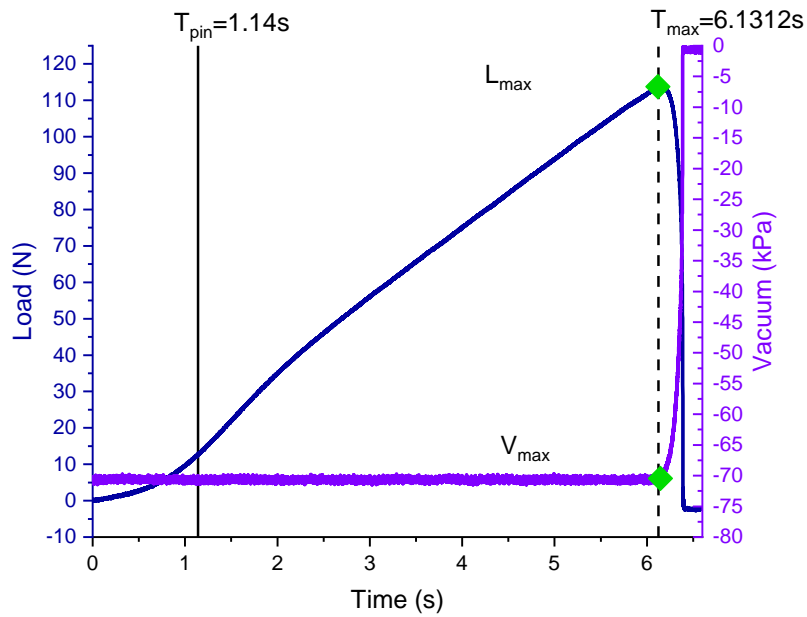


Figure 4-28: Time-series data acquisition of the traction load and vacuum level for the experimental capture at 100Hz

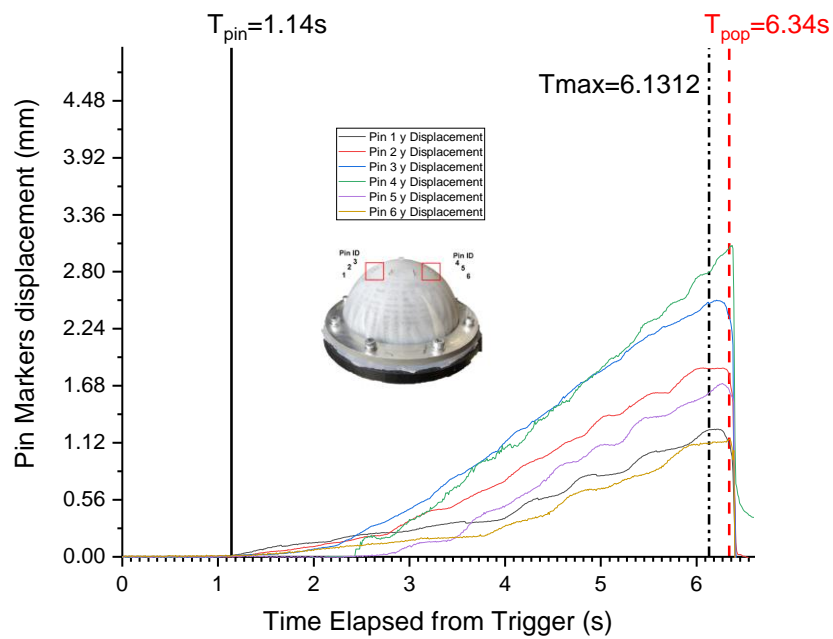


Figure 4-29: Post-Processed Time-series data acquisition of the displacement of the pin markers displacement (mm) data for the experimental capture at 100Hz. T_{pin} shows initial movement of the pin markers, T_{max} is the maximum identified Traction load. T_{pop} is the detected time at which Pop Off arises through threshold setting on the differentiated time series profile of the acquisition of the displacement of the pin markers.

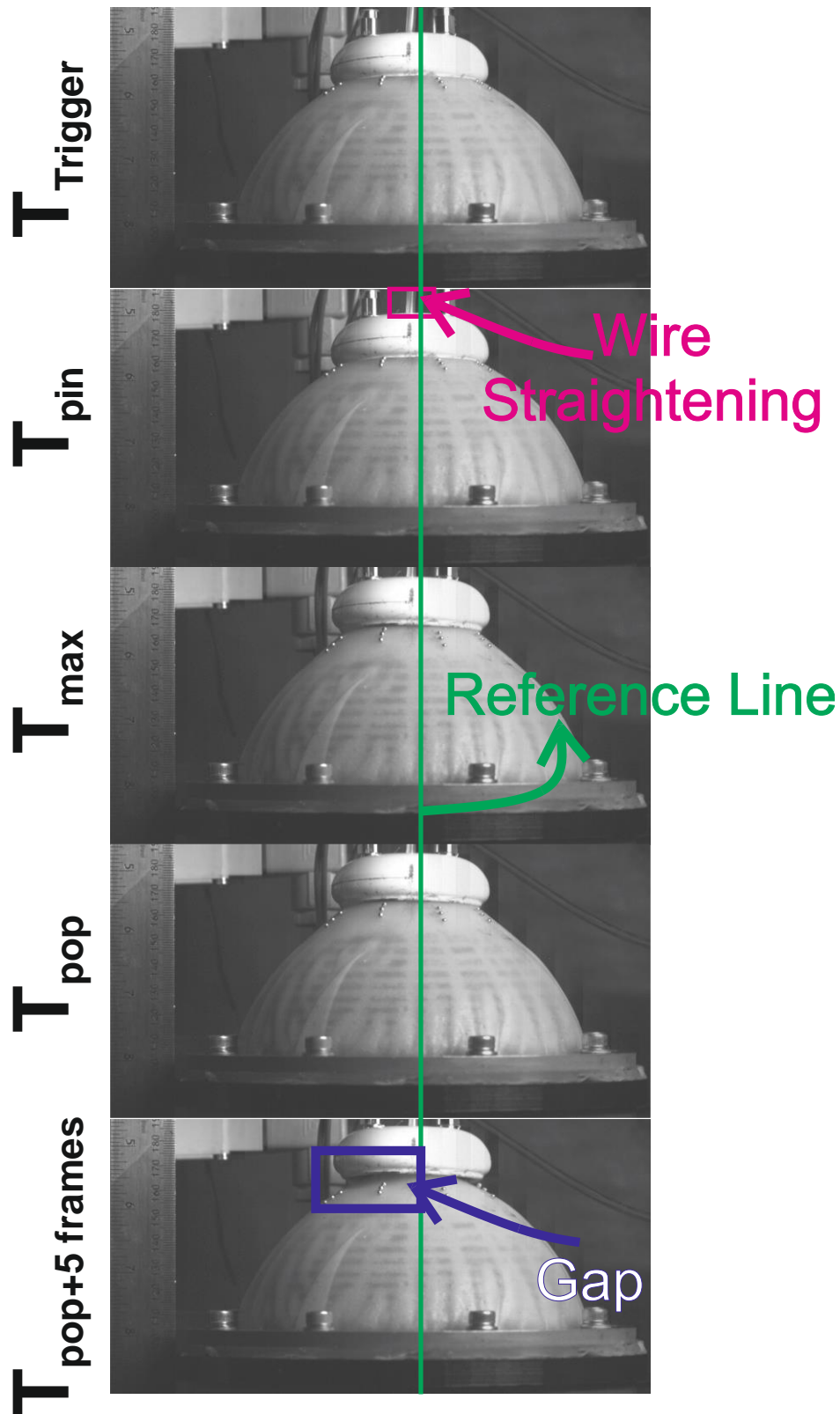


Figure 4-30: Chain of events at different time points registered on the test and the relevant capture image of the test associated with each time stamp described in Figure 4-29.

4.5.2 System dynamics

At the start of the simulation of over traction, there appears to be no movement of the marker pins but an initial load response is observed (Figure 4-30). This is attributed to the tensioning of the wire of the instrumented VAD and confirmed by the acquired images at the time frame of the event (T_{Trigger} and T_{pin}). After the wire stretch, the motion of the place pin markers affirms the uniform straining of the soft elastomeric material until a maximum load is reached (L_{max}) at a specific time (T_{max}) and vacuum (V_{max}). At this point, it is interesting to note the gradual decrease in the vacuum inside the VAD cup (Figure 4-33). Imminently after T_{max} , in this phase, a drastic change in displacement is noticed. A slow exponential decreasing slope in the transient of the vacuum changes suggests the inclusion of a leak affecting the net flow rate of the system. This continues up until T_{pop} . At this moment (T_{pop}) in the time series of test, it is highly likely that the scalp material has lost contact with the VAD cup and a drop in the scalp is observed by the increase in velocity of the side pin markers (Figure 4-31& Figure 4-32). Visual confirmation is provided by the high-speed imagery footage indicates that the likelihood of pop detachment happened in between T_{max} and T_{pop} (Figure 4-34). 10 frames after T_{pop} , the net flow equilibrium inside the cup is completely disrupted and the vacuum has been phased off by the inclusion of atmospheric pressure in the system (Figure 4-34). A distinctive “cup detachment” pop sound is shortly heard.

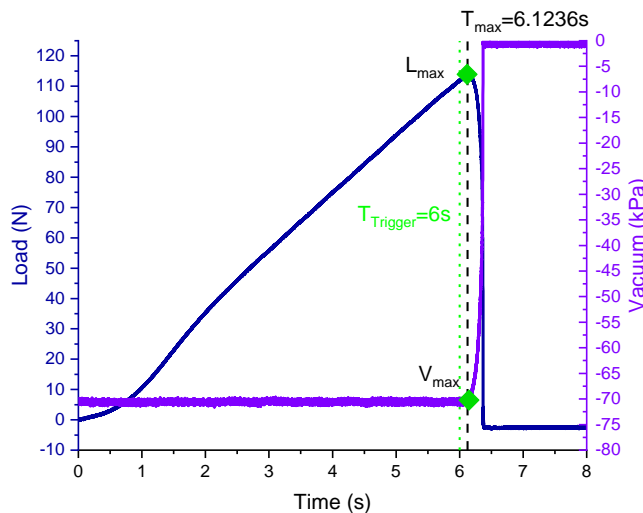


Figure 4-31: Time-series data acquisition of the traction load and vacuum level for the experimental capture at 1600Hz

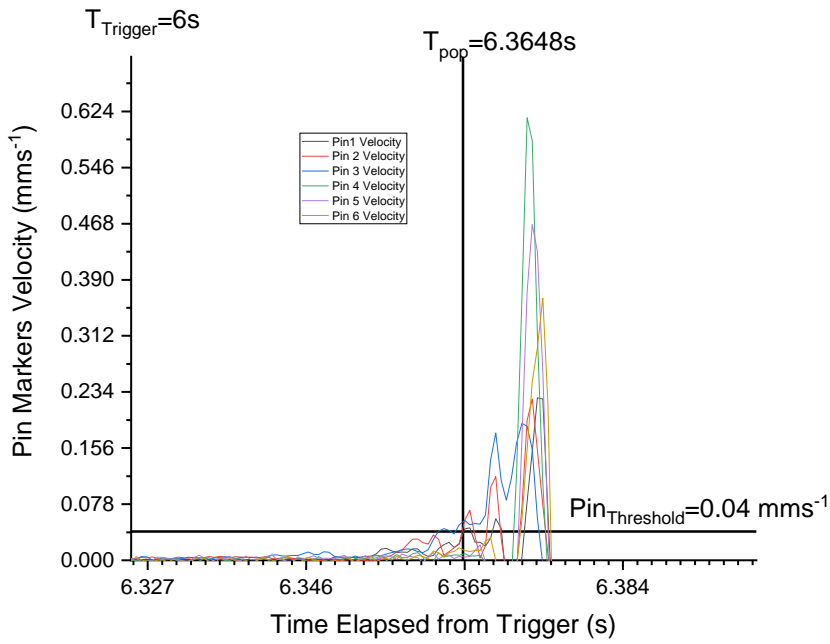


Figure 4-32 : Pin Marker Threshold setting of 0.04mms-1 to detect the Pop-Off event on the differentiated displacement pin markers dataset (velocity) against time elapsed from trigger for the experimental capture at 1600Hz.

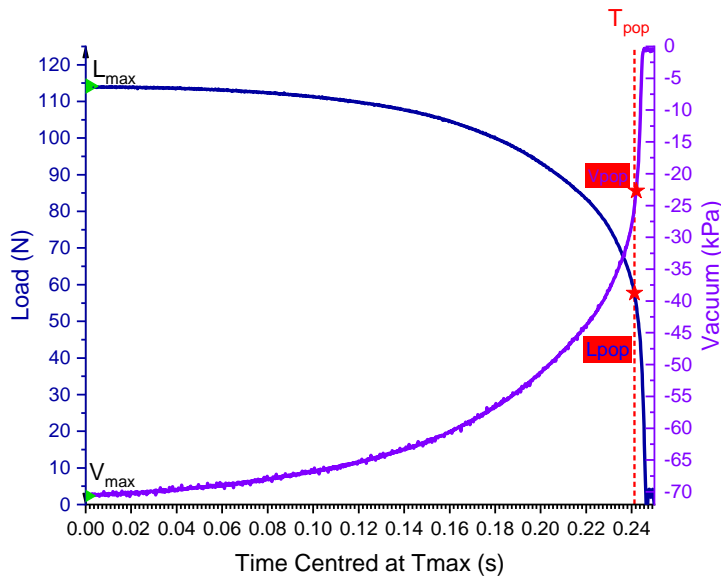


Figure 4-33: Time-series data acquisition centred around T_{max} of the traction load and vacuum level for the experimental capture at 1600Hz. T_{max} is the maximum traction load identified. T_{pop} is the location of the pop-off event. Events of $T_{pop} \pm 10$ frames or $\pm 0.000625s$ are also indicated.

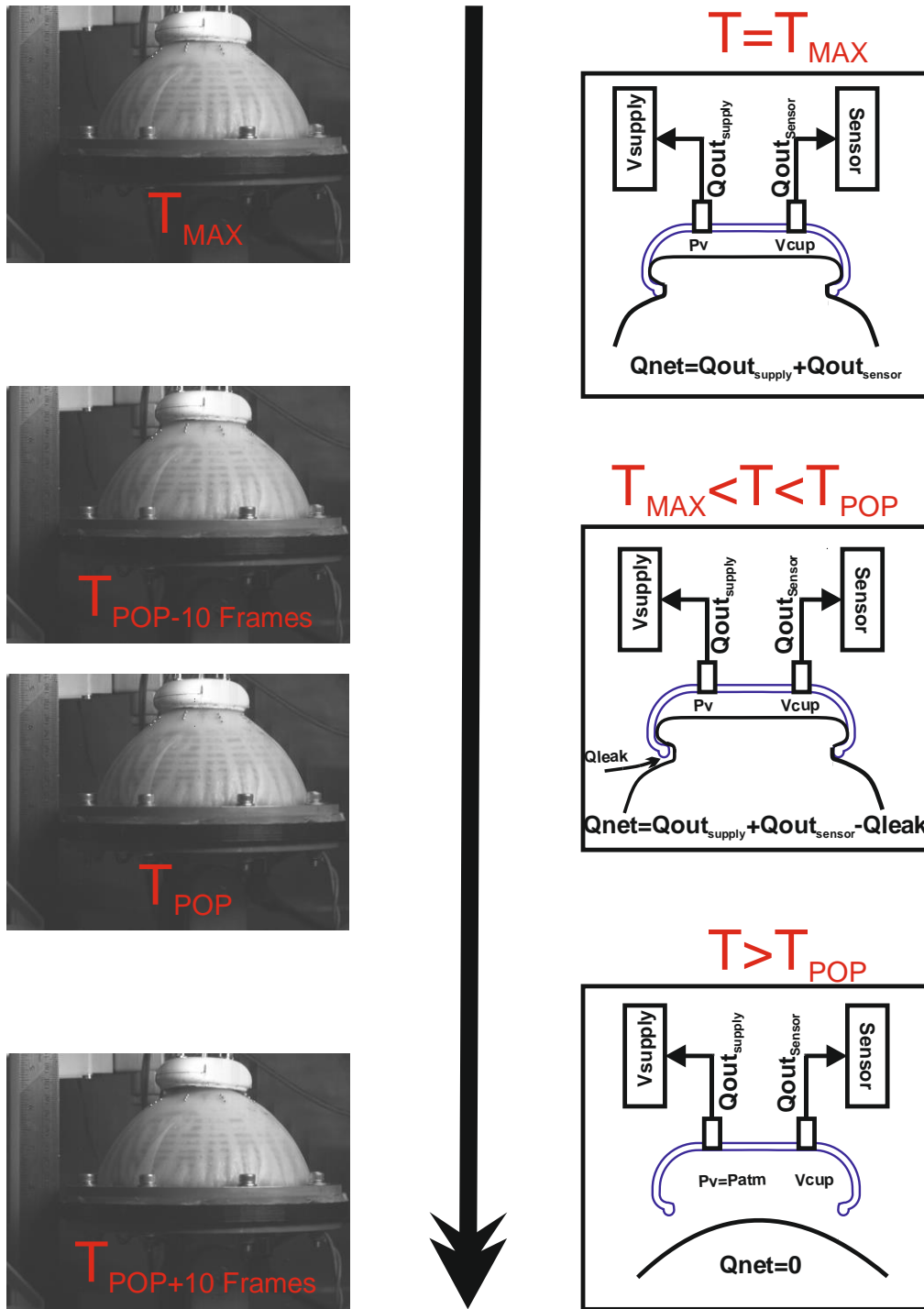


Figure 4-34: Chain of events leading to a cup detachment starting from T_{max} to $T_{pop} + 10$ Frames. The time points registered on the test and the relevant capture image of the test associated with each time stamp described in Figure 4-33. On left a schematic on the net flowrate (Q_{net}) inside the cup is shown at various time events during the test. Q_{out} represents suction flow rate towards the vacuum supply or the sensor. Q_{leak} represents the leak introduced in the closed system.

4.5.3 Repeatability and Reproducibility

An evaluation of the manufacture of the scalps produced with the current fabrication technique was performed. Another test scalp (Scalp 2) was manufactured to be compared against the already manufactured scalp to understand the reproducibility of the acquisition of data with the current experimental set up (Scalp 1). 5 experimental repeats of an over traction were performed on each scalp at a traction speed of 100mmmin^{-1} and at a vacuum level of -70kPa supplied to the pneumatic were performed on each manufactured scalp.

It was expected that with the current fabrication technique that the manufactured scalp will exhibit different elastic profile due to the nature of the compressive nature and control of the embodiment of the textile material inside the scalps. From the experimental results, different profiles of elastic deformation in initial straightening were observed (Figure 4-37). It is interesting to note that minimal variations were recorded around the set of experimental repeats for each tested configuration. A Tukey Simultaneous test for differences of Means was used to identify differences in the means in L_{max} and T_{max} at a 95% confidence interval. The pairwise comparisons in between the different groups of speed shows that there is no difference in the means of L_{max} and T_{max} with high p-value reported across groups ranging from ($p= 0.641$ & 0.826). No observable difference in V_{max} was noticed when the vacuum applied was constant. The details of the statistical analysis can be viewed in the Appendix A3. An interval plot summary of the collected metrics can be viewed in Figure 4-35 & Figure 4-36. The interval displays the mean of the test metrics and a deviation of experimental repeats performed for each evaluated scalp.

There were observable differences during the quantification of the load and vacuum metrics at the time of cup detachment provided by the visual system (L_{pop} and V_{pop}). The latter could have been influenced by the change in scalp material properties but as well from the physical positioning of the cup onto the scalp. This will certainly need to be further verified by automated experimental control and more extensive material characterisation and testing which wasn't possible within the time of this study. Nevertheless, whilst the scalps exhibit different characteristics, the system dynamics of cup detachment using the current methodology remains unaffected as the same chain of events are observed. Metrics such as the load and the vacuum at T_{max} (L_{max} and V_{max}) and the time of at cup detachment (T_{pop}) can be utilised to quantify the dynamics of cup detachment.

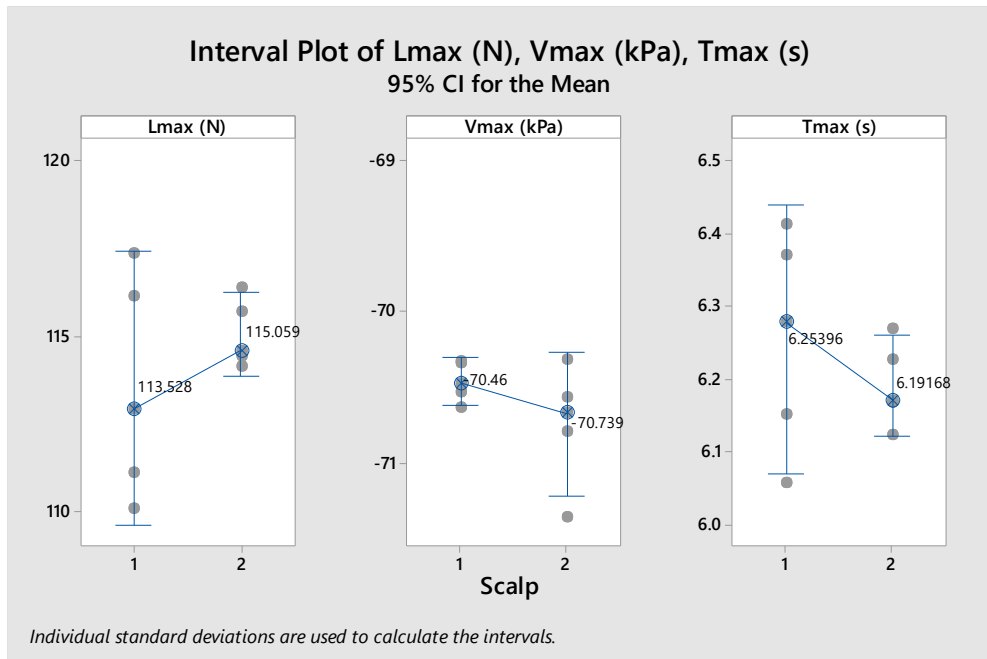


Figure 4-35: Interval plots of L_{max}, V_{max}, and T_{max} for evaluating Two manufactured scalps. Y axis represents the L_{max}, V_{max} & T_{max} and X axis represents tested scalps.

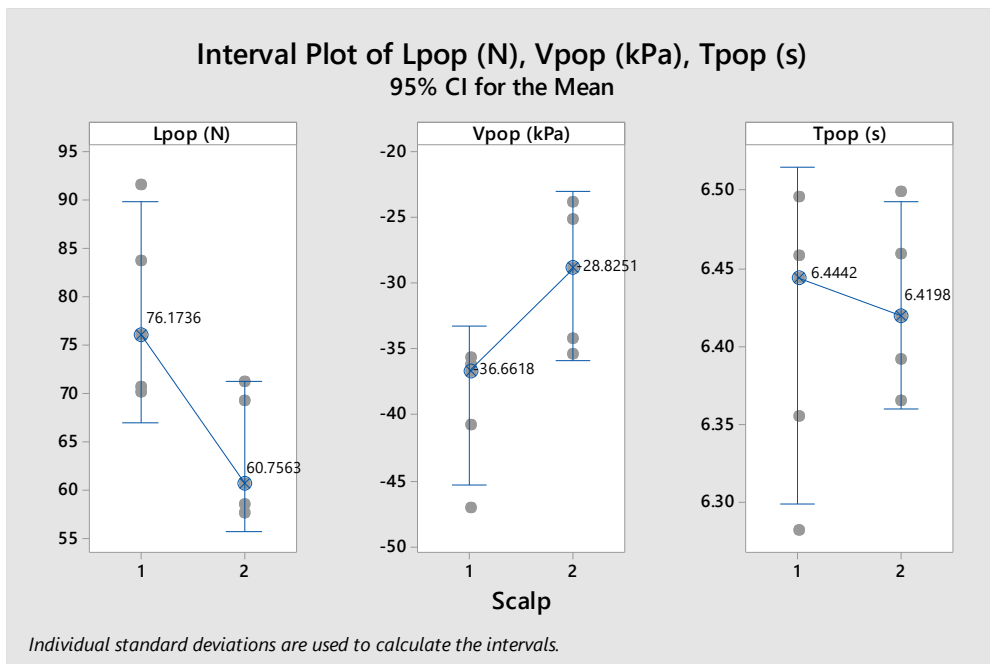


Figure 4-36: Interval plots of L_{pop}, V_{pop}, and T_{pop} for evaluating Two manufactured scalps. Y axis represents the L_{pop}, V_{pop} & T_{pop} and X axis represents tested scalps.

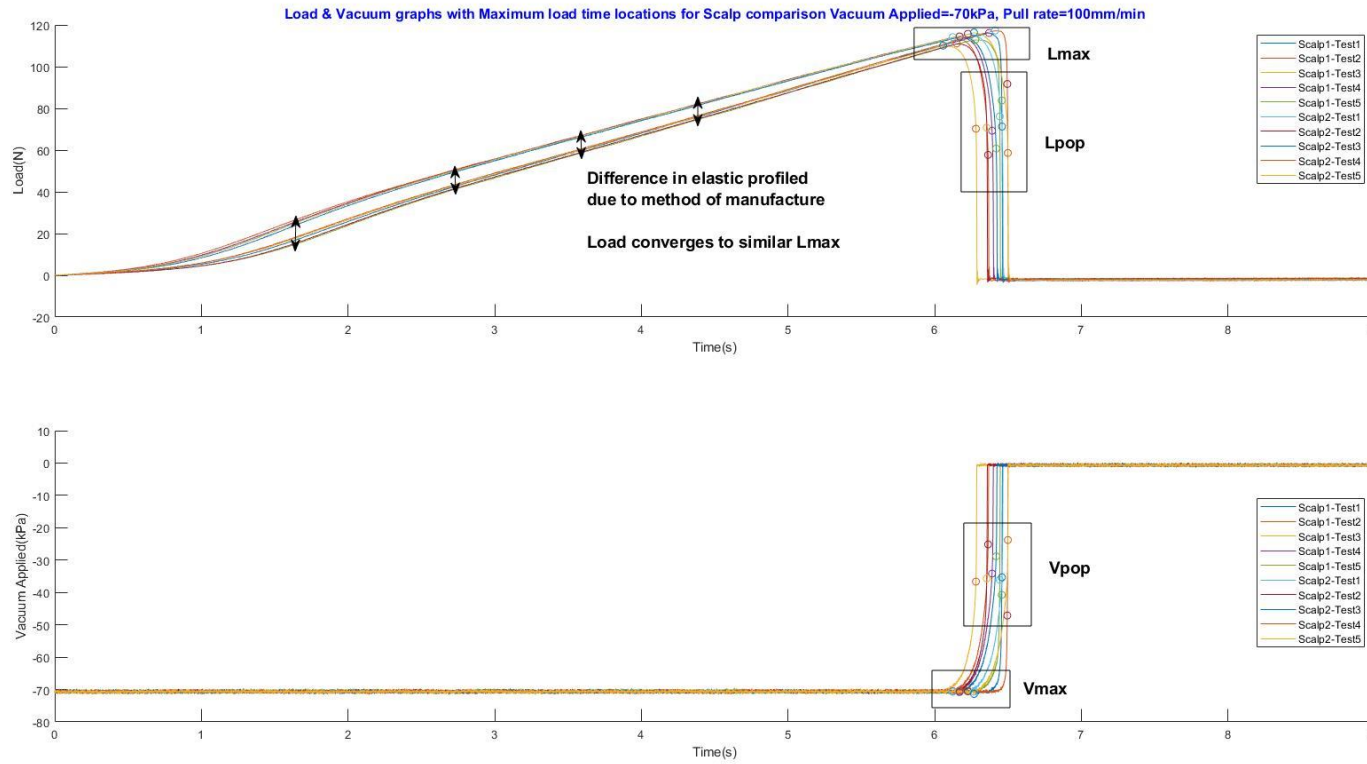


Figure 4-37: Times-series plot of 5 experimental repeats of the load (N) & Vacuum (-kPa) acquired at 5000Hz with load and vacuum markers at T_{max} and T_{pop} reported for the evaluation of 2 scalps.

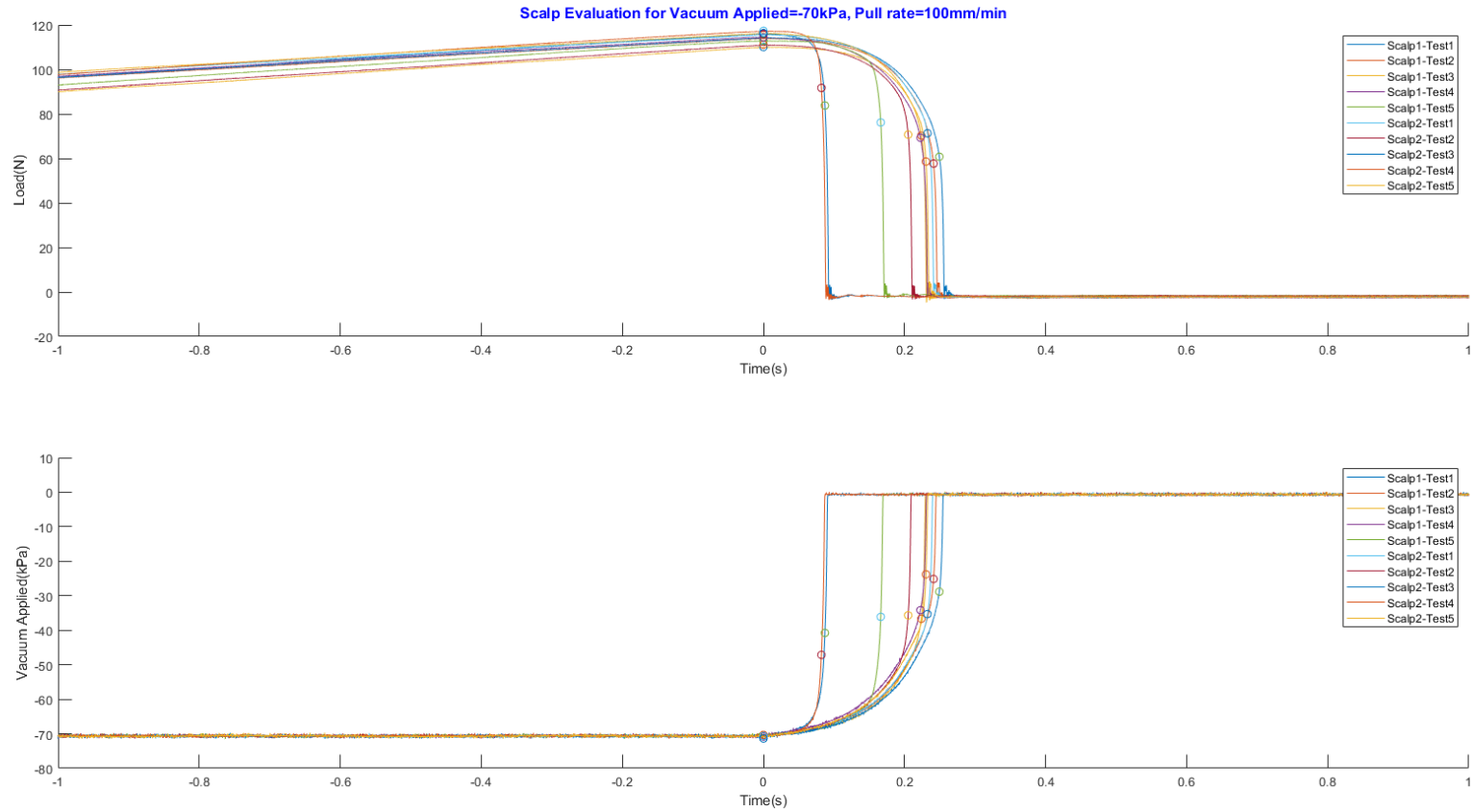


Figure 4-38 :Time series plot in Figure 1 37, centred around T_{max} with load and vacuum markers at T_{max} and T_{pop} reported for the evaluation of 2 scalps.

4.6 Chapter Summary

Following the definition of the system requirements in the previous chapter, an instrumented experimental simulation of VAD has been conceived. First, the design and manufacture of this VAD simulator considered the design and development of a representative head scalp model with a silicone-textile formulate to replicate the mechanical properties of the scalp. The Kiwi Omnicup™ was then used as a template for instrumentation and coupled to a uni-axial tensile testing machine for the simulation of traction experiments. The control, sensing & data acquisition aspects were devised to control and provide sensory feedback on the vacuum inside the VAD cup. Pin markers were placed onto the head scalp model, combined with a high-speed camera system provide a qualitative tracking of scalp deformation during mechanical simulation of obstetric traction. Inherently, this was used to aid in the visual detection of cup detachment. In combination with measurement datasets of the load and vacuum levels acquired by the acquisition unit, the dynamics of cup detachment were then informed. The evaluation of the measurement system has shown that a simulated obstetric VAD traction produces a characteristic response from which a number of key metrics can be determined. Experiments will be devised from the proposed methodology to investigate the clinical impact of system variables including the applied traction speed, magnitude of vacuum imposed, and changes in the geometry of the VAD cup and pneumatic architecture in the next chapter.

Chapter 5

Experimental Evaluation of VAD Systems

This chapter details the experimental approach taken to identify clinical and mechanical factors capable of affecting the propensity of cup detachment. Following the insight provided into the dynamics of cup detachment in the previous chapter, the next objective of this research consists of assessing the performance of current VAD cup systems with the VAD simulator to provide engineering recommendations into the conception of an atraumatic device. Different experimental configurations surrounding the instrumented VAD cup will then be evaluated to understand their contribution to the failure dynamics with VAD simulator developed in the previous chapter. The outcomes will be evaluated to inform engineering actions which can improve performance of VAD and reduce trauma occurring due to unintentional cup detachments.

5.1 Investigation of Clinical and Mechanical Factors affecting VAD Performance

A range of different factors are recognised to affect the performance of VAD delivery (1). For instance, clinical training is fundamental to ensure safe and consistent application of VAD. There have been considerable efforts to improve the proficiency of obstetric trainees through simulation-based workshops focussed on cup placement and the theory of vacuum delivery(21). However, there remains a lack of basic knowledge into the mechanics of VAD use to inform best practice, in particular understanding what constitutes safe application of a vacuum and tractive forces.

The design of the VAD cup system can affect the performance in achieving and retaining physical contact with scalp upon application of a vacuum. Commercially, variants of VAD pneumatic architecture consists of either electric or manual supply of vacuum (Hand/Foot Pumps). Electric pumps for VAD use (Medela Basic) can provide a more regulated, faster and steady supply of vacuum at high flow rates (30L/min) and in combination with the large residual volume (Reservoir) can help compensate for air leakages. There still remains unverified commercial claims on whether such pneumatic components can reduce rate of cup detachment and are more beneficial for safely performing VAD. In addition, those systems are often thought to be bulky and impose constraints to the healthcare professional as assistance would be required when clinical events which require vacuum level readjustments, such as cup malposition or trapped maternal tissue ,occur. Alternatively, hand operated pumps as utilised in Mityvac or the Utah Medical (UM) VAD systems can be regarded as more cost beneficial but require clinical preparation such as sterilisation. Integrated hand pumped traction system, for example, the Kiwi Omni cup has been the latest commercial development known in the VAD market but reports of high rates of cup detachment puts concern on the optimisation of its design to resist cup detachment albeit being clinically intuitive (30.1%) (86). There needs to be more objective evidence in recognising the contribution of the concerning VAD pumping components as it can have a significant impact on the dynamics of cup detachment.

With, the mechanics of the cup-scalp interlock requiring improved definition, the importance of the mechanical interlock created by the recessed edges of the cup design is crucial to the performance of VAD. Furthermore, a better understanding of how clinical factors influence the dynamics of cup detachment can help device manufacturers to develop more robust training material for clinicians. This can

raise awareness in the limitation in performance of those medical devices in different conditions and make the latter more adept in their decision-making process to perform safer VAD.

Subsequently, clinical factors and mechanical factors such as cup geometry or changes in the volumetric attributes of the VAD system will be added to the scope of study; to provide a quantifiable comprehension of how they affect device performance (ability to apply traction) and clinical outcome (i.e. scalp trauma).

5.2 Parametric experimental Study

In this section, a parametric experimental test protocol was developed based around the investigation of the clinical and mechanical factors. The study of clinical factors comprised of an investigation around the applied vacuum magnitude inside the instrumented VAD, speed of traction and the frictional attributes of the maternal environment. The study on mechanical factors focused on observing effect on changes in cup geometry of the instrumented VAD cup and simulation of various pneumatic configurations adopted in current VAD devices. The simulation of the traction will be based on the similar methodology as introduced in Section 4.4.2. A depiction of the test plan can be seen in Figure 5-1 and further details will be provided in the sub-sections.

5.2.1 Test Protocol

Experimental tests were performed according to the test protocol matrix highlighted above on the developed VAD simulator and its alteration to fit the requirements of each individual study as detailed in this section (Table 5-1). Five experimental repeats (n=5) of each study were performed on the developed VAD simulator for each tested configuration, using the same experimental methodology introduced in the previous chapter (Section 4.4.2). As previously utilised during the understanding of chain of events leading to a cup detachment with the current set up, the rate of capture of the visual system was set to 1600Hz. Any notable deviation to the experimental study will be listed as a deviation. The test protocol matrix is summarised in Table 5-1 and the study conditions of the vacuum level and the traction speed were chosen to meet the clinical requirements in Section 3.4.

Table 5-1: Test protocol matrix during this parametric study of clinical and mechanical factors.

Study ID	Investigation Title	Type of Factor	Pneumatic Configuration ID	Set Vacuum (kPa)	Speed of Traction (mm/min)	Cup Geometry	Frictional Attribute	Head Scalp Model
1	Vacuum magnitude inside the VAD	Clinical	1 (State 1)	Multiple ¹	100	Unchanged	Dry	1
2	Impact of Speed of Traction	Clinical	1 (State 1)	-70	Multiple ²	Unchanged	Dry	1
3	Changes in Cup Geometry	Mechanical	1 (State 1)	-70	100	Multiple ³	Dry	1
4	Frictional Attributes of the Maternal Environment	Clinical	1 (State 1)	-70	100	Unchanged	Multiple ⁴	Deviation ⁴ Scalp2 used
5	Changes in Pneumatic VAD Configuration	Mechanical	Multiple ⁵	-70	100	Unchanged	Dry	Deviation ⁵ Scalp2 used

1 Refer to Section 5.2.2

2 Refer to Section 5.2.3

3 Refer to Section 5.2.4

4 Refer to Section 5.2.5

5 Refer to Section 5.2.6

Investigation of Clinical & Mechanical Factors capable influencing VAD Performance

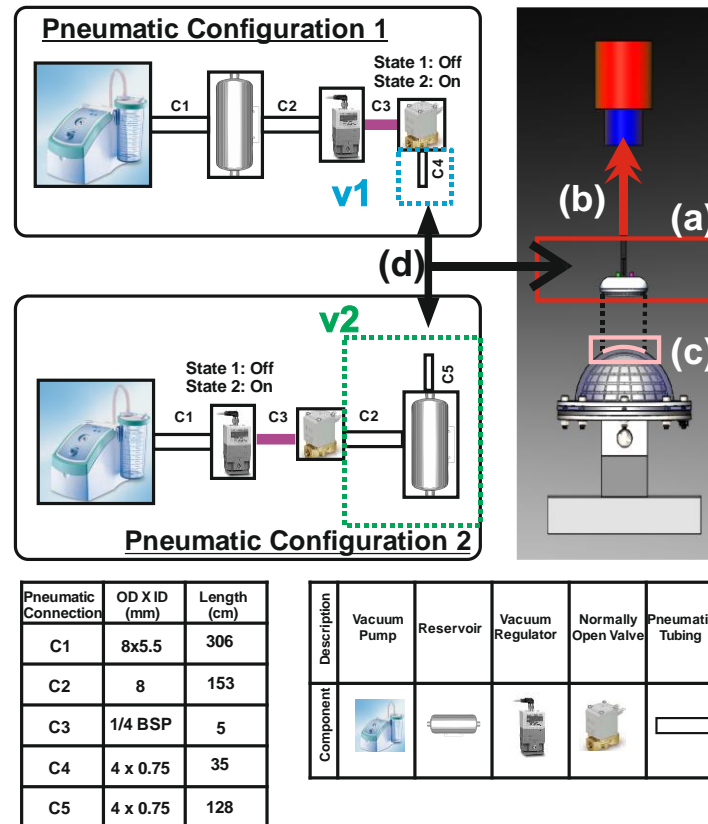


Figure 5-1: Pneumatic Test configurations for the study of the regulated buffered vacuum source. The configuration 1, state 1 is the control simulations for all the cases in all presented studies. (a)- relates to changes in cup geometry , (b)-relates to changes in traction speed, (c)-relates to addition of lubricants on the surface of the foetal head scalp, (d) relates to pneumatic changes in the control & delivery of the vacuum by the pneumatic unit.

5.2.2 Study 1: Vacuum magnitude inside instrumented VAD

The experimental investigation into the physical simulation of over-traction at a set tractive speed of 100mmmin^{-1} will be performed at 4 different vacuum levels (-55,-60,-65 & -70 kPa as control) set using the LabVIEW VI and delivered by the pneumatic controller unit (configuration 1 state 1) to the instrumented VAD set up with unchanged cup geometry. The test configuration at -70kPa will be used as control for the data analysis of the collected results. The aim of this study is to understand to develop a working principle of how the vacuum magnitude influences the retention of the chignon and influence the dynamics of cup detachment.

5.2.3 Study 2: Traction Speed




The experimental investigation into physical simulation of over-traction at different traction speed (50,100 as control,150, 200 mmmin^{-1}) and with a set vacuum level of -70 kPa set using the LabVIEW VI and delivered by the pneumatic controller unit (configuration 1 state 1) to the instrumented VAD set up with unchanged cup geometry. The test configuration at 100mmmin^{-1} will be used as control for the data analysis of the collected results. The aim of this study is to understand to develop a working principle of how the traction speed imposed by the obstetrician can contribute to the retention forces of the chignon and influence the dynamics of cup detachment.



5.2.4 Study 3: Changes in Cup Geometry

In this study, the effect of the mechanical interlock will be investigated based on the depiction in Figure 5-2. In the absence of a mechanical interlock the maximum retention forces (F_{popoff}) would be reduced as the forces due to the contribution of the mechanical interlock (F_m) will be impacted. To investigate into this working principle, two inserts were designed and manufactured using PLA (Ultimaker Extended 2+) to limit the coverage of the mechanical interlock thereby reducing the effects of the term F_m . When the inserts are combined with the unchanged VAD cup, the volume capacity of the original cup (V_{cup}) and impacts the expected surface scalp contact area upon chignon built up after vacuum exposure (SCA). Once inserted, the percentage difference in SCA and V_{cup} to the unchanged VAD configuration are 2.3% & 10.4 % (Insert A) and 5.4% and 13.6% (Insert B). See Appendix B1 for the profile of the scalp expected in the presence of the Inserts. The design intent of insert B can be considered as worst case since

it limits the coverage of the mechanical interlock the most. The provided model The experimental investigation of the changes in cup geometry was performed at set tractive speed of 100mmmin⁻¹. An applied vacuum level of -70 kPa was first set using the LabVIEW VI and delivered by the pneumatic controller unit (configuration 1 state 1) to the instrumented VAD set up with different Cup geometry VAD configurations (Table 5-2). The test configuration with the unchanged cup geometry will be used as control for the data analysis of the collected results.

Table 5-2: Cup profile tested with their cross section, surface area, contact volume and schematic upon combination with the respective insert.

	Cup geometry Configuration		
	Unchanged (Control)	Insert A	Insert B
Cup Profile Schematic			
Scalp contact Area excluding sponge volume (mm²)	6634.23	6481.20	6278.61
% Change to Unchanged Configuration		2.3	5.4
Cup Volume excluding sponge volume (mm³)	22939.03	20558.08	19817.88
% Change to Unchanged Configuration		10.4	13.6

				Cup geometry Configuration		
		Unchanged (Control)	Insert A	Insert B		
Inserts Fabrication						

VAD Cup Geometry Changes

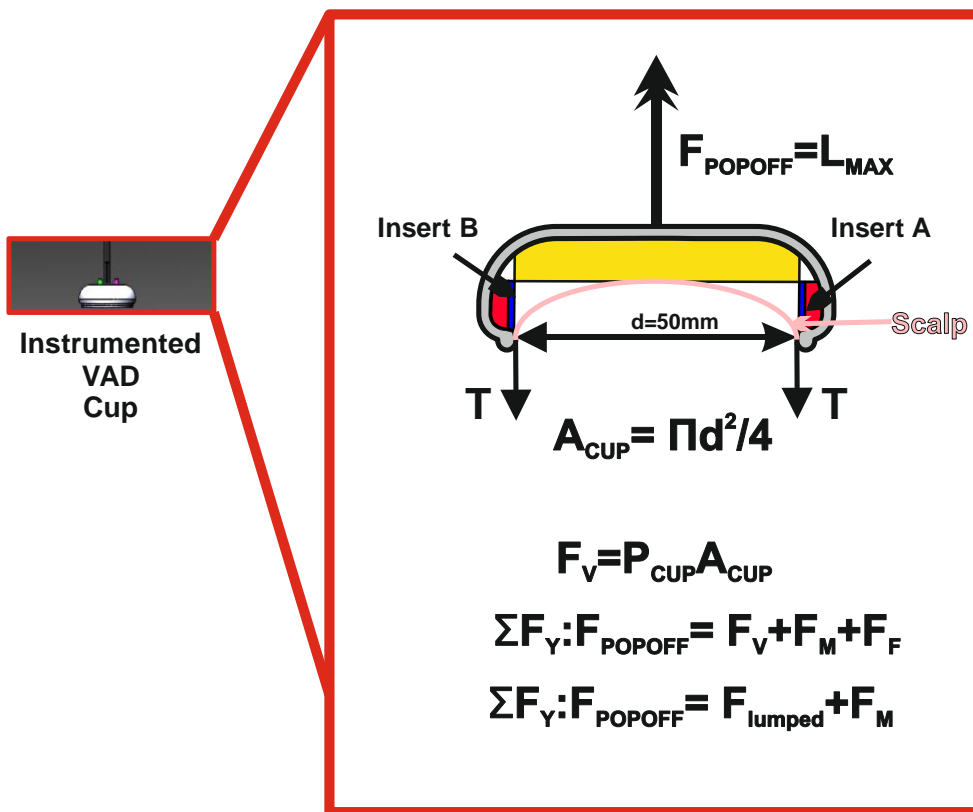


Figure 5-2: Cup Geometry changes in instrumented VAD. In diagram annotations shows the cup geometry changes upon insertion of fabricated inserts to reduce the contact area of the scalp and volume capacity of the VAD cup. In the displayed constitutive equation, the impact of F_m will be investigated through different addition of inserts. F_{lumped} will contain the terms (F_v : Force due to the applied vacuum and F_f : Force due to frictional effects). T represents the Tension in the scalp.

5.2.5 Study 4: Frictional Attributes of the Maternal Environment

This experimental study concerned the assessment of the frictional impact of 5 different lubricants applied onto the surface of the foetal head scalp model based on the depiction shown in Figure 5-3. The impact of sliding friction (μ_k) will be studied since it can affect the tangential forces present on the contact surfaces of the cup and the foetal scalp (F_f). Since the maternal environment consists of vaginal discharge, foetal matter and blood, a variety of lubricated formulations were applied on the foetal head scalp model to simulate the frictional attributes of the maternal environment as defined in Section 3.3. The latter consist of a leak detector, a silicone based lubricant, aqueous surfaces (water misted and water soaked VAD sponge) and a commercially available gynaecological lubricant as used in VAD (Table 5-3). A physical simulation of over-traction at different traction speed of 100 mmmin^{-1} and at a vacuum level of -70 kPa set using the LabVIEW VI and delivered by the pneumatic controller unit (configuration 1 state 1) to the instrumented VAD set up to initiate contact with the pre-conditioned foetal head model. After each test, the surface of the scalp was cleaned with distilled water and wiped dry. The dry test configuration with no lubrication will be used as control performed on Scalp 1 for the data analysis of the collected results. During the performance of the studies, a deviation was observed during the testing of Lubricant A, B and D. For those tested configurations, the dry test configuration with no lubrication will be used as control performed on Scalp 2 for the data analysis of the collected results (Table 5-3).

Table 5-3: List of lubricants used during the study of assessing the impact of lubricant on the traction force

Lubricant ID	Lubricant Description	Lubricant Manufacturer	Scalp Tested
A	Leak Detector Spray (Aqueous blend of surfactants)	Rocol™ Leak Detector (115)	2
B	Silicone based Lubricant	Servisol® Super 40 (116)	2
C	Distilled Water mist	Vaporiser with Milli-Q Distilled water (117)	1
D	Water based Lubricant and additives	Pelican™ PELIJelly Lubricant (118)	2

Lubricant ID	Lubricant Description	Lubricant Manufacturer	Scalp Tested
E	Distilled water Soaked Sponge	Kiwi Omni Cup™ Sponge soaked in Milli-Q Distilled Water for 30 Seconds (117)	1
Dry	Control- No Lubricant	N/A	1 & 2

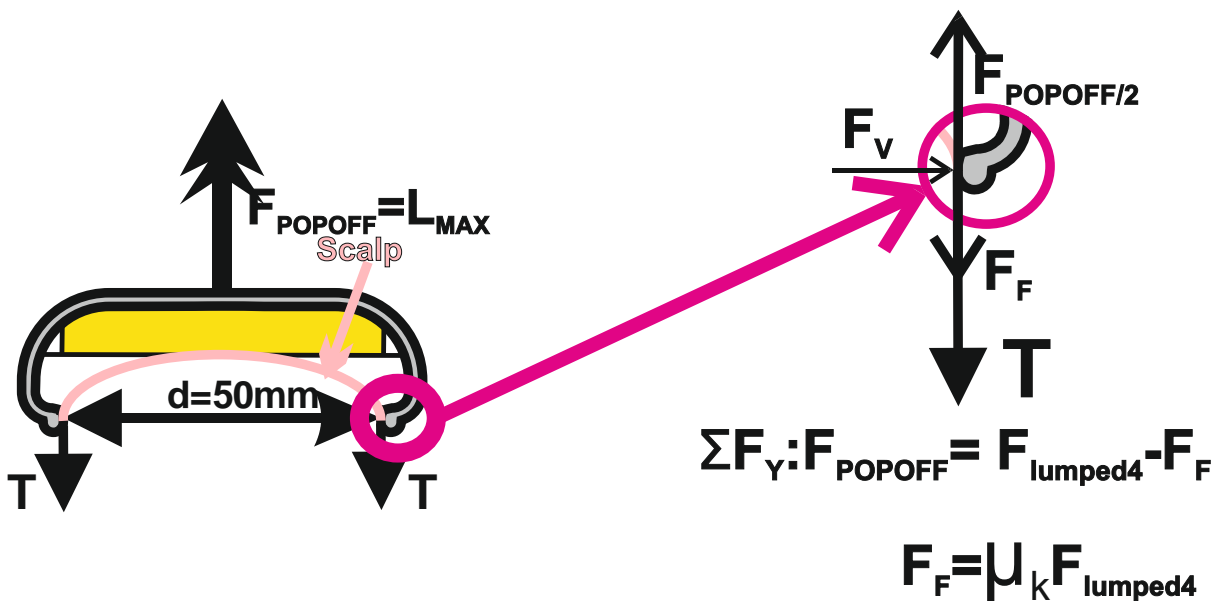


Figure 5-3: Investigation of the Frictional Attributes of the maternal environment using different formulation of lubricants (low viscosity to high viscosity) to provide an insight the tribology of the cup interaction. (μ_k -Sliding Coefficient of Friction). In the displayed constitutive equation, the impact of F_F will be investigated through application of different lubricant formulations on the foetal head scalp model. F_{lumped} will contain the terms (F_V :Force due to the applied vacuum and F_m :Force due to mechanical interlock). T represents the Tension in the scalp.

5.2.6 Study 5: Changes in Pneumatic VAD Configuration

This study considered an investigation of the volumetric flow rate effects of the pneumatic architecture (Q_{net}) adopted by current commercially available VAD design displayed in Figure 5-4. The connection of the pneumatic components in the first state of the first pneumatic configuration are organised in such a way to investigate the impact of using a continuous supply of regulated vacuum to the instrumented cup (V1). This test configuration will be used as control to this experiment. The second state of that pneumatic configuration emulates the

simulation of a vacuum and atypical to instrumented hand-help pump systems as shown in Figure 2-9. This involves an initial development of the chignon and then turning on the normally open solenoid valve prior to the over traction experiment.

The connection of the pneumatic components in the first state of the second pneumatic configuration features a continuous supply of regulated vacuum (V2) but connected in line with a volumetric tank (2L reservoir) can buffer the dynamics by deferring the timing of cup detachment due to a greater volumetric flowrate (capable of compensating for leaks) atypical of an electric pump system shown in Figure 2-10. The sizing of the pneumatic lines was chosen due to physical constraint of the test bed in the tensile testing machine (E10000) affecting the optimal placement of the pneumatic components.

The second state of that pneumatic configuration offers the similar characteristics as the second state of the first configuration but with a bigger residual volume of buffered vacuum. This experiment was performed on scalp 2 due to deviation during the study addressed in section 5.2.5. The tests were performed at an applied pull rate of 100 mmmin^{-1} and with a set vacuum level of -70 kPa set using the LabVIEW VI and delivered by 2 configuration pneumatic controller unit in 2 controllable states to the instrumented VAD set up with unchanged cup geometry (Figure 5-1).

Table 5-4: The pneumatic configuration and the effective volume after valve based on the schematic shown in Figure 5-1 & Table 5-1.

Pneumatic ID	Pneumatic configuration	State	Control Volume (CV) (cm ³)
1	1	1	0.0015463
2	1	2	
3	2	1	165.49899
4	2	1	

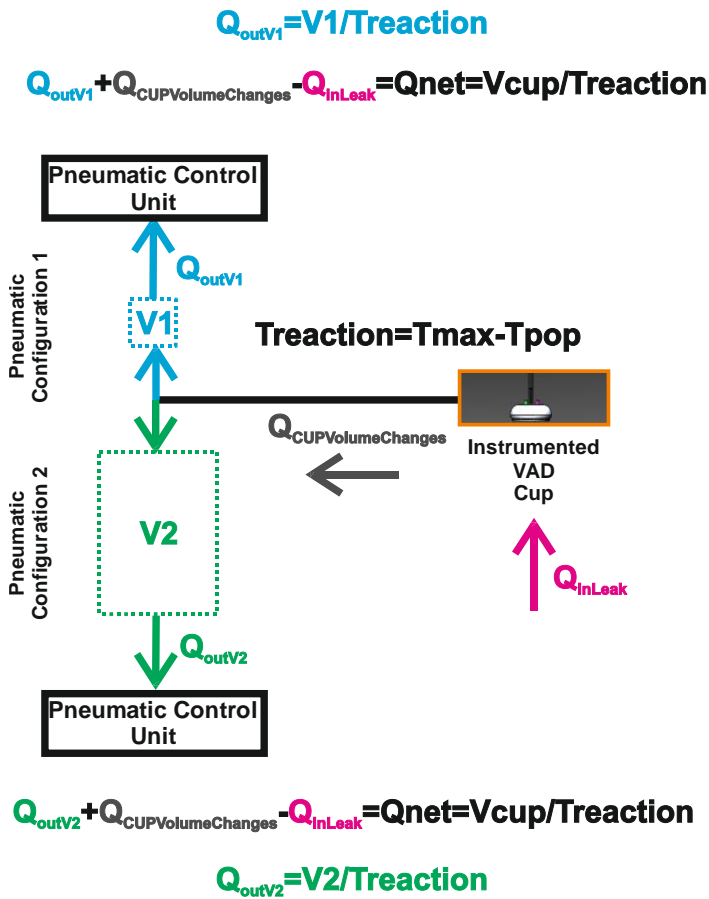


Figure 5-4: Pneumatic Architecture volumetric flow rate changes as a function of volume

5.3 Experimental Results

The full Load-Time and Vacuum-Time traces with an indication of the Load & Vacuum (L_{max} , V_{max} & L_{pop} , V_{pop}) at their respective time events (T_{max} & T_{pop} respectively) and the representative interval plots of the test metrics used for the statistical analysis can be viewed in Appendix B2. Representative time centred series centred plot at maximum traction time ($T = T_{max}$): Load-Time and Vacuum-Time traces during the typical simulation of an over traction performed per the presented Test Methodology in the previous chapter (Section 4.4.2), are shown in Figure 5-5, Figure 5-6, Figure 5-7, Figure 5-8 and Figure 5-9 (Pneumatic Configuration 1) & Figure 5-10 (Pneumatic Configuration 2) for each concerned study and their concerned test configurations testing according to the test protocol matrix in Table 5-1. The results will be evaluated in the next section. After the evaluation of the results, a discussion of the experimental observations based on the clinical and mechanical factors evaluated in this experimental study will be made.

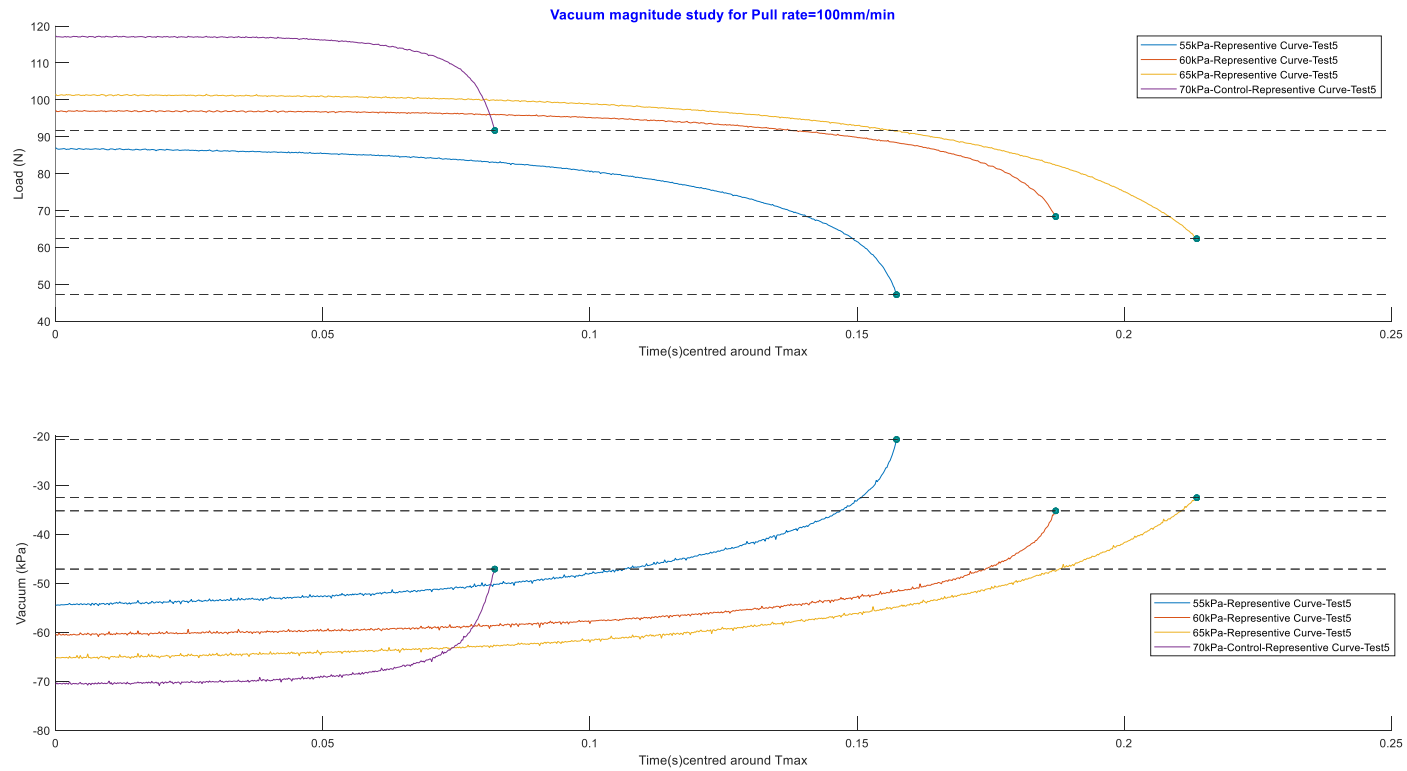


Figure 5-5: A representative time centred series centred plot at maximum traction time ($T=T_{max}$) of the sensory output of the load and the vacuum detected by the VAD simulator with graph markers indicated at T^*_{Pop} ($T=T_{max}-T_{pop}$) for each Test configuration in Study ID 1

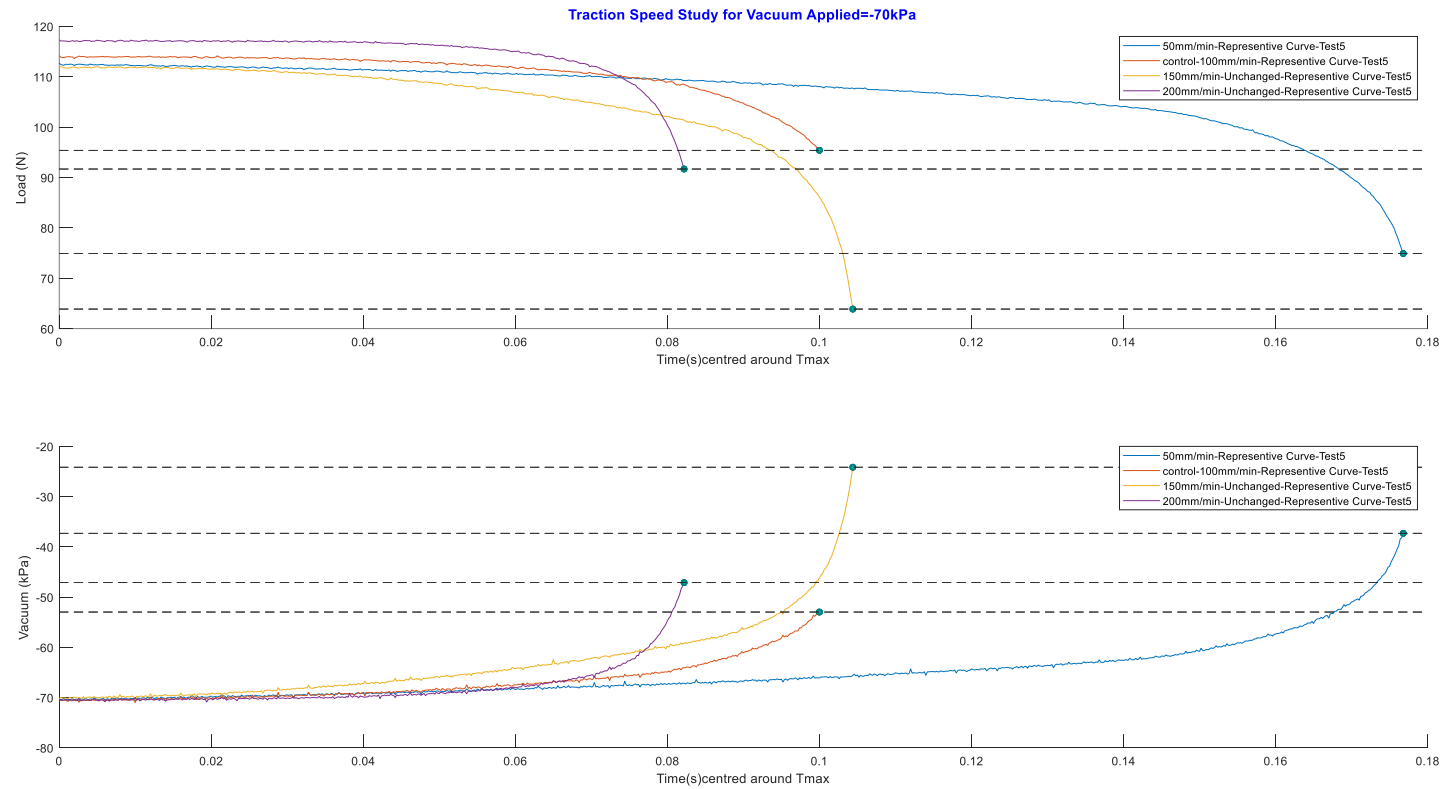


Figure 5-6: A representative time centred series centred plot at maximum traction time ($T=T_{\max}$) of the sensory output of the load and the vacuum detected by the VAD simulator with graph markers indicated at T^*_{Pop} ($T=T_{\max}-T_{pop}$) for each Test configuration in Study ID 2

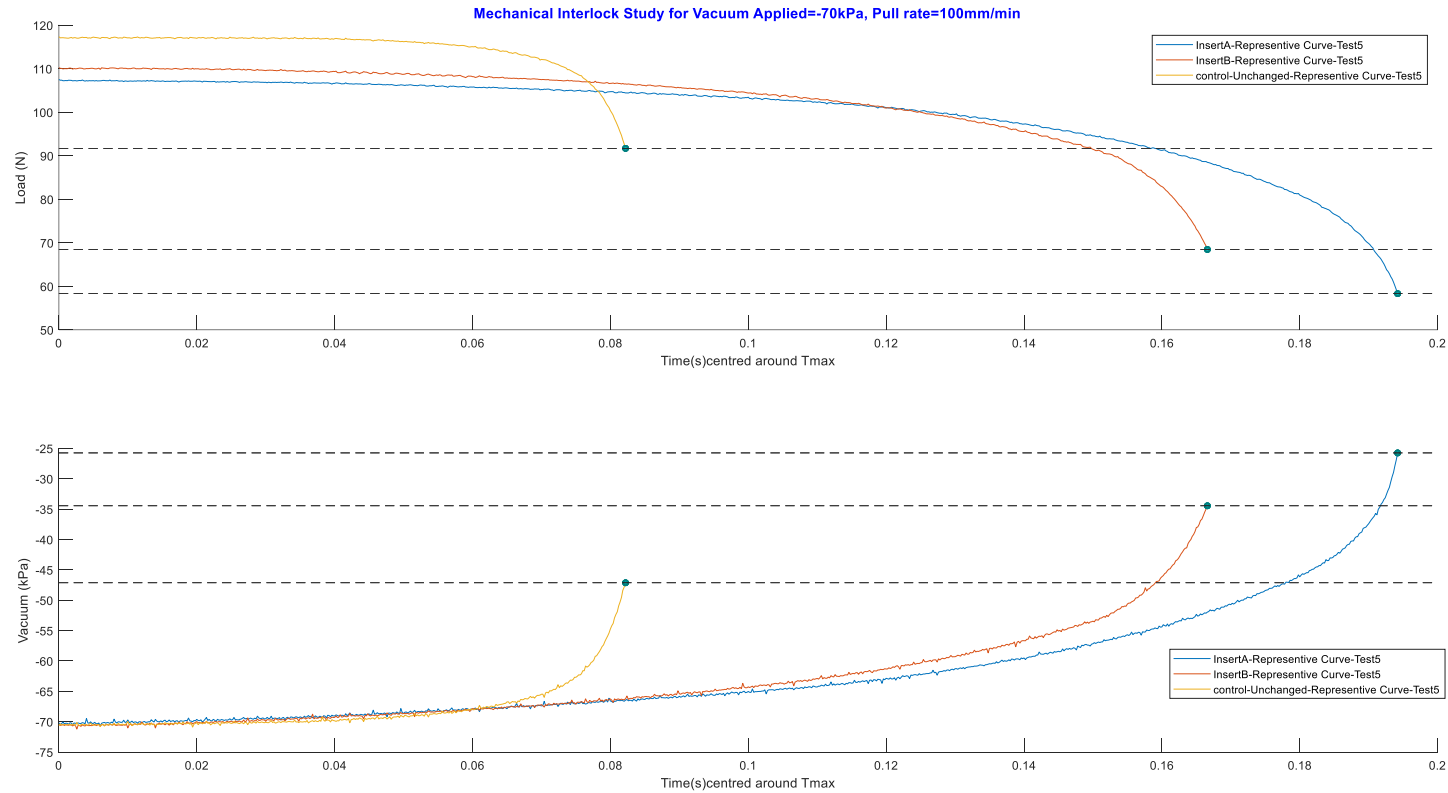


Figure 5-7: A representative time centred series centred plot at maximum traction time ($T=T_{max}$) of the sensory output of the load and the vacuum detected by the VAD simulator with graph markers indicated at T^*_{Pop} ($T=T_{max}-T_{pop}$) for each Test configuration in Study ID 3

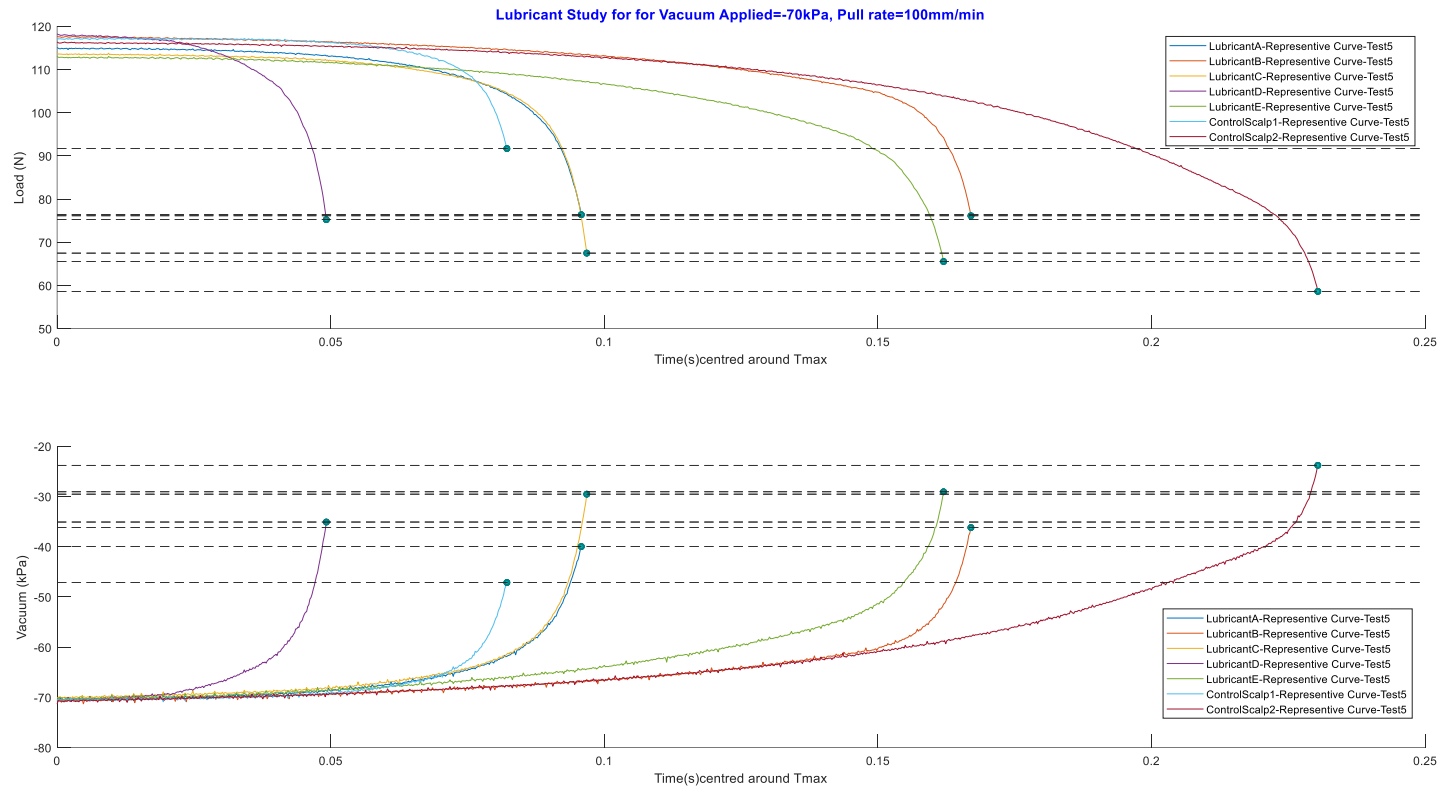


Figure 5-8: A representative time centred series centred plot at maximum traction time ($T=T_{max}$) of the sensory output of the load and the vacuum detected by the VAD simulator with graph markers indicated at $T+Pop$ ($T=T_{max}-T_{pop}$) for each Test configuration in Study ID 4

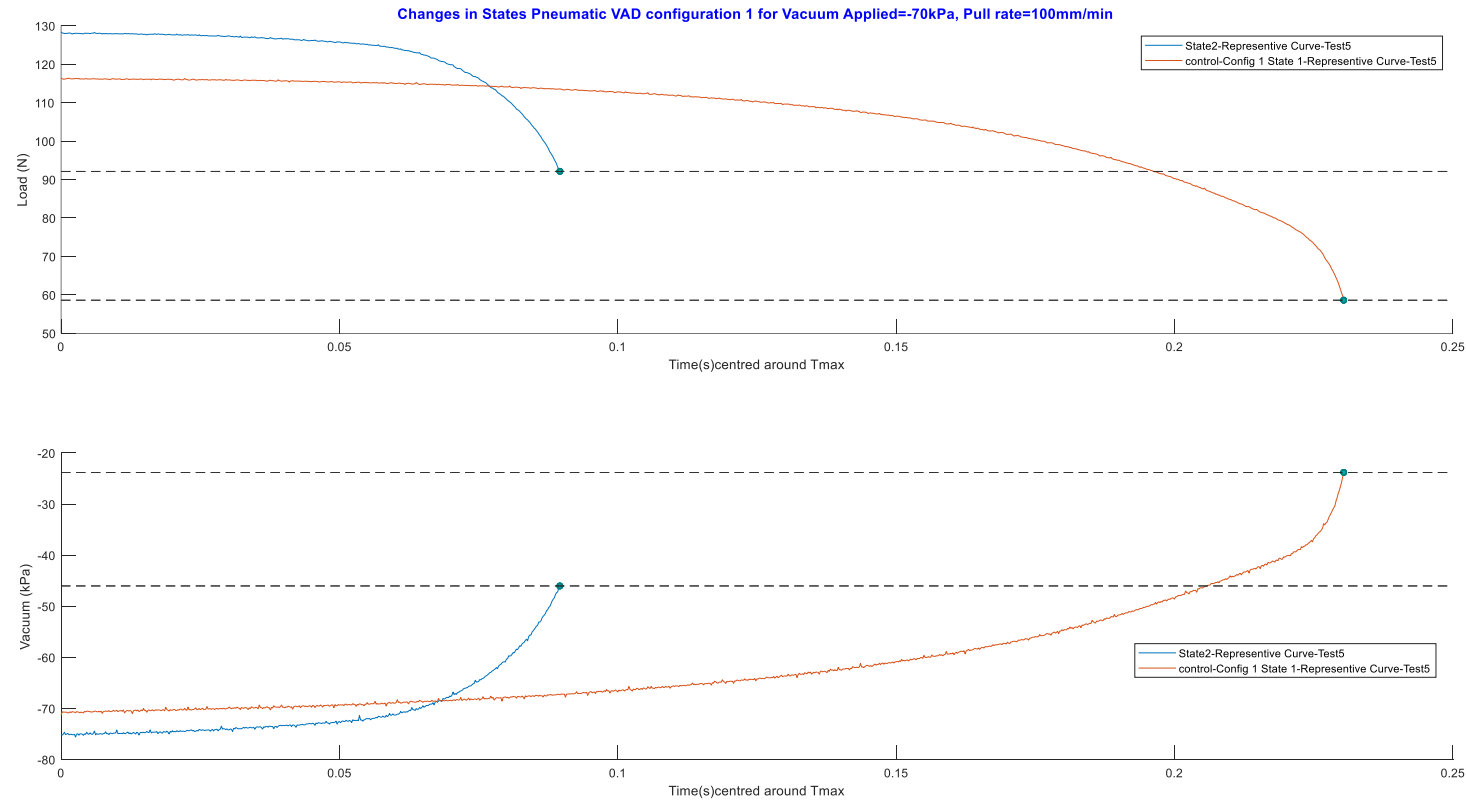


Figure 5-9: A representative time centred series centred plot at maximum traction time ($T=T_{max}$) of the sensory output of the load and the vacuum detected by the VAD simulator with graph markers indicated at T^*_{Pop} ($T=T_{max}-T_{pop}$) for each Test State in Pneumatic VAD configuration 1 in Study ID 5

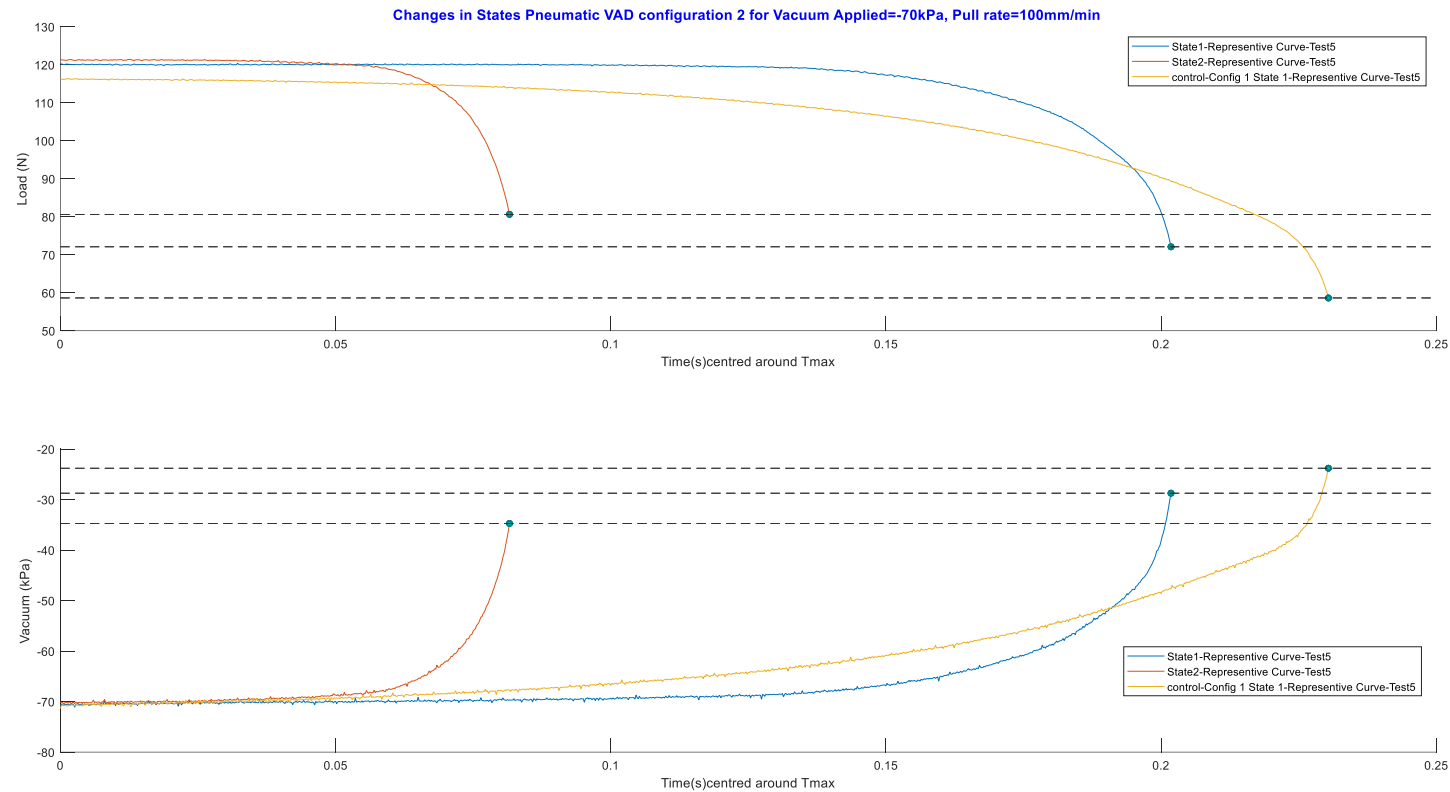


Figure 5-10: A representative time centred series centred plot at maximum traction time ($T=T_{max}$) of the sensory output of the load and the vacuum detected by the VAD simulator with graph markers indicated at T^*_{Pop} ($T=T_{max}-T_{pop}$) for each Test State in Pneumatic VAD configuration 2 in Study ID 5.

5.4 Experimental Evaluation

Acquired responses shared similar trends as the observed time-series graphs presented during the evaluation of the scalp material in Section 4.5.3. The same dynamic profile of loading and stable vacuum (except for Study 2- Pneumatic configuration 1 State 2) were observed up until time of maximum scalp retention load (T_{max}) was reached. After T_{max} , noticeable differences were noted which lead to the statistical analysis of the test metrics (T_{max} , L_{max} , V_{max} & T_{pop} , L_{pop} , and V_{pop}) to comment on the significance of those differences. An empirical statistical evaluation, based on observation of defined metrics (L_{max} , V_{max} , T_{max} , L_{pop} , V_{pop} , T_{pop}) against a systematically controlled experimental test configuration (control) present in each study was performed to conclude on the effects of the observed differences associated with the experimented conditions.

The means of the metrics were compared using a Tukey Simultaneous test for differences of Means across experimental conditions for each individual study at a 95% confidence interval. During the comparison, a null hypothesis testing of equal means ($p > 0.05$) and the alternative hypothesis highlighting unequal means ($p < 0.05$) were used. A regression analysis was performed to comment on the significance of the interactions of test metrics showing identifiable trends at a 95% confidence interval. An example generated report of both set of statistical analysis can be viewed in Appendix B3 for relevant studies.

5.4.1.1 Vacuum magnitude inside the VAD

The study results indicate that the working principle of the vacuum applied inside the VAD cup has a direct correlation with the maximum retention load of the scalp (L_{max}) due to an increased time to break contact with the scalp (T_{max}). It is interesting to note that the vacuum (V_{max}) sensed by the sensory unit of the instrumented VAD device at T_{max} hasn't deviated from the initially applied vacuum suggesting that the cup is still in contact with the scalp. Cup detachment was visually detected at T_{pop} and L_{max} increases proportionally as the vacuum magnitude is increased. Regression analysis on the collected data ($n=20$) shows that there is a strong correlation between the following set of data L_{max} & V_{max} ($R^2=96.7\%$), L_{pop} and V_{pop} ($R^2=96.3\%$), T_{max} and T_{pop} ($R^2=98.4\%$) (Figure 5-11).

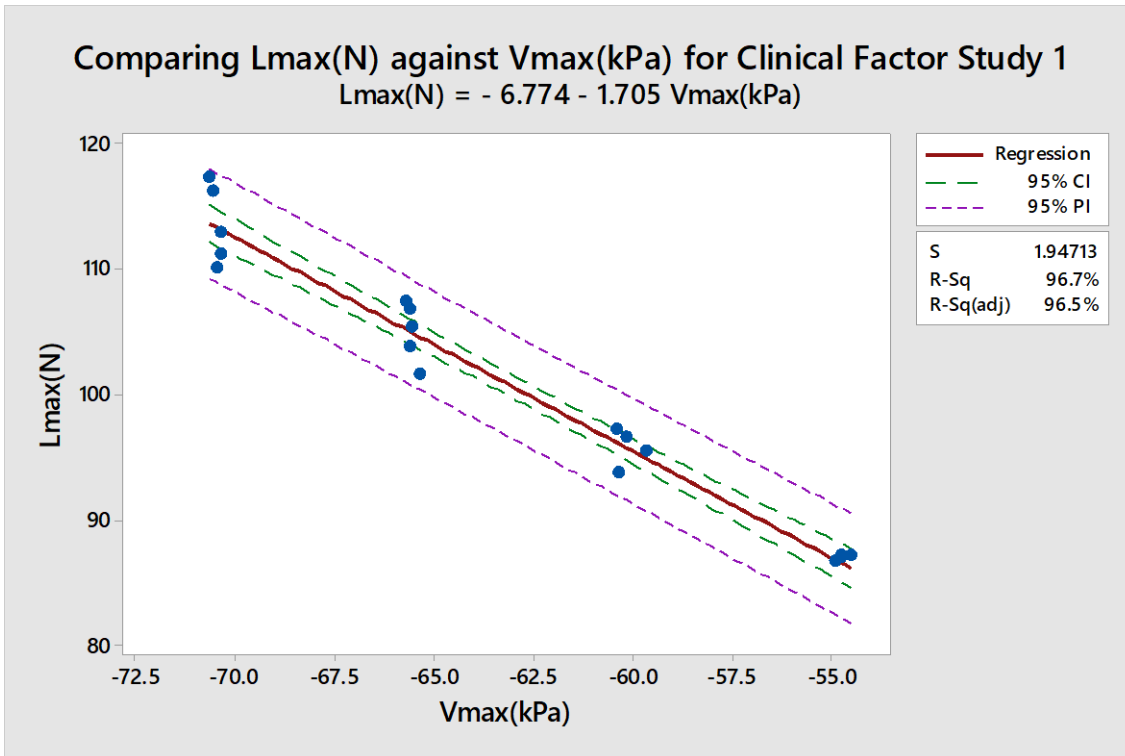


Figure 5-11: Regression line showing relationship between Lmax(N) and Vmax for each tested Traction speed (mm/min) for Study 1

5.4.1.2 Traction Speed

From the acquired results, no changes in Lmax and Vmax were observed as the speed of traction/pull has increased (Figure 5-12). A Tukey Simultaneous test for differences of Means showed no differences in the means in Lmax and Tmax at a 95% confidence interval with high p-value reported across groups ranging from (p= 0.111 to 0.975). The vacuum applied was regulated and there were no differences in Vmax. As anticipated, the most noticeable difference observed in this study is the decrease in the time to reach Lmax (Tmax) (p=0) as speed of traction is increased. Regression analysis on the collected data (n=20) shows also that there is a strong correlation between the following set of data Tmax(s) & Speed of Traction ($R^2=85.59\%$) and Tpop & Tmax ($R^2=100\%$) (Figure 5-13)

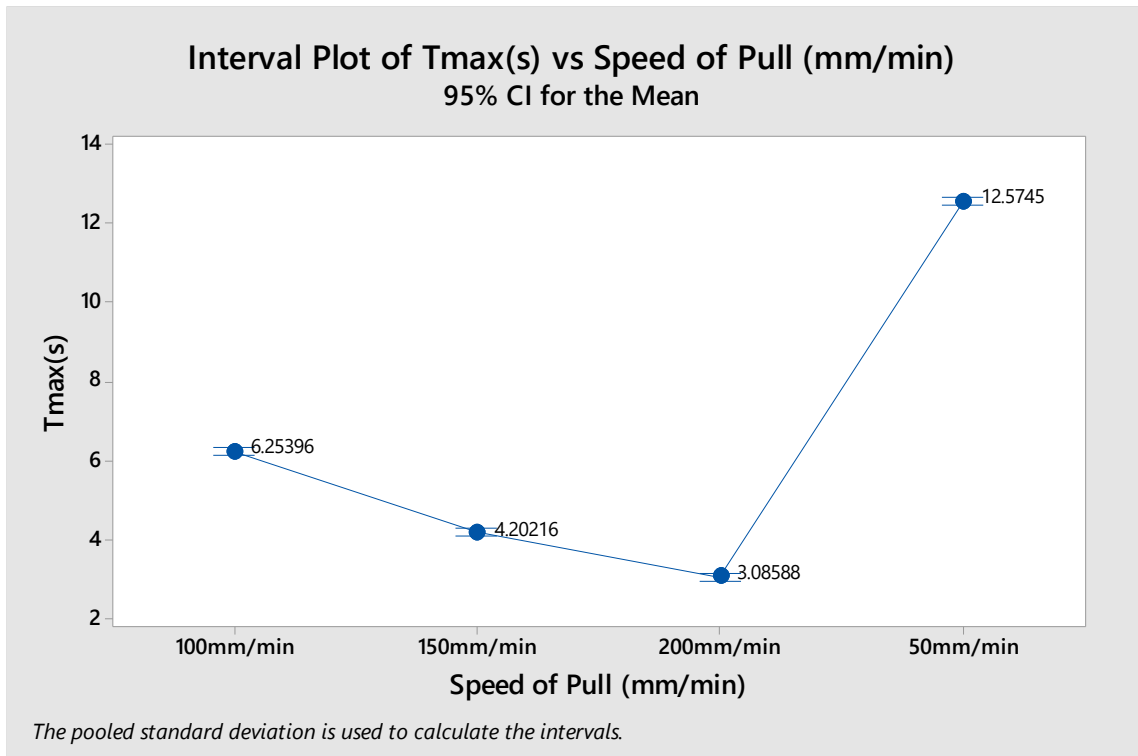


Figure 5-12: Interval plot of Tmax (N) against tested Traction speed (mm/min) conditions for Study 2

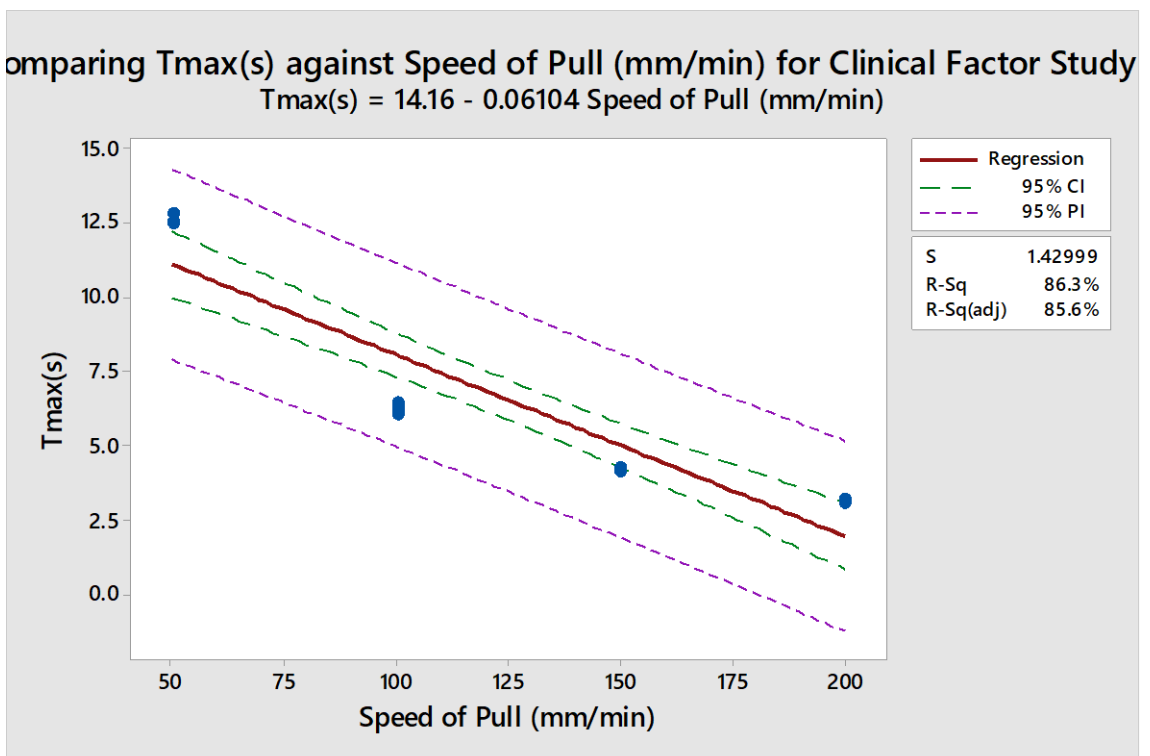


Figure 5-13: Regression line showing relationship between Tmax(s) and tested Traction speed (mm/min) conditions for Study 2

5.4.1.3 Changes in Cup Geometry

This study highlights the importance of the mechanical interlock as a function of the design intent of the recessed edges contributing to additional retention load of the scalp prior to cup detachment. The interval plots show that the maximum retention forces (L_{max}) were influenced by the changes in cup geometry experimented conditions (Figure 5-14). The pairwise comparisons in between the different groups of varying cup geometry demonstrates that there is a statistically significant difference in the means of L_{max} with a low p-value when means of the unchanged configuration was compared to the one with Insert B ($p=0.040$) (Figure 5-15). However there were no significant differences in means of T_{max} ($p=0.233-0.706$) across all groups evaluated in this study. The analysed results highly suggest that changes in the mechanical interlock has a statistically significant impact on the maximum retention forces of the scalp and therefore impact the timing of failure (T_{max}). By design, Insert B presented with the worst cased approach with limiting the effects of the mechanical and observations at the maximum tractive forces (L_{max}) were subsequently different from the unchanged configuration (Figure 5-15).

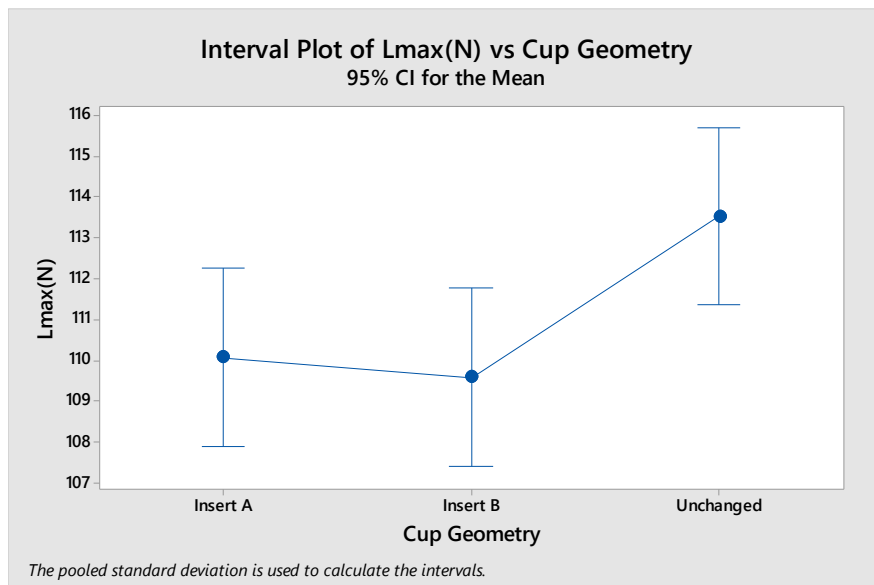


Figure 5-14: Interval Plot of L_{max} (N) against changes in cup geometry for Study 3

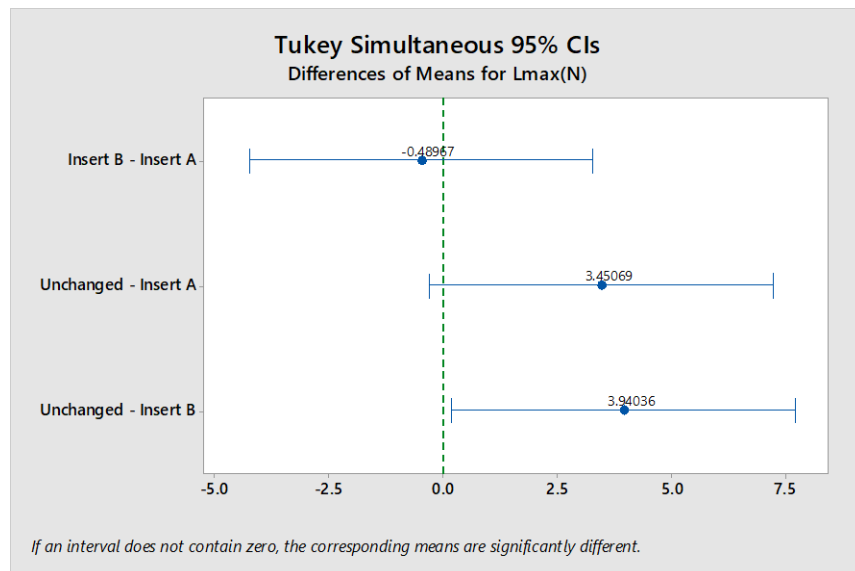


Figure 5-15: Tukey simultaneous analysis of means of Lmax against tested experimental condition for study ID 3. Only Insert B showed difference in means compared to unchanged configuration.

5.4.1.4 Frictional Attributes of the Maternal Environment

The addition of the lubricants used in the study increased the retention forces with the most viscous lubricants (B&E) having the most impacting effect compared to water based lubricants (C & D) (Figure 5-16). The pairwise comparisons between all the different groups tested aside the control scalps shows statistically significant differences in the means of both Lmax & Tmax with a very low p-value reported across groups of lubricants tested ($p=0$) (Figure 5-17). This contradicts the working principle introduced on the effects of lubricants in Section 1.3.4. A possible explanation would be that the presence of the layer of lubricants used in this study offered more resistance to leaks (Similar to lubricating sealant). As previously demonstrated in Section 4.5.3, there were no noticeable differences in performance between dry scalp 1 and dry scalp 2. There were not noticeable differences in L_{max} between the water based lubricants (A & C & E) (Figure 5-17). Lubricant B and D had the greatest effect on the maximum tractive forces indicating their chemical formulation might have adhered better to the tested head scalp surface as compared to the other tested lubricants .

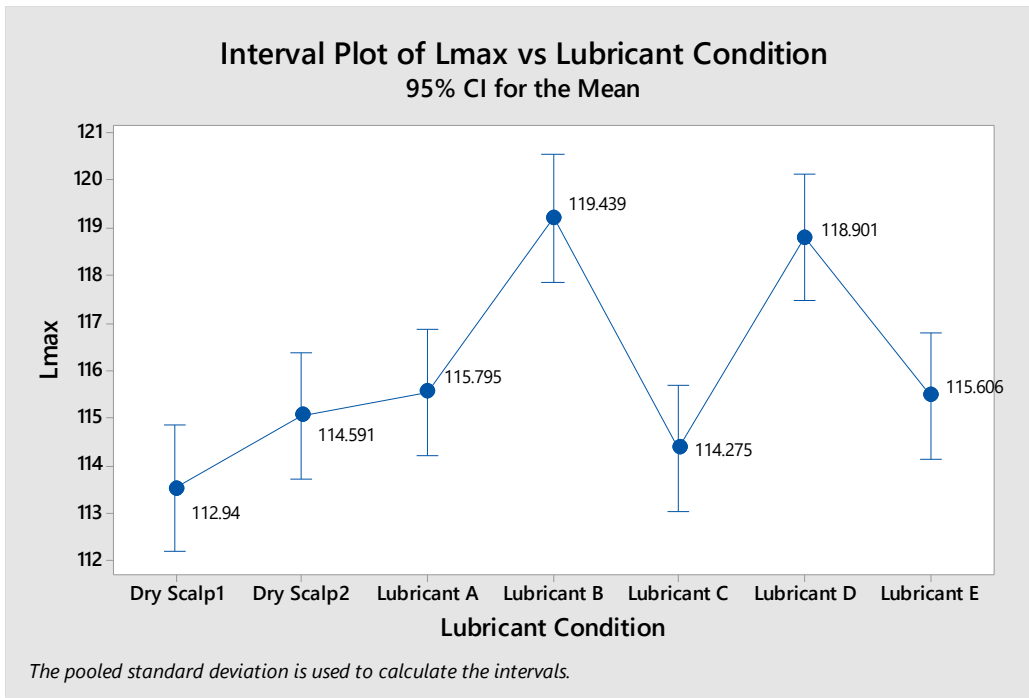


Figure 5-16: Interval plot of Lmax (N) against test lubricant formulation in Study 4

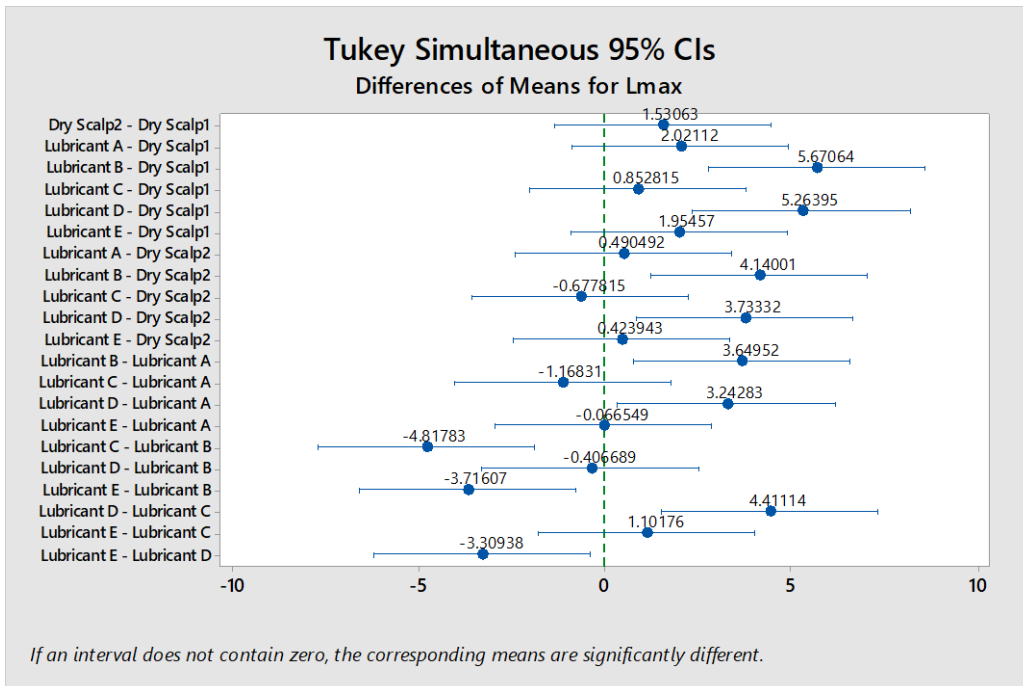


Figure 5-17: Tukey simultaneous analysis of means of Lmax against tested across all tested experimental condition and the scalps control for study ID 4

5.4.1.5 Changes in Pneumatic VAD configuration

Pair-wise comparison across the states of each pneumatic configuration shows a significant difference in observed means of L_{max} across all the experimented conditions compared to the control (Pneumatic ID 1) (Figure 5-18). The noticeable increase in vacuum experienced (with Pneumatic ID 2 (similar to the Kiwi OmniCup system) can be explained by the changes in volume inside the cup as a result of scalp stretching. Figure 5-19 shows that there are considerable vacuum differences (V_{max}) at L_{max} between the 2 states in that pneumatic configuration. This intensified the vacuum originally applied leading to higher retention load (Figure 5-20). However, the time-series trace reveals a faster time to reach T_{pop} from T_{max} (Figure 5-9). This suggest that control of the vacuum compensates for volume changes in the cup but also buffers potential introduction of leaks as demonstrated by the delaying effects of the trace of the pneumatic configuration 2 from T_{max} to T_{pop} (Figure 5-10). The results indicate that Q_{net} has an observable impact on the dynamics of cup detachment.

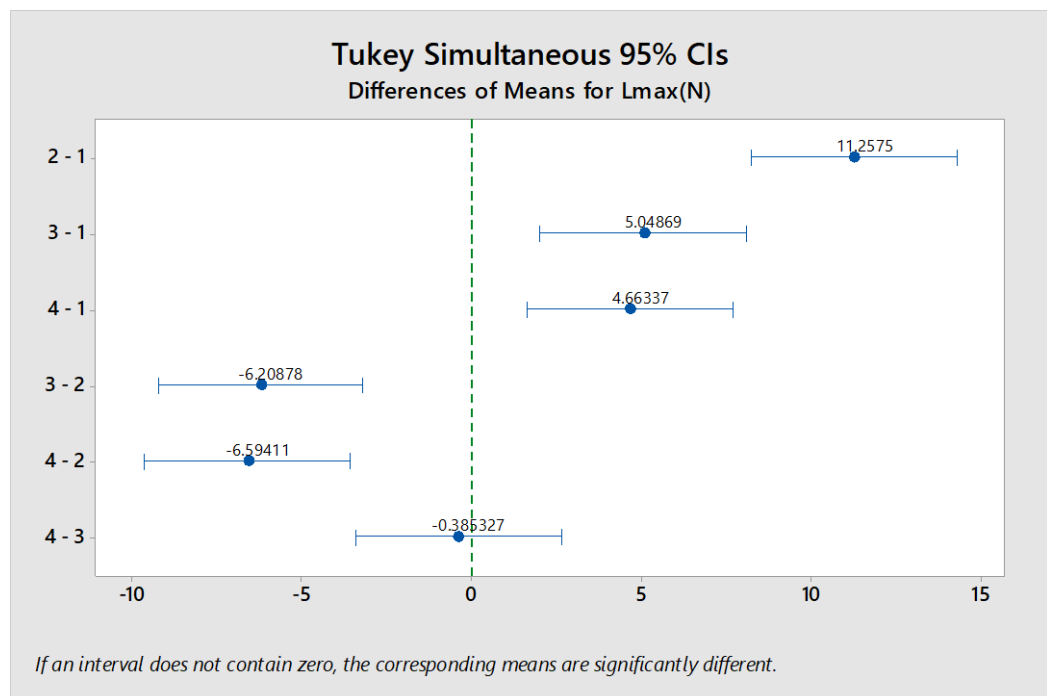


Figure 5-18: Comparison of means of L_{max} (N) against tested Pneumatic configuration ID for study 5.

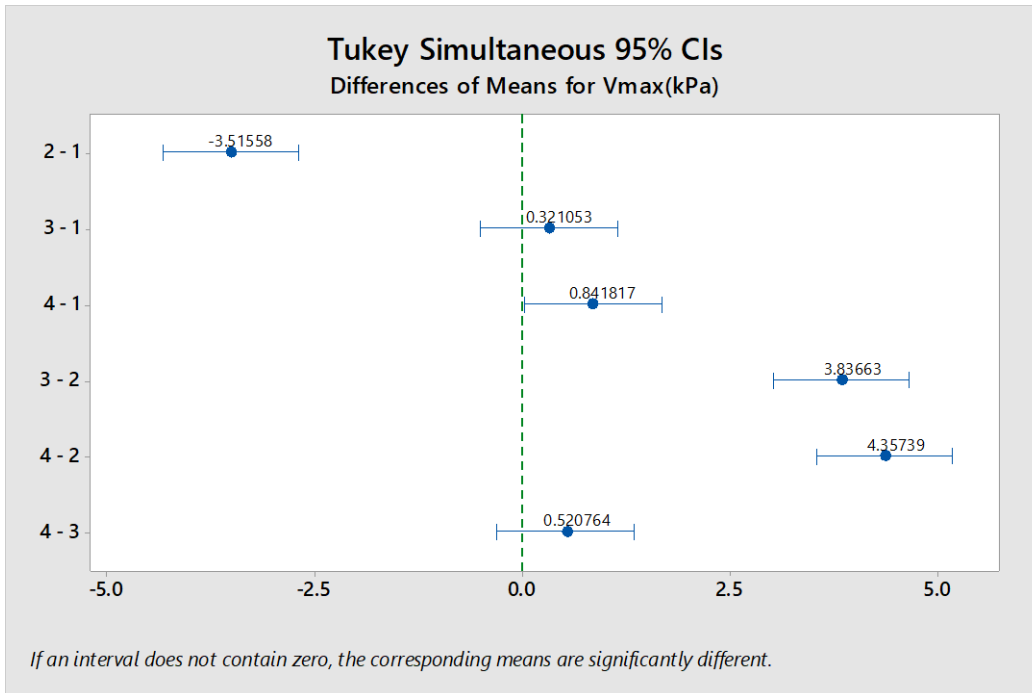


Figure 5-19: Comparison of means of Vmax (kPa) against tested Pneumatic configuration ID for study 5.

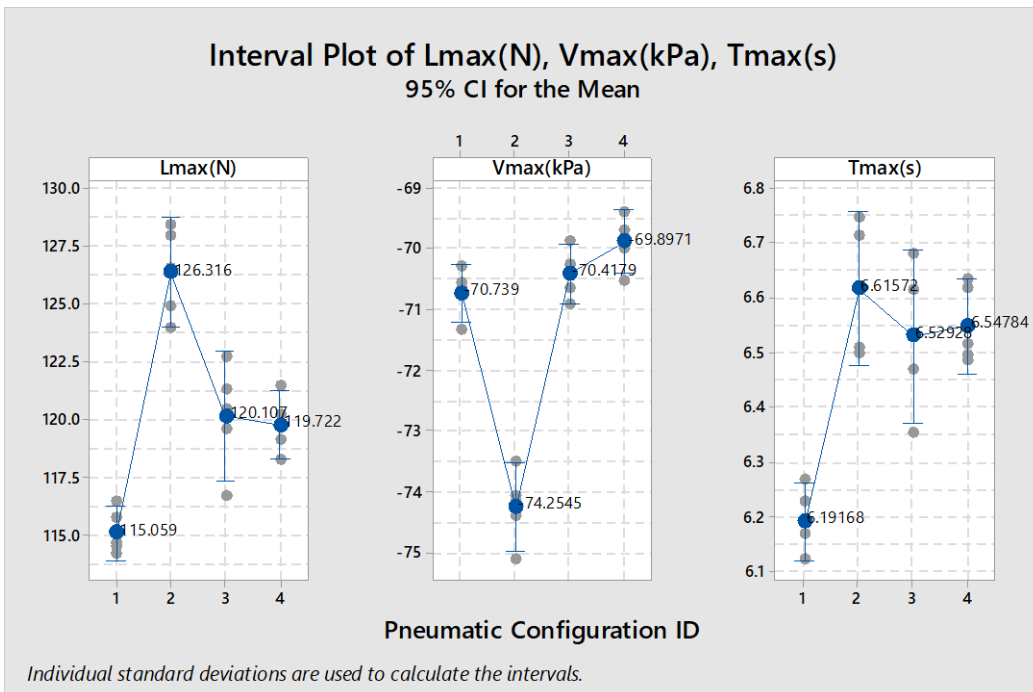


Figure 5-20: Interval plots of test metrics- Lmax(N), Vmax(kPa), Tmax(s) against tested Pneumatic configuration ID for study 5

5.5 Discussion

The evaluation of the results provided in the previous section, study 1 revealed that the maximum retention forces prior to cup detachment (L_{\max}) have a proportional linear relationship with the vacuum applied (V_{\max}). This suggests that obstetricians need to be cautious when load dependency is dependent on the vacuum level in the cup. It is critical to monitor the vacuum inside the cup as this inherently influences scalp retention inside the cup. Study 2 shows that the speed of traction influences the time at which the maximum retention forces occur (T_{\max}). If the obstetrician is tempted to pull faster, the likelihood of cup detachment will increase. Training may be required to develop awareness on what the appropriate speed of traction should be to reduce unintentional cup detachment. Study 3 highlighted the importance of the mechanical interlock (formed between the scalp and recessed edges of the cup) in increasing the load retention of the device (and thus decreasing unintentional cup detachments). This is an important aspect which should be considered in the design of future VAD devices. However, this finding should be approached with caution as more load retention does not necessarily increase the likelihood of successful application of VAD devices and would require clinical verification. Study 4 demonstrated that lubricants used on the surface of the head can increase retention forces by creating a sealing interface capable of reducing micro leaks at the cup scalp interface. The findings in Study 5 demonstrated changes in the pneumatic VAD architecture can have a significant impact on the dynamics of cup detachment. This confirms that regulating the vacuum source inside the cup could compensate for any associated volumetric changes inside the VAD cup system as the scalp deforms. A similar effect is observed by using a reservoir system which delays the onset of unintentional cup detachment by minimising changes in the vacuum inside the cup.

In comparison to previous studies on the mechanics of VAD devices as indicated in Section 2.6, this experimental evaluation provides an objective and quantitative investigation into the mechanical and clinical factors which impact on VAD performance. Considered together, the results suggest that there are opportunities to improve VAD device design; such as changes in cup geometry and pneumatic architecture to reduce the likelihood of unintentional cup detachment.

5.6 Chapter Summary

Experiments have been devised to investigate the clinical and mechanical factors including applied force rate, magnitude of vacuum imposed, and the impact of lubrication, the effect of vacuum buffered source and geometry alterations of the VAD cup.

The results from the performed parametric experimental studies in the previous section, demonstrate the importance of both clinical and mechanically related factors on the dynamics of cup detachment and on the performance of VAD devices. The research outcomes generated from this experimental evaluation of VAD system provided an insight on the mechanics of interaction of the VAD cup system and a representative foetal head scalp model and provided a quantifiable way to assess the impact of clinical & mechanical factors on the dynamics of cup detachment. The following outcomes will be translated in the next chapter to improve the performance of VAD cup system to reduce the effect of failure rate associated with cup detachment.

Chapter 6

Translating research outcomes to the design of a commercial system

This chapter evaluates how the research outcomes generated from the previous chapter, could be translated into a commercial system in the form of new market introduction (NPI) of an atraumatic VAD device. The evaluation will focus on the improvement of clinical outcomes associated with VAD device performance to reduce the risk of cup detachment during an obstetric over-traction. This work was performed in collaboration with the industrial partner of this project: Eakin Healthcare Group (EHG), with the aim of translating the outcomes of this research towards a new commercial Vacuum Assisted Delivery (VAD) device to reduce unintentional cup detachments. EHG contributed to this process by facilitating interaction and discussion with relevant subject matter experts (SMEs) to evaluate the proposed opportunity technically and commercially.

6.1 Assessment of Clinical and Commercial Opportunities

Vacuum Assisted Delivery (VAD) devices have emerged as the instrument of choice for assisted delivery, surpassing forceps due to ease of use, decrease in maternal morbidity and improved cosmetic outcome for the baby.

In the VAD market, as highlighted by the literature review, a variety of device configurations exist commercially. In the single use instrumented category, the Kiwi Omni cup as manufactured by Clinical Innovation (CI) with its hard low profile Polyethylene VAD cup is the market choice. Another single use system is provided by Cooper Surgical Ltd (CS). CS traditionally sells single piece models with an integrated pump design alongside different cup designs (Mystic 2 with a semi rigid-stem or Mityone with a rigid stem). In addition, a reusable pump (mityvac) can be used to deliver vacuum to cup systems with different shape factors (mushroom shaped with a flexible joint and bell shaped with a soft lip). Other notable competitors in the market are device manufacturers of more conventional types of VAD system such as Utah medical and Medela AG (Figure 2-3). Conventional cup systems feature an optimised version of the Malmstrom device (Bird low profile 2nd generation) in transparent plastic or metal format with an add-on traction handle.

Despite the growing popularity of VAD, the clinical evidence on the safety and efficacy of such devices remains unclarified with an elevated propensity for delivery failures (30.1%) occurring due to VAD cup detachment associated with the leader in the field (86). However, the healthcare economics evaluating the potential financial impact arising as a function of cup detachment hasn't been yet established. The causation of a pop-off leads to a decision pathway to further obstetric care/surgical procedures. The decision making of the obstetrician is important in the clinical care pathway (21). After electing to use VAD, the obstetrician follows a clinical pathway based on guidelines and experience (119) (Figure 6-1). In the event of a cup detachment, either a repeat is performed (pathway 2a) or the process is completely aborted and a low-section C section is performed (pathway 3). If a repeat of the procedure is unsuccessful, pathway 3 is followed. Any deviation by the decision factors in the decision tree proposed below leads to a cost introducing event. The reimbursement opportunities as results of events in the clinical care pathway can be viewed in Figure 6-2.

Instrumental delivery rates in the majority of EU countries range between 7.2% to 10.9% (23) (Table 2-2). Table 6-1 shows a summary of the market potential of

VAD. For example, in UK (England), in 2017, 5% of all registered birth (31,311 procedures) contributed a total available market (TAM) of £782,775, factoring the cost of £25 for the market leader in VAD devices (Kiwi Omni Cup). The estimated market share of the Kiwi Omni cup is rated at 70% and the rest is assumed to be shared with all the other VAD device manufacturers present in the market. Based on the clinical care pathway listed above, the differential in cost of pathway 2 and 3 to pathway 1 ranges in between £1680-£5623 (119) (Figure 6-2). With the reported failure rate of 30.1% of the Kiwi device and 18.2% with other VAD devices, there are 6313 births at risk, which leads to a potential estimated cost of £10,605,840-£35,498,000 to the NHS as a result of unintentional cup detachments. The monetary benefit associated with this reimbursement opportunity shows promise for future progression to commercial development of the proposed concept especially in the key identified markets (USA and EU) established in Table 6-1.

Clinical Care Pathway

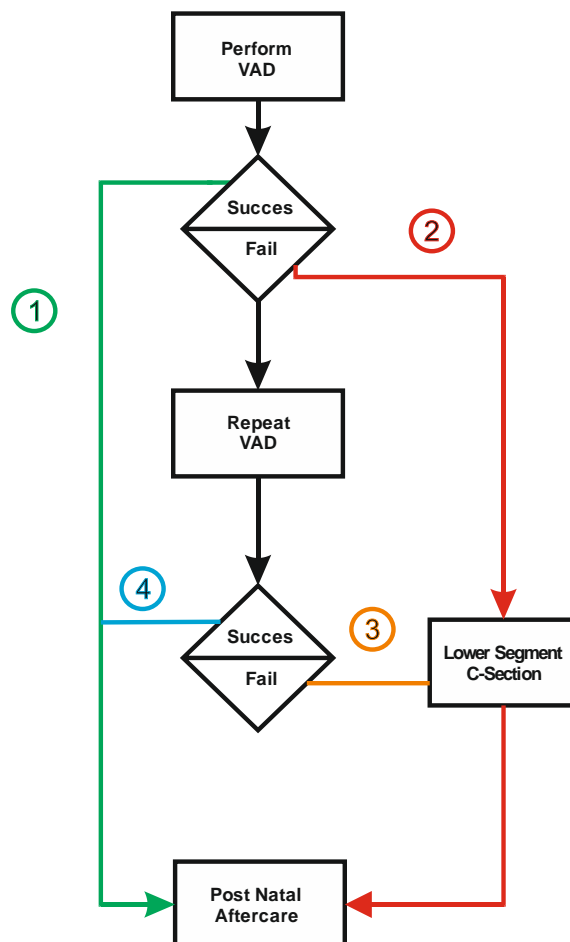


Figure 6-1: Clinical care pathway behind operative delivery and clinical outcomes in the event of VAD failure (21, 119)

Table 6-1 : Market opportunity analysis based Total Available Market (TAM), Serviceable available market (SAM), and serviceable obtainable market (SOM) of the identified countries with a receptive VAD market in Table 2-2

	Countries			
	UK (England)(120)	Australia(121)	USA(17, 122)	EU Countries (n=26)(23)
No of Registered births in 2017	626,203	309,142	3,855,500	5,075,000
TAM [All Instrumental Deliveries- Forceps+VAD] (Percentage Total Birth- Births) [Monetary Market @ £25 per Birth]	12%-75,145 £1,878,625	11%-34,006 £850,150	3.1%-119,521 £2,988,025	6.84%-347,130 £8,678,250
SAM [Instrumental Deliveries-VAD Only] (Percentage Total Birth-Births) [Monetary Market @ £25 per Birth]	5%-31 311 £782,775	6.6%-20,404 £510,100	2.6%-100,243 £2,506,075	4.1%-208,278 £5,206,950
SOM (30% Market Capture from SAM) [Monetary Market @ £25 per Birth]	9393 £234,825	6121 £153,025	30,073 £751,825	62,484 £1,562,100

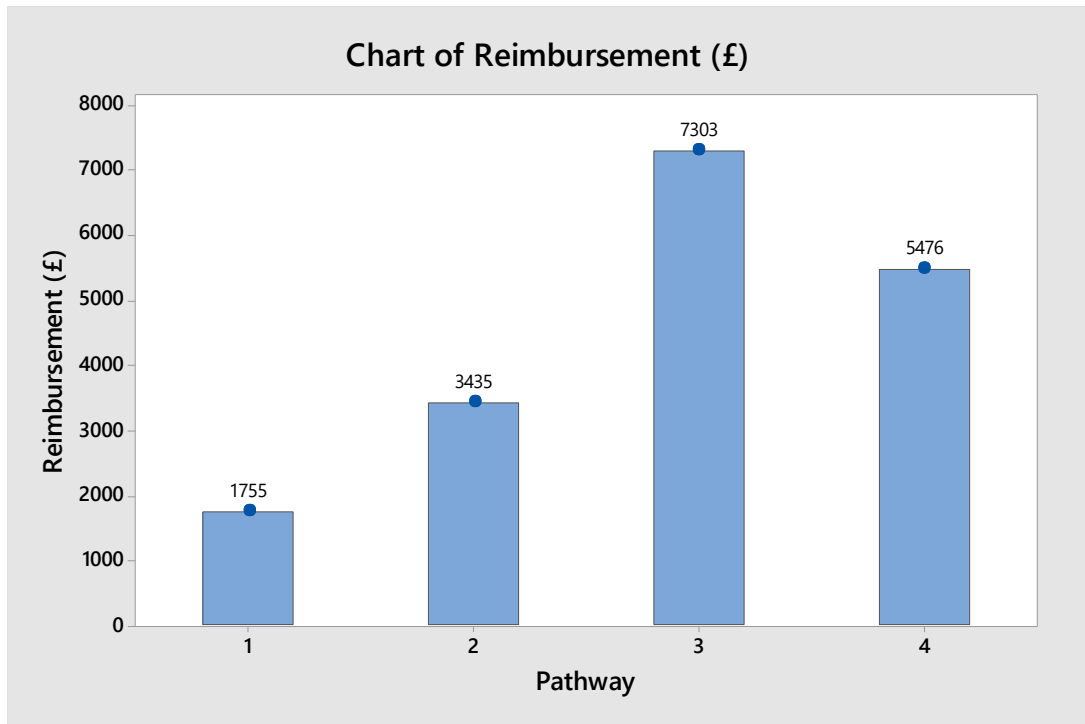


Figure 6-2: Reimbursement chart showing NHS operational cost associated with clinical costs linked to clinical care pathway as shown in Figure 6-1 (119)

Table 6-2: Estimated calculations for the cost saving potential of the proposed device in UK

Determining Cost saving Potential of new Device in UK	
Cost Difference Range (£)	£1680-5623 [Comparison of Pathway 2 & 3 to Pathway 1]
Cost Saving Potential of preventing Cup Detachment	Total Births at risk:6313 [£10,605,840-£35,498,000] (30.1% devices failing of 21918(Kiwi Market share: 70% of 31,311 births in UK)=4603 Births at risk) (18.2% devices failing of 9394 (Other VAD Market share: 30% of 31,311 births in UK)=1710 Births at risk)

6.2 Assessing technical opportunities to improve VAD performance

From the assessment provided in the previous section, it is evident that there is a clinical and commercial need for an atraumatic VAD capable of preventing unintentional cup detachments. In this section, key design opportunities, identified through the research outcomes established in Chapter 5, will be assessed in terms of their technical and commercial feasibility to realise an atraumatic VAD system which offers improved performance.

6.2.1 Evaluation of Design Opportunities

The research outcomes from Chapter 5 have identified three main design opportunities which offer the potential to improve VAD performance. In this section, the technical feasibility of their integration into the proposed concept will be evaluated, prior to investigating their commercial and clinical value. Figure 6-3 shows the design opportunities in relation to the VAD system which comprise three main areas:

- A. Changing the cup geometry to improve scalp retention
- B. Optimising pneumatic architecture to minimise vacuum degradation
- C. Integration of sensors to determine vacuum level in the VAD cup

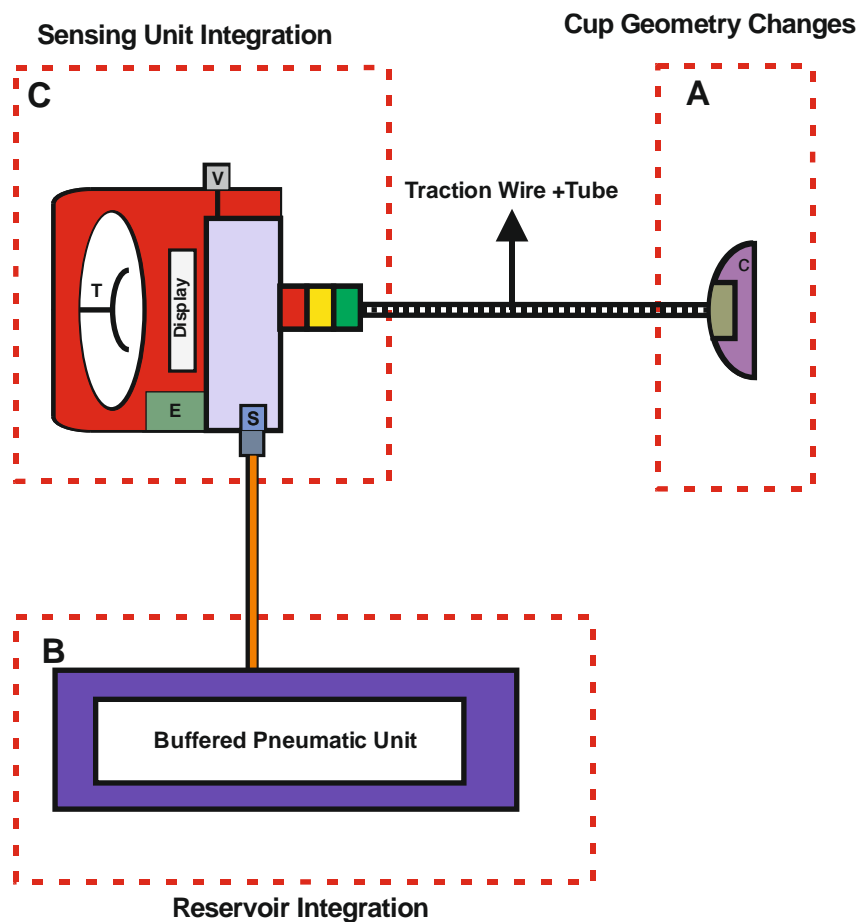


Figure 6-3: Design aspects considered during the conception of an atraumatic VAD cup system. A: Changing the cup geometry to improve scalp retention. B: Integration of a reservoir to provide a continuous volumetric flow rate to the pneumatic architecture C: Sensing unit integration in the dynamically sensing the vacuum inside the VAD cup system.

Design Opportunity A: Changing Cup Geometry

From the experimental evaluation in section 5.4.1.3, the mechanical interlock at the recessed edges remains an important aspect to consider as it offers additional retention of the scalp. However, designing a device with optimised recessed edges can be perceived as a radical change to healthcare professionals; introducing a risk to product adoption. It could also present a constraint to commercial development as further clinical evaluations will be required to demonstrate safety and efficacy against current systems. Changing the cup geometry presents limited novelty and falls back into the loop of product differentiation but with added costs and potentially no added clinical benefits. A fail safe option is to adopt the current VAD cup in the Kiwi Omni cup.

Design Opportunity B: Pneumatic Architecture

The pneumatic vacuum control of the vacuum flow rate is instrumental in maintaining stability of the applied vacuum in a VAD cup system and as well delaying the dynamics of cup detachment. Therefore, it was important to consider the integration of a buffered vacuum regulated system capable of hosting a significantly high volumetric flow rate such as an external reservoir to counteract not only downstream unwanted vacuum changes but also the intrusion of potential leaks. Leaks can be manifested in various forms. Hair on the baby's head or entrapment of maternal tissue (detrimental to vacuum integrity), the presence of already present caputs (reduction of contact area), cup malposition (uneven surface placement) or incorrect vector of traction (tilting or vacuum line pinching) can all contribute to the formation of leaks affecting the performance of the VAD device. However, despite the functional advantages in maintaining the vacuum inside the VAD cup system, connection to an external reservoir can be cumbersome. An inbuilt consideration of pneumatic architecture will need to be considered in the overall design of the concept.

Design Opportunity C: Integration of Sensing Systems

Equipping a VAD device with a controlled vacuum and an alarm system to warn of changes in the vacuum applied could be a unique product offering. This could help resolve escalation to further care and reduce associated costs incurred during the operational management of the event. However, choosing the right sensing system is important. Following the insight provided in Chapter 4, it is now known that the vacuum degradation leads on to cup detachment. Equipping the device with a fast reacting digital vacuum sensor capable of sensing changes (1000Hz) is essential to sense the initial drop in vacuum noticed after the maximum retention force. However, from the displayed dynamics of cup detachment within the presented studies on clinical & mechanical factors in Section 5.3, the healthcare professional will not be be capable of manually reacting in the time frame of cup detachment between T_{max} and T_{pop} (0.05s-0.25s). Therefore, an alternative automated approach is proposed in the following section to address this opportunity.

6.2.2 Concept for an atraumatic VAD device

Through evaluation of the technical opportunities A-C with EHG, the new VAD concept will integrate improvements in pneumatic architecture, combined with the integration of a vacuum sensing system, as shown in Figure 6-4.

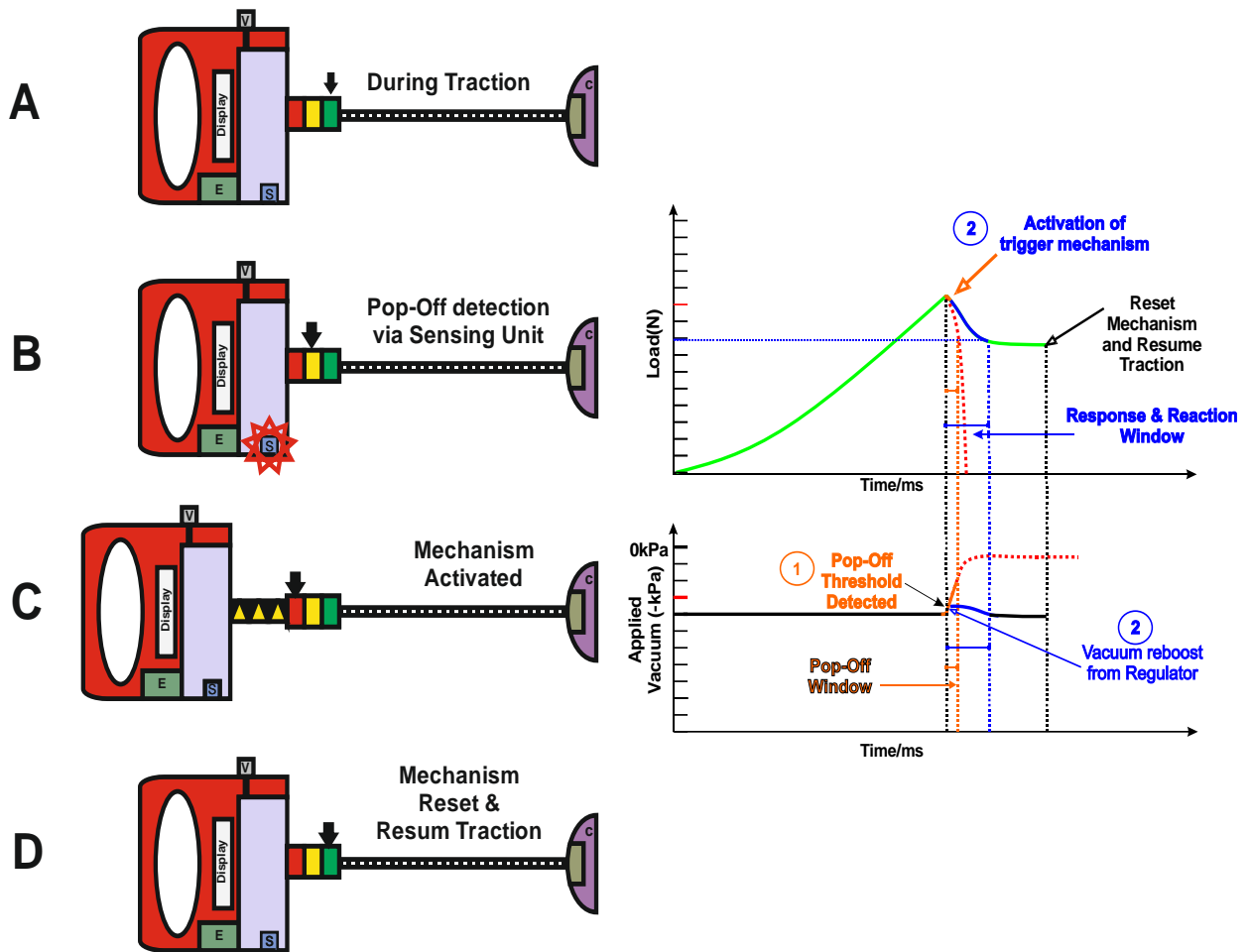


Figure 6-4 : Concept of the device operation to reduce cup detachment by an adaptive tensioning mechanism triggered by vacuum sensing input. Left: Device and Operations. Right: Dynamic monitoring control and monitoring of cup detachment.

Unlike the current state of art (Kiwi Omni Cup from CI), the proposed innovation will be capable of adaptively warning the end user of potential unintentional cup detachment during the VAD procedure leading to better clinical outcomes. In terms of device configuration, the concept atraumatic device will feature a single-use cup with an integrated electric pump. The suction cup will be powered by a re-usable electronic instrumented hand grip pump. The latter is equipped with a vacuum sensor and a retractable mechanism to apply and maintain traction on

the cup and counter unintentional cup detachment. The device is designed for transient use and is capable of adaptively warning the obstetrician of a potential unintentional cup detachment during the VAD procedure. Figure 6-4 shows the working operation of the concept device in the event of a cup detachment during normal VAD use. When vacuum degradation is observed during traction, the sensor activates a mechanism. This relieves tension but maintains the original positioning of the VAD cup on the baby's head ensured by the continuous regulation of the vacuum by the electric pump.

6.2.3 Intellectual Property (IP) Analysis

The proposed device comprises of key technologies requiring a regulated source of vacuum, a vacuum sensing module, and an activated mechanism to perform VAD delivery and counter cup detachment. The IP state of art was analysed to identify the potential of protecting the key technological claims of the proposed VAD device. Table 6-3 shows a summary of potential infringement of currently filed/ expired IP around the novel contribution aspects of the proposed VAD device.

In the IP state of art of VAD devices, CI holds a significant number of patents around their present invention of the Kiwi Omni Cup. The main patent (ID 1) combining the use of a vacuum sensor to carry out VAD expires in 2022. However, there is workability around the patent as the core technology will be based on a predictive metric. The patent around the design of the Kiwi Omni cup (ID 2) has expired and can be used as a template for the design of new VAD products. The main constraint of achieving IP around the concept design will be from the patent surrounding the invention by Meditech Development Inc. (ID3). They have devised a system capable of a portable vacuum regulated source which could have impact on the general concept of the proposed VAD invention. With regard to potential instrumentation such as the addition of a vacuum sensor to interface with an ECG monitor, the product patent associated with Texas Tech University (ID 4) has expired. Any invention comprising of a pull sensing module with alarms will be influenced by the technology proposed by Advanced Obstetric Systems (ID 5).

There has clearly been efforts in the past to control/mitigate pop-offs. However, the knowledge brought forward by the research provides a new perspective on controlling the event via the detection of a vacuum degradation and then a reactive mechanism to prevent unintentional cup detachment. This provides a real opportunity for further research and development with an offering not seen so far in the current IP state of art.

Table 6-3: IP Analysis to identify IPs which can be a barrier to innovation. The relevance in risk is colour coded. Green-Free to operate, Yellow- Presented IP might be a concern but there might be workability around it.

ID	Patent	Assignee	Analysis	Status	Relevance/Risk
1	US20020165556A1	Clinical Innovations Llc, Murray, Utah 84123 (US)	Instrumented Palm Pump	Valid but Expiry in 2022	Claims related to the monitoring of the vacuum and thresholding of the vacuum as a magnitude. The patent expires in 2022. The patent can be worked around as the core technology of vacuum degradation will be based on a predictive metric.
2	EP 1152702 B1 US6355047B1	Clinical Innovations Llc, Murray, Utah 84123 (US)	Kiwi Device with Traction indicator. This is the only VAD device with a traction indicator on the market.	Expired	The re-usable cup of the proposed VAD device will be identical to the Kiwi Device.
3	US 9138216 B2	Meditech Development incorporated, CA (US)	Controllable vacuum output from vacuum source with tuneable LED display bar	TBA	The main claims in this patent comprises of a system capable of a portable vacuum pump as a standalone unit to connect to a VAD device and regulate the internal pressure inside the cup.

ID	Patent	Assignee	Analysis	Status	Relevance/Risk
4	WO 2002/043599 A1, US 6620171 B2 US 7069170 B2	Texas Tech University System (Formerly Medevco Inc)	VACULINK, MODEL VCL 3000: Wireless Add on accessory to existing VAD devices connected to a foetal HR monitor. Device is capable of detecting pressure changes inside the cavity of the VAD cup and	Expired/Not Renewed	Can impose constraints on design in case of adding a vacuum sensor for in line vacuum detection. This needs to be further evaluated. However, this is an add on device and the sensor in the proposed device is integrated in the embodiment of the handle
5	US 7291156 B1	Advanced Obstetric Systems Llc	Pull sensing module on handle capable of emitting alarms on load thresholding	Priority in 2007	The emission of alarms as a result of potential risk to cup detachment is based on load thresholding technology however the proposed device uses vacuum degradation metrics.

6.2.4 Regulatory requirements

In an effort to help ensure clinical acceptance and usage, it is important that the proposed device does not differ significantly from currently available VAD cup system formats. As such, the proposed concept should feature a sterile, disposable suction cup attached to the scalp with a soft inner liner/mesh to prevent tissue damage and satisfy the regulatory requirement established below.

If a manufacturer intends to sell medical devices in the EU, the latter must conform to the regulations of the Medical Device Directive (93/42/EEC). As outlined by Annex IX of the directive, the proposed re-usable non-invasive instrumented pump handle system is considered as an active medical device due to the presence of external power source i.e. AC mains or battery powered. Subsequently, the full assembly is considered of the pump and the single use invasive cup is considered as a Class 2a medical device according Rule 2 & 5. The device development of the product should follow all stipulated annexes of the directive except section 4 of Annex II & Annex III. The technical dossier for regulatory submission as defined by guidance on Design-Dossier Examination and Report (NBOG BPG 2009-1) will comprise of the following main documentations:

- Manufacturer details & Notified Body review
- Device description and product specification & Classification Statement
- Requirements regarding manufacturing, Design and construction
- Pre-clinical evaluation
- Clinical evaluation/performance evaluation
- Risk analysis and risk management
- Review of declaration of conformity
- Post-market surveillance

A manufacturer who intends to sell VAD devices in the USA must conform to the regulations of the 21 CFR § 884.4340 as established by the Federal Food, Drug, and Cosmetic Act (FDA) (Table 6-4). The new VAD device should demonstrate substantial equivalence to a legally marketed predicate device marketed interstate commerce prior to May 28, 1976, the enactment date of the Medical Device Amendments. The introduction of a new VAD device will not necessitate a stringent premarket approval application process. A 510(k) premarket notification of intent to market the device with substantially equivalent devices listed in Table 6-4, should be sufficient. As a result, the proposed will occupy a Class 2 (Performance standards) status and will be registered under the product code: HDB. Compliance to registration and listing 21 CFR Part 807, labelling (21 CFR Part 801), good manufacturing practice requirements as set by the quality

system regulation (21 CFR 820) and the electronic product radiation control provision (21 CFR 1000-1050).

Table 6-4: Regulatory pathway of predicate/substantially equivalent VAD devices following the 510(k) route in USA

Product code: HDB, Regulation no: 884.4340, Class: 2 (Performance standards)		
Notified bodies: Accelerated Device Approval Services, Llc, Regulatory Technology Services, Llc, Third Party Review Group, Llc, Tuv Sud America Inc.		
Premarket Review code: OHT3 & DHT3B		
Product code for Powered/Manual Suction pump: BTA		
Device/Model	Supplier	Applicable 510K
M-Style/Mushroom Cup with MityVac M-style with wall suction and Universal release valve	Cooper Surgical	K020447 K934011 K890307
VAC-6000M/MTE (Traction indicator)	Clinical Innovations	K011532 K981260
Powered Suction PUMP	Medela AG	K130123 K041579
CMI-H671001C0 Pump CMI (H671101A1)	Utah Medical	K881967 K895446

6.3 Discussion

The analysis in this chapter shows that there is commercial potential for an atraumatic VAD device. Furthermore, this is technically feasible. However, there will be significant risks/challenges in the development of the concept towards a final product. The inclusion of electronic hardware, for vacuum sensing purposes and control of the relative motion of the traction system, can impose a technical and regulatory barrier. This will be dependent on the resources and capabilities available to the device manufacturer, as the integration of electronics will require further verification and validation to ensure compliance with appropriate medical device development standards. Clinical challenges may also be a barrier in demonstrating that there is a significant improvement in VAD performance. In this clinical domain, conducting an appropriate clinical study with child delivery will carry significant risks to the company. In addition, there are currently no methods for evaluating the performance of VAD devices to mitigate cup detachment. Whilst, increased litigation resulting from VAD incidents can deter manufacturers from entering this complex market, there is a necessity to create more advanced prototypes and achieve clinical validation. Clear clinical outcomes/benefits need to be demonstrated compared to the current state of the art. Building an informed position in the market (clinical evidence, market appreciation and optimisation of training material) would be beneficial for the introduction of this concept to the market. Even modest changes could enhance the performance of the VAD devices and thus reduce the costs and risks of commercialisation; although the performance gains would be lower.

6.4 Chapter Summary

The concept of a portable device used in emergency childbirth to assist delivery of babies that allows medical professionals to perform safer VAD delivery during difficult labour, was introduced in this chapter. This is achieved by using an active sensing attachment device with a feedback mechanism aimed at reducing unintentional cup detachment. The cost to healthcare provision behind the occurrence of an unintentional VAD cup detachment was calculated based on the clinical care path decisions associated with this undesired healthcare outcome. An IP analysis was performed to understand the patent landscape and the regulatory aspects. The next stages of development for the proposed concept will be further discussed in the following chapter.

Chapter 7

General Discussion, Future Works and Conclusion

The concluding chapter of this thesis provides a review of the presented research against defined research objectives outlined in Chapter 1. A general discussion of the produced works and suggestions about future work for the continuation of the intended research will be detailed. Concluding remarks will establish the closure of the presented work.

7.1 Assessment of Research Objectives

Section 1.1 detailed defined research objectives established during the conception of the main research aim. The research aim was to achieve a robust engineering understanding of the key design parameters of commercially available VAD devices and their impact on performance and trauma in order to evaluate the design of a less traumatic device. This section provides an assessment on how each objective was addressed in the presented research.

1. Perform a review of published literature to identify the clinical gaps of understanding in VAD device design

The literature review revealed that cup detachment can lead to an escalation of further obstetric care and is closely linked to the end use of VAD devices. The occurrence of uncontrolled cup detachments was identified to instigate head trauma to the baby and lead to profound change in delivery plans which could lead to higher risks of morbidity and poorer outcomes for mother and baby. An investigation into the evolution of VAD devices demonstrated that there have been minimal changes in the design of VAD cup systems since its original inception by Malmström. The most noticeable design changes, identifiable in the most up-to-date devices, for example the Kiwi® Omni Cup™ focus on usability concerns such as insertion of the device into the birth canal (low profiled cup) and gauging the level of traction with visual indicators. The outcomes of these improvements have the end use of the devices but the details of the biomechanics behind the contact of the cup with the foetal head remains under investigated. Rigorous evidence-based research on its influence on clinical outcomes is much needed.

2. Understand and characterise the mechanics of VAD device performance based on the prevalent form of trauma during VAD: Cup Detachment

Based on the findings established in the previous objective, the motivation behind the presented research was formulated to improve an appreciation of clinical gaps of understanding surrounding device performance and its influence on cup detachment from an engineering perspective. In order to accomplish this objective, an expert clinical opinion by Dr John Anderson helped the research team to develop the conception of a VAD simulator.

This led to a comprehensive understanding of the biomechanics of VAD device performance and its resulting effects on the dynamics of cup detachment in Chapter 3. The detailed design and development of the model features alongside the technical requirements of the simulator in Chapter 4. An experimental methodology was then proposed to inform on the dynamics of cup detachment. From the experimental evaluation of the test measurement system, an introductory but quantifiable approach to inform the dynamics of cup detachment, a medium for characterisation of the performance of VAD devices was assessed to investigate the next objective in Chapter 5.

3. Investigate VAD device design improvements to improve VAD performance

A parametric study based on the investigation of selected experimental factors associated with VAD device performance (clinical and mechanical factors) was performed to report on its subjected impact on the dynamics of cup detachment. The aim of this study was to provide recommendations to improve their end use based on objective observations. Five experimental studies were performed per a test protocol matrix and the results were evaluated empirically against a defined control condition for each study. Findings in Study 1 & 2 demonstrated that cup detachment can be intensified at a lower vacuum magnitude and at high traction speed. Study 3 demonstrated the importance of the mechanical interlock. However, this necessitates further work to achieve a better understanding. Study 4 demonstrated that the practice of smearing lubricant around the cup edges helps in reducing micro-leaks at the cup scalp interface. Further tribology studies would be required to provide further insight into the observed effects. Study 5 revealed that changes in the pneumatic VAD architecture showed the significance of having a regulated source of vacuum to compensate for any associated volume changes inside the VAD cup system. Combined with a reservoir, a delay in the dynamics of cup detachment is observed. The observed results were judged to be sufficient to meet the requirements of these objectives and suggestions on improving the current VAD cup system investigation were made in an effort to deter the occurrence of cup detachment.

4. Recommend engineering design inputs for an atraumatic VAD device and evaluate the feasibility of commercial translation and clinical implementation.

In Chapter 6, the details of a conceptual design for atraumatic VAD capable of sensing the dynamics of cup detachment and offering a control mechanism to deter cup detachment was evaluated based on the research outputs gathered from the experimental study performed in Chapter 5. The outcomes of this assessment showed that design opportunities to improve VAD performance could be introduced. Unlike the passive vacuum assisted device from current competitors, the proposed innovation would reduce the failure of existing devices as a result of unintentional cup detachment. The costs to healthcare provision incurred by VAD cup detachment was then calculated based on the clinical care path decisions induced by the occurrence of cup detachment. The patent landscape and the pathway to commercialisation were considered as routes to clinical implementation. From this initial due diligence, it is anticipated that there would be associated risks involved in engineering the product as it features integration of electronic components for sensing purposes and programming of processors capable of controlling the relative motion of the traction system. These aspects will be proposed in the future works section of this chapter.

7.2 General Discussion and Future works

The presented work will be assessed in this section to address the limitations experienced in the stages of development of the VAD test simulator and the relevant experimental studies performed to evaluate VAD device performance. Furthermore, details of future works will be provided to advance the state of the research, validate designs of new VAD devices and assess their performance against commercially available devices. Upon achievement of such task, further details on progressing the introduced concept of an atraumatic VAD set up to the commercial phase will be evaluated in the form of a risk register.

7.2.1 Discussion

Following the review of the literature, a more rigorous evidence-base to inform on the biomechanics of VAD systems and quantification of its impact on clinical outcomes was required. This motivated the presented research in assessing the performance of commercially available VAD cup systems. Inspired by clinical requirements, the design and development of a VAD simulator entailed the creation of a novel head scalp model onto which in-vitro simulation of VAD was performed by means of an instrumented VAD test set up. The presented research work was the first quantifiable approach in evaluating the performance of VAD devices in comparison to previously reported physical VAD models (36, 93, 97). The chain of events leading to a cup detachment was successfully characterised; providing a much needed insight into the dynamics of cup detachment. Upon construction of the VAD test simulator and its detailed experimental methodology to quantifiably assess cup detachment, combinatorial studies focused on the clinical and mechanical factors associated with device performance. Engineering recommendations were then provided in an effort to engineer improvements to improve VAD device performance. The research outcomes were translated into the design of a commercial system capable of reacting to dynamics changes associated with cup detachment by identifying key design opportunities. Compared to previous work on cup detachment warning mechanisms(98-100), the technical feasibility assessment of the identified opportunities revealed that adaptively reacting to sensed vacuum changes can help prevent cup detachment. Furthermore, clinical and commercial avenues were explored to provide justification for the future development of the atraumatic VAD cup system concept.

Despite all the advancements proposed by the presented research, certain aspects of the proposed research endured technical limitations. For example, the current model is simplified to look into axial traction. Oblique traction can contribute to unequal vector forces which disturb the overall performance of the VAD devices, significantly influenced by constraints in the maternal environment such as maternal tissue and the bony pelvis. To investigate on such effects, improvement to the capabilities of the VAD simulator will have to be addressed. The load sensing aspect of the VAD will have to be upgraded to a multi-axial load cell to measure the effect of angular traction. The base of the head scalp model will need to incorporate a tilting mechanism as the actuator end of the tensile tester needs to be constrained axially to the load cell.

The evaluation of the effects of mechanical interlock on the biomechanics of cup detachment will be more complete if the profile of the chignon can be detected during the relative motion of the developed chignon. This requires further instrumentation in the VAD cup system to enhance the detectability of the profile through improvements of the transparency of the cup system and visual detection methods. By means of such improvements, different cup profiles can be investigated to contribute to the learning of the contact mechanics of the scalp and the cup system.

Supplementing the investigation of clinical factors, the consideration of the shape factor of the baby's head with presence of caputs or hair can be integrated in the overall design of the head scalp model. To experiment on such conditions, significant design adaptations to the current head scalp model would have to be considered. However, the robustness of the method of manufacture of the moulded silicone-textile scalps will need to be improved with more advanced techniques such as vacuum casting and embodiment of preformed textile sheet inside the built design of the casting moulds. Within the design of the mould, defined depots can be accommodated for silicone extrusions and can act as visual markers to improve the detectability of silicone strain. Advanced video measurement systems such as digital image correlation (DIC) can aid in the quantitative measurement of strain on the surrogate scalp during VAD simulation. Reflecting on clinical practice, the process of adding a smear of lubricant can help in improving retention forces. However, it would be interesting to investigate on the tribology aspects influencing the contact mechanics at the cup and scalp interface by a detailed study of the thickness of the lubricants to evaluate the effective coefficient of friction and its underlying impact on the dynamics of cup detachment.

The discussed enhancements to the VAD test simulator can bring the latter into contention for a test evaluation method of new conceptions of VAD devices to supplement device development activities.

7.2.2 Future Works

Based on the discussion on the research outputs delivered from the presented research, the future direction for the continuation of activities related to the research and commercial aspects of the project will be suggested in this section. Certainly, there will be challenges in the developmental path of the atraumatic device which could impact the delivery of the solution to be clinically implemented. An initial risk register was conceived to understand the risks associated with the advancement of the newly conceived atraumatic VAD system from the conception stage to the developmental stages. Table 7-1 provides a summary of key considerations of the technical, clinical & commercial challenges, the presented risks which should be mitigated to progress from the current concept to a commercially viable offering on the market. In future considerations, from a research point of view, advanced prototypes of the atraumatic VAD concept will need to be functionally evaluated and IP filing around the technological advancements will be required. Before entering commercial development for further verification and validation activities, usability studies or stake holder validation will need to be addressed to ensure that the product can be easily adopted in clinical practices. Business processes will then follow to achieve a market place for the supply and distribution of the device for the chosen route to market.

Table 7-1: Risk register for Future works of technical and commercial development of VAD device

Risk Register for new VAD Device Development			
Risk ID	Risk	Description	Mitigation
1	Technical Challenges	Further Research Considerations	Advanced prototypes need to be generated to demonstrate functionality. Work on predictive method will be further established.
		Transition to Commercial Development	Further verification and validation work of test metrics and predictive metric to design. Further validation of rig in scope that it becomes an approved industrial standard for testing new VAD devices

Risk Register for new VAD Device Development			
Risk ID	Risk	Description	Mitigation
2	Clinical Challenges	Product difficult to clinically validate	<p>Since there is no immediate change in the cup design, the only clinical impact is to assess the usability impact of the traction mechanism and its impact with the stakeholders (Table 2-3)</p> <p>Long term study, Multicentre study in the form of clinical trials.</p>
3	Industrialisation Capabilities	Lack of expertise in area	<p>Contracted Manufacturer needs to be identified if capability is not possible in house. Licensing opportunity might need to be considered.</p>
4	Product Adoption	Resistance to uptake new product	<p>Stakeholder Validation will be performed prior to commercialisation. Develop training material and use sales channels to deliver training.</p>

Risk Register for new VAD Device Development			
Risk ID	Risk	Description	Mitigation
5	Reimbursement	New medical products experience problems in cost coverage in healthcare system	Existing reimbursement code will be used but a premium price will be charged since there is significant contribution to the clinical pathway in cost saving benefits of preventing a pop-off. Business assessment and new trends in VAD usage needs to be used. Further discussion with stakeholders responsible for purchasing.
6	Competition	Gaining market Share	If patent is filed around technology, there will be no freedom to operate for competitors
		Competitor decides to implement a traction control system	Licensing opportunities required or advice from patent attorney required. If financial gain exceeds cost of licensing, then a business opportunity.

Risk Register for new VAD Device Development			
Risk ID	Risk	Description	Mitigation
7	Patent	Patent is not granted	Concept is novel, inventive and innovative and is backed with structured research from a PhD thesis.
8	Regulatory	EU regulatory framework is changing and becoming more stringent. Approval times might have an impact on product launch	Documentations will need to be created to address the EU MDR directive. Regulatory timeline for approval typically 9 months for class 2a.
9	Route to Market	Commercial partner does not have a sales & distribution network	A distributor with market access to hospitals or clinics and capable of handling commercial orders will need to be considered

7.3 Concluding Remarks

The research presented in this thesis has investigated an area of key clinical need, improving the performance of VAD devices, which has seen minimal technical development since their inception. The literature review highlighted a lack of rigorous understanding in how VAD devices function, in particular the mechanics of their use.

This research therefore addressed these limitations and developed evidence-based means of investigating and documenting VAD performance. The methods developed in this work have enabled further experimental investigation to understand the mechanical interaction of the VAD cup with the foetal head scalp during the occurrence of unintentional cup detachment. The physical in-vitro simulation of VAD procedures proposed an original assessment of VAD device performance against a robust controlled test methodology. The experimental studies undertaken provided a deeper insight into mechanical and clinical factors associated with VAD.

Considering the current state of research of VAD was clinically oriented, this was the first known approach to propose improvements to VAD based on quantifiable research outcomes with an engineering focus. However, the presented research can be further advanced to improve the visibility of demonstrable objective evidence in this critical area of care. To achieve a better state of understanding around the biomechanics of VAD devices, elaboration on the current limitations discussed in the previous section is needed to progress the current state of research.

In conclusion, informing stakeholders of VAD involved in the clinical outcomes about the impact of cup detachment and its outlying links to clinical and mechanical factors can complement best practice in training for, and performing, VAD. In addition, improved understanding of VAD mechanics is critical to inform the development of new atraumatic VAD devices appropriate for modern healthcare systems. These have a direct opportunity to bring improvements in healthcare delivery, reducing healthcare costs, improving efficiency by avoiding unnecessary operative delivery and most crucially, by reducing maternal and child trauma.

References

1. O'Mahony, F., G.J. Hofmeyr and V. Menon. Choice of instruments for assisted vaginal delivery. *The Cochrane Library*, 2010.
2. Awon, M.P. The vacuum extractor-extractor-experimental demonstration of distortion of the foetal skull. *BJOG: An International Journal of Obstetrics & Gynaecology*, 1964, **71**(4), pp.634-636.
3. Pettersson, K., J. Ajne, K. Yousaf, D. Sturm, M. Westgren and G. Ajne. Traction force during vacuum extraction: a prospective observational study. *BJOG*, 2015, **122**(13), pp.1809-16.
4. Turkmen, S. Maternal and neonatal outcomes in vacuum-assisted delivery with the Kiwi OmniCup and Malmström metal cup. *Journal of Obstetrics and Gynaecology Research*, 2015, **41**(2), pp.207-213.
5. Baskett, T.F. and A.A. Calder. *Munro Kerr's Operative Obstetrics E-Book*. Elsevier Health Sciences, 2014.
6. Milton, S.H. *Normal Labor and Delivery* [online]. 2016. [Accessed]. Available from: <http://emedicine.medscape.com/article/260036-overview>.
7. Baum, J.D. and D. Searls. Head shape and size of newborn infants. *Developmental Medicine & Child Neurology*, 1971, **13**(5), pp.572-575.
8. Di Renzo, G.C. and U. Simeoni. *The pre-nate and neonate: an illustrated guide to the transition to extrauterine life*. CRC Press, 2006.
9. Sorbe, B. and S. Dahlgren. Some important factors in the molding of the fetal head during vaginal delivery - A photographic study. *International Journal of Gynecology & Obstetrics*, 1983, **21**(3), pp.205-212.
10. Al-Mufti, R., A. McCarthy and N. Fisk. Obstetricians' personal choice and mode of delivery. *The Lancet*, 1996, **347**(9000), p.544.
11. Macfarlane, A., B. Blondel, A. Mohangoo, M. Cuttini, J. Nijhuis, Z. Novak, H. Ólafsdóttir and J. Zeitlin. Wide differences in mode of delivery within Europe: risk-stratified analyses of aggregated routine data from the Euro-Peristat study. *BJOG: An International Journal of Obstetrics & Gynaecology*, 2015.
12. Murphy, D.J., R.E. Liebling, L. Verity, R. Swingler and R. Patel. Early maternal and neonatal morbidity associated with operative delivery in second stage of labour: a cohort study. *The Lancet*, 2001, **358**(9289), pp.1203-1207.
13. NHS. Caesarean section
14. Berger, K.S. *The Developing Person Through the Life Span*. Ninth Edition ed. Worth Publishers, 2014.
15. Ontario. *Labour Progress* [online]. [Accessed]. Available from: <http://www.ontarioprenataleducation.ca/labour-progress/>.
16. Thomas, J. and S. Paranjothy. National sentinel caesarean section audit report. Royal College of Obstetricians and Gynaecologists Clinical Effectiveness Support Unit. London: RCOG Press, 2001, **200**(1), p.43.
17. Martin, J.A., B.E. Hamilton, P.D. Sutton, S.J. Ventura, F. Menacker, S. Kirmeyer and M.L. Munson. Births: final data for 2005. *National vital statistics reports*, 2007, **56**(6), pp.1-103.
18. RCOG. *Green-top Guideline No.26*. RCOG, 2011.

19. Cass, G.K.S., J.F. Crofts and T.J. Draycott. The Use of Simulation to Teach Clinical Skills in Obstetrics. *Seminars in Perinatology*, 2011, **35**(2), pp.68-73.
20. Lepage, J., M. Cosson, O. Mayeur, M. Brieu and C. Rubod. Pedagogical childbirth simulators: utility in obstetrics. *Eur J Obstet Gynecol Reprod Biol*, 2016, **197**, pp.41-7.
21. Bahl, R., D.J. Murphy and B. Strachan. Decision-making in operative vaginal delivery: when to intervene, where to deliver and which instrument to use? Qualitative analysis of expert clinical practice. *Eur J Obstet Gynecol Reprod Biol*, 2013, **170**(2), pp.333-40.
22. Macleod, M. and D.J. Murphy. Operative vaginal delivery and the use of episiotomy—a survey of practice in the United Kingdom and Ireland. *European Journal of Obstetrics and Gynecology and Reproductive Biology*, 2008, **136**(2), pp.178-183.
23. Euro-Perisat-Project. *European Perinatal Health Report- Core Indicators of the health and care of pregnant women and babies in Europe in 2015*. November 2018.
24. Johanson, R. Choice of instrument for vaginal delivery. *Current Opinion in Obstetrics and Gynecology*, 1997, **9**(6), pp.361-365.
25. Grossbard, P. and S. Cohn. The Malmstrom vacuum extractor in obstetrics. *Obstetrics & Gynecology*, 1962, **19**, pp.207-211.
26. PFH. *Sales Representative Training guide*. 2011.
27. Ross, M.G. *Forceps Delivery* [online]. 2020. [Accessed]. Available from: <http://emedicine.medscape.com/article/263603-overview>.
28. Dunn, P. Sir James Young Simpson (1811–1870) and obstetric anaesthesia. *Archives of Disease in Childhood-Fetal and Neonatal Edition*, 2002, **86**(3), pp.F207-F209.
29. ---. Dr Christian Kielland of Oslo (1871–1941) and his straight forceps. *Archives of Disease in Childhood-Fetal and Neonatal Edition*, 2004, **89**(5), pp.F465-F467.
30. Ross, M.G. *Forceps Delivery Treatment & Management*.
31. Rather, H., J. Muglu, L. Veluthar and K. Sivanesan. The art of performing a safe forceps delivery: a skill to revitalise. *Eur J Obstet Gynecol Reprod Biol*, 2016, **199**, pp.49-54.
32. Benavides, L., J.M. Wu, A.F. Hundley, T.S. Ivester and A.G. Visco. The impact of occiput posterior fetal head position on the risk of anal sphincter injury in forceps-assisted vaginal deliveries. *Am J Obstet Gynecol*, 2005, **192**(5), pp.1702-6.
33. Drife, J.O. Choice and instrumental delivery. *BJOG: An International Journal of Obstetrics & Gynaecology*, 1996, **103**(7), pp.608-611.
34. Science Museum, L. *Keilland obstetrical forceps, England, 1979*. Television advertisement. Screened
35. ---. Simpson type obstetrical forceps, London, England, 1871-1900.
36. Malmström, T. The Vacuum Extractor an Obstetrical Instrument and the Parturiometer a Tokographic Device. *Acta Obstetrica et Gynecologica Scandinavica*, 1957, **36**(S3), pp.5-87.
37. Vacca, A. VACUUM-ASSISTED DELIVERY-Improving patient outcomes and protecting yourself against litigation. [online], 2004, p.12.

- Available from: <http://clinicalinnovations.com/wp-content/uploads/2015/03/OBGMgmtSupplement.pdf>.
38. Buttin, R., F. Zara, B. Shariat, T. Redarce and G. Grange. Biomechanical simulation of the fetal descent without imposed theoretical trajectory. *Comput Methods Programs Biomed*, 2013, **111**(2), pp.389-401.
 39. Vacca, A. *Handbook of vacuum extraction in obstetric practice*. London: Arnold, 1992.
 40. ANTIPUESTO, D.J. *Difference between Caput Succedaneum and Cephalhematoma* [online]. 2011. [Accessed]. Available from: <http://nursingcrib.com/nursing-notes-reviewer/maternal-child-health/difference-between-caput-succedaneum-and-cephalhematoma/>.
 41. Nicholson, L. Caput succedaneum and cephalohematoma: the Cs that leave bumps on the head. *Neonatal Network*, 2007, **26**(5), pp.277-281.
 42. Rydberg, E. Mechanism of labor. *Archiv für Gynäkologie*, 1951, **180**, p.171.
 43. Bird, G. The importance of flexion in vacuum extractor delivery. *BJOG: An International Journal of Obstetrics & Gynaecology*, 1976, **83**(3), pp.194-200.
 44. Vacca, A. Vacuum-assisted delivery: An analysis of traction force and maternal and neonatal outcomes. *Australian and New Zealand Journal of Obstetrics and Gynaecology*, 2006, **46**(2), pp.124-127.
 45. ---. Reducing the risks of a vacuum delivery. *Fetal and Maternal Medicine Review*, 2006, **17**(04), pp.301-315.
 46. Winter, G.A.T.D.A.G.D.S.C. *ROBuST:RCOG operative birth simulation training*. Cambridge University Press, 2014.
 47. Attilakos, G., A. Gale, T. Draycott, D. Siassakos and C. Winter. *ROBuST: RCOG operative birth simulation training*. Cambridge University Press, 2013.
 48. Young, R.W. Age changes in the thickness of the scalp in white males. *Human biology*, 1959, **31**(1), pp.74-79.
 49. Harris, C.M. *Scalp Anatomy* [online]. 2013. [Accessed]. Available from: <http://emedicine.medscape.com/article/834808-overview>.
 50. Agur, A.M. and A.F. Dalley. *Grant's atlas of anatomy*. Lippincott Williams & Wilkins, 2009.
 51. Logan, B.M., R.T. Hutchings and R.M.H. McMinn. *Color atlas of head and neck anatomy*. 2nd ed. Edinburgh; New York: Mosby, 1995.
 52. Snell, R.S. and A.A. Travill. Clinical Anatomy for Medical Students. *Annals of Plastic Surgery*, 1979, **2**(6), p.542.
 53. Oomens, C., D. Van Campen and H.J.J.o.b. Grootenboer. A mixture approach to the mechanics of skin. 1987, **20**(9), pp.877-885.
 54. ---. In vitro compression of a soft tissue layer on a rigid foundation. 1987, **20**(10), pp.923-935.
 55. Falland-Cheung, L., M. Scholze, P.F. Lozano, B. Ondruschka, D.C. Tong, P.A. Brunton, J.N. Waddell and N. Hammer. Mechanical properties of the human scalp in tension. *Journal of the mechanical behavior of biomedical materials*, 2018.
 56. *Differences between caput succedaneum, cephalhematoma, and subgaleal hemorrhage*. [online]. [Accessed 08/02/2020]. Available from:

https://evolve.elsevier.com/objects/apply/RN/HealthyNewborn/RN_HealthyNewborn_04.html.

57. Baskett, T.F., C.A. Fanning, D.C.J.J.o.O. Young and G. Canada. A prospective observational study of 1000 vacuum assisted deliveries with the OmniCup device. 2008, **30**(7), pp.573-580.
58. Uchil, D. and S. Arulkumaran. Neonatal subgaleal hemorrhage and its relationship to delivery by vacuum extraction. *Obstetrical & gynecological survey*, 2003, **58**(10), pp.687-693.
59. Plauche, W.C. Fetal cranial injuries related to delivery with the Malmstrom vacuum extractor. *Obstetrics & Gynecology*, 1979, **53**(6), pp.750-757.
60. Govaert, P., P. Vanhaesebrouck, C. De Praeter, K. Moens and J. Leroy. Vacuum extraction, bone injury and neonatal subgaleal bleeding. *European Journal of Pediatrics*, 1992, **151**(7), pp.532-535.
61. Davis, D.J. Neonatal subgaleal hemorrhage: diagnosis and management. *Canadian Medical Association Journal*, 2001, **164**(10), pp.1452-1453.
62. Amar, A.P., H.E. Aryan, H.S. Meltzer and M.L. Levy. Neonatal subgaleal hematoma causing brain compression: report of two cases and review of the literature. *Neurosurgery*, 2003, **52**(6), pp.1470-1474.
63. Cavlovich, F.E. Subgaleal Hemorrhage in the Neonate. *Journal of Obstetric, Gynecologic, & Neonatal Nursing*, 1995, **24**(5), pp.397-405.
64. Eliachar E, B.A., Bardiaux M, Tassy R, Pheulpin J, Schneider M. Hématome souscutané crânien du nouveau-né. *Arch Fr Pédiatr*, 1963, (20:1105-11).
65. Boo, N.Y., K.W. Foong, Z.A. Mahdy, S.C. Yong, R.J.B.A.I.J.o.O. Jaafar and Gynaecology. Risk factors associated with subaponeurotic haemorrhage in full-term infants exposed to vacuum extraction. 2005, **112**(11), pp.1516-1521.
66. Haikin, E.H. and D. Mankuta. Vacuum cup placement during delivery – A suggested obstetric quality assessment measure. *The Journal of Maternal-Fetal & Neonatal Medicine*, 2012, **25**(10), pp.2135-2137.
67. Johanson, R. and V. Menon. Soft versus rigid vacuum extractor cups for assisted vaginal delivery. *The Cochrane Library*, 2000.
68. Eskander, R., M. Beall and M.G. Ross. Vacuum-assisted vaginal delivery simulation – quantitation of subjective measures of traction and detachment forces. *The Journal of Maternal-Fetal & Neonatal Medicine*, 2012, **25**(10), pp.2039-2041.
69. Simpson, J.Y. *The obstetric memoirs and contributions of James Y. Simpson*. Lippincott, 1855.
70. Eustace, D. James Young Simpson: the controversy surrounding the presentation of his Air Tractor (1848-1849). *Journal of the Royal Society of Medicine*, 1993, **86**(11), p.660.
71. Hibbard, B.M. *The obstetrician's armamentarium: historical obstetric instruments and their inventors*. Norman Publishing, 2000.
72. Lövset, J. Modern techniques of vaginal operative delivery in cephalic presentation. *Acta Obstetrica et Gynecologica Scandinavica*, 1965, **44**(1), pp.102-106.
73. Couzigou, Y. La ventouse eutocique. *Travail, extrait d'une communication faite le*, 1947, **25**.

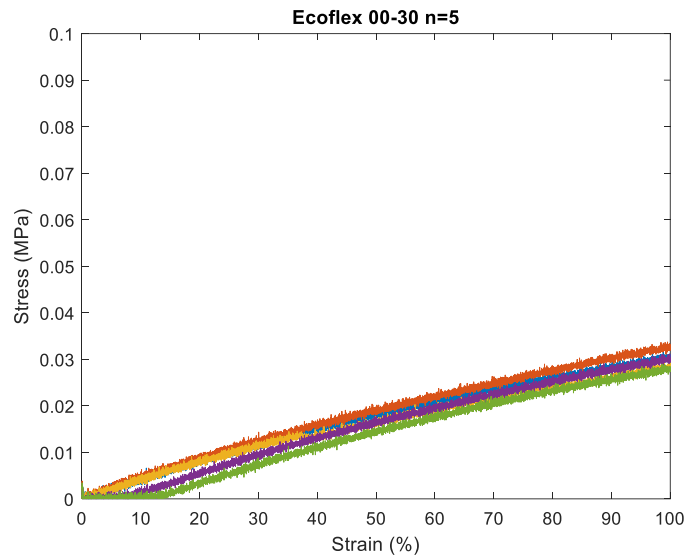
74. Sjöstedt, J.E. The vacuum extractor and forceps in obstetrics a clinical study. *Acta Obstetrica et Gynecologica Scandinavica*, 1967, **46**(sup10), pp.1-208.
75. Škrobonja, A., V. Uremović, A. Finderle and H. Haller. Two anniversaries related to Dr. Viktor Finderle (1902–1964). *Wiener klinische Wochenschrift*, 2004, **116**(24), pp.858-860.
76. Malmstrom, T.J.N.M. * SUGKLOCKA-EN ERSATTARE FOR GALEATANG. 1953, **50**(38), pp.1311-1311.
77. Kuit, J. *Clinical and physical aspects of obstetric vacuum extraction*. thesis, Erasmus University Rotterdam, 1997.
78. Thiery, M., R. Van Den Broecke, G. Kermans, W. Parewijck, M. Dhont, M. Vanlancker, H. Van Kets, P. Defoort, R. Derom and P. Vanhaesebrouck. A randomized study of two cups for vacuum extraction. *Journal of Perinatal Medicine-Official Journal of the WAPM*, 1987, **15**(2), pp.129-136.
79. DELL, D.L., S.E. SIGHTLER and W.C. PLAUCHE. Soft cup vacuum extraction: a comparison of outlet delivery. *Obstetrics & Gynecology*, 1985, **66**(5), pp.624-628.
80. Kuit, J.A., H.C.S. Wallenburg and F.J.M. Huikeshoven. The pliable obstetrical vacuum cup: application and opinions in The Netherlands. *European Journal of Obstetrics & Gynecology and Reproductive Biology*, 1992, **44**(2), pp.107-110.
81. Chalmers, J.A. *The ventouse: the obstetric vacuum extractor*. London: Lloyd-Luke, 1971.
82. Lo, C.L.D.G.J. First UK experience of Mityvac vacuum delivery system. *Journal of Obstetrics and Gynaecology*, 2001, **21**(6), pp.601-602.
83. Clinical-Innovations. A Complete Vacuum Delivery System to Assist in Fetal Delivery.
84. Deruelle, P., E. Queste-Bothuyne, S. Depret and D. Subtil. Cinq questions à propos de la ventouse Kiwi OmniCup™ ☆. *Gynécologie Obstétrique & Fertilité*, 2007, **35**(6), pp.582-586.
85. Hayman, R., J. Gilby and S. Arulkumaran. Clinical evaluation of a "hand pump" vacuum delivery device. *Obstetrics & Gynecology*, 2002, **100**(6), pp.1190-5.
86. Groom, K., B. Jones, N. Miller and S. Paterson-Brown. A prospective randomised controlled trial of the Kiwi Omnicup versus conventional ventouse cups for vacuum-assisted vaginal delivery. *BJOG: An International Journal of Obstetrics & Gynaecology*, 2006, **113**(2), pp.183-189.
87. Chalmers, J. and R. Fothergill. Use of a vacuum extractor (ventouse) in obstetrics. *British medical journal*, 1960, **1**(5187), p.1684.
88. Svenningsen, L. Birth progression and traction forces developed under vacuum extraction after slow or rapid application of suction. *European Journal of Obstetrics & Gynecology and Reproductive Biology*, 1987, **26**(2), pp.105-112.
89. Glaser, L.M., F.A. Alvi and M.P. Milad. Trends in malpractice claims for obstetric and gynecologic procedures, 2005 through 2014. *American Journal of Obstetrics & Gynecology*, 2017, **217**(3), pp.340. e1-340. e6.

90. Saling, E. and M. Hartung. Analyses of tractive forces during the application of vacuum extraction. *Journal of Perinatal Medicine-Official Journal of the WAPM*, 1973, **1**(4), pp.245-251.
91. Saling, E., U. Blücher and H. Sander. Equipment for the recording of tractive power in vacuum extractions. 1973.
92. MUISE, K.L. and R.H. BROWN. The effect of artificial caput on performance of vacuum extractors. *Obstetrics & Gynecology*, 1993, **81**(2), pp.170-173.
93. Muise, K.L., M.A. Duchon and R.H. Brown. Effect of angular traction on the performance of modern vacuum extractors. *American Journal of Obstetrics and Gynecology*, 1992, **167**(4), pp.1125-1129.
94. DUCHON, M.A., M.A. DeMUND and R.H. BROWN. Laboratory Comparison of Modern Vacuum Extractors. *Obstetrics & Gynecology*, 1988, **71**(2), pp.155-158.
95. Loudon, J., K. Groom, L. Hinkson, D. Harrington, S.J.J.o.O. Paterson-Brown and Gynaecology. Changing trends in operative delivery performed at full dilatation over a 10-year period. 2010, **30**(4), pp.370-375.
96. Ismail, N.A.M., W.S.L. Saharan, M.A. Zaleha, R. Jaafar, J.A. Muhammad, Z.R.M.J.J.o.O. Razi and G. Research. Kiwi Omnicup versus Malmstrom metal cup in vacuum assisted delivery: a randomized comparative trial. 2008, **34**(3), pp.350-353.
97. Bestgen, R. *FORCE AND PRESSURE MEASUREMENT DURING VACUUM EXTRACTIONS IN OBSTETRICS*. REPORTS IN APPLIED MEASUREMENT, HOTTINGER BALDWIN MESSTECHNIK, vol. 9, no. 1, 1995, pages 1-4, XP000521570 ISSN: 0930-7923. DARMSTADT, DE.
98. Korell, M., S. King and H. Hepp. [Dual chamber safety vacuum--initial experiences with a new suction cup]. *Geburtshilfe und Frauenheilkunde*, 1994, **54**(6), pp.367-371.
99. ---. [A new vacuum extraction system with a ball joint and detachment warning--in vitro studies and clinical use]. *Zeitschrift fur Geburtshilfe und Neonatologie*, 1999, **204**(3), pp.93-98.
100. ---. Untersuchungen an einem neuen Saugglockensystem mit Kugelgelenk und Abrisswarnung-In-vitro-Studien und klinische Anwendung. *Zeitschrift fur Geburtshilfe und Neonatologie*, 2000, **204**(03), pp.93-98.
101. Pettersson, K., K. Yousaf, J. Ranstam, M. Westgren and G. Ajne. Predictive value of traction force measurement in vacuum extraction: Development of a multivariate prognostic model. *PloS one*, 2017, **12**(3), p.e0171938.
102. Bahl, R., D. Murphy and B. Strachan. Qualitative analysis by interviews and video recordings to establish the components of a skilled low-cavity non-rotational vacuum delivery. *BJOG: An International Journal of Obstetrics & Gynaecology*, 2009, **116**(2), pp.319-326.
103. Calvert, K., M. Epee, A. Karzcub, C. Neppe, M. Allen, W. Hughes, P. McGurgan, R. King, A. Maouris and D. Doherty. Novel Simulation Workshop Improves Performance in Vacuum Delivery. *Open Journal of Obstetrics and Gynecology*, 2016, **6**(08), p.439.
104. Rosa, P.e.P. Analyse de 100 cas de ventouses. *Bull. Soc. roy. beige Gynéc. Obstét*, **27**.

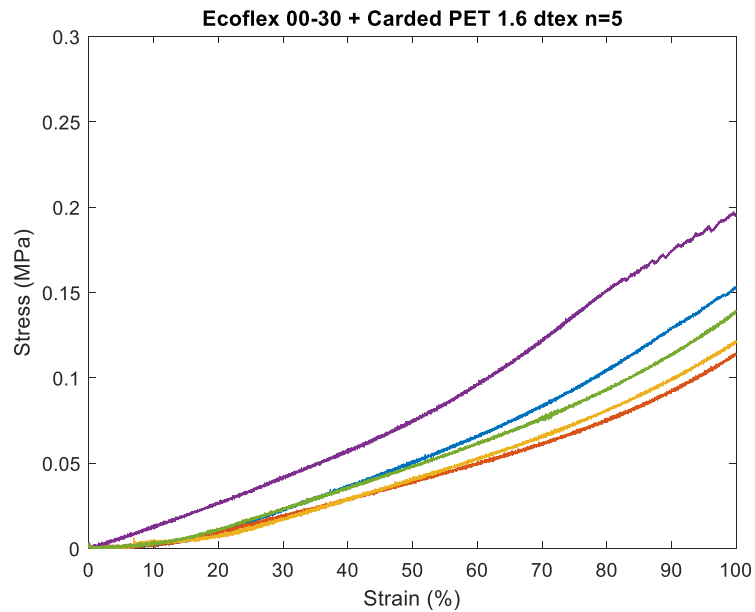
105. Rosati, P., P. Pola, P. Riccardi, R. Flore, P. Tondi, U.J.I.J.o.G. Bellati and Obstetrics. The use of amniotic fluid viscosity measurements to establish fetal lung maturity. 1991, **35**(4), pp.351-355.
106. Vacca, A. Vacuum-assisted delivery: An analysis of traction force and maternal and neonatal outcomes. *Australian and New Zealand Journal of Obstetrics and Gynaecology*, 2006, **46**(2), pp.124-127.
107. Nachman, M. and S. Franklin. Artificial Skin Model simulating dry and moist in vivo human skin friction and deformation behaviour. *Tribology International*, 2016, **97**, pp.431-439.
108. Trotta, A., D. Zouzias, G. De Bruyne and A. Ní Annaidh. The Importance of the Scalp in Head Impact Kinematics. *Annals of Biomedical Engineering*, 2018, **46**(6), pp.831-840.
109. O'Connor, H.J., A.N. Dickson and D.P.J.A.M. Dowling. Evaluation of the mechanical performance of polymer parts fabricated using a production scale multi jet fusion printing process. 2018, **22**, pp.381-387.
110. Sparks, J.L., N.A. Vavalle, K.E. Kasting, B. Long, M.L. Tanaka, P.A. Sanger, K. Schnell and T.A. Conner-Kerr. Use of Silicone Materials to Simulate Tissue Biomechanics as Related to Deep Tissue Injury. *Advances in skin & wound care*, 2015, **28**(2), pp.59-68.
111. Tausif, M., A. Pliakas, T. O'Haire, P. Goswami and S.J. Russell. Mechanical Properties of Nonwoven Reinforced Thermoplastic Polyurethane Composites. *Materials*, 2017, **10**(6), p.618.
112. Silver, F.H., J.W. Freeman and D. DeVore. Viscoelastic properties of human skin and processed dermis. *Skin Research and Technology*, 2001, **7**(1), pp.18-23.
113. SMC. *SMC ITV2090-31F2BN5 regulator, electro-pneumatic, IT2000/ITV2000 E/P REGULATOR* [online]. 2020. [Accessed]. Available from: <https://www.smc pneumatics.com/ITV2090-31F2BN5.html>.
114. Matlab. *detectHarrisFeatures* [online]. 2020. [Accessed]. Available from: <https://uk.mathworks.com/help/vision/ref/detectharrisfeatures.html>.
115. Rocol. Rocol Leak Detector Spray. 2020.
116. CRC. *Servisol Super 40* [online]. 2020. [Accessed]. Available from: http://www.crcind.com/csp/web/msds.csp?document=UDS000110_3_0_&idx=2552.
117. Merck. *Milli-Q® Reference Water Purification System* [online]. 2020. [Accessed]. Available from: https://www.merckmillipore.com/GB/en/product/Milli-Q-Reference-Water-Purification-System,MM_NF-C79625.
118. Medisave. *Material Safety Data sheet for PELJelly lubricant* [online]. 2007. [Accessed]. Available from: https://www.medisave.co.uk/media//documents/MATERIALSAFETYD ATASHEET-PELjelly_000.pdf.
119. NHS-Digital. *NS Maternity Statistics,2017-2018:HES NHS Maternity*.
120. ONS. *Annual Reference Tables:Birth Stats*. 2017.
121. RANZCOG. Instrumental vaginal birth. 2016.
122. Joyce A. Martin, M.P.H., Brady E. Hamilton, Ph.D., Michelle J.K. Osterman, M.H.S., Anne K. Driscoll, Ph.D., and Patrick Drake, M.S., Division of Vital Statistics. *National Vital Statistics Reports*. 2018.

Appendices

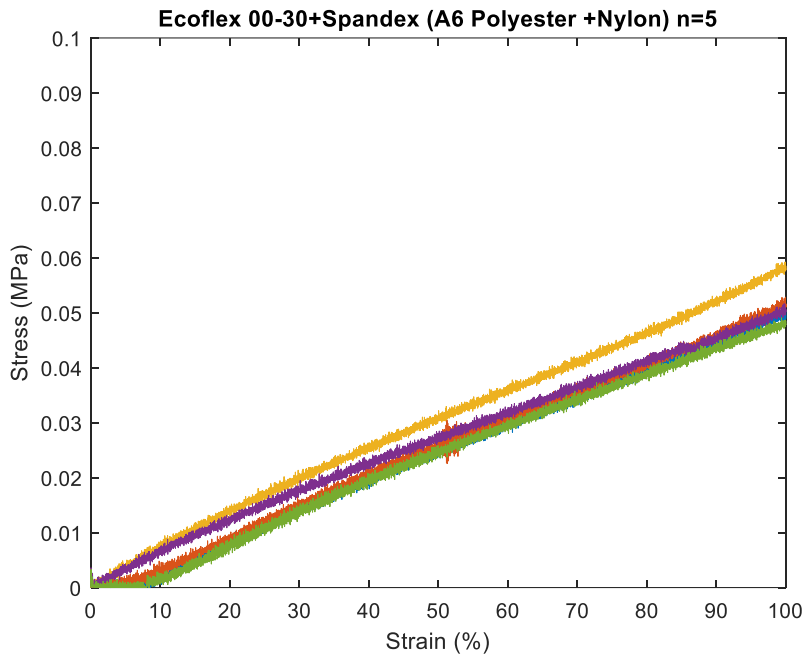
Appendix A1-Results for Evaluation for silicone textile foetal head scalp



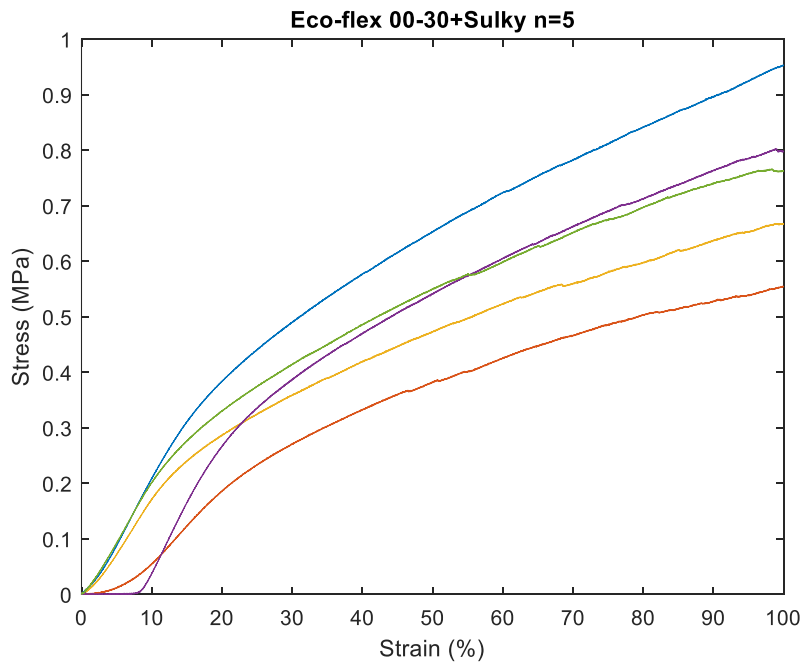
A1. 1: Stress(MPa) against Strain (%) for Ecoflex 00-30 (n=5)



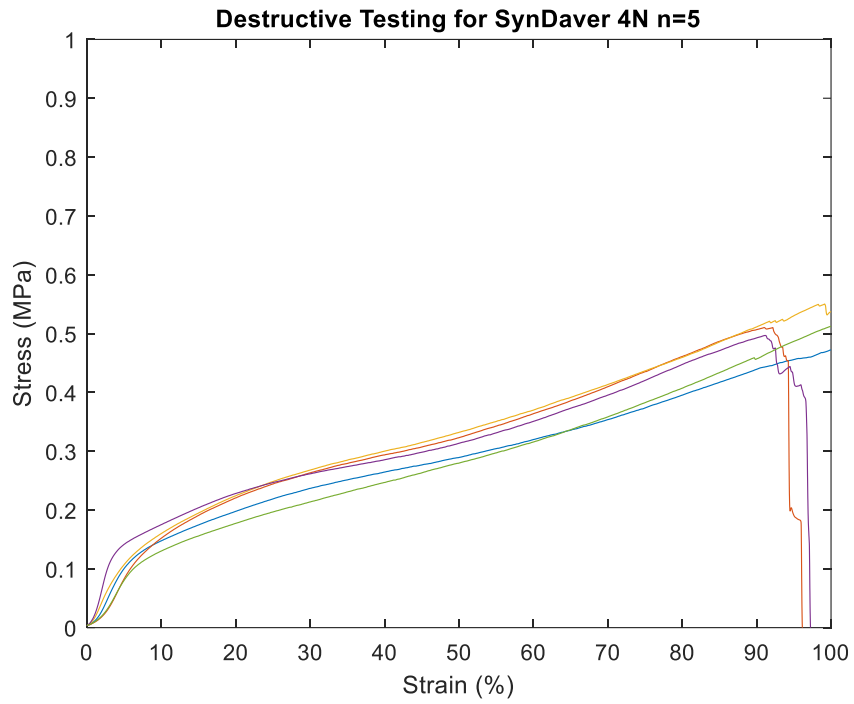
A1. 2: Stress(MPa) against Strain (%) for Ecoflex 00-30+Carded PET 1.6 dtex (n=5)



A1. 3: Stress(MPa) against Strain (%) for Ecoflex 00-30 +Spandex (A6 Polyester+Nylon) (n=5)

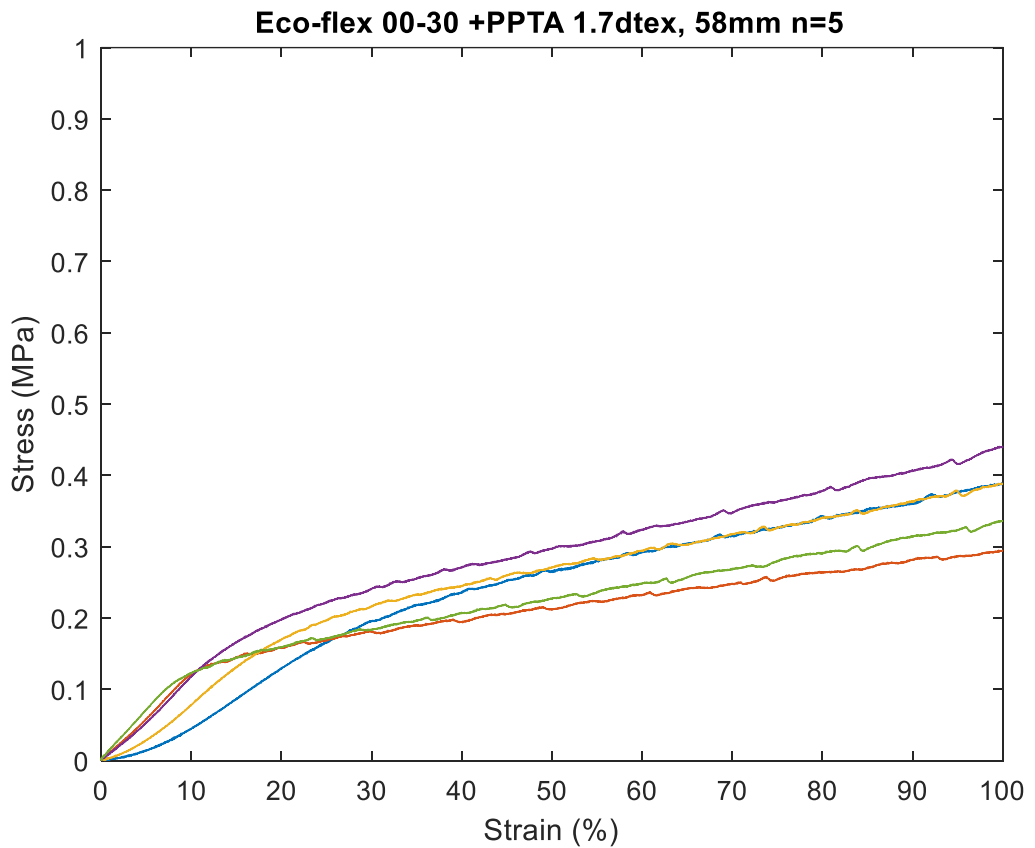


A1. 4: Stress(MPa) against Strain (%) for Ecoflex 00-30+Sulky (n=5)

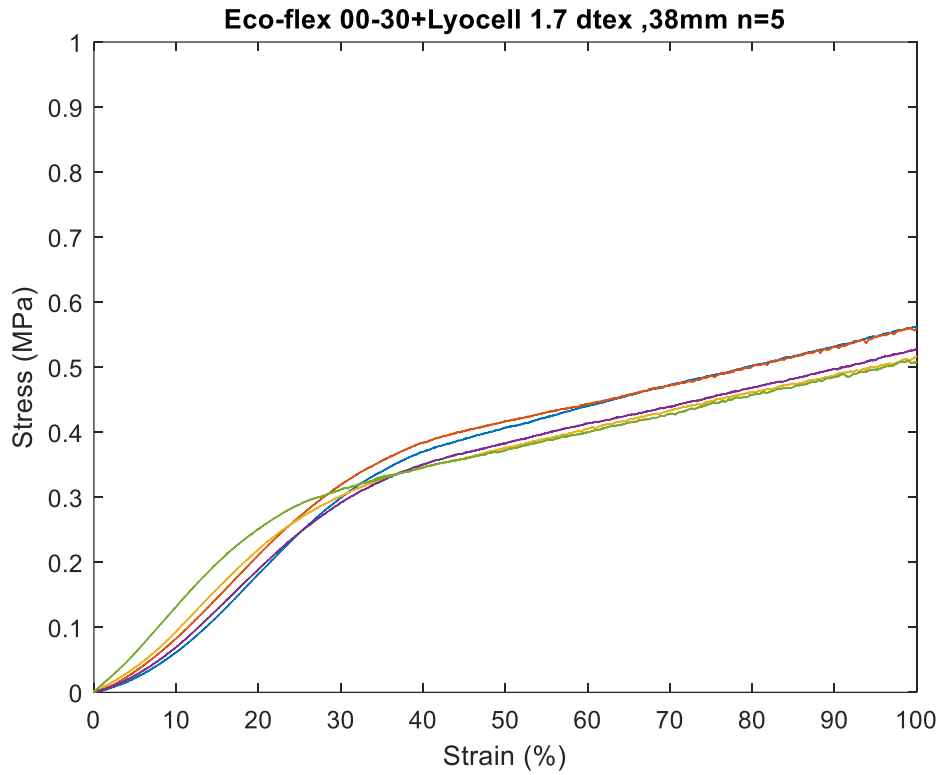


8.9

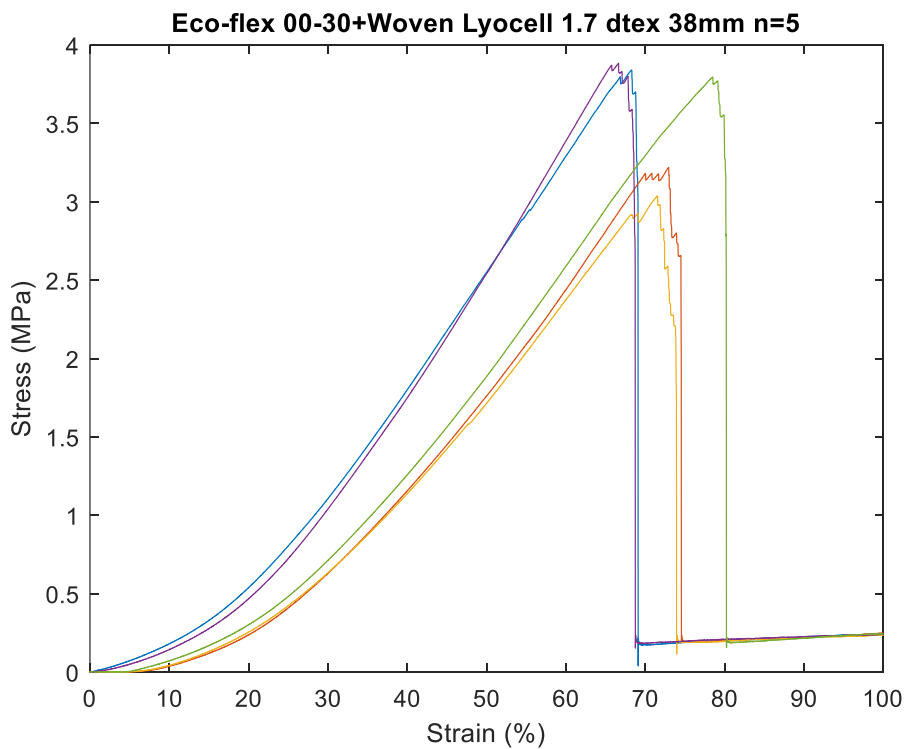
A1. 5 Stress(MPa) against Strain (%) for SynDaver 4N (n=5)



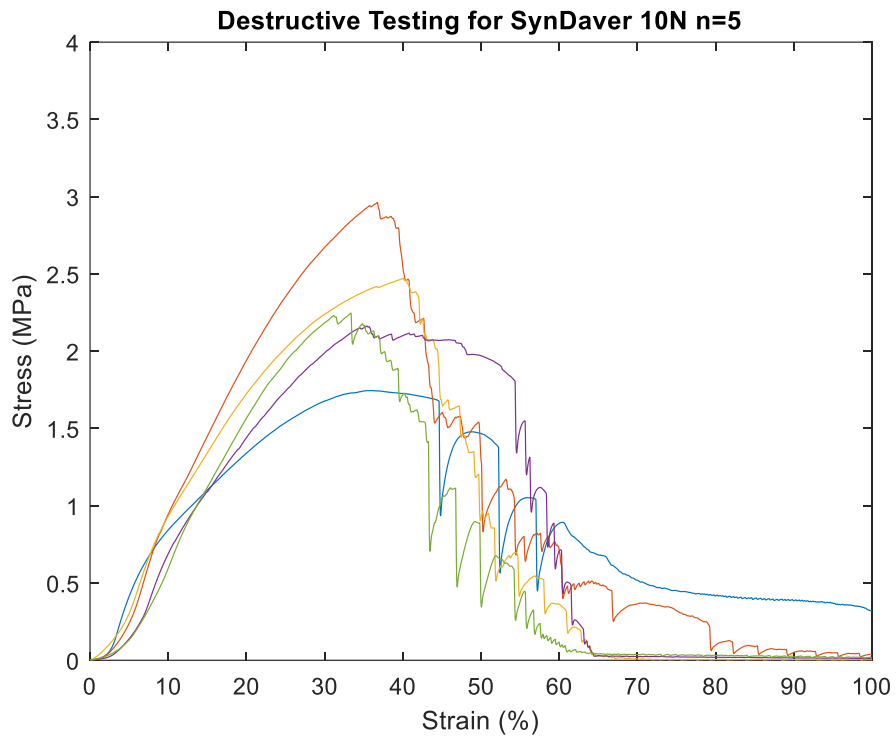
A1. 6: Stress(MPa) against Strain (%) for Ecoflex 00-30+PPTA 1.7dtex, 58mm (n=5)



A1. 7: Stress(MPa) against Strain (%) for Ecoflex 00-30+Lyocell 1.7 dtex,38mm (n=5)

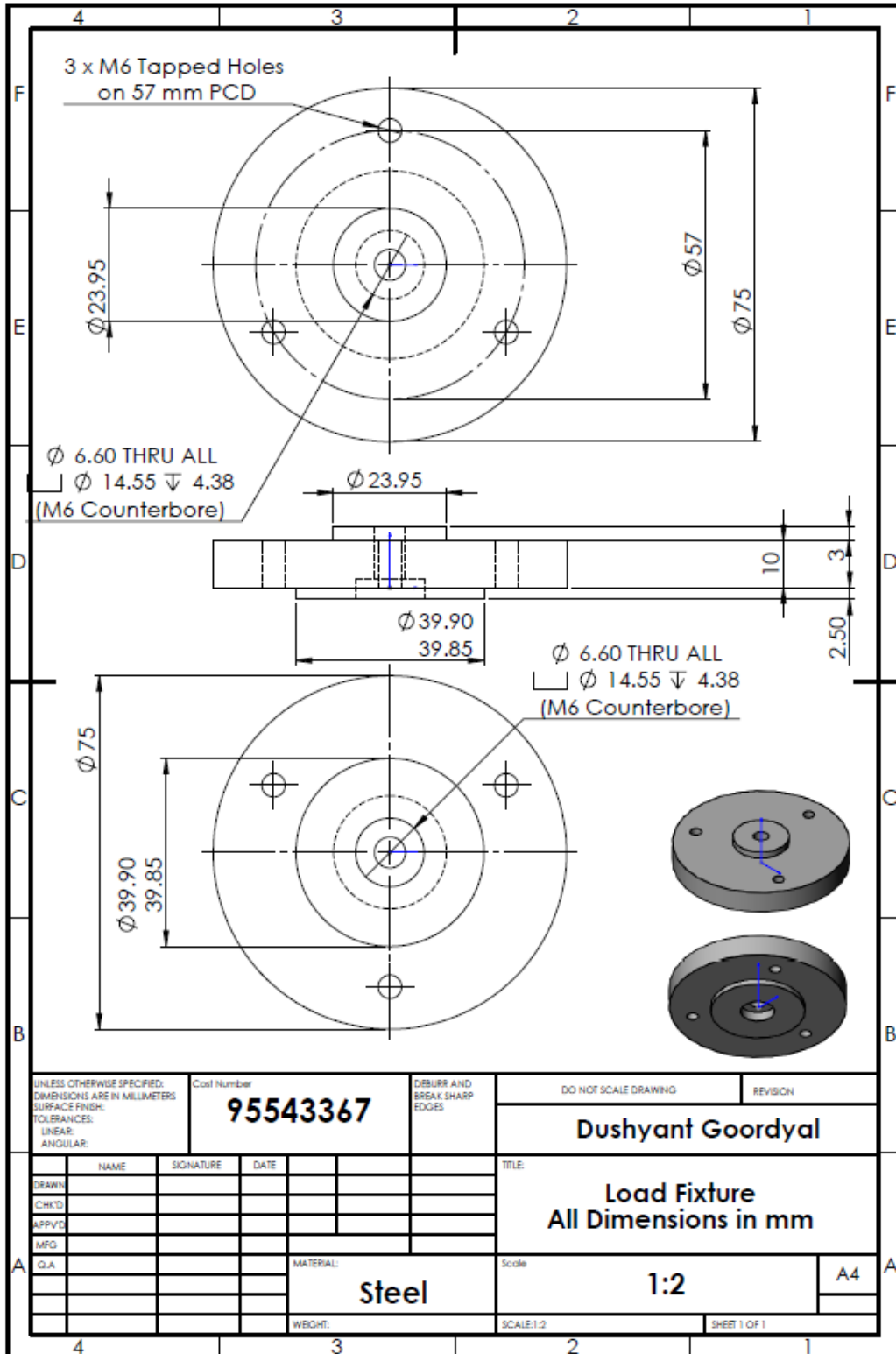


A1. 8: Stress(MPa) against Strain (%) for Ecoflex 00-30+Woven Lyocell 1.7 dtex 38mm (n=5)

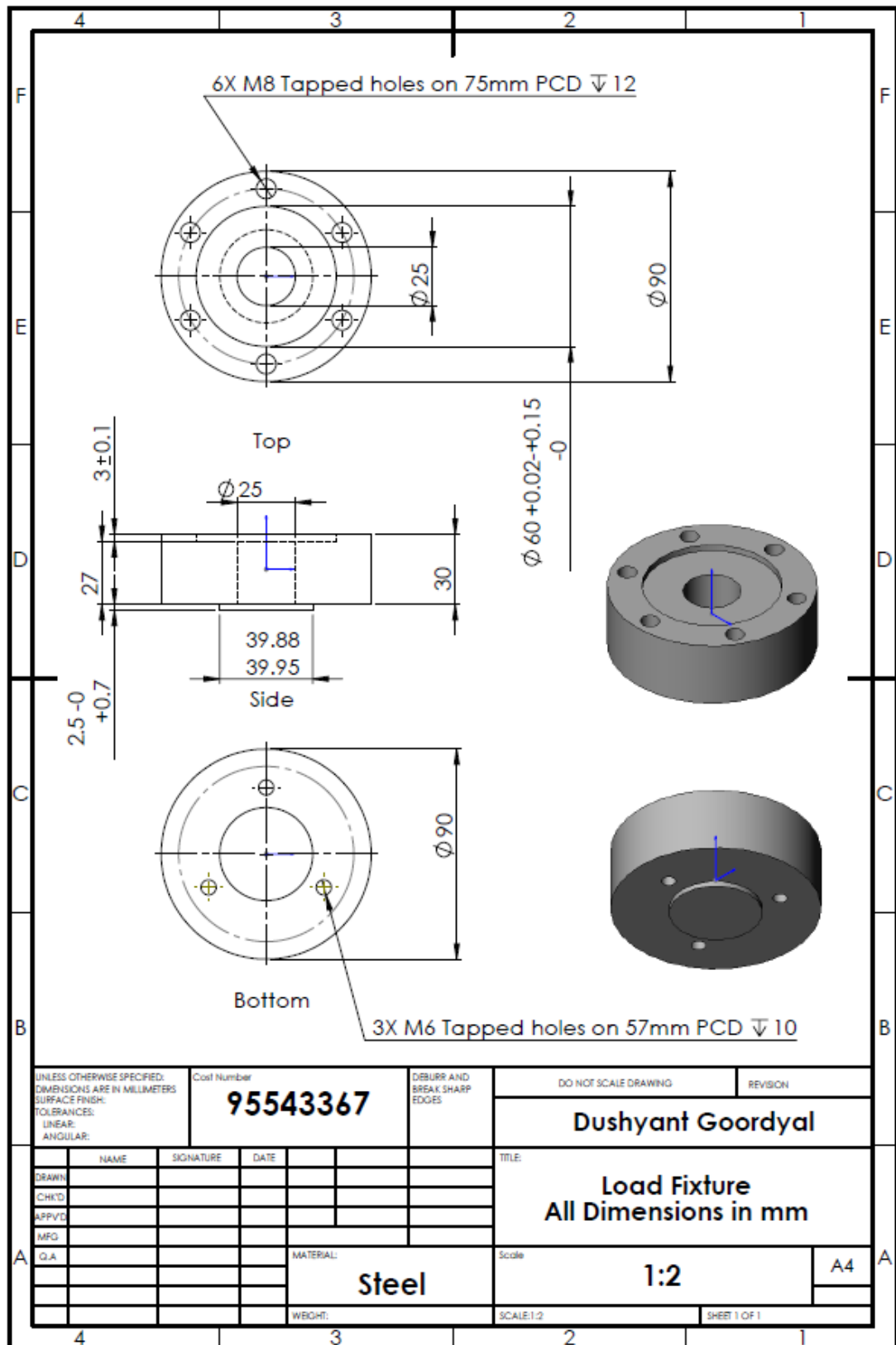


A1. 9: Stress(MPa) against Strain (%) for SynDaver 10N (n=5)

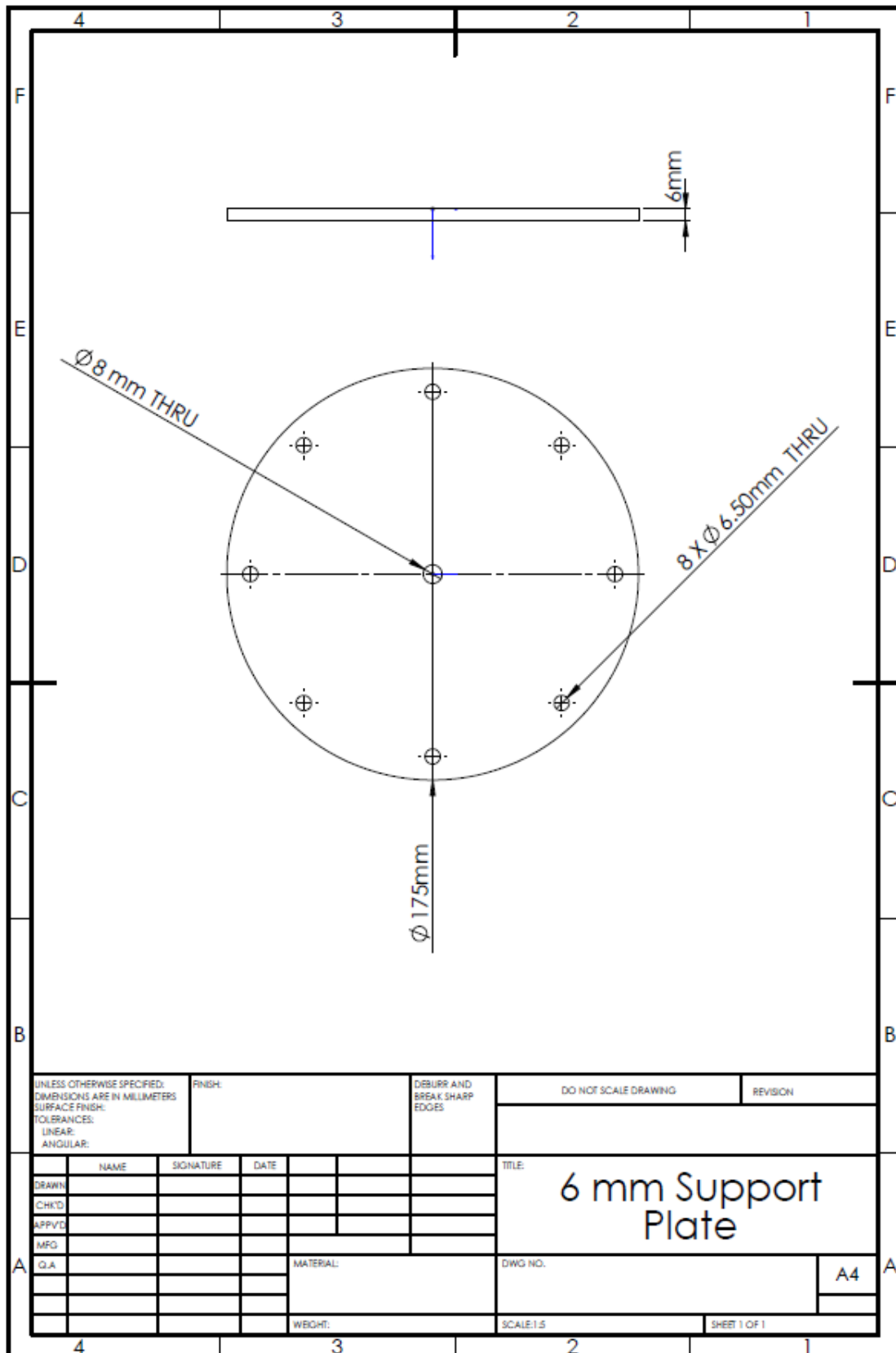
Appendix A2- E10000 Fixtures Design



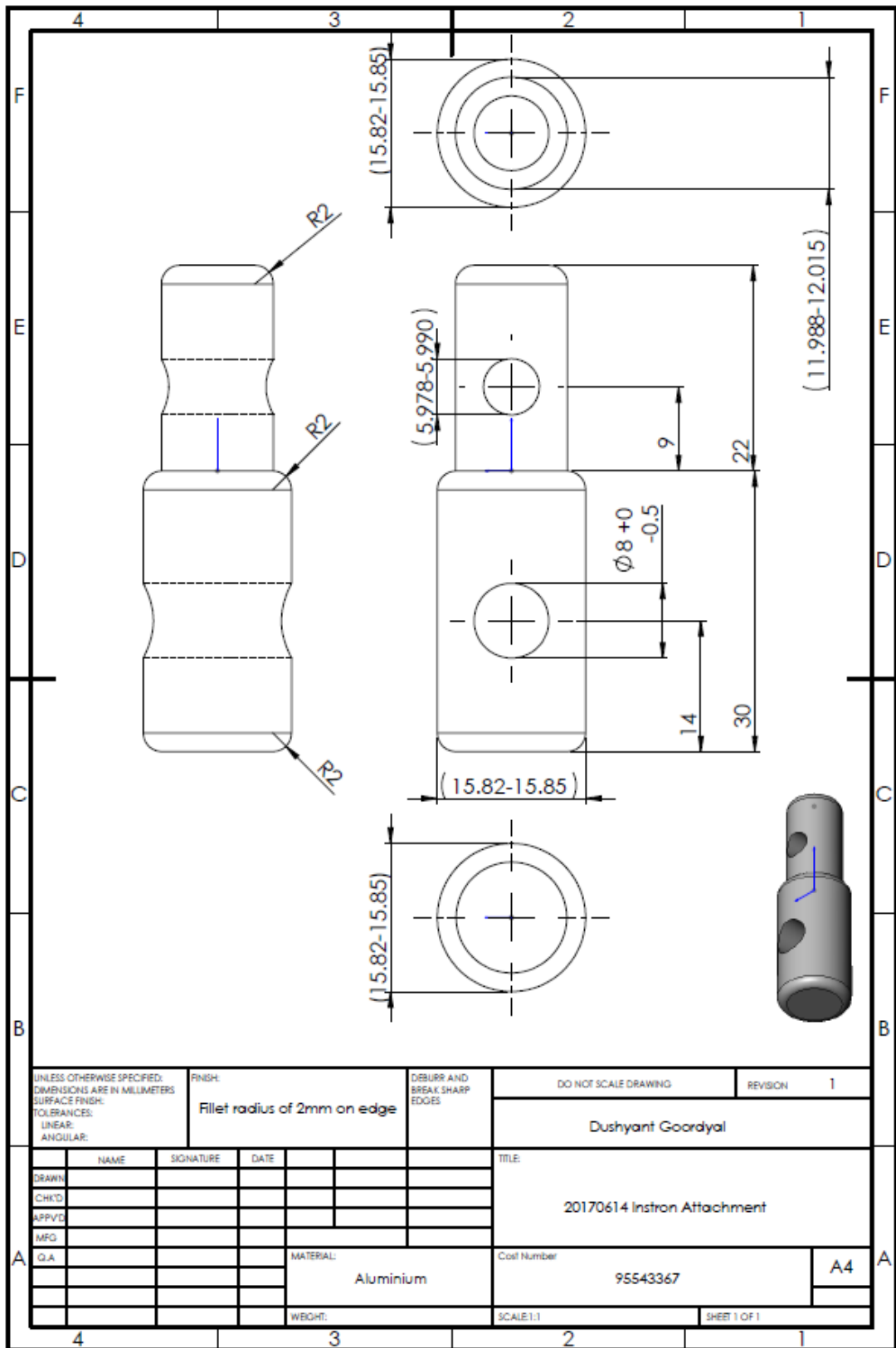
A2. 1: Coupling fixture to base of Instron E10000



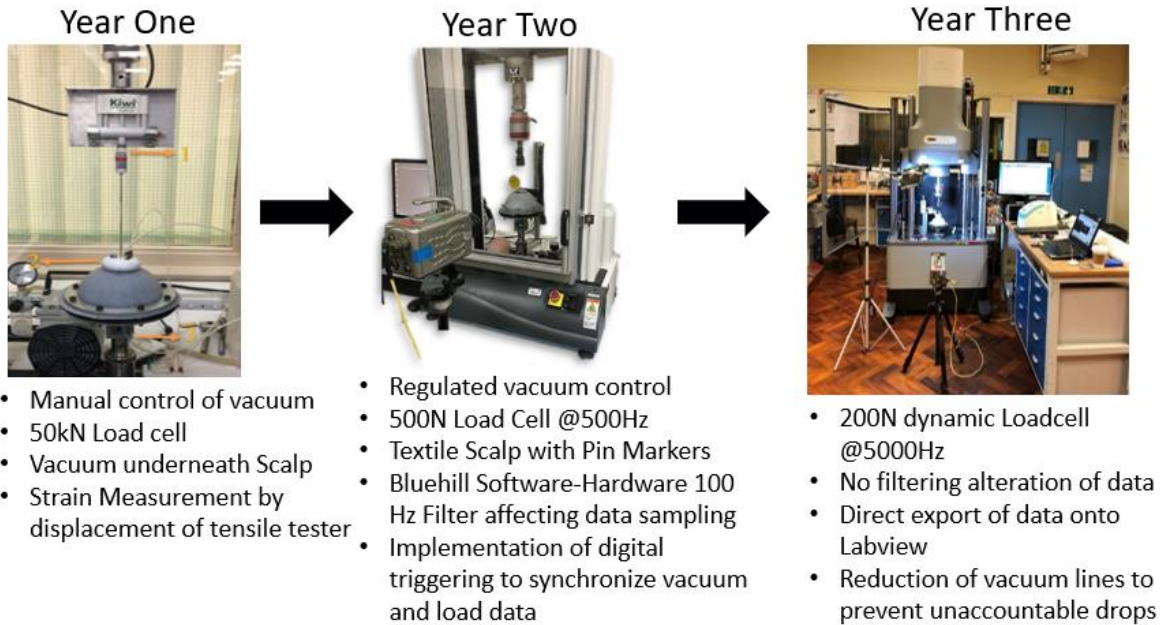
A2. 2 Coupling Fixture to 200N LoadCell



A2. 3: Fixture underneath Foetal Head Scalp model to connect to Instron Base Coupling



A2. 4: Gripping Fixture Attachment



A2. 5:Rig Development

Appendix A3: Statistical Evaluation of Scalps

Tukey comparison of means

One-way ANOVA: Lmax (N) versus Scalp Method

Null hypothesis All means are equal
 Alternative hypothesis Not all means are equal
 Significance level $\alpha = 0.05$

Equal variances were assumed for the analysis.

Factor Information

Factor	Levels	Values
Scalp	2	1, 2

Analysis of Variance

Source	DF	Adj SS	Adj MS	F-Value	P-Value
Scalp	1	5.857	5.857	1.09	0.327
Error	8	43.020	5.377		
Total	9	48.877			

Model Summary

S	R-sq	R-sq(adj)	R-sq(pred)
2.31893	11.98%	0.98%	0.00%

Means

Scalp	N	Mean	StDev	95% CI
1	5	113.53	3.14	(111.14, 115.92)
2	5	115.059	0.951	(112.667, 117.450)

Pooled StDev = 2.31893

Tukey Pairwise Comparisons

Grouping Information Using the Tukey Method and 95% Confidence

Scalp	N	Mean	Grouping
2	5	115.059	A
1	5	113.53	A

Means that do not share a letter are significantly different.

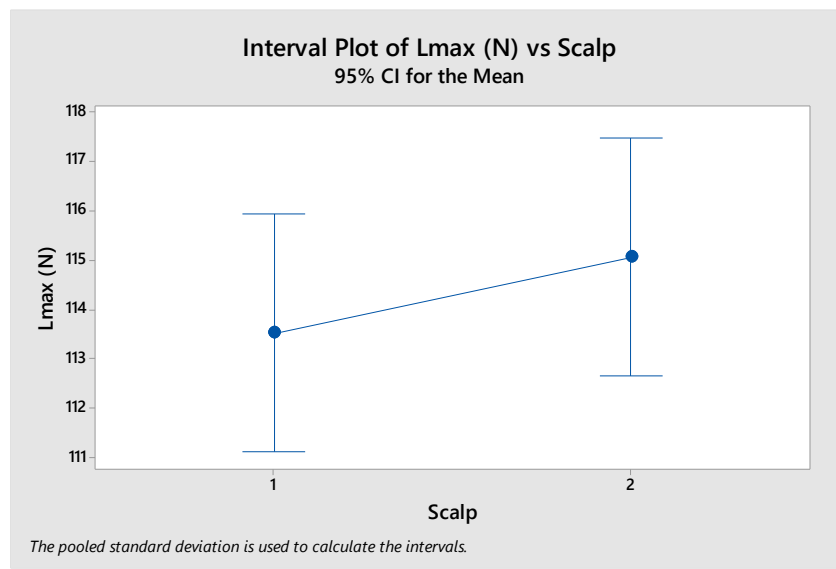
Tukey Simultaneous Tests for Differences of Means

Difference of Levels	Difference of Means	SE of Difference	95% CI	T-Value	Adjusted P-Value
2 - 1	1.53	1.47	(-1.85, 4.91)	1.04	0.327

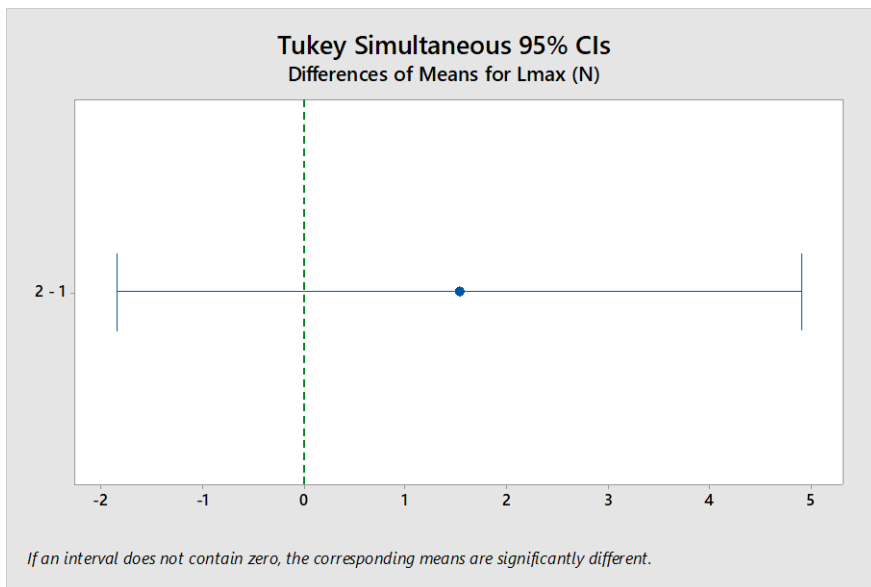
Individual confidence level = 95.00%

Tukey Simultaneous 95% CIs

Interval Plot of Lmax (N) vs Scalp



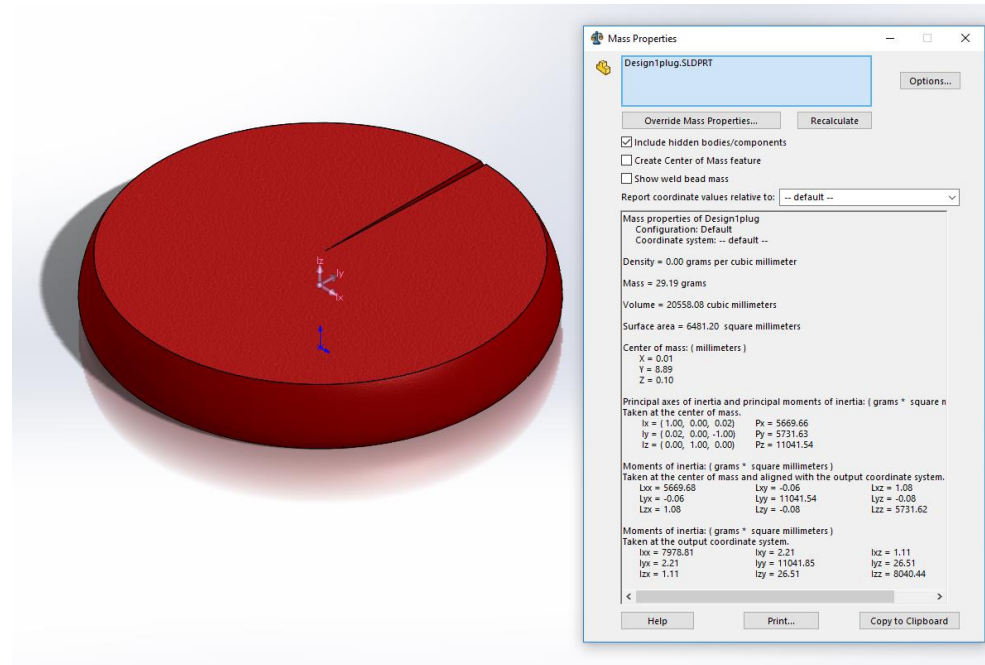
A3. 1 Interval plot of Lmax(N) against test lubricant formulation for comparison of scalps



A3. 2 Tukey simultaneous analysis of means of Lmax against tested across all tested experimental condition and the scalps control for comparison of scalps

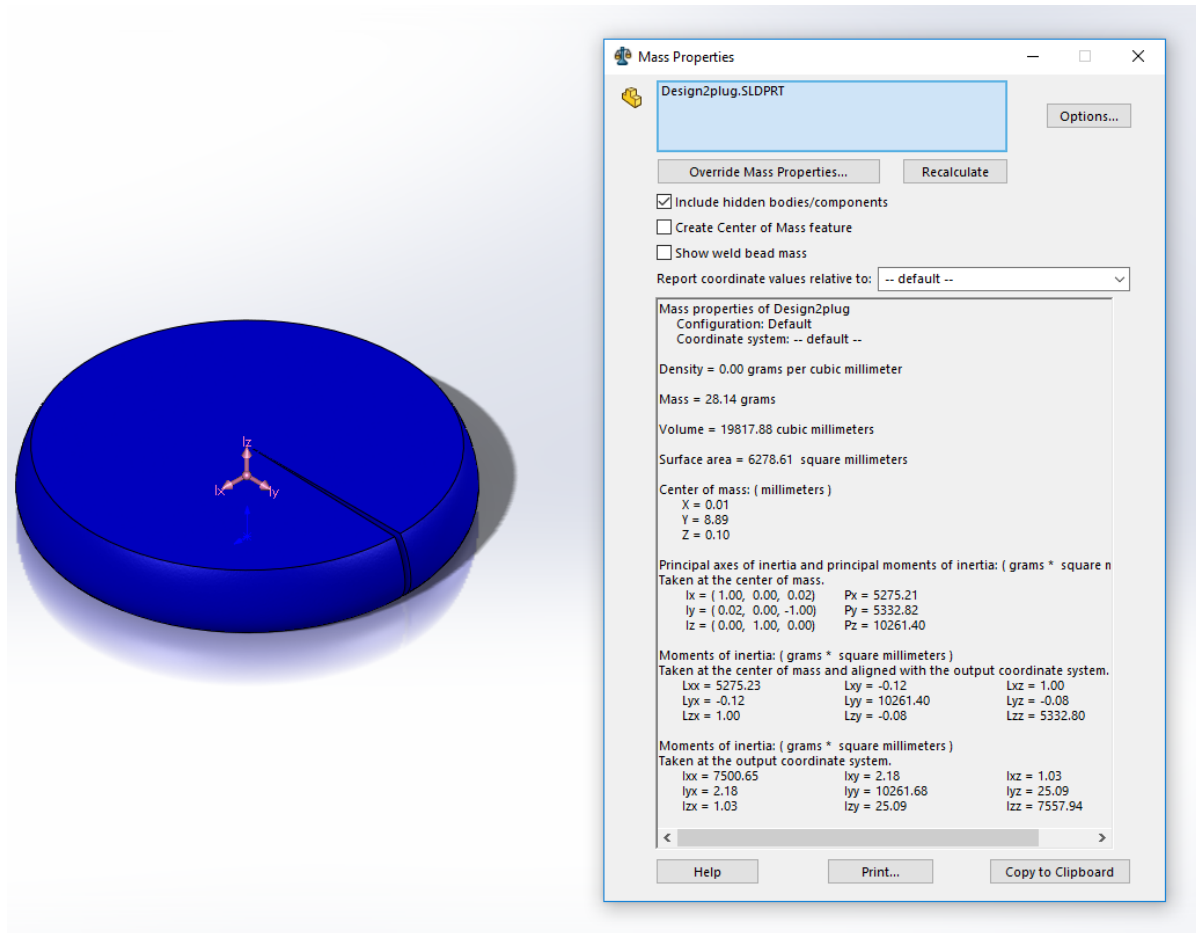
Appendix B1- Calculation of Contact Area and Volume with Inserts

Plug profile for Insert A



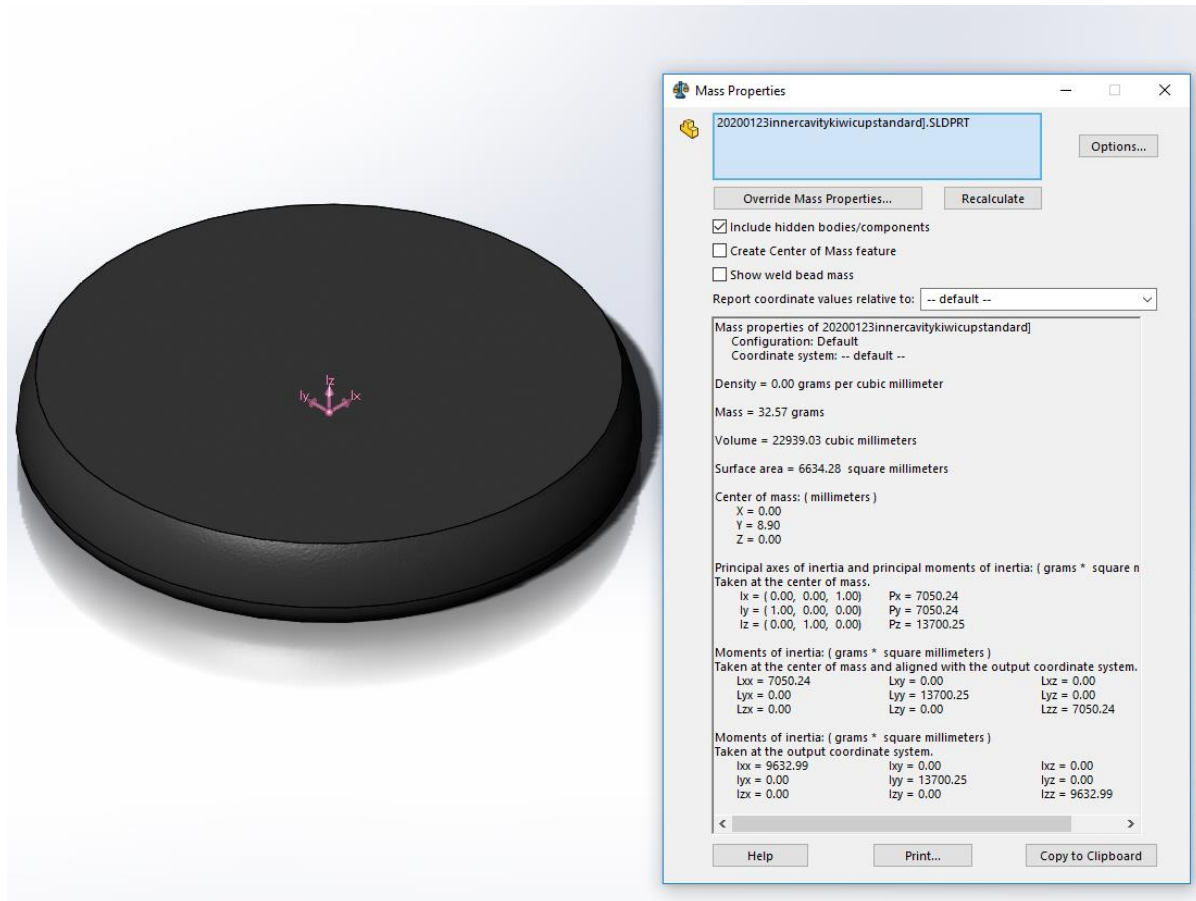
B1. 1: Calculation of mass properties of scalp plug formed due to presence of Insert A

Plug profile for Insert B



B1. 2: Calculation of mass properties of scalp plug formed due to presence of Insert B

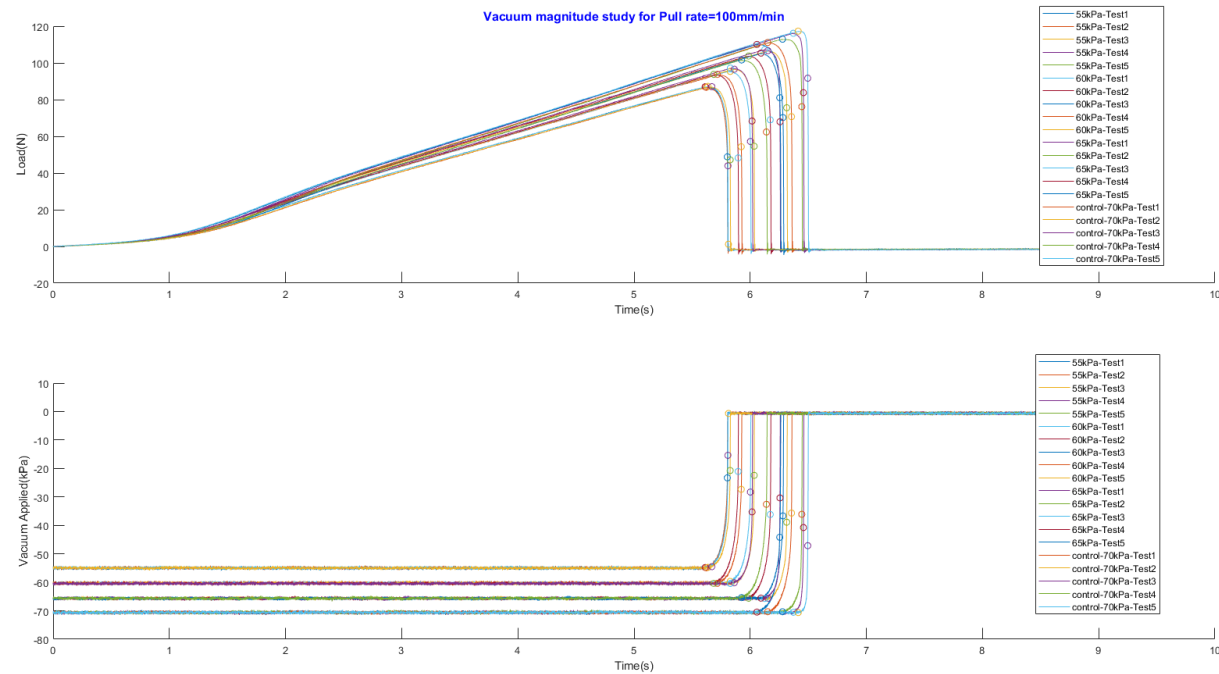
Plug profile for Unchanged Configuration



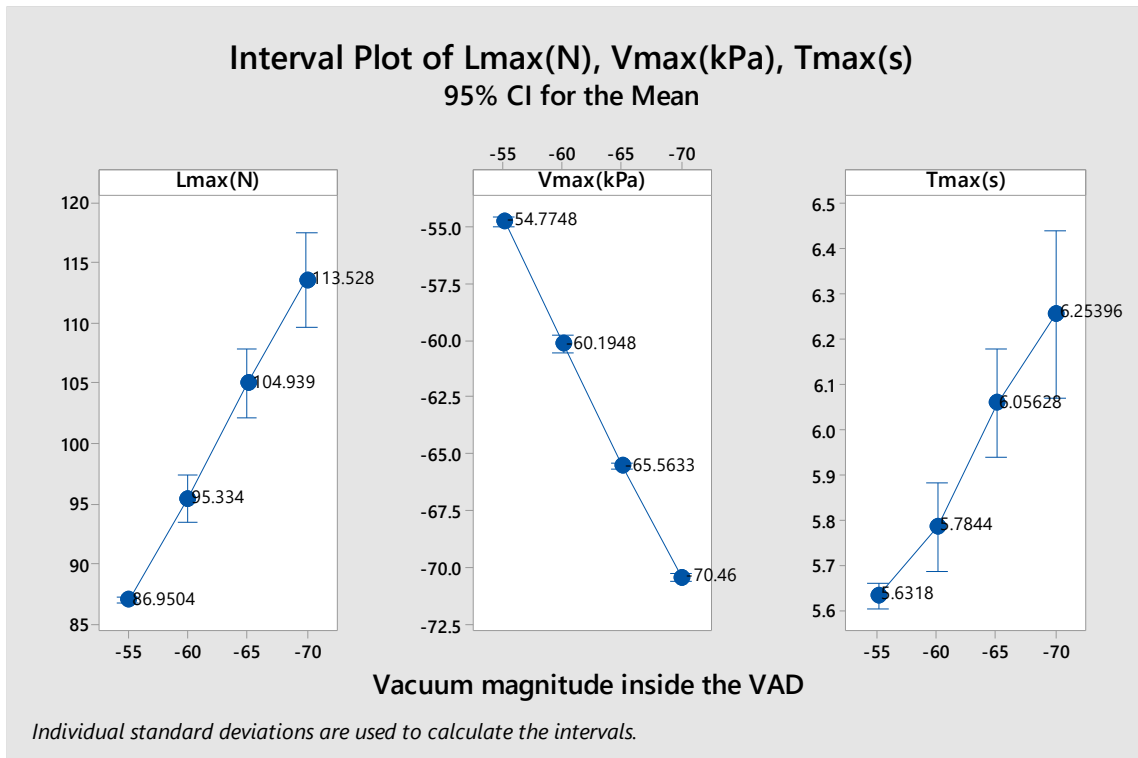
B1. 3: Calculation of mass properties of scalp plug formed with Kiwi cup

Appendix B2-Experimental Results

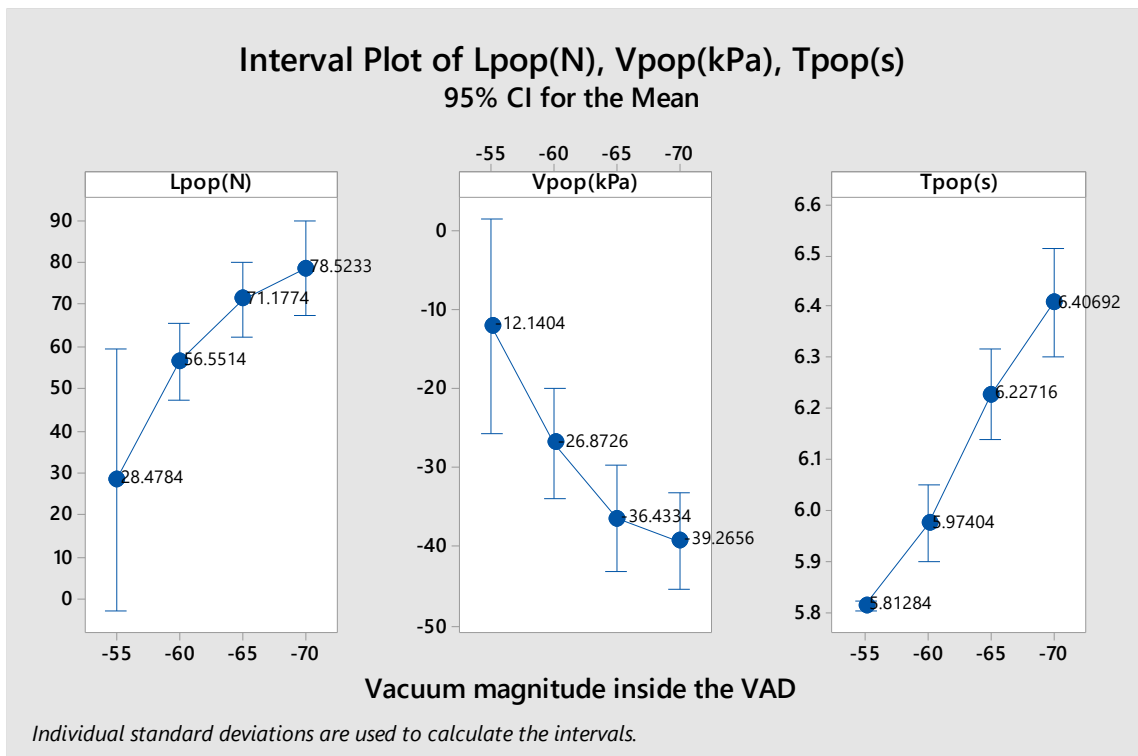
Vacuum magnitude inside the VAD



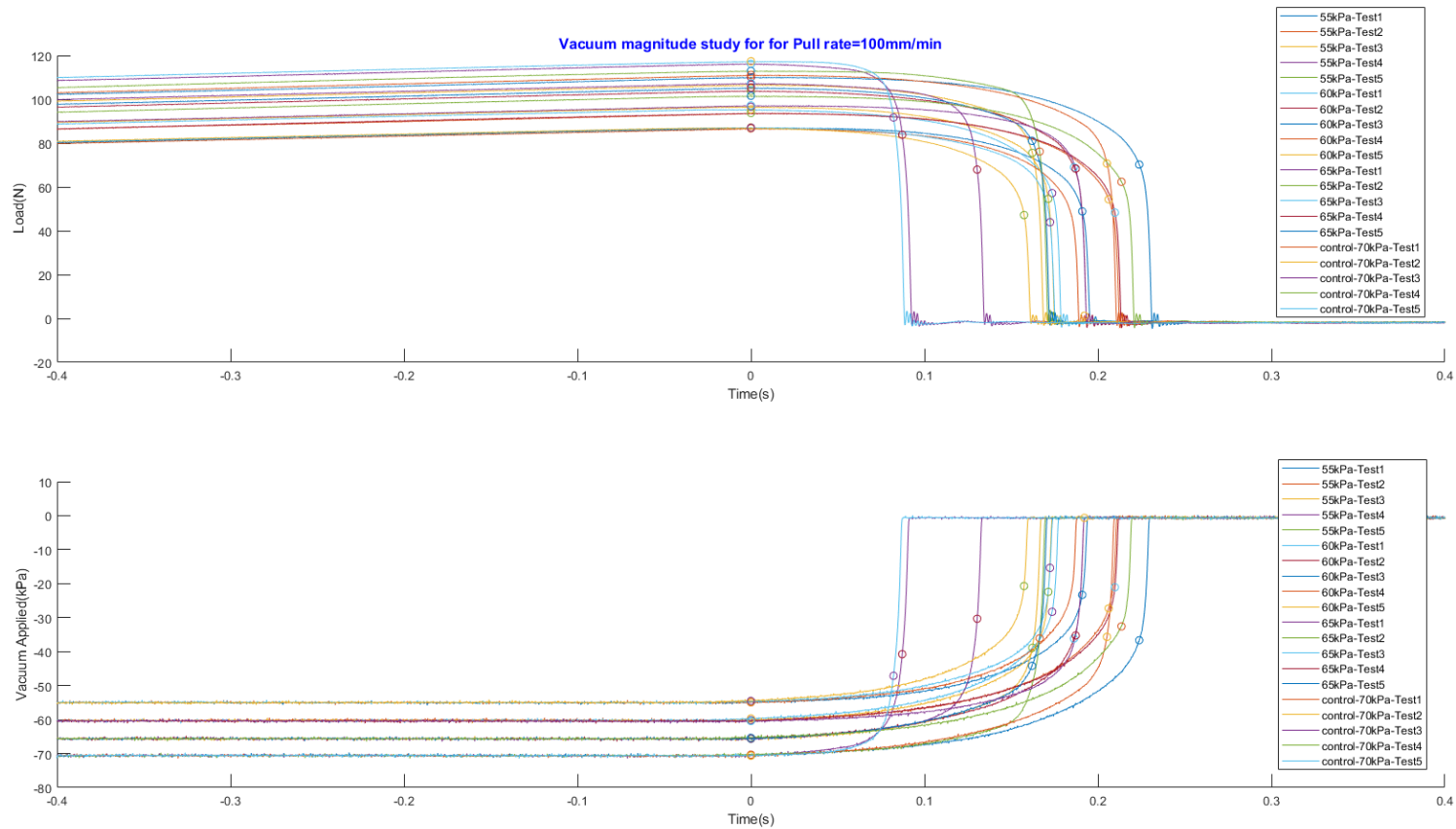
B2. 1: Time Series of sensory output of the load and the vacuum detected by the VAD simulator with graph markers of value of Load (L_{max}) and Vacuum (V_{max}) at T_{max} and Load (L_{pop}) and Vacuum (V_{pop}) for Study ID 1



B2. 2: Interval plots of metrics used for analysis- Lmax(N), Vmax(kPa), Tmax(s) for Study ID 1

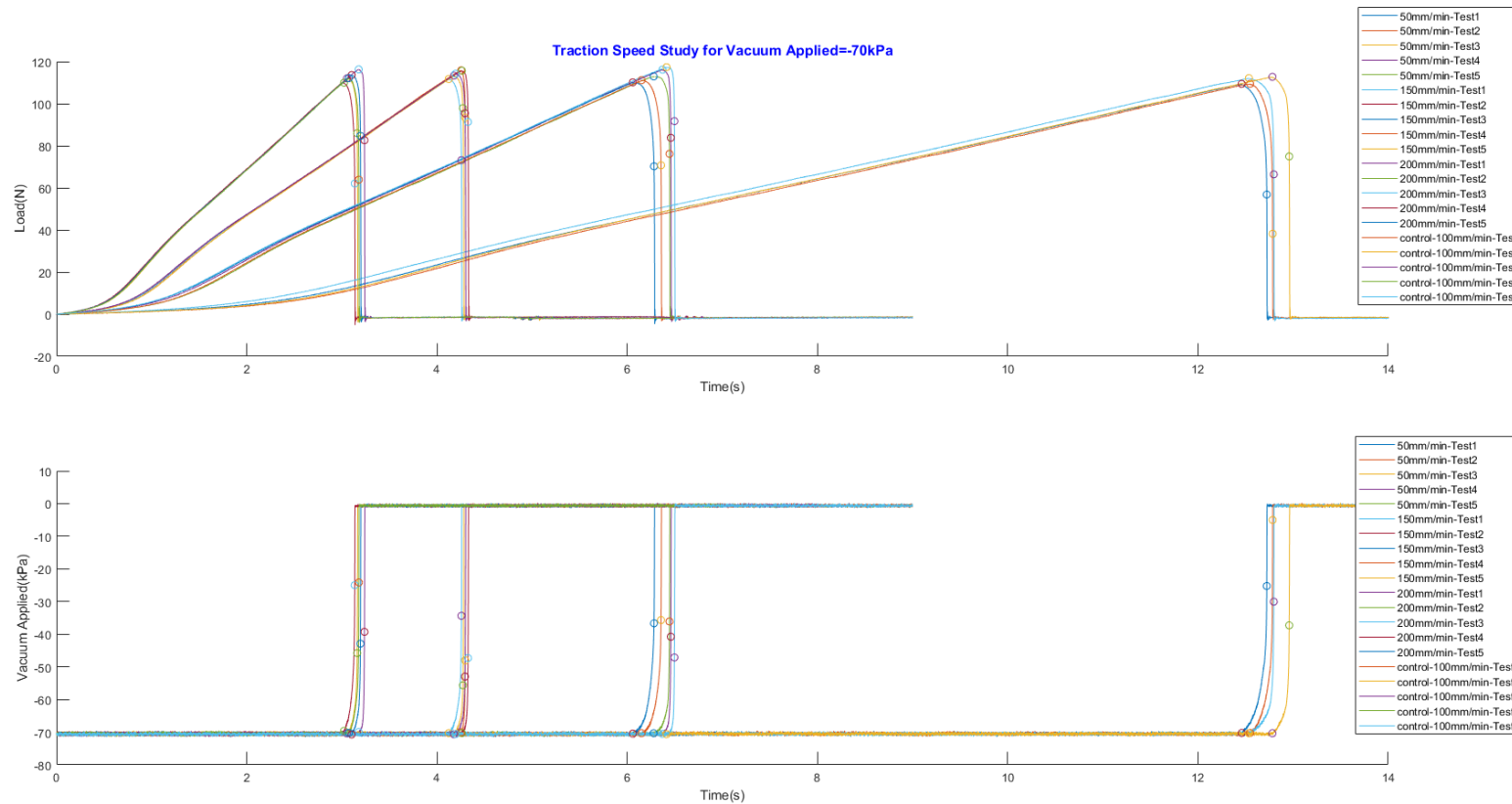


B2. 3: Interval plots of metrics used for analysis- Lpop,Vpop,TPop for Study ID 1



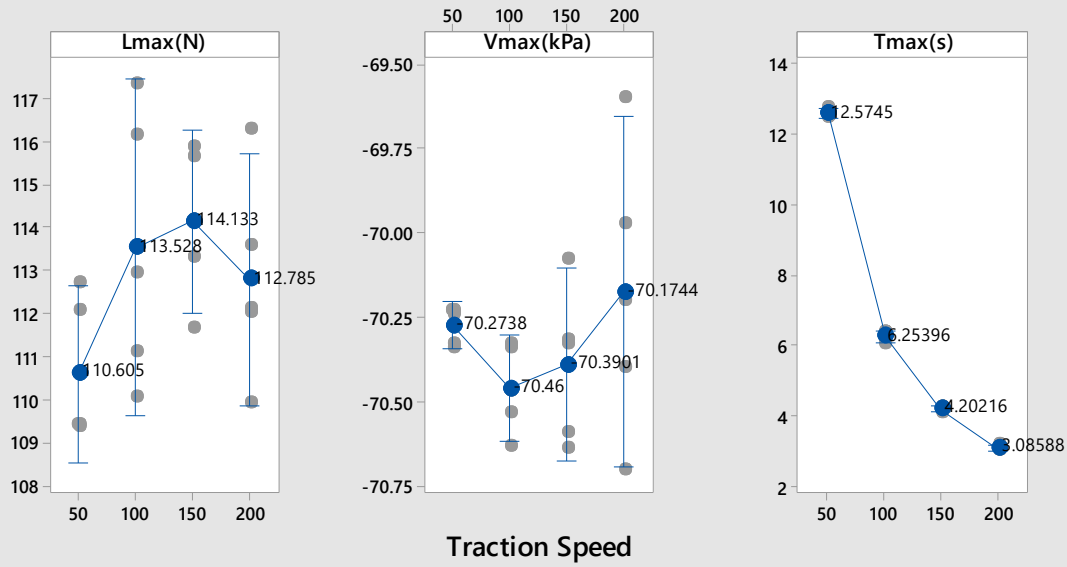
B2. 4: Time centred at series centred at maximum traction time of sensory output of the load and the vacuum detected by the VAD simulator with graph markers of value of Load (L_{max}) and Vacuum (V_{max}) at T^*_{max} ($T=T_{max}-T_{max}=0s$) and Load (L_{pop}) and Vacuum (V_{pop}) the time of cup detachment (T^*_{pop}) ($T=T_{max}-T_{pop}$) respectively. for Study ID 1

Traction Speed



B2. 5: Time Series of sensory output of the load and the vacuum detected by the VAD simulator with graph markers of value of Load (Lmax) and Vacuum (Vmax) at Tmax and Load (Lpop) and Vacuum (Vpop) for Study ID 2

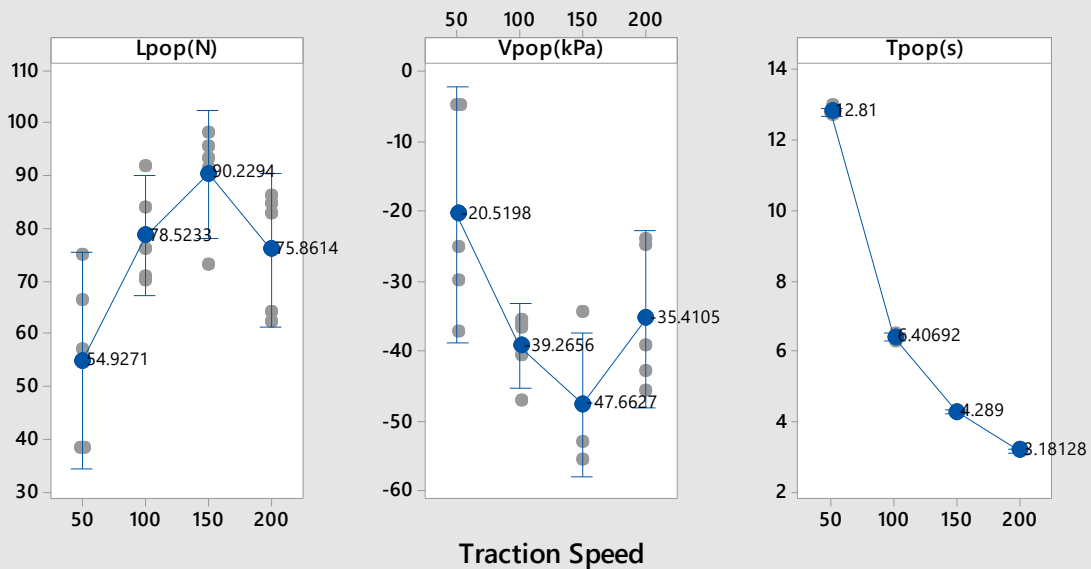
Interval Plot of Lmax(N), Vmax(kPa), Tmax(s)
95% CI for the Mean



Individual standard deviations are used to calculate the intervals.

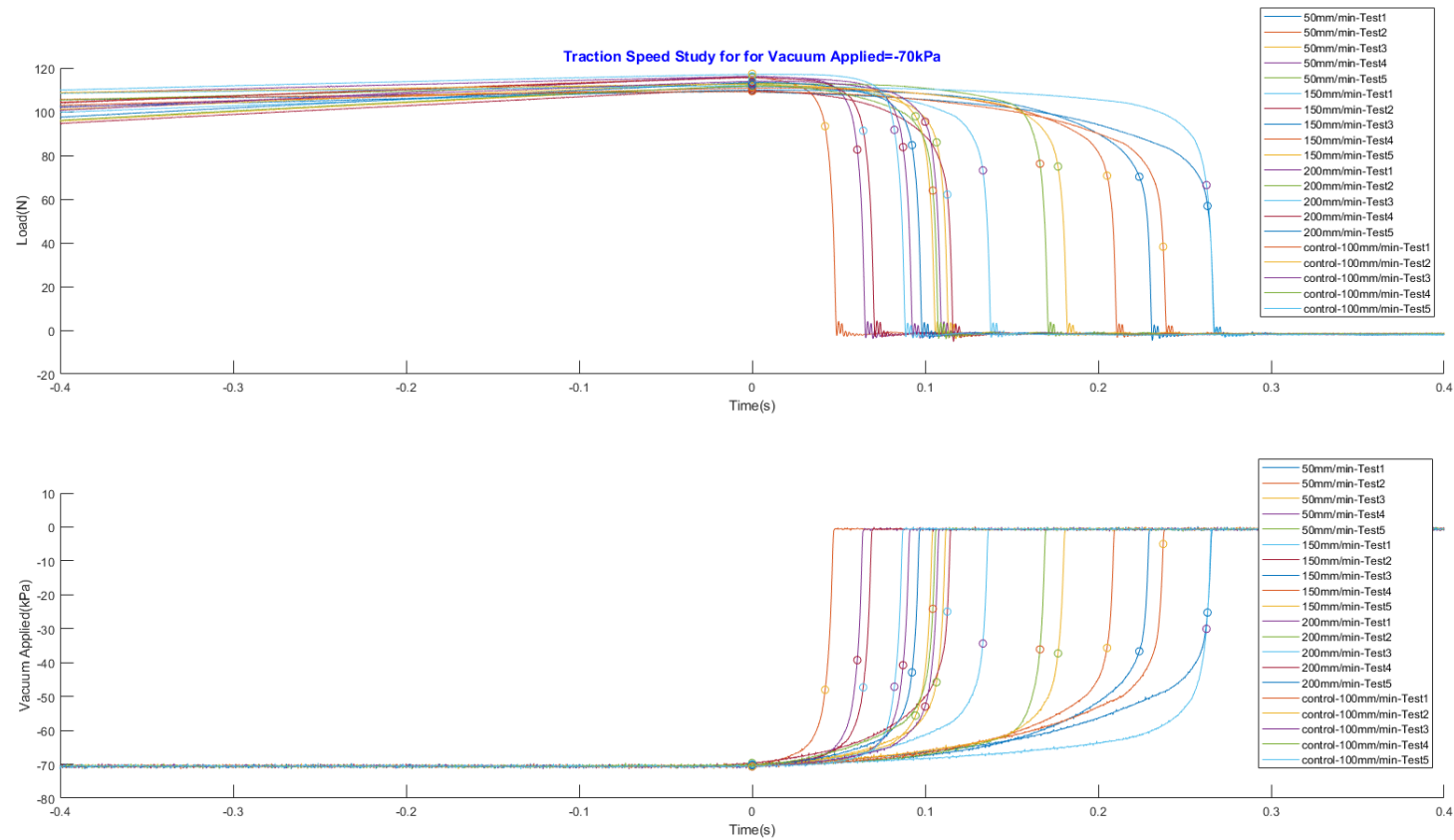
B2. 6: Interval plots of metrics used for analysis- Lmax, Vmax, Tmax for Study ID 2

Interval Plot of Lpop(N), Vpop(kPa), Tpop(s)
95% CI for the Mean



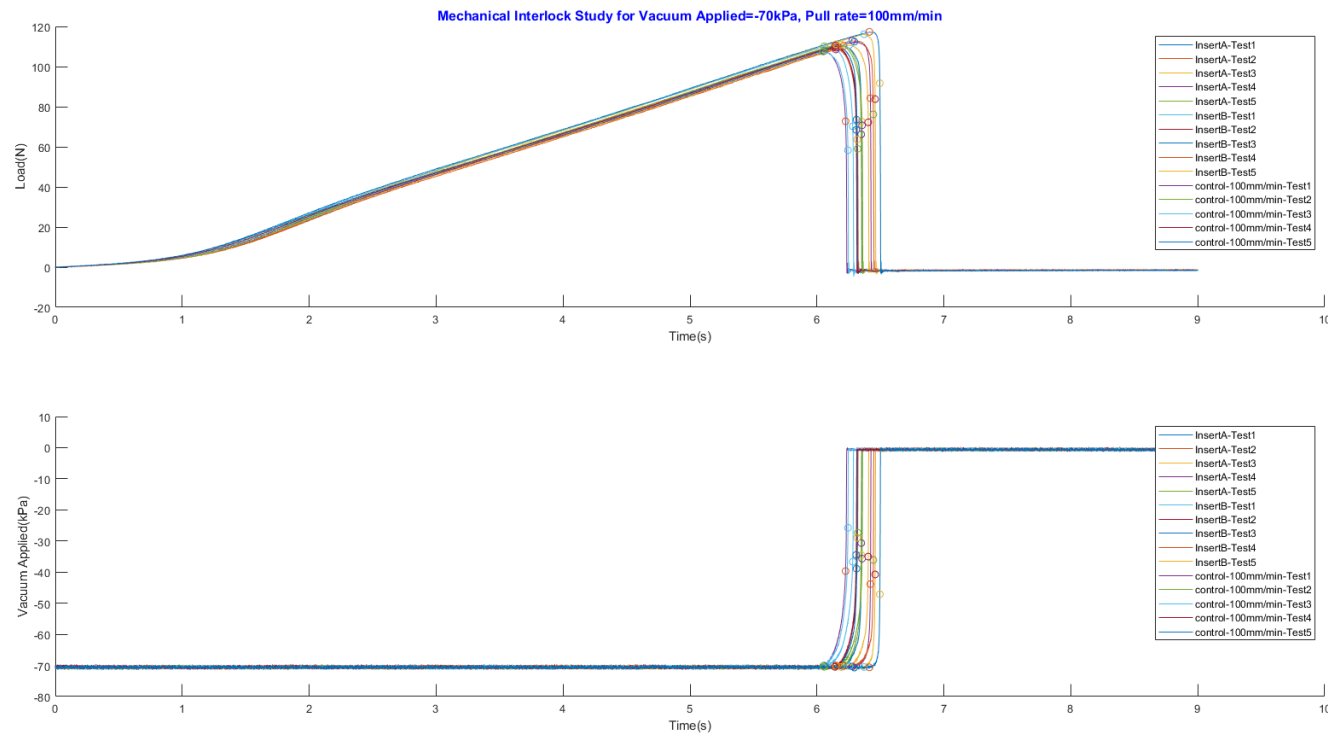
Individual standard deviations are used to calculate the intervals.

B2. 7: Interval plots of metrics used for analysis- Lpop,Vpop,TPop for Study ID 2



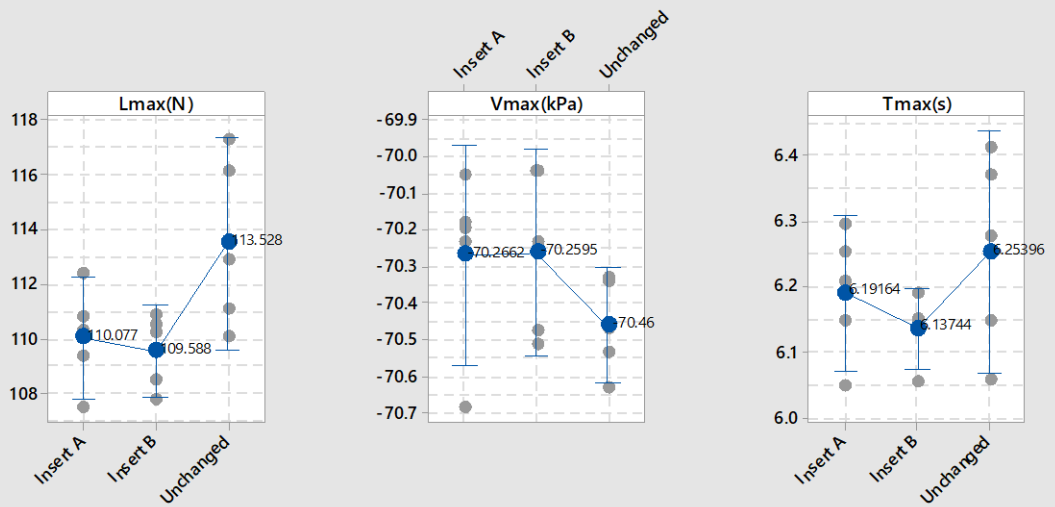
B2. 8: Time centred at series centred at maximum traction time of sensory output of the load and the vacuum detected by the VAD simulator with graph markers of value of Load (L_{max}) and Vacuum (V_{max}) at T^*_{max} ($T=T_{max}-T_{max}=0s$) and Load (L_{pop}) and and Vacuum (V_{pop}) the time of cup detachment (T^*_{pop}) ($T=T_{max}-T_{pop}$) respectively. for Study ID 2

Changes in Cup Geometry



B2. 9: Time Series of sensory output of the load and the vacuum detected by the VAD simulator with graph markers of value of Load (L_{max}) and Vacuum (V_{max}) at T_{max} and Load (L_{pop}) and Vacuum (V_{pop}) for Study ID 3

Interval Plot of Lmax(N), Vmax(kPa), Tmax(s)
95% CI for the Mean

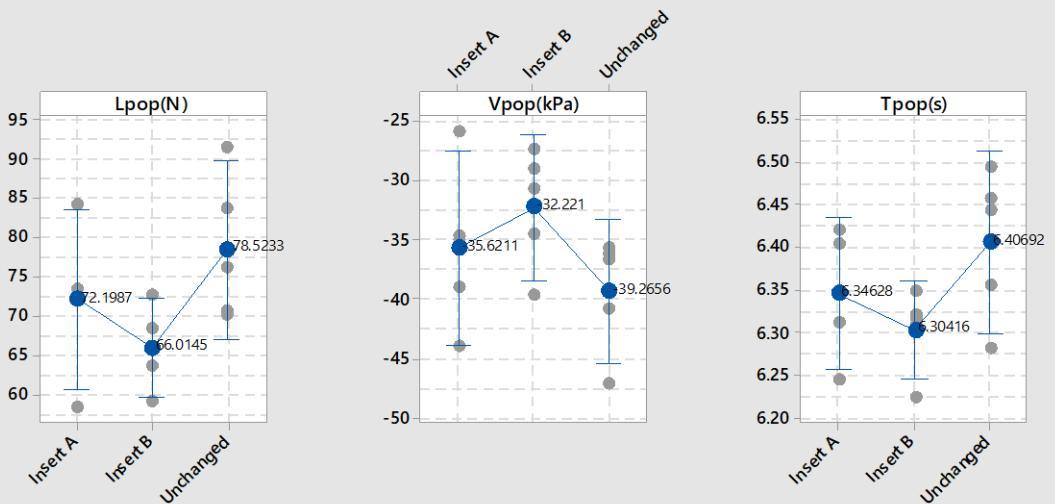


Changes in Cup Geometry

Individual standard deviations are used to calculate the intervals.

B2. 10: Interval plots of metrics used for analysis- Lmax, Vmax, Tmax for Study ID 3

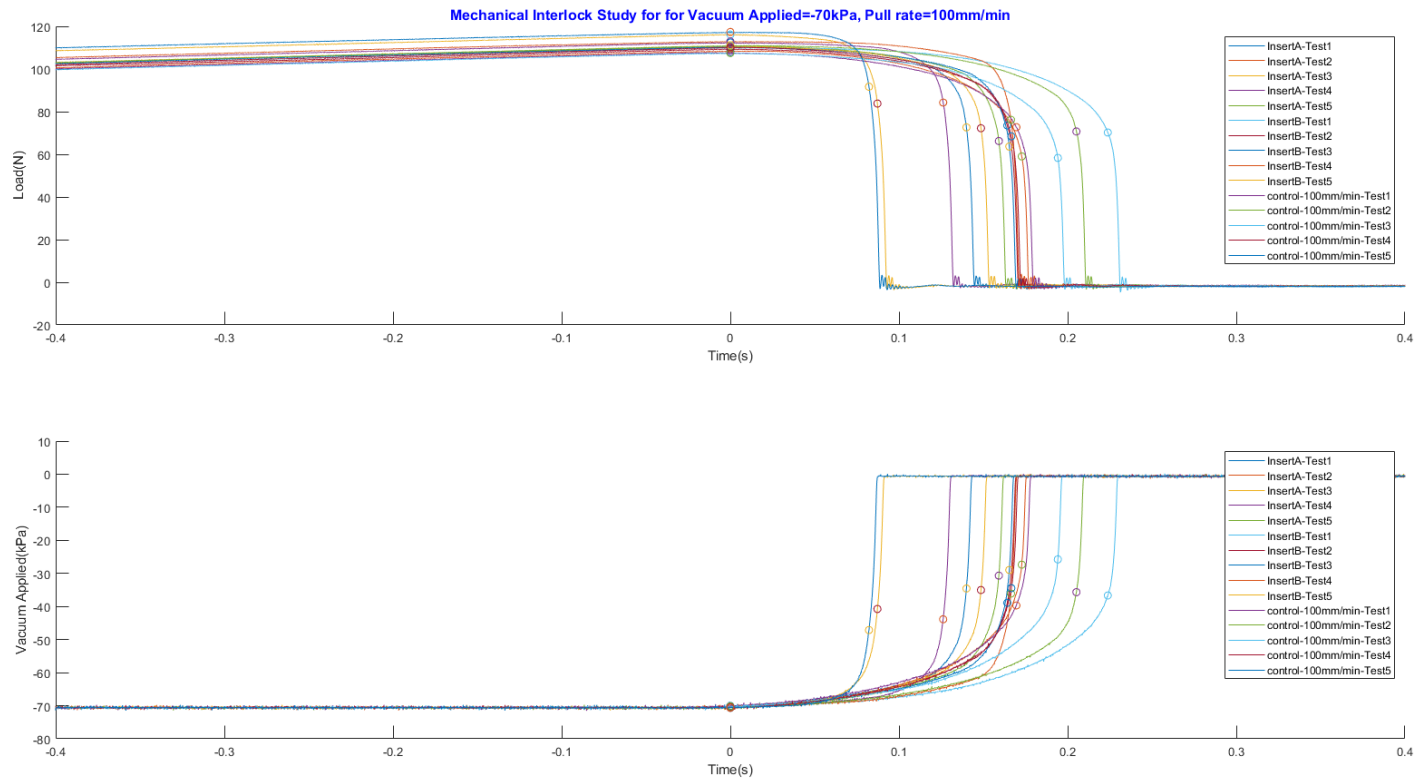
Interval Plot of Lpop(N), Vpop(kPa), Tpop(s)
95% CI for the Mean



Changes in Cup Geometry

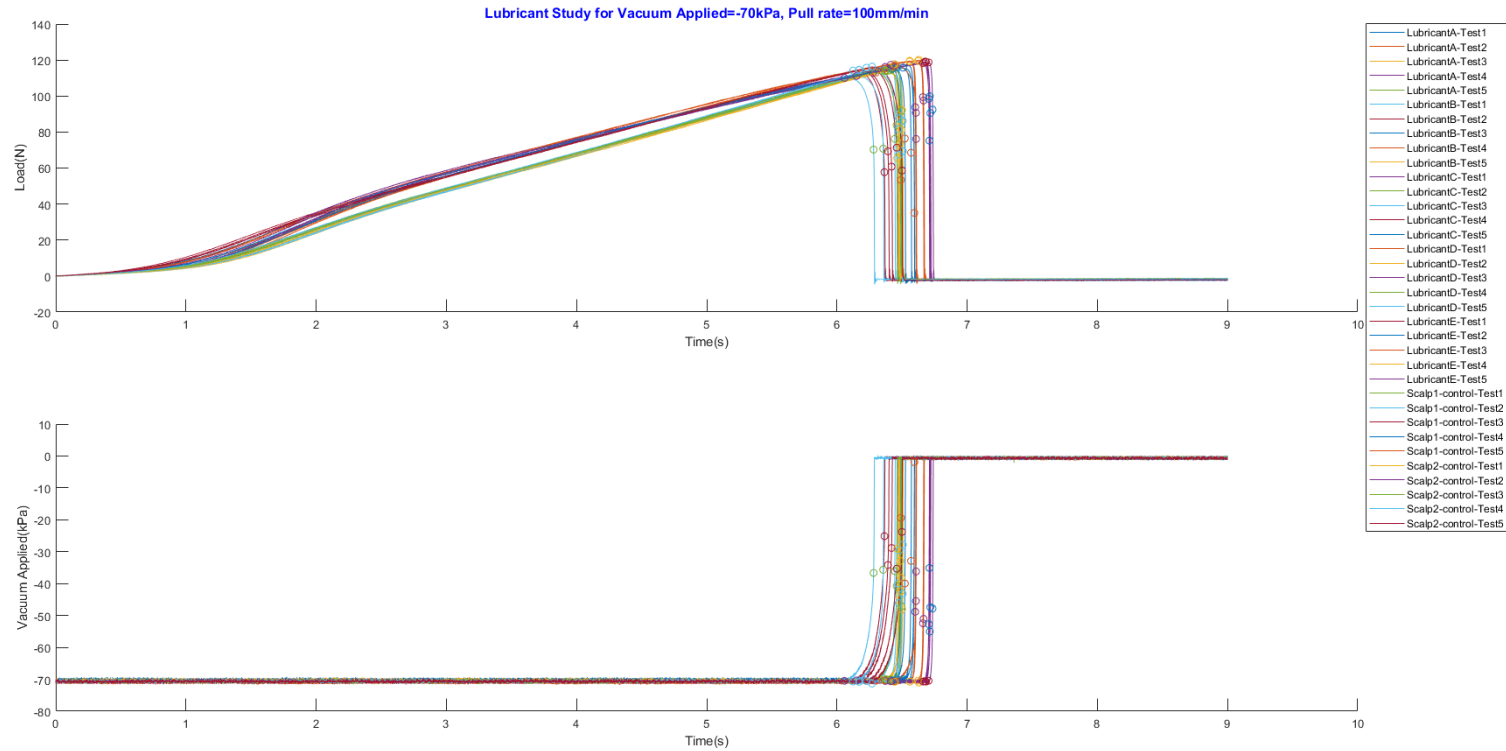
Individual standard deviations are used to calculate the intervals.

B2. 11: Interval plots of metrics used for analysis- Lpop, Vpop, Tpop for Study ID 3

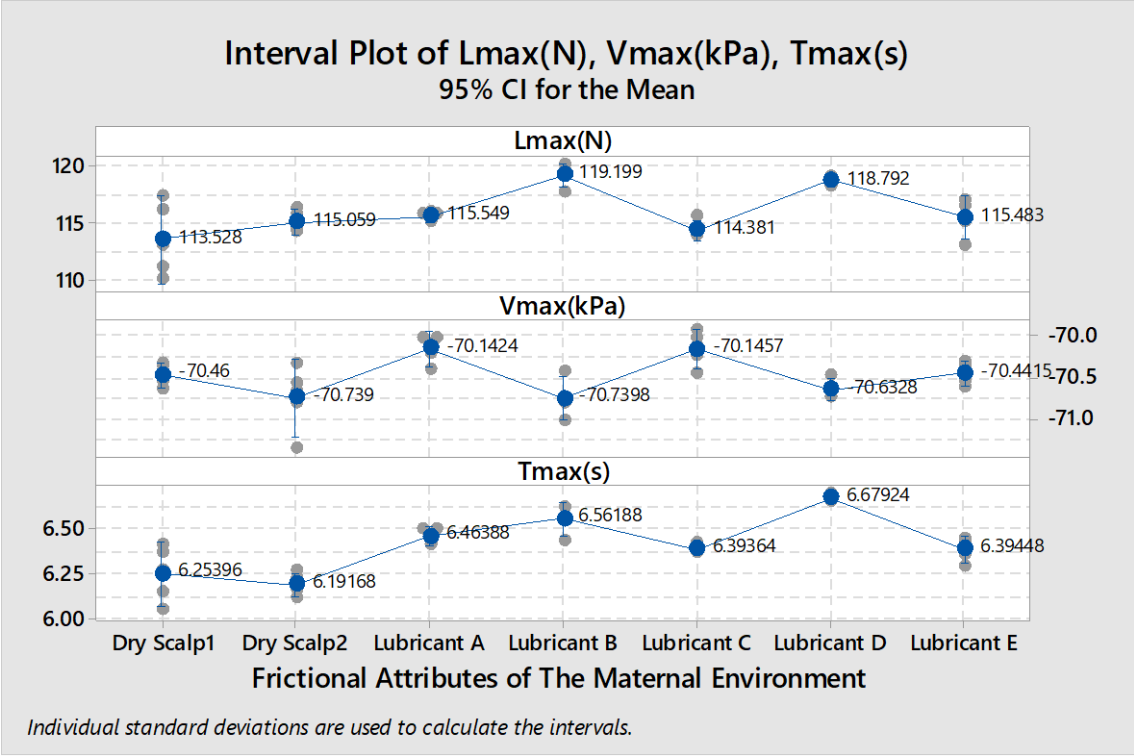


B2. 12: Time centred at series centred at maximum traction time of sensory output of the load and the vacuum detected by the VAD simulator with graph markers of value of Load (L_{max}) and Vacuum (V_{max}) at T^*_{max} ($T=T_{max}-T_{max}=0s$) and Load (L_{pop}) and Vacuum (V_{pop}) the time of cup detachment (T^*_{pop}) ($T=T_{max}-T_{pop}$) respectively. for Study ID 3

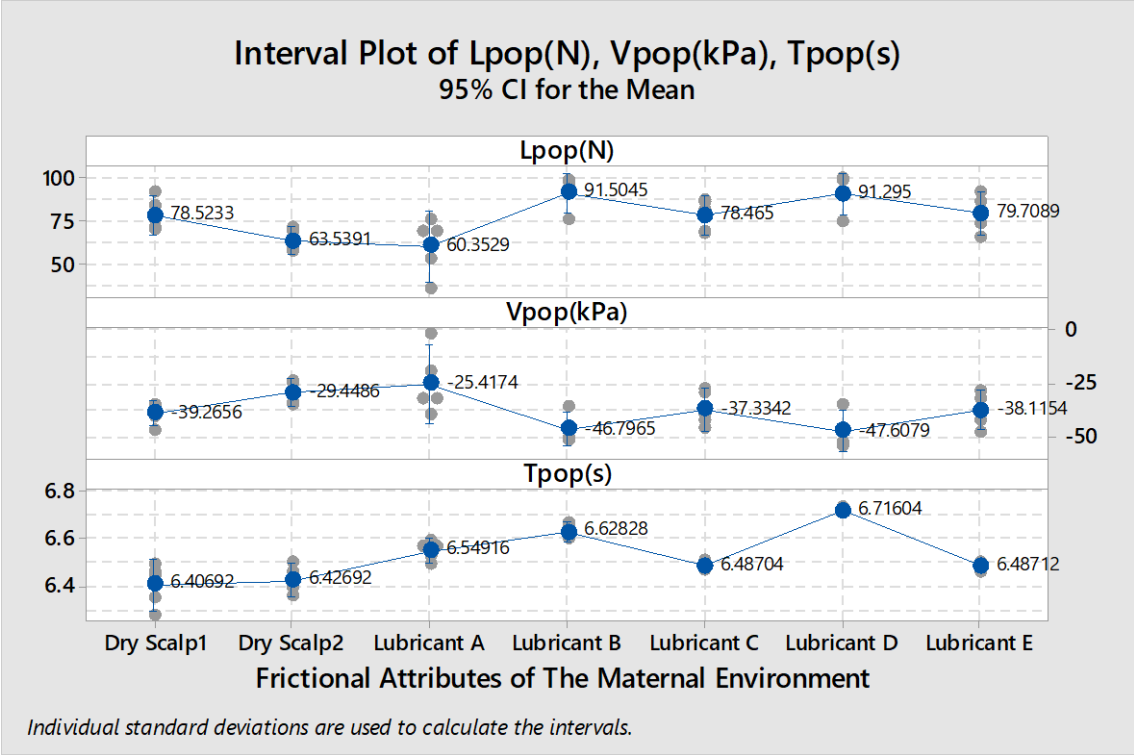
Frictional Attributes of The Maternal Environment



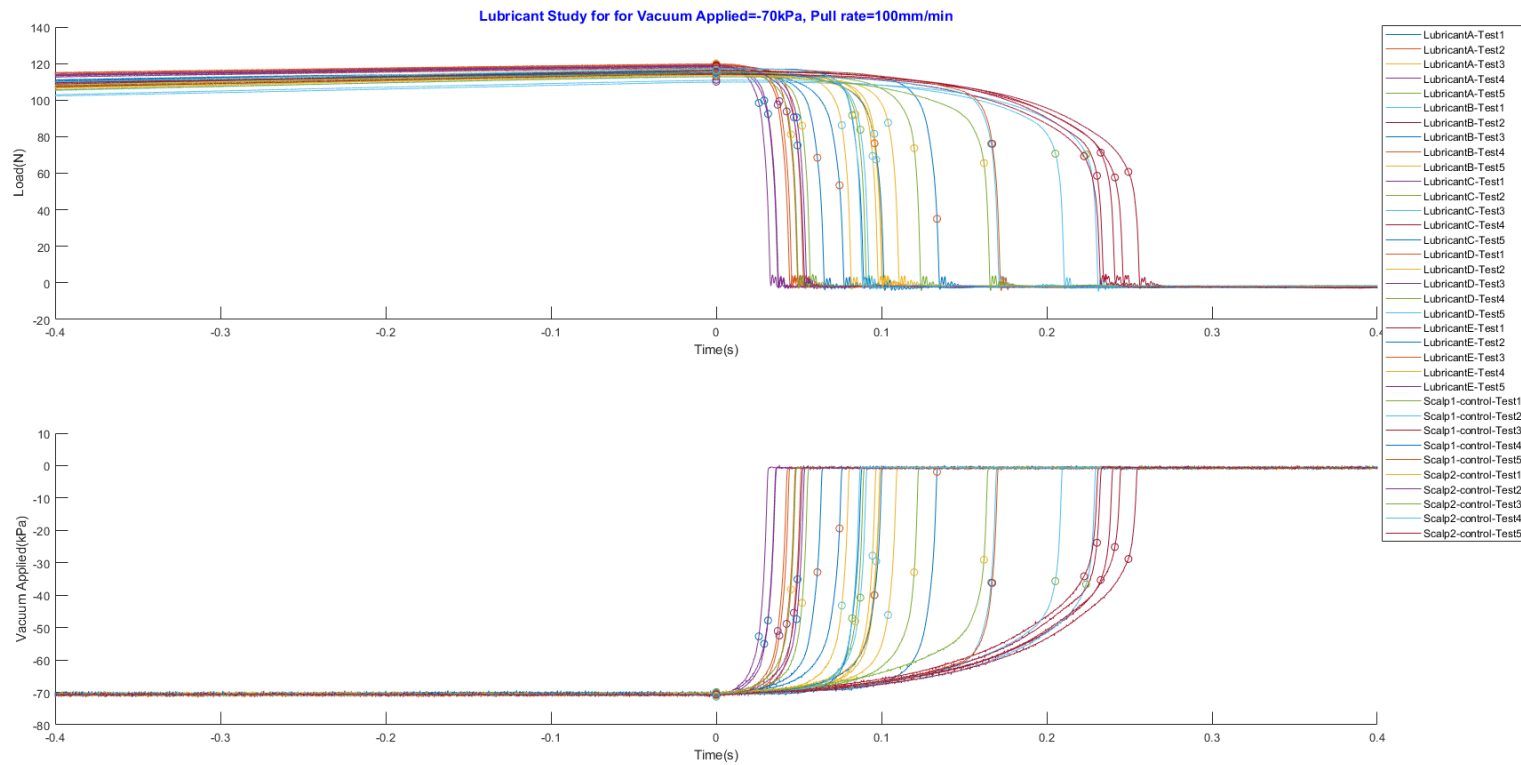
B2. 13: Time Series of sensory output of the load and the vacuum detected by the VAD simulator with graph markers of value of Load (Lmax) and Vacuum (Vmax) at Tmax and Load (Lpop) and Vacuum (Vpop) for Study ID 4



B2. 14: Interval plots of metrics used for analysis- Lmax, Vmax, Tmax for Study ID 4

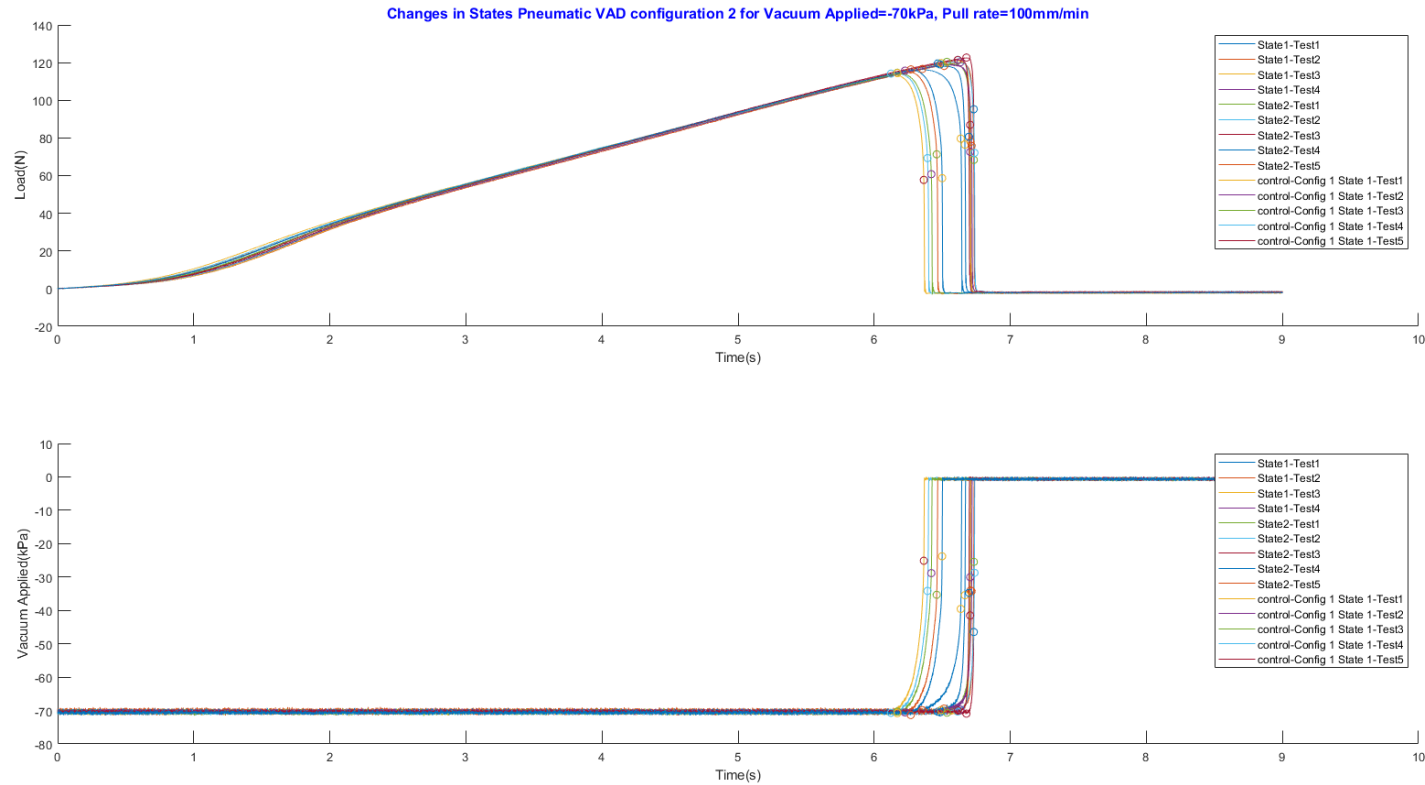


B2. 15: Interval plots of metrics used for analysis- Lpop, Vpop, Tpop for Study ID 4

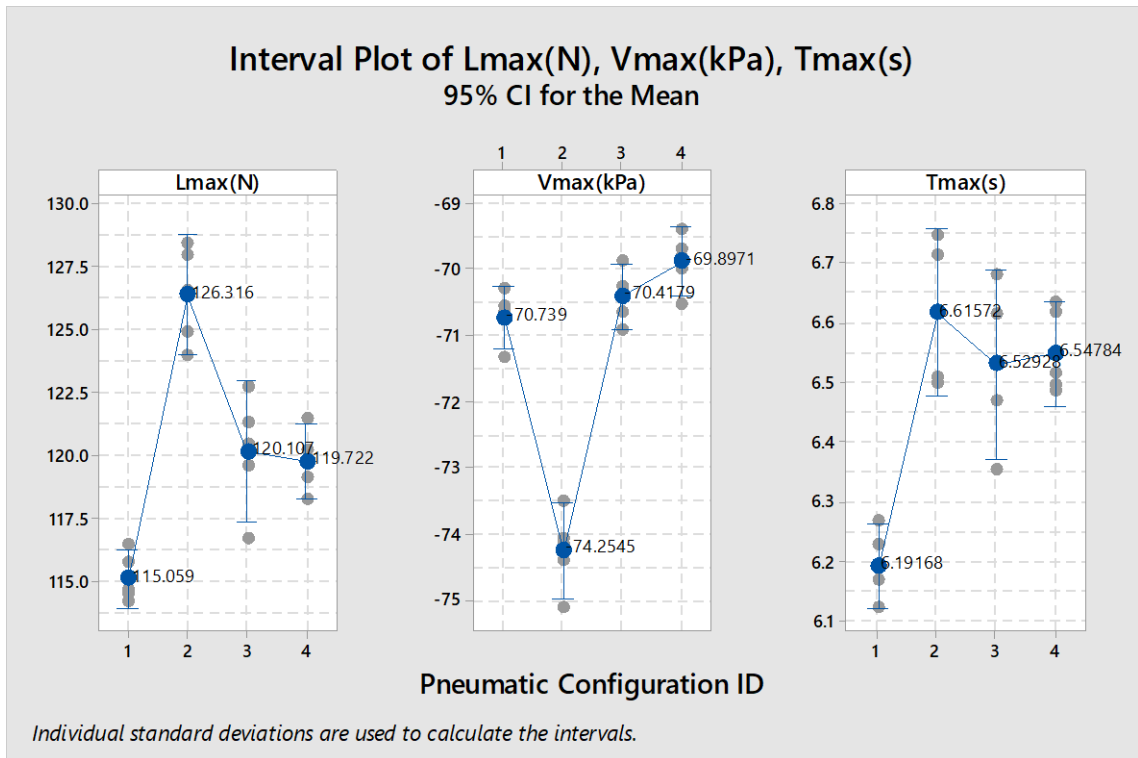


B2. 16: Time centred at series centred at maximum traction time of sensory output of the load and the vacuum detected by the VAD simulator with graph markers of value of Load (L_{max}) and Vacuum (V_{max}) at T^*_{max} ($T=T_{max}-T_{max}=0s$) and Load (L_{pop}) and Vacuum (V_{pop}) the time of cup detachment (T^*_{pop}) ($T=T_{max}-T_{pop}$) respectively. for Study ID 4

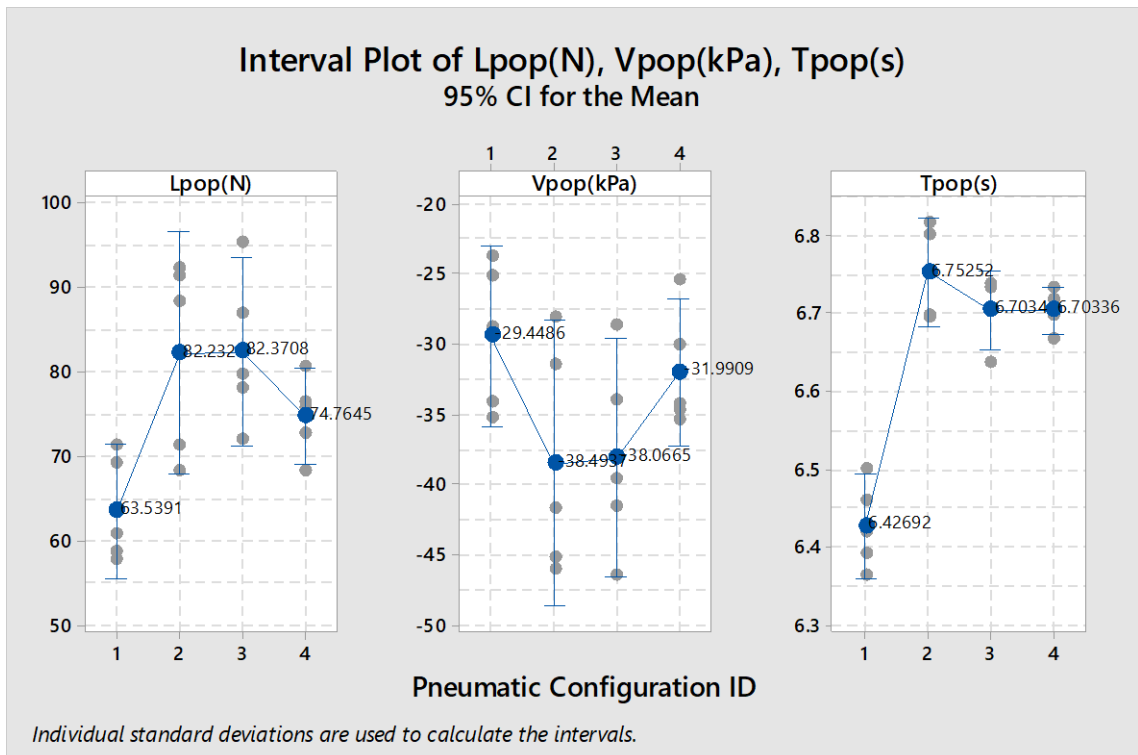
Changes in Pneumatic VAD configuration



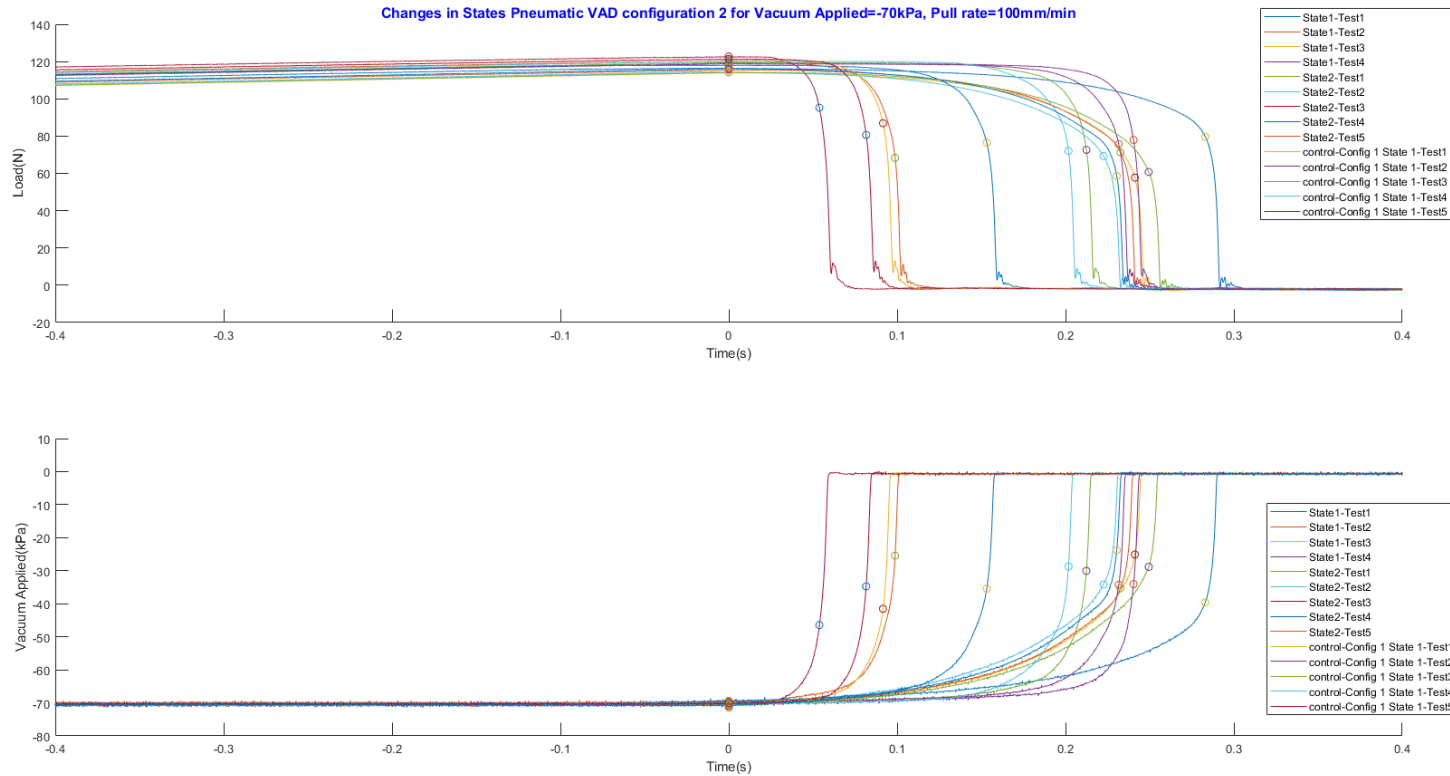
B2. 17: Time Series of sensory output of the load and the vacuum detected by the VAD simulator with graph markers of value of Load (Lmax) and Vacuum (Vmax) at Tmax and Load (Lpop) and Vacuum (Vpop) for Study ID 5



B2. 18: Interval plots of metrics used for analysis- Lmax, Vmax, Tmax for Study ID 5



B2. 19: Interval plots of metrics used for analysis- Lpop,Vpop,TPop for Study ID 5



B2. 20: Time centred at series centred at maximum traction time of sensory output of the load and the vacuum detected by the VAD simulator with graph markers of value of Load (L_{max}) and Vacuum (V_{max}) at T^*_{max} ($T=T_{max}-T_{max}=0s$) and Load (L_{pop}) and Vacuum (V_{pop}) the time of cup detachment (T^*_{pop}) ($T=T_{max}-T_{pop}$) respectively. for Study ID 5

Appendix B3-Example report generated by Minitab for the statistical analysis of the metrics

Regression Analysis for Study ID 1

Regression Analysis: Lmax(N) versus Vmax(kPa)

The regression equation is $L_{max}(N) = -6.774 - 1.705 V_{max}(kPa)$

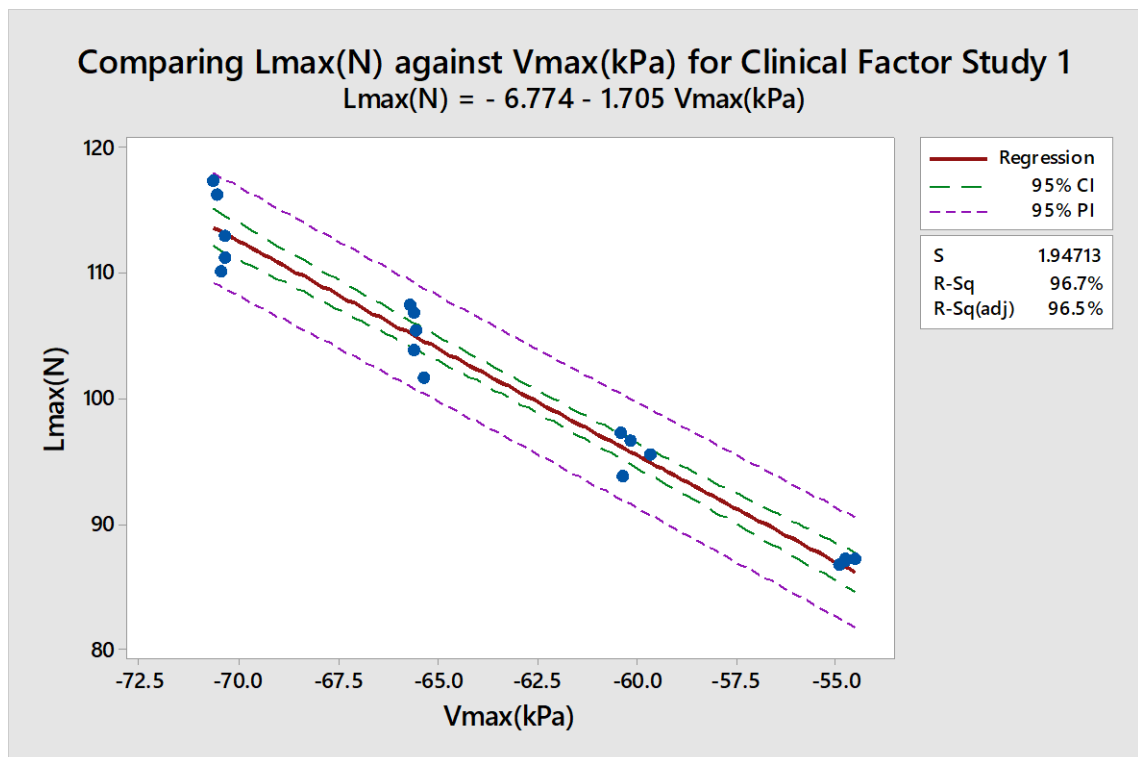
Model Summary

S	R-sq	R-sq(adj)
1.94713	96.70%	96.52%

Analysis of Variance

Source	DF	SS	MS	F	P
Regression	1	1999.36	1999.36	527.35	0.000
Error	18	68.24	3.79		
Total	19	2067.60			

Fitted Line: Lmax(N) versus Vmax(kPa)



B3. 1 Regression line showing relationship between Lmax(s) and tested Traction speed (mm/min) for Study 1

Tukey Simultaneous comparison of means (Lmax) for Study ID 4

One-way ANOVA: Lmax versus Lubricant Condition

Method

Null hypothesis All means are equal
 Alternative hypothesis Not all means are equal
 Significance level $\alpha = 0.05$

Equal variances were assumed for the analysis.

Factor Information

Factor	Levels	Values
Lubricant Condition	7	Dry Scalp1, Dry Scalp2, Lubricant A, Lubricant B, Lubricant C, Lubricant D, Lubricant E

Analysis of Variance

Source	DF	Adj SS	Adj MS	F-Value	P-Value
Lubricant Condition	6	140.58	23.430	11.15	0.000
Error	28	58.84	2.101		
Total	34	199.42			

Model Summary

S	R-sq	R-sq(adj)	R-sq(pred)
1.44959	70.50%	64.17%	53.90%

Means

Lubricant Condition	N	Mean	StDev	95% CI
Dry Scalp1	5	113.53	3.14	(112.20, 114.86)
Dry Scalp2	5	115.059	0.951	(113.731, 116.387)
Lubricant A	5	115.549	0.392	(114.221, 116.877)
Lubricant B	5	119.199	0.884	(117.871, 120.527)
Lubricant C	5	114.381	0.700	(113.053, 115.709)
Lubricant D	5	118.792	0.352	(117.464, 120.120)
Lubricant E	5	115.483	1.551	(114.155, 116.811)

Pooled StDev = 1.44959

Tukey Pairwise Comparisons

Grouping Information Using the Tukey Method and 95% Confidence

Lubricant Condition	N	Mean	Grouping
Lubricant B	5	119.199	A
Lubricant D	5	118.792	A
Lubricant A	5	115.549	B
Lubricant E	5	115.483	B
Dry Scalp2	5	115.059	B
Lubricant C	5	114.381	B

Dry Scalp1 5 113.53 B

Means that do not share a letter are significantly different.

Tukey Simultaneous Tests for Differences of Means

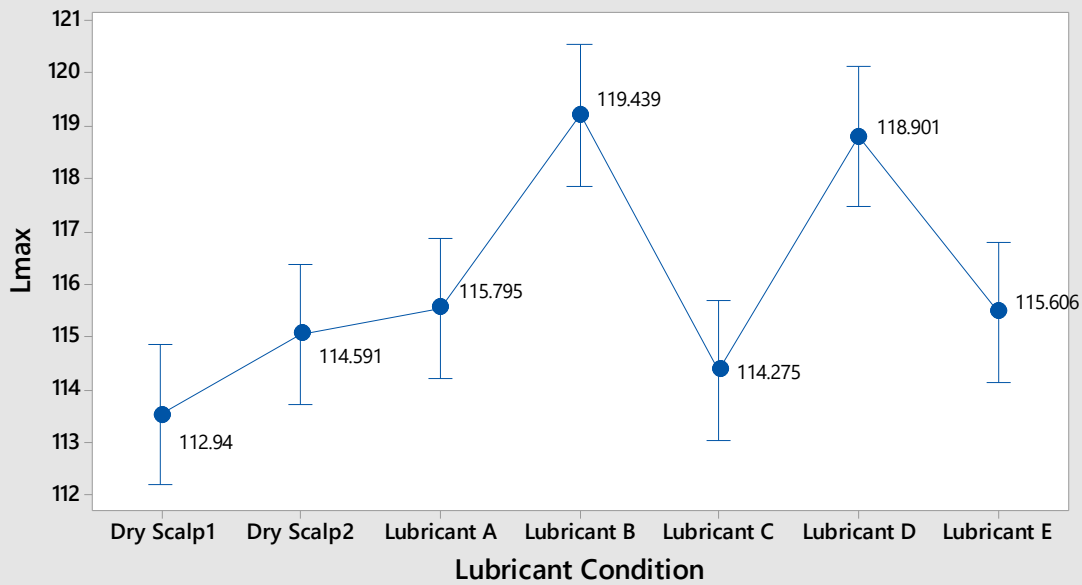
Difference of Levels	Difference of Means	SE of Difference	95% CI	T-Value	Adjusted P-Value
Dry Scalp2 - Dry Scalp1	1.531	0.917	(-1.380, 4.441)	1.67	0.641
Lubricant A - Dry Scalp1	2.021	0.917	(-0.890, 4.932)	2.20	0.325
Lubricant B - Dry Scalp1	5.671	0.917	(2.760, 8.581)	6.19	0.000
Lubricant C - Dry Scalp1	0.853	0.917	(-2.058, 3.764)	0.93	0.964
Lubricant D - Dry Scalp1	5.264	0.917	(2.353, 8.175)	5.74	0.000
Lubricant E - Dry Scalp1	1.955	0.917	(-0.956, 4.865)	2.13	0.363
Lubricant A - Dry Scalp2	0.490	0.917	(-2.420, 3.401)	0.54	0.998
Lubricant B - Dry Scalp2	4.140	0.917	(1.229, 7.051)	4.52	0.002
Lubricant C - Dry Scalp2	-0.678	0.917	(-3.589, 2.233)	-0.74	0.989
Lubricant D - Dry Scalp2	3.733	0.917	(0.823, 6.644)	4.07	0.006
Lubricant E - Dry Scalp2	0.424	0.917	(-2.487, 3.335)	0.46	0.999
Lubricant B - Lubricant A	3.650	0.917	(0.739, 6.560)	3.98	0.007
Lubricant C - Lubricant A	-1.168	0.917	(-4.079, 1.742)	-1.27	0.858
Lubricant D - Lubricant A	3.243	0.917	(0.332, 6.154)	3.54	0.021
Lubricant E - Lubricant A	-0.067	0.917	(-2.977, 2.844)	-0.07	1.000
Lubricant C - Lubricant B	-4.818	0.917	(-7.729, -1.907)	-5.26	0.000
Lubricant D - Lubricant B	-0.407	0.917	(-3.317, 2.504)	-0.44	0.999
Lubricant E - Lubricant B	-3.716	0.917	(-6.627, -0.805)	-4.05	0.006
Lubricant D - Lubricant C	4.411	0.917	(1.500, 7.322)	4.81	0.001
Lubricant E - Lubricant C	1.102	0.917	(-1.809, 4.013)	1.20	0.888
Lubricant E - Lubricant D	-3.309	0.917	(-6.220, -0.399)	-3.61	0.018

Individual confidence level = 99.64%

Tukey Simultaneous 95% CIs

Interval Plot of Lmax vs Lubricant Condition

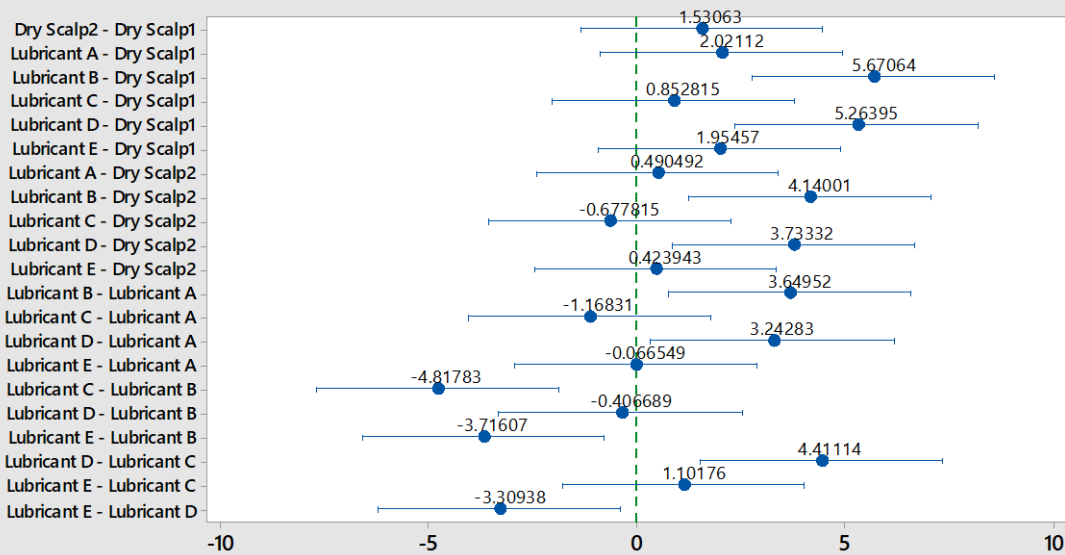
Interval Plot of Lmax vs Lubricant Condition 95% CI for the Mean



The pooled standard deviation is used to calculate the intervals.

B3. 2: Interval plot of Lmax(N) against test lubricant formulation in Study 4

Tukey Simultaneous 95% CIs Differences of Means for Lmax



If an interval does not contain zero, the corresponding means are significantly different.

B3. 3 Tukey simultaneous analysis of means of Lmax against tested across all tested experimental condition and the scalps control for study ID 4